Long-term trends of ambient gaseous concentrations at South African DEBITS sites and wet deposition at Cape Point

J Swartz

orcid.org 0000-0003-4552-9111

Thesis submitted in fulfilment of the requirements for the degree *Doctor of Philosophy in Environmental Sciences with Chemistry* at the North-West University

Promoter:	Dr PG van Zyl
Co-promoter:	Prof JP Beukes

Graduation July 2019

20564759

ACKNOWLEDGEMENTS

It has been said that the journey toward completing a PhD is a lonely one that will test you in every facet of your academic, professional and personal life. Although I was certainly tested, it was far from a lonely journey and I would like to acknowledge the colleagues, family and friends who made it possible.

I would like to extend my heartfelt gratitude to my two promoters, Prof PG van Zyl and Prof JP Beukes. Long before I started this body of work, when I had only just completed under graduate studies, several obstacles arose that at the time seemed insurmountable and would cut my academic endeavours short. What started as a request for a referral for my CV and some advice turned into a discussion about my aspirations and I was offered an opportunity that would irrevocably change my life. During the course of my honours, master's and now PhD studies, I witnessed and greatly benefitted from your guidance, patience and devotion to your students. The support you gave and understanding you showed me are things that I will always remember and be grateful for. I would also like to thank you both for all the advice you gave.

My family also deserves more gratitude than I can ever show. The influence of your love and support is immeasurable. To my mother Magda and late father Jan, thank you for the innumerable sacrifices you made to afford me every opportunity that you possibly could, and for teaching me the value of hard work, dedication and perseverance during my formative years. To my sister Annalé, your strength, courage and headstrong nature are things I have always admired. To my in-laws, Piet and Caren, thank you for your support and words of encouragement.

I would like to make special mention of the love my life, my wife Alta. Thank you for all your love and support. When I thought that I had no more to give, you would inspire me to dig deeper to hidden reserves you somehow always knew I would find. Thank you for always believing in me. The many sacrifices that you made that aided in me completing this immense task is something that I can never repay and will always be very grateful for. Thank you for being the wonderful mother that you are to our son. If I were to lose everything but the two of you, I would still be a very rich and happy man.

It is with gratitude that I would like to acknowledge the input and assistance of the team from the South African Weather Service operating the measurement site at Cape Point, C. Labuschagne, Dr E.-G. Brunke and T Mkololo for their assistance in sample collection as well as for their various inputs throughout the duration of this study. I would also like to thank Prof JJ Pienaar for his valuable inputs and assistance.

I would also like to thank the Atmospheric Research in Southern Africa and Indian Ocean (ARSAIO) programme established by the National Centre for Scientific Research (CNRS) and the National Research Foundation (NRF) for their respective contributions toward the completion of this study.

It is, however, the Lord and Saviour Jesus Christ who deserves my humble gratitude the most. By bringing people and opportunities across my path that I could never have deserved, You guided me to where I am now and moulded me to become the person I have become. I am looking forward to being moulded further to become the person You want me to be. Thank you for allowing me a tiny glimpse of Your handy work. You are truly the Great Teacher.

Thank you

` Jan-Stefan Swartz

for Alta and Liam

PREFACE

This thesis is submitted for examination in article format in accordance with the academic rules of the North-West University, wherein provision is made for the article model. All requirements laid out by the North-West University regulations have been adhered to in this thesis. The three articles and four supplementary chapters that comprise this article-based thesis aim to demonstrate the contribution to knowledge in the field similar to a traditional format thesis.

The structure of this thesis adheres to the traditional format in that it comprises an introductory chapter that includes the motivation for the study (Chapter1), a chapter providing an overview of the relevant literature (Chapter 2), a chapter on the experimental methodology (Chapter 3), as well as a concluding chapter in which the project is evaluated, and future recommendations are made (Chapter 7). A complete bibliography is also provided. This thesis deviates from the traditional format by not presenting conventional results chapters. Instead, three research articles are presented as Chapters 4, 5 and 6. Of the three manuscripts presented in this thesis, at least one had been submitted to a peer-reviewed journal (a prerequisite by the North-West University), while the other two had been prepared for submission to peer-reviewed journals. Each of the three articles comprises their own introduction, experimental, results and conclusions sections, as well as a relevant reference list. As a consequence, some repetition of material might occur in the thesis. However, this thesis has been kept as concise as possible and forms a cohesive body of work supporting the themes articulated in the introductory chapter. The author would like to note that the fonts, numbering and layout of Chapters 4, 5 and 6 are inconsistent with the rest of the thesis, since these manuscripts were prepared according to the guidelines of journals.

Rationale for submitting thesis in article format

From the outset of the study, the intention was to prepare three individual papers to submit for publication in scientific journals. The traditional PhD thesis generally reaches a smaller audience than articles published in peer-reviewed journals. The nature of this study facilitated an article approach as separate, yet interconnected research questions were addressed during the course of the study. The decision was made that emphasis should be placed on the improvement of the quality of research rather than writing a lengthy traditional thesis. The

three articles in Chapters 4, 5 and 6 each addresses a unique scientific question or research objective, while being connected to the central theme of this study to form a cohesive narrative.

Contextualising the articles in the overall storyline

The general topic of this PhD was associated with long-term trends, which included assessments of atmospheric SO_2, NO_2 and O_3 concentration measurements at four South African DEBITS sites representative of different ecosystems (semi-arid savannah and marine), as well as an evaluation of wet deposition at a marine site that was not previously conducted. Three articles are presented in this PhD thesis, each focusing on different aspects related to the topic. In the first article, presented in Chapter 4, the author focused on assessing long-term temporal trends of SO_2, NO_2 and O_3 concentrations measured at the Cape Point marine site, and developing a model to identify important factors influencing levels of these species. The second article, presented in Chapter 5, assessed long-term temporal patterns of SO_2, NO_2 and O_3 levels at three sites located in the north-eastern interior of South Africa by performing statistical modelling on long-term datasets. The third article, presented in Chapter 6, investigates the chemical composition of rainwater and wet deposition fluxes based on long-term precipitation collection at the marine site located at Cape Point.

The following manuscripts have been submitted or prepared for submission to a journal;

- Article 1: **Swartz, J.-S.,** Van Zyl, P.G., Beukes, J.P., Labuschagne, C., Brunke, E.-G., Portafaix, T., Galy-Lacaux, C., Pienaar, J.J. **Twenty-one years of passive sampling monitoring of SO_2, NO_2 and O_3 at the Cape Point GAW station, South Africa.** Submitted to ***Atmospheric Environment***, an Elsevier journal. The article was formatted according to the guidelines for authors of the journal.
- Article 2: **Swartz, J.-S.,** Van Zyl, P.G., Beukes, J.P., Galy-Lacaux, C., Pienaar, J.J. **Statistical modelling of long-term atmospheric SO_2, NO_2 and O_3 trends within the interior of South Africa.** Prepared for submission to ***Atmospheric Environment***, an Elsevier journal. The article was formatted according to the guidelines for authors of the journal.
- Article 3: Swartz, J.-S., Van Zyl, P.G., Beukes, J.P., Galy-Lacaux, C., Labuschagne, C., Brunke, E.-G., Mkololo, T., Pienaar, J.J. **Chemical composition of atmospheric wet deposition at the Cape Point GAW site, South Africa.** Prepared for submission

to ***Atmospheric Environment***, an Elsevier journal. The article was formatted according to the guidelines for authors of the journal.

Other articles, to which the author collaborated during the duration of this study as a co-author, but not included for examination purposes, are:

- Venter, A.D., Van Zyl, P.G., Beukes, J.P., **Swartz, J.-S.,** Josipovic, M., Vakkari, V., Laakso, L., Kulmala, M. 2018. Size-resolved characteristics of inorganic ionic species in atmospheric aerosols at a regional background site on the South African Highveld. *Journal of Atmospheric Chemistry*, 75(3):285-304., doi:10.1007/s10874-018-9378-z
- Dunnink, J.A., Curtis, C.J., Beukes, J.P., Van Zyl, P.G., **Swartz, J.-S.** 2016. The sensitivity of Afromontane trans in the Maloti-Drakensberg region of South Africa and Lesotho to acidic deposition. *African Journal of Aquatic Scien*ce, 41(4):431-426., doi:10.2989/16085914.2016.1244509

ABSTRACT

Although South Africa is considered an important source region for atmospheric pollutants, this region is considered to be understudied with regard to atmospheric composition, especially in terms of long-term assessments of atmospheric pollutant concentrations. The Deposition of Biogeochemically Important Trace Species (DEBITS) task of the International Global Atmospheric Chemistry (IGAC) programme was initiated in 1990 in collaboration with the Global Atmosphere Watch (GAW) network of the World Meteorological Organisation (WMO) to investigate long-term concentrations and deposition of biogeochemical species in the atmosphere for regions in the tropics for which limited long-term datasets exist. Four DEBITS sites, representative of semi-arid savannah, are located in the north-eastern interior of South Africa, i.e. Amersfoort (AF), Louis Trichardt (LT), Skukuza (SK) and the Vaal Triangle (VT), while one South African coastal site is also included, i.e. the Cape Point Global Atmosphere Watch (CPT GAW) station. The general aim of this study was to assess the long-term trends of SO_2, NO_2 and O_3 concentrations measured with passive samplers at the South African DEBITS sites located in the interior, and the marine background site, as well as to evaluate long-term wet deposition at CPT GAW. Since measurements were only conducted from 2009 to 2014 at VT, this site was not considered in this study, while comprehensive assessments of precipitation chemistry were previously reported for AF, LT and SK.

A 21-year (1995 to 2015) SO_2, NO_2 and O_3 passive sampling dataset was available for CPT GAW, while 19- (1997 to 2015), 21- (1995 to 2015) and 16-year (2000 to 2015) SO_2, NO_2 and O_3 passive sampling datasets were available for AF, LT and SK, respectively. The first part of the study entailed an evaluation of the long-term temporal trends at the marine CPT GAW site, as well as development of a multiple linear regression model in order to assess the influence of variances in source contribution, as well as local, regional and global meteorology on SO_2, NO_2 and O_3 concentrations. Thereafter, the statistical model developed for CPT GAW was employed in an assessment of long-term SO_2, NO_2 and O_3 concentration measurements at the sites located in the north-eastern interior of South Africa (AF, LT and SK) for which the influence of local, regional and global factors was also considered in the model. Finally, the chemical composition of rain water samples collected from 2004 to 2012 at CPT GAW during the wet season (May to October) was determined.

The SO_2, NO_2 and O_3 monthly mean concentrations determined at CPT GAW showed seasonal variability, which can be attributed to various factors influencing levels of these species at CPT GAW. These factors are generally season specific, which include changes in meteorological conditions and source contributions. Higher SO_2 and NO_2 concentrations during winter could be attributed to pollution build-up, as well as being more frequently impacted by air masses passing over the Cape Town metropole. Higher NO_2 concentrations were also attributed to increased microbial activity in the wet season. The O_3 seasonal pattern corresponded to the NO_2 seasonality, which was attributed to their related chemistry. SO_2 and NO_2 concentrations displayed inter-annual variability, while O_3 did not indicate significant inter-annual fluctuations. The seasonal and inter-annual variability was explored with a multilinear regression model, in which global, regional and local meteorological factors, as well as population growth were included. Modelling results indicated that variances in SO_2 concentrations were predominantly influenced by changes in global forcing factors. Global, regional and local factors played a significant role in NO_2 trends, which included the influence of population growth and associated increased anthropogenic activities. It was also established that variances in O_3 concentrations were predominantly associated with regional and local factors. Trend analysis indicated that SO_2, NO_2 and O_3 concentrations remained relatively constant over the 21-year sampling period at CPT GAW. A comparison between the SO_2, NO_2 and O_3 concentrations measured at CPT GAW with other African DEBITS sites indicated that levels of these species were generally similar to other African inland ecosystems, but lower compared to the industrially impacted AF site.

Long-term temporal trends indicated seasonal and inter-annual variability at AF, LT and SK, which could be ascribed to changes in meteorological conditions and/or variances in source contribution. Local, regional and global parameters contributed to SO_2 variability with total solar irradiation (TSI) being the most significant factor at the regional background site, Louis Trichardt (LT). Temperature (T) was the most important factor at Skukuza (SK), located in the Kruger National Park, while population growth (P) made the most substantial contribution at the industrially impacted Amersfoort (AF) site. Air masses passing over the source region also contributed to SO_2 levels at SK and LT. Local and regional factors made more substantial contributions to modelled NO_2 levels, with P being the most significant factor explaining NO_2 variability at all three sites, while relative humidity (RH) was the most important local and regional meteorological factor. The important contribution of P to modelled SO_2 and NO_2 concentrations was indicative of the impact of increased anthropogenic activities and energy

demand in the north-eastern interior of South Africa. Higher SO_2 concentrations associated with lower temperatures, as well as the negative correlation of NO_2 levels to RH, reflected the influence of pollution build-up and increased household combustion during winter. ENSO made a significant contribution to modelled O_3 levels at all three sites, while the influence of local and regional meteorological factors was also evident. Trend lines for SO_2 and NO_2 at AF indicated an increase in SO_2 and NO_2 concentrations over the 19-year sampling period, while an upwards trend in NO_2 levels at SK signified the influence of growing rural communities. Marginal trends were observed for SO_2 at SK, as well as for SO_2 and NO_2 at LT, while O_3 remained relatively constant at all three sites. SO_2 and NO_2 concentrations were higher at AF, while the regional O_3 problem was evident at all three sites in the South African interior.

The chemical composition of rain samples collected at CPT GAW indicated that the VWM concentrations of Na^+ and Cl^- were significantly higher compared to the VWM concentrations of other ionic species, as well as VWM concentrations thereof at the sites in the South African interior. The average pH of rainwater was slightly lower than the pH of unpolluted rainwater, mainly due to NO_3^- associated with the occasional influence of the Cape Town metropole. In contrast to the sites situated in the north-eastern South African interior, where anthropogenic SO_4^{2-} was the major constituent in rainwater, SO_4^{2-} at CPT GAW was entirely associated with marine air with no anthropogenic contribution. Sulphur and nitrogen depositions at CPT GAW were two orders of magnitude lower than sulphur and nitrogen depositions in the South African interior. It was also indicated that 94% of the chemical content at CPT GAW can be attributed to the marine source.

Keywords: Sulphur dioxide (SO_2), nitrogen dioxide (NO_2), ozone (O_3), DEBITS, IDAF, INDAAF, multiple linear regression, long-term trends, wet deposition

LIST OF ABBREVIATIONS

^{222}Rn	Radon 222
$(NH_4)_2SO_4$	Ammonium sulphate
%TP	Percentage total precipitation
AE	Anion equivalents
AF	Amersfoort
AMMA	African Monsoon Multidisciplinary Analysis
Amsl	Above mean sea level
AN-STO	Australian Nuclear Scientific and Technology Organisation
Ar	Argon
ARL	Air Resources Laboratory
ARSAIO	Atmospheric Research in Southern Africa and Indian Ocean
$C_2H_5COO^-$	Propionic acid (propionate)
$C_2O_4^{2-}$	Oxalic acid (oxalate)
$C_3H_8O_3$	Glycerol
$C_6H_8N_2O_2S$	Sulphanilamide/4-Aminobenzenesulfonamide
$C_{12}H_{14}N_2.2HCl$	N-1-Naphthylethylenediamine dihydrochloride / NEDA
Ca^{2+}	Calcium
CAM	Continental air masses
CNRS	National Centre for Scientific Research
CCN	Cloud condensation nuclei
CE	Cation equivalents
CFRPA	Cape Floral Region Protected Areas
CH_3COO^-	Acetic acid (acetate)

CH_4	Methane
Cl^-	Chloride
CO	Carbon monoxide
CO_2	Carbon dioxide
COO^-	Formic acid (formate)
CPT	Cape Point
DAAC	Distributed Active Archive Centres
DEBITS	Deposition of Biogeochemically Important Trace Species
DFE	Difference between RFE and LFE
DMS	Dimethylsulphide
DQO	Data quality objectives
ECMWF	European Centre for Medium-Range Weather Forecasts
EC	Electro-conductivity
EF	Enrichment factors
EN	El-Niño
ENSO	El-Niño Southern Oscillation
EOS	Earth Observation System
ERA	ECMWF reanalysis-interim archive
F^-	Fluoride
Fe^{2+}	Iron (II)
Fe^{3+}	Iron (III)
GAW	Global Atmosphere Watch
GDAS	Global Data Assimilation System
H_2O	Water
H_2O_2	Hydrogen peroxide
H_2S	Hydrogen sulphide

H_2SO_4	Sulphuric acid
$HO_2^{\bullet}$	Hydroperoxy radicals
HNO_3	Nitric acid
HYSPLIT	Hybrid Single-Particle Lagrangian Integrated Trajectory
I^-	Iodide
I_2	Molecular iodine
IC	Ion chromatography
ID%	Ion difference percentage
IDAF	IGAC DEBITS Africa
IGAC	International Global Atmospheric Chemistry
INDAAF	International network to study Atmospheric Chemistry and Deposition in Africa
INI	International Nitrogen Initiative
IOD	Indian Ocean Dipole
IQR	Interquartile range
IVL	Swedish Environment Research Institute
K^+	Potassium
K_2CO_3	Potassium carbonate
KOH	Potassium hydroxide
LFE	Local fire events
LIS	Laboratory Inter-comparison Study
LT	Louis Trichardt
MeOH	Methanol
Mg^{2+}	Magnesium
MLR	Multiple linear regression
Mn^{2+}	Manganese

MODIS	Moderate Resolution Imaging Spectrometer
MSA	Methane sulphonic acid
N_2	Molecular nitrogen
N_2O	Nitrous oxide
N_2O_5	Dinitrogen pentoxide
NASA	National Aeronautics and Space Administration
Na^+	Sodium
NaI	Sodium iodide
$NaNO_2$	Sodium nitrite
NaOH	Sodium hydroxide
NCEP	National Centre for Environmental Prediction
NDIR	Non-dispersive infrared
NF	Neutralisation factors
NH_3	Ammonia
NH_4^+	Ammonium
NH_4HSO_4	Ammonium bisulphate
NH_4NO_3	Ammonium nitrate
NO	Nitrogen oxide
NO_2	Nitrogen dioxide
NO_2^-	Nitrite
NO_3^-	Nitrate
$NO_3^\bullet$	Nitrogen trioxide radical
NOAA	National Oceanic and Atmospheric Administration
NO_X	$NO + NO_2$
NRF	National Research Foundation
nssf	Non-sea-salt fraction

o-H_3PO_4	Ortho-phosphoric acid
$O^{\bullet}$	Oxygen radical
O_2	Oxygen
O_3	Ozone
OA	Organic acids
OAM	Oceanic air masses
ODM	Overberg District Municipality
$OH^{\bullet}$	Hydroxyl radical
OH^-	Hydroxide
P	Population
pA	Potential acidity
PAN	Peroxyacetyl nitrate
PBL	Planetary boundary layer
ppb	Parts per billion
$PM_{2.5}$	Particulate matter in the sub 2.5 µm size range
PTFE	Teflon® / polytetrafluoroethylene
QBO	Quasi-biennial Oscillation
R	Rain depth
RF	Radiative forcing
RFE	Regional fire events
RH	Relative humidity
RIW	Relative important weight
RMSE	Root mean square error
$RO_2^{\bullet}$	Peroxyl radical
SAM	Southern Annular Mode
SAWS	South African Weather Service

SK	Skukuza
SO	Southern oscillation
SO_2	Sulphur dioxide
SO_3^{2-}	Sulphite
SO_4^{2-}	Sulphate
SR	Source region
ssf	Sea-salt fraction
SST	Sea surface temperature
T	Temperature
TEI	Thermo-environmental Instrument
TSI	Total solar irradiation
UNESCO	United Nations Educational, Scientific and Cultural Organization
USNWS	United States National Weather Service
UV	Ultra-violet
Uv/vis	Ultra-violet/visible
VOCs	Volatile organic compounds
v/v	Volume per volume
VWM	Volume weighted mean
Wd	Wind direction
WMO	World Meteorological Organisation
Ws	Wind speed

TABLE OF CONTENTS

LIST OF TABLES

CHAPTER 4

CHAPTER 5

CHAPTER 6

LIST OF FIGURES

CHAPTER 2

CHAPTER 3

CHAPTER 4

CHAPTER 5

CHAPTER 6

CHAPTER 1

INTRODUCTION

1.1 Background and motivation

Atmospheric pollutants are introduced into the atmosphere through various anthropogenic and natural emission sources (Abiodun *et al.*, 2014; Adon *et al.*, 2010; Connell, 2005; Mphepya *et al.*, 2004; Seinfeld & Pandis, 2006), while they are predominantly removed from the atmosphere through wet- and dry deposition processes or chemical transformation (Josipovic *et al.*, 2011). The impacts of atmospheric pollutants are most commonly associated with climate change and/or air quality. Increased levels of these species can either have a net warming or cooling effect on the climate of the earth. Greenhouse gases, for instance, absorb outgoing infrared radiation that causes an increase in temperature. Climate change is globally regarded as one of the most important occurrences, as it has large-scale political, social and economic impacts. Furthermore, air pollutants can cause serious human health problems by affecting, for example, the respiratory and cardiovascular systems, with the degree to which these effects are manifested depending on the pollutant concentration and duration of exposure to these species. Ecotoxicological research also indicates that the impact of air pollution on ecosystems ranges from small changes in the populations of terrestrial and aquatic ecosystems, up to the extinction of vulnerable species (Scholes *et al.*, 1996).

Although Africa is one of the most sensitive continents with regard to air pollution and climate change, it is also the least studied. South Africa is among the largest industrialised economy economies in Africa, with significant mining and metallurgical activities, which is also the only industrialised regional energy producer in the southern part of the continent as of 2014 (Rorich & Galpin, 1998; Sivertsen *et al.*, 1995; Tiitta *et al.*, 2014). Its continued economic growth has led to an increase in industrial activity, which, in turn, has led to higher electricity demand and increased fossil fuel combustion (Tiitta *et al.*, 2014). It is therefore important that long-term atmospheric monitoring programmes are established for this region in order to assess the impacts of increased anthropogenic activities on the environment. By studying the spatial and temporal evolution of the chemical composition of the atmosphere, as well as the atmospheric

dry deposition of chemical species, the extent of anthropogenic and natural influences on the atmosphere can be evaluated and monitored (Martins *et al.*, 2007).

The Deposition of Biogeochemically Important Trace Species (DEBITS) task of the International Global Atmospheric Chemistry (IGAC) programme was initiated in 1990 in collaboration with the Global Atmosphere Watch (GAW) network of the World Meteorological Organisation (WMO) to investigate long-term concentrations and deposition (wet and dry) of biogeochemical species (mainly C, N and S species) in the atmosphere for regions in the tropics for which limited long-term datasets exist (Lacaux *et al.*, 2003). The African component of this initiative is known as IGAC DEBITS Africa (IDAF) and consists of ten strategically positioned deposition sites in southern and western Africa that are representative of important African ecosystems (IDAF, 2011). Wet and dry depositions, as well as long-term trends of atmospheric pollutant concentrations are determined within the IDAF framework. There are four South African IDAF sites situated in the interior of the country, which include Louis Trichardt (LT), Amersfoort (AF), Skukuza (SK) and the Vaal Triangle (VT) (Adon *et al.*, 2010; Martins *et al.*, 2007). However, measurements were only conducted from 2009 to 2014 at VT. In addition to these sites located in the interior, one coastal South African DEBITS site is situated at Cape Point (CPT), which is also included in the Global Atmosphere Watch (GAW) network of the World Meteorological Organisation (WMO) (Brunke *et al.*, 2004).

AF, LT and SK are situated in a semi-arid savannah region in the north-eastern interior of South Africa at 1628 m, 1300 m and 267m above mean sea-level (amsl), respectively. AF is located in proximity of anthropogenic activities approximately 200 km south-west of the Johannesburg metropole, and approximately 50 km south-east of the highly industrialised Mpumalanga Highveld. LT is located in a rural region of the Limpopo Province, mainly characterised by agricultural activity, while SK is situated in the Kruger National Park – a well-known, large conserved protected area (Conradie *et al.*, 2016). CPT GAW is located approximately 60 km south of the Cape Town metropole, which is predominantly exposed to air masses representative of clean maritime air from the southern hemispheric mid-latitudes (Baker *et al.*, 2002; Brunke *et al.*, 2010; Brunke *et al.*, 2004).

Comprehensive assessments of precipitation chemistry at AF, LT and SK were presented by Conradie *et al.* (2016), Mphepya *et al.* (2004), and Mphepya *et al.* (2006). However, assessments of long-term temporal and spatial patterns of atmospheric inorganic species concentrations measured at these South African DEBITS sites, as well as possible sources

thereof, are not well documented in peer-reviewed literature (Martins *et al.*, 2007). Therefore, in this study, the long-term trends of ambient concentrations of inorganic gaseous species, i.e. SO_2, NO_2 and O_3 measured at South African DEBITS sites will be assessed. A statistical model will be developed in which the influence of local, regional and global meteorology, as well as variances in source contribution, will be considered. In addition, precipitation chemistry at the CPT GAW station, which has never been reported, will also be assessed.

1.2 Objectives

The general aim of this study will be to assess the long-term trends of inorganic gaseous species measured with passive samplers at the South African DEBITS sites, which include three sites located in the South African interior, i.e. AF, LT and SK, as well as the marine background CPT GAW site. It is also aimed at assessing the long-term wet deposition at CPT GAW in order to contextualise in relation to wet deposition determined at DEBITS sites in the interior of South Africa, previously reported by Conradie *et al.* (2016). In order to achieve the general aim of the study, specific objectives include:

I. Assessing monthly mean long-term seasonal and inter-annual trends of SO_2, NO_2 and O_3 measured with passive samplers at the CPT GAW atmospheric monitoring station, as well as determining possible sources of these species;

II. Developing and employing a statistical model to establish the influence of local and regional meteorology together with source contribution, as well as global climate drivers at CPT GAW on long-term trends;

III. Conducting statistical modelling of SO_2, NO_2 and O_3 long-term trends in the north-eastern interior of South Africa by utilising long-term passive sampling datasets available for AF, LT and SK in order to determine the influence of changes in source contributions, as well as local, regional and global meteorological parameters on long-term temporal trends;

IV. Contextualising SO_2, NO_2 and O_3 concentrations measured at South African DEBITS sites with other regions; and

V. Assessing the chemical composition of rainwater and wet deposition fluxes at CPT GAWs.

1.3 Methodology

Passive samplers are used to determine SO_2, NO_2 and O_3 concentrations at all the South African DEBITS sites, while rainwater samples are collected at CPT GAW with a wet-only sampler. A Dionex ICS 3000 ion chromatograph is used to perform analyses of passive samplers and rainwater samples. pH and conductivity of rain water are determined with a Hanna HI 255 combined pH and conductivity meter. Data processing is performed with relevant programmable software, which is also utilised in the development of a statistical model for long-term trend analysis. Air mass back trajectories are calculated with a Hybrid Single-Particle Lagrangian Integrated Trajectory (HYSPLIT) model (version 4.8) developed by the National Oceanic and Atmospheric Administration (NOAA) Air Resources Laboratory (ARL).

Local and global-scale meteorological and atmospheric measurements are obtained as relevant input parameters for the development of the statistical model. Local parameters (e.g. wind speed, ambient temperature, relative humidity) are obtained from the South African Weather Service and/or European Centre for Medium-Range Weather Forecasts (ECMWF). Global input parameters (e.g. El-Niño Southern Oscillation, Indian Ocean Dipole) are obtained from relevant databases, i.e. NOAA, Royal Netherlands Meteorological Institute and National Environmental Research Council's British Antarctic Survey. Daily fire distribution data are derived from the National Aeronautics and Space Administration's (NASA) Moderate Resolution Imaging Spectrometer (MODIS) satellite retrievals.

1.4 Thesis overview

This thesis comprises seven chapters. i.e.:

- Chapter 1: Provides the background, motivation and research objectives of this study.

- Chapter 2: Literature survey – presents a literature review of all relevant literature related to this study, which includes atmospheric composition, characteristics of pollutants and South Africa meteorology.
- Chapter 3: Experimental methods – presents information on the South African DEBITS sites, measurements, analytical methods, quality control and -assurance protocols, and the statistical model utilised.
- Chapter 4: Presents research article 1, which is related to long-term passive sampling measurements of SO_2, NO_2 and O_3 at a southern-hemispherical marine background site located on the south-western coast of South Africa, i.e. CPT GAW.
- Chapter 5: Presents research article 2, in which long-term trends of SO_2, NO_2 and O_3 measured with passive samplers at three South African DEBITS sites located in the north-eastern interior are assessed with a statistical model.
- Chapter 6: Presents research article 3 related to rainwater chemistry and wet deposition fluxes at CPT GAW.
- Chapter 7: Project evaluation – presents an evaluation of the study by discussing successes and shortcomings, as well as making recommendations for future work.

CHAPTER 2

LITERATURE SURVEY

2.1 Atmospheric composition

The lower atmosphere consists of the troposphere, which extends to an altitude of approximately 12 km at the mid-latitudes above the earth's surface (Connell, 2005; Seinfeld & Pandis, 2006). Between 85 and 90% of the atmospheric mass is in the troposphere, which consists of various gases and particulates. Gaseous composition in the troposphere comprises approximately 78% N_2, 21% O_2, 1% Ar and less than 1% trace gases. The troposphere essentially contains all the atmospheric water vapour and is a region characterised by constant mixing of air masses, giving rise to the observed frontal systems and various weather patterns (Harrison, 1999; Seinfeld & Pandis, 2006). In addition, the troposphere also facilitates basic natural energy conversion cycles, namely photosynthesis and respiration (Brasseur *et al.*, 1999; Connell, 2005).

Extending to an approximate altitude of 1 km above the earth's surface is a region referred to as the planetary boundary layer (PBL). It is characterised as a turbulent atmospheric region where aerosols, heat and moisture from the earth's surface can be exchanged with the free atmosphere, which is most often observed as an inversion in potential dew point and temperature or even a peak in low-level wind. The most common route by which pollutants are introduced into the atmosphere is by emission from anthropogenic and natural sources on the earth's surface into the PBL, making it the most impacted atmospheric region with regard to atmospheric pollution. Various processes serve to disperse pollutants through the lower atmosphere (Harrison, 1999; Schmid & Niyogi, 2012; Seinfeld & Pandis, 2006) such as deep convection that removes pollutants from the lower atmosphere, which is then rapidly injected into the middle and upper troposphere (Thompson *et al*., 1997).

2.2 Air pollution

As defined by Eby (2004), air pollution is the presence of substances in the atmosphere that are irritant, toxic or harmful to humans, vegetation and animals, as well as damaging to property, which can be divided into two main categories, namely primary and secondary pollutants. Primary pollutants are directly produced through combustion and/or evaporation, while their reactions in the atmosphere lead to the formation of secondary pollutants (Eby, 2004). The chemical properties, composition and the sources of air pollutants differ on local, regional and global scales (Kampa & Castanas, 2008).

2.2.1 Types of air pollutants

Atmospheric pollutants are categorised as gaseous or aerosol species (Conradie, 2018). Gaseous pollutants include inorganic species, e.g. sulphur dioxide (SO_2), nitrogen dioxide (NO_2), ozone (O_3) and ammonia (NH_3), as well as organic compounds such as volatile organic compounds (VOCs) and methane (CH_4) (Eby, 2004; Kampa & Castanas, 2008). Some of these gaseous species can be directly emitted into the atmosphere or are secondary pollutants formed through chemical reactions. NO_2, for instance, is formed rapidly from NO emissions from plants or can be directly emitted from combustion processes. Furthermore, these gaseous species can also result in the formation of aerosols, such as the oxidation of SO_2 and NO_2, leading to the formation of SO_4^{2-} (sulphate) and NO_3^- (nitrate), respectively. Vakkari *et al.* (2013) have indicated the significance of SO_4^{2-} related to high SO_2 emissions to new particle formation in southern Africa. Furthermore, O_3 is a secondary pollutant formed for the photosynthetic oxidation of NO_2.

Aerosols are defined as solid or liquid particles ranging from 1 nm to up to 20 µm in radius (Eby, 2004). Atmospheric particulates can either absorb or scatter incident solar radiation influencing the radiative budget of the atmosphere. These species can also affect the microphysical and optical properties of cloud condensation nuclei (CCN) (Takemura, 2005), since water droplet and ice particle formation in the atmosphere requires a nucleation site, which particulates in a certain size range can present (Andreae & Rosenfeld, 2008). The mean effective radius of the formed droplets decreases as the number of aerosol particles in the atmosphere increases, which increases the cloud albedo and reflection of incoming solar

radiation. Additionally, as the mean effective radius of formed droplets decreases, precipitation also decreases. Although atmospheric pollutants can be characterised as either particulate matter or gaseous pollutants, they are inter-correlated through various chemical, physical and meteorological processes present in the atmosphere (Josipovic *et al.*, 2011; Martins *et al.*, 2007; Petäjä *et al.*, 2013).

2.2.2 Gaseous pollutants

Since the primary focus of this study was on gaseous species, the sources, fate and impacts of major gaseous atmospheric pollutants are further discussed. Although trace gases comprise less than 1% of the tropospheric gaseous composition, these species affect the radiative budget of the earth and play an important role in atmospheric chemistry (Seinfeld & Pandis, 2006).

Sources and fates

It has become more apparent that the atmospheric chemical composition is being altered by increased anthropogenic activities, as large amounts of organic and inorganic trace gases are emitted into the troposphere (Monks & Leigh, 2009). The combustion of fossil fuels, pyrometallurgical processes and household biomass combustion are major contributors to anthropogenically emitted atmospheric gaseous species (Fields, 2004; Hao & Liu, 1994; Josipovic *et al.*, 2011).

Natural sources of atmospheric sulphurous compounds include volcanic activity, which emits SO_2 and H_2S, and oceanic biological processes that produce dimethylsulphide (DMS). DMS undergoes photochemical reaction to form methane sulphonic acid (MSA), along with SO_2 and sulphates (Ayers *et al.*, 1997; Monroe *et al.*, 2007). Increased SO_2 concentrations observed over urban and industrialised areas can mainly be ascribed to the increased combustion of coal and coal-derived fuels, as well as refinement and smelting of sulphur-containing ores. Therefore, atmospheric SO_2 concentrations are directly impacted by increases/changes in industrial and economic development (Connell, 2005; McGranahan & Murray, 2003). The atmospheric sulphur dioxide cycle is presented in Fig. 2.1.

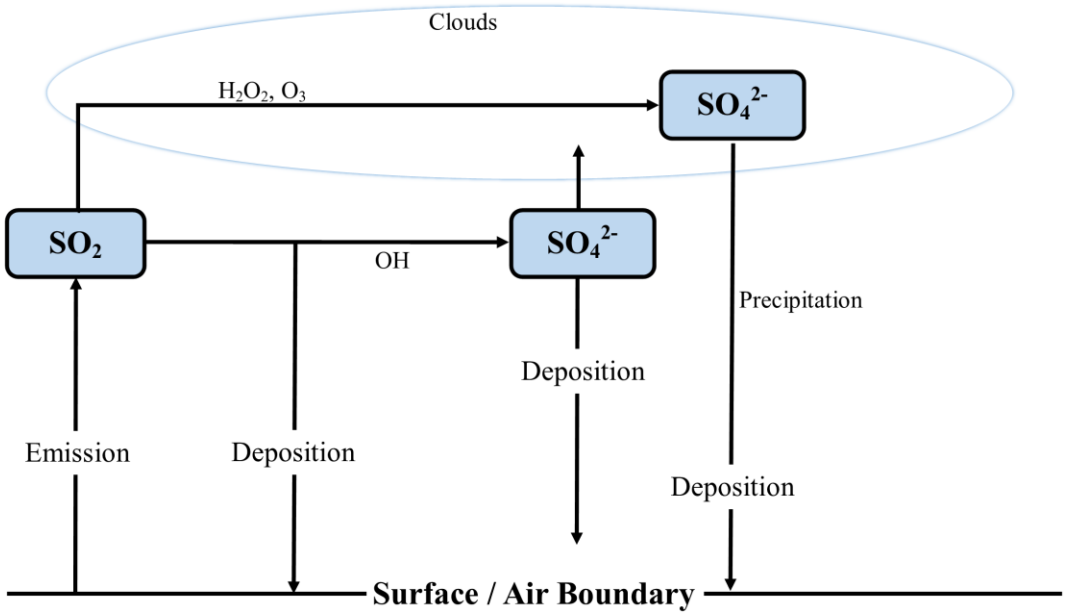

Figure 2.1: Atmospheric SO_2 cycle as adapted from Popescu & Ionel (2010)

Approximately 1.9 million tons of SO_2 is released into the southern African atmosphere annually from coal combustion on the Mpumalanga Highveld – constituting approximately 94% of the total emitted atmospheric SO_2 (Josipovic *et al.*, 2007) in southern Africa. SO_2 emitted into the atmosphere can be oxidised to form sulphates (SO_4^{2-}), which, in the presence of moisture, form sulphuric acid (Adon *et al.*, 2010; Connell, 2005; McGranahan & Murray, 2003);

$$2SO_2 + O_2 + 2H_2O \rightarrow 2H_2SO_4 \quad (2.1)$$

The presence of NH_3 in the atmosphere serves to neutralise atmospheric acids and, in the case of its reaction with sulphuric acid, either $(NH_4)_2SO_4$ or NH_4HSO_4 is produced, depending on the atmospheric availability of NH_3 (Seinfeld & Pandis, 2006);

$$NH_3 + H_2SO_4 \rightarrow NH_4HSO_4 \quad (2.2)$$

$$2NH_3 + H_2SO_4 \rightarrow (NH_4)_2SO_4 \quad (2.3)$$

Nitrogen is an essential component in sustaining biological life on earth. In Fig. 2.2, the nitrogen biogeochemical cycle is presented.

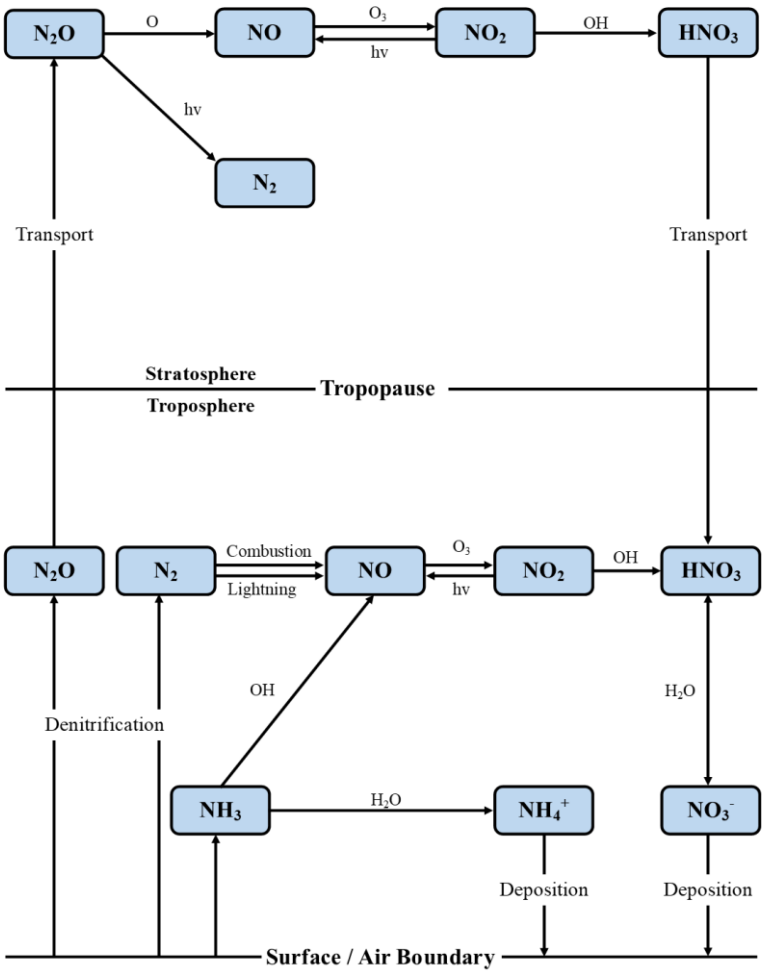

Figure 2.2: The most common atmospheric nitrogenous compounds and reactions of the nitrogen cycle as adapted form Seinfeld & Pandis (2006)

Nitrogen is converted into various chemical forms through biological and physical processes as it circulates among atmosphere, terrestrial and marine ecosystems. The mostly inert N_2 molecules in the atmosphere must be transformed (referred to as nitrogen fixation) into compounds that can be taken up by biological systems (Seinfeld & Pandis, 2006). Nitrogen oxide (NO), NO_2, nitrous oxide (N_2O), nitric acid (HNO_3) and NH_3 are considered to be the most important nitrogenous trace gas species in the atmosphere (Seinfeld & Pandis, 2006). One of the main anthropogenic nitrogen fixation processes includes the combustion of fossil fuels, which produces nitrogen oxides (NO_X = NO + NO_2). It is estimated on a global scale that as much as 50% of the total NO_X present in the atmosphere results from fossil fuel combustion (Fields, 2004; Hao & Liu, 1994; Josipovic *et al.*, 2011). Reactive NO_X can be transported over distances of up to hundreds of kilometres. Another source of anthropogenic NO_2 is the

oxidation of reactive nitrogenous compounds during the Haber-Bosch process used in the production of fertiliser (Zbieranowski & Aherne, 2012), while natural sources of NO_2 include lightning and microbial activity producing NO, which is readily oxidised to NO_2 (Connell, 2005). As mentioned previously, NO_2 can be formed through the reaction of NO and O_2 as a secondary pollutant species (Connell, 2005; Seinfeld & Pandis, 2006);

$$2NO + O_2 \rightarrow NO + NO_2 \quad (2.4)$$

NO_X is a precursor in the formation of photochemical smog and acid rain (Chameides *et al.*, 1994). Atmospheric NO_X is oxidised to form, among other compounds, HNO_3, which is readily deposited through wet deposition owing to its high solubility in water (Fields, 2004). The chemical reaction path through which atmospheric HNO_3 is formed is illustrated by equations 2.5 to 2.9. The oxidation of NO_2 by O_3 produces a relatively stable nitrogen trioxide radical ($NO_3^{\bullet}$), which is broken down by incident solar radiation to form either NO_2 or the oxygen radical ($O^{\bullet}$), depending on the frequency of the radiation (Connell, 2005);

$$NO_2 + O_3 \rightarrow NO_3^{\bullet} + O_2 \quad (2.5)$$

$$NO_3^{\bullet} \xrightarrow{h\nu} NO^{\bullet} + O_2 \text{ or } NO_2 + O^{\bullet} \quad (2.6)$$

In the absence of sunlight at night, $NO_3^{\bullet}$ reacts with excess NO_2 and NO to form dinitrogen pentoxide (N_2O_5), which in the presence of moisture, leads to the production of HNO_3. This is illustrated by reaction equations 2.7, 2.8 and 2.9 (Connell, 2005);

$$NO_3^{\bullet} + NO \rightarrow 2NO_2 \quad (2.7)$$

$$NO_3^{\bullet} + NO_2 \rightarrow N_2O_5 \quad (2.8)$$

$$N_2O_5 + H_2O \rightarrow 2HNO_3 \quad (2.9)$$

In much the same way as in the case of atmospheric H_2SO_4, HNO_3 is neutralised by NH_3 to form ammonium nitrate (NH_4NO_3) (Seinfeld & Pandis, 2006);

$$HNO_3 + NH_3 \rightarrow NH_4NO_3 \quad (2.10)$$

The process by which ammonium (NH_4^+) salts are oxidised as a result of microbial action is referred to as nitrification and leads to the production of nitrite (NO_2^-) and NO_3^- with N_2O and NO as by-products. The opposite process to nitrification, i.e. denitrification, refers to the

process by which NO_3^- is reduced to form species such as N_2, NO_2, N_2O or NO (Seinfeld & Pandis, 2006).

Volatile organic compounds (VOCs) are considered to be of natural and anthropogenic origin (Brasseur *et al.*, 1999), with the petrochemical industry, fossil fuel combustion and solvents used in industrial processes being the most important of anthropogenic sources (Jaars *et al.*, 2014). The most important natural source of VOCs within the South African context is considered to be open biomass combustion (Jaars *et al.*, 2014).

VOCs, together with NO_2, are important precursor species in the formation of tropospheric O_3 through complex reactions occurring in the atmosphere. O_3 commonly occurs in smog, together with other oxidants and aerosols (Abiodun *et al.*, 2014; Adon *et al.*, 2010; McGranahan & Murray, 2003). Fig. 2.3 presents the physical and chemical processes controlling O_3 in the atmosphere.

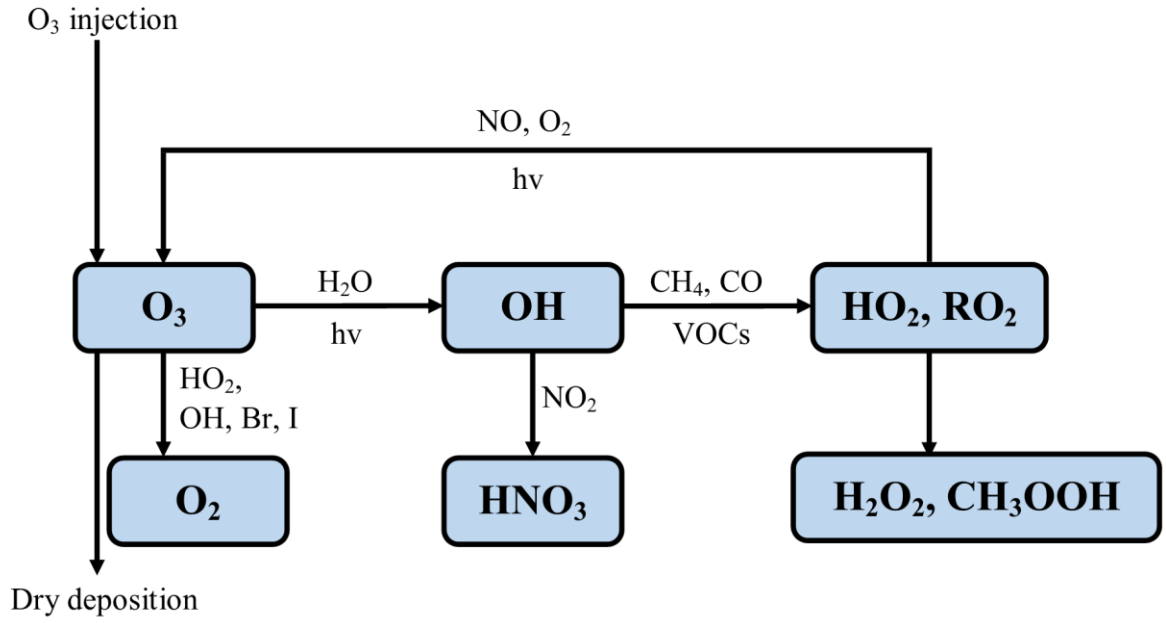

Figure 2.3: Physical and chemical processes controlling the production of O_3 as adapted from Galbally *et al.*, (2013)

The photochemical reduction of NO_2 to produce O_3 is the only known reaction through which O_3 is formed in the troposphere (Connell, 2005; Seinfeld & Pandis, 2006);

$$NO_2 \xrightarrow{h\nu} NO^{\bullet} + O^{\bullet} \quad (2.11)$$

$$O^{\bullet} + O_2 + X \rightarrow O_3 + X \quad (2.12)$$

with X = N_2 or O_2. In the atmosphere, Reactions 2.11 and 2.12 form a null-cycle through which the O_3 formed reacts with NO to form NO_2. However, in the presence of VOCs (including carbon monoxide, CO), this null-cycle is perturbed, resulting in the build-up of tropospheric O_3. Hydroxyl radicals ($OH^{\bullet}$) are produced through the photolysis of O_3 in the presence of H_2O, which contributes to the removal of trace gases from the atmosphere (Connell, 2005; Wilson *et al.*, 2007);

$$O_3 \xrightarrow{h\nu} O_2 + O^{\bullet} \quad (2.13)$$

$$O^{\bullet} + H_2O \rightarrow 2OH^{\bullet} \quad (2.14)$$

VOCs are oxidised by hydroxyl radicals ($OH^{\bullet}$) to produce peroxyl radicals ($RO_2^{\bullet}$) and hydroperoxy radicals ($HO_2^{\bullet}$), which, in turn, oxidise NO and thereby effectively removing surface O_3 (Atkinson, 2000).

Although chemical reactions are considered to be the major pathway through which atmospheric gases are removed from the atmosphere, wet and dry deposition also plays a significant role in the removal of atmospheric chemical compounds (Josipovic *et al.*, 2011; Waldman *et al.*, 1992). Dry deposition refers to the removal of pollutants through impaction, where species either make contact with the biosphere, e.g. sticking to the surface of a tree leaf or trunk, or though sedimentation. Dry deposition is largely influenced by the turbulence of the atmosphere, the nature of the surface being deposited onto and the chemical properties of the depositing chemical species. Natural vegetation generally promotes this process (Seinfeld & Pandis, 2006).

Wet deposition refers to the removal of particles from the atmosphere through precipitation. Condensation should occur when the atmosphere is saturated with water vapour, implying that the humidity should be close to 100%. When the newly formed cloud droplets are large enough, precipitation occurs, and the species are removed from the atmosphere. This is referred to as rainout, while aerosol collection by rain, fog and snowfall below the cloud base is referred to as washout. Acidic and basic atmospheric compounds are water soluble, meaning that they are readily dissolved into rain-, fog and cloud water (Eby, 2004; Josipovic *et al.*, 2011; Kajino &

Aikawa, 2015; Waldman *et al.*, 1992). By studying the chemical composition of wet deposition, the interaction between various chemical and physical mechanisms in the atmosphere can be better understood. These mechanisms include emission and source magnitude, processes governing atmospheric transport, chemical reactions in the atmosphere, and removal processes (Galy-Lacaux *et al.*, 2009). Furthermore, insight is also obtained regarding the chemical composition of the atmosphere caused by changes in meteorology and variances in source contribution (Vet *et al.*, 2014).

Impacts

Changes in atmospheric composition have an influence on climate, human health and ecosystems. It also affects the ability of governments to adapt to social and environmental changes (Laj *et al.*, 2009). One of the factors influenced by a change in the atmospheric composition is the radiative budget of the earth, which is expressed as radiative forcing (RF). A positive RF is associated with heating of the earth's surface associated with a climate driver, while a negative RF reflects surface cooling (IPCC, 2013). In Fig. 2.4, RF estimates in 2011 are related to RF values in 1750. It is evident that sulphates (SO_4^{2-}) and nitrates (NO_3^-), i.e. secondary aerosols formed from SO_2 and NO_2, respectively as previously mentioned, are shown to have a net cooling effect (negative RF) on the atmosphere with a high level of scientific understanding (H). In contrast, O_3, which is generally considered a short-lived greenhouse gas, has a net heating effect on the atmosphere (IPCC, 2013), with a medium level of scientific understanding. The medium level of confidence associated with tropospheric O_3 can be attributed to the complexity associated with this secondary pollutant.

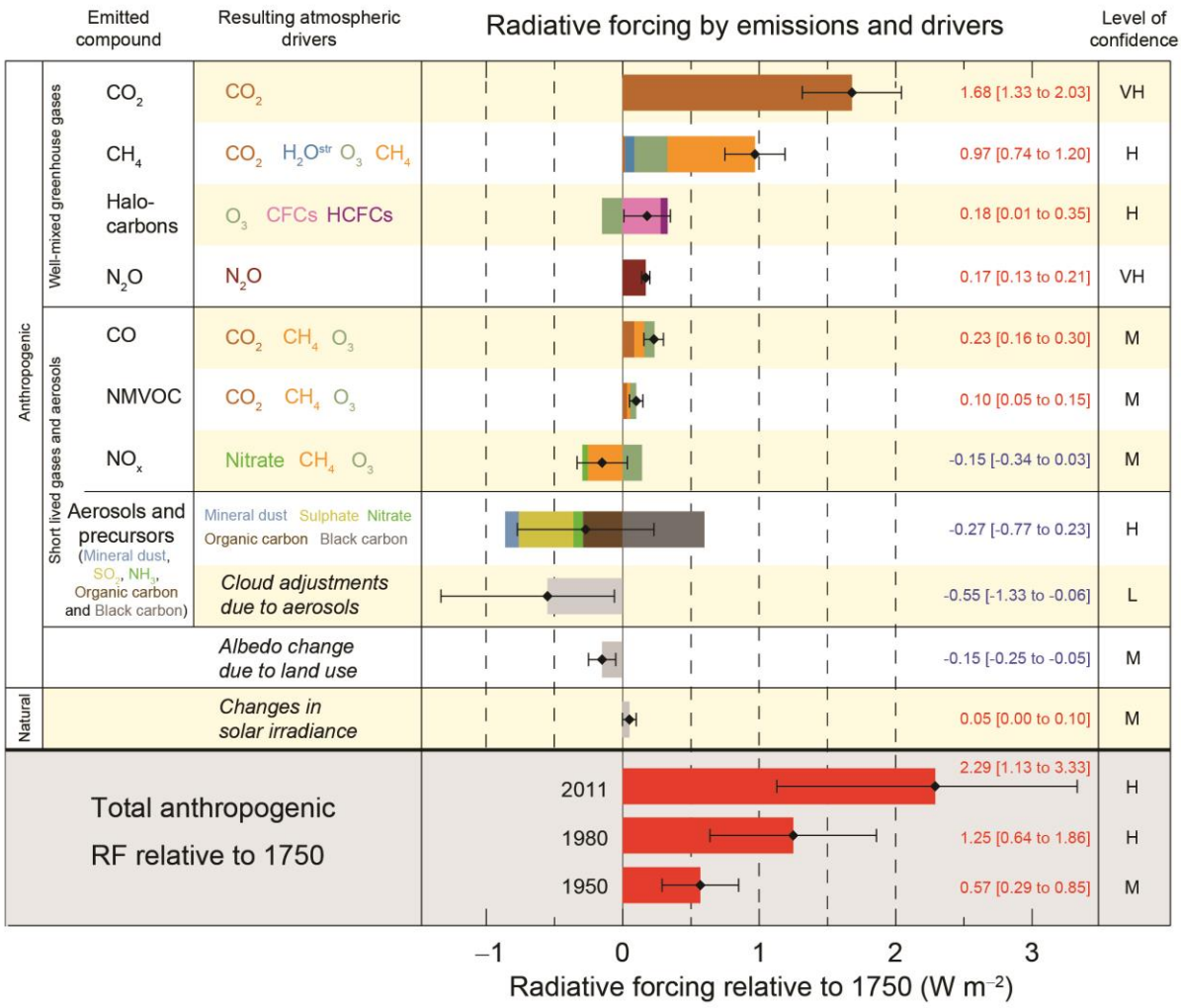

Figure 2.4: Relative 2011 radiative forcing estimates as compared to 1750 with associated uncertainties for major climate change drivers (IPCC, 2013)

High exposure to gaseous atmospheric pollutant species such as SO_2, NO_2 and O_3 can have detrimental impacts on human health. SO_2 can irritate the skin and mucosal membranes as well as aggravate heart and respiratory diseases. NO_2 is known to increase respiratory infections such as pneumonia and bronchitis and to impair lung growth in children, while it also weakens immune system functionality (McGranahan & Murray, 2003; USEPA, 2014; USNPS, 2013). The impacts of O_3 with regard to human health relate to the respiratory system, which include reduced lung function and lung irritation (Jerrett *et al.*, 2009; Ojumu, 2013). O_3, together with particulates smaller than 2.5 µm ($PM_{2.5}$), is considered, among atmospheric pollutants, to have the most significant impacts on human health (IPCC, 2013; NRC, 1991).

These species can also either be sources of important nutrients to the environment or be harmful to ecosystems through processes such as eutrophication of soils and surface/ground water. Although NO_X is essential for the photosynthetic and biological processes that sustain life on earth, excess NO_X can be detrimental to the environment (Connell, 2005). The limiting factor in the dynamics and productivity of terrestrial and marine ecosystems is biological nitrogen (Galloway *et al.*, 1995). Nitrogen availability influences the production and accumulation of biomass and consequently the global carbon cycle (Schimel *et al.*, 1995; Vitousek & Howarth, 1991). The rates at which nitrogen is taken up and removed from ecosystems are affected by changing biodiversity in affected ecosystems. Biodiversity generally decreases as nitrogen levels increase beyond a critical level as processes such as eutrophication tend to disrupt the nitrogen balance in soils and aquatic systems (Fields, 2004). Nitrates are leached from soil into surface- and groundwater, effectively removing minerals and leading to soil acidification, while downstream freshwater and coastal ecosystems are also affected by increased levels of nitrogenous compounds (Likens *et al.*, 1996; Nixon *et al.*, 1996). Lower pH of soil and terrestrial water increase the solubility and mobility of heavy/toxic metals such as iron (Fe^{2+}/Fe^{3+}) and manganese (Mn^{2+}), which can damage or be fatal to aquatic life. In addition, alkaline ions (e.g. Na^{+}, K^{+}, Ca^{2+} and Mg^{2+}) are removed from soils, negatively impacting the ability of soils to support plant life. In the long term, acidification of soils negatively affects the buffering capacity of soils. Not only does acidic precipitation adversely affect biological life and ecosystems, it also negatively affects economies through adverse effects on agriculture, infrastructure and architecture (Seinfeld & Pandis, 2006). As previously indicated, SO_2 and NO_2 are also associated with the formation of acid rain, which also contributes to the acidification of soil and aquatic systems.

O_3 can have negative impacts on agricultural activities by damaging crops and decreasing yields (Krupa *et al.*, 2001). Damage caused by O_3 to plants and crops includes visible injury, biomass loss, as well as physiological damage such as reduced photosynthesis, stomatal closure, reduced leaf area index, inhibition of transpiration, altered carbon allocation, reduced yield quality, and damage to reproductive ability (Felzer *et al.*, 2007).

2.3 Measurement of atmospheric gaseous species – passive sampling

Various active and passive sampling techniques exist through which the atmospheric concentrations of gaseous species can be measured. Typical active monitoring techniques to measure atmospheric trace gas concentrations include analytical methods such as chemiluminescence, fluorescence and absorption (Dhammapala, 1996; Jaars *et al.*, 2014; Kulmala *et al.*, 2013; Petäjä *et al.*, 2013; Saltzman *et al.*, 1993; Tiitta *et al.*, 2014; Venter *et al.*, 2012). Passive samplers provide a cost-effective solution to measure concentrations of atmospheric pollutants in regions that are logistically restrained by not being easily accessible or through lack of human capacity (Cox, 2003). Furthermore, passive samplers can also be utilised to increase the spatial resolution within an existing active monitoring network in a cost-effective manner. Passive samplers can also be useful for the initial screening of regions in order to identify pollution hotspots for which infrastructure and capacity could be invested to conduct active measurements. Passive samplers were essential in obtaining long-term measurements of atmospheric species at remote sites located in the western, central and southern African Deposition of Biogeochemical Important Trace Species (DEBITS) project.

A cost-effective passive sampler was developed by Dhammapala (1996), which is based on the samplers developed by the Swedish Environment Research Institute (IVL) (Ferm, 1991) and functions through diffusion of the atmospheric pollutant. Ambient air is sampled at a rate that is determined by molecular diffusion through a volume of air trapped inside the sampler in the absence of active air movement through the sampler, which yields averaged time-weighted gaseous concentrations (Aiuppa *et al.*, 2004). Fig. 2.5 illustrates the components of the passive sampler developed by Dhammapala (1996). The top assembly comprises a punched snap-on cap, used to hold a polytetrafluoroethylene (PTFE) filter and stainless-steel mesh in place. A paper disc impregnated with a chemically selective absorbing solution is placed in another plastic snap-on cap indicated as the lower assembly. These top and bottom assemblies are snapped together with a polypropylene ring, which holds the sampler together. The PTFE filter and stainless-steel mesh serve to prevent active air movement through turbulent diffusion (Carmichael *et al.*, 2003).

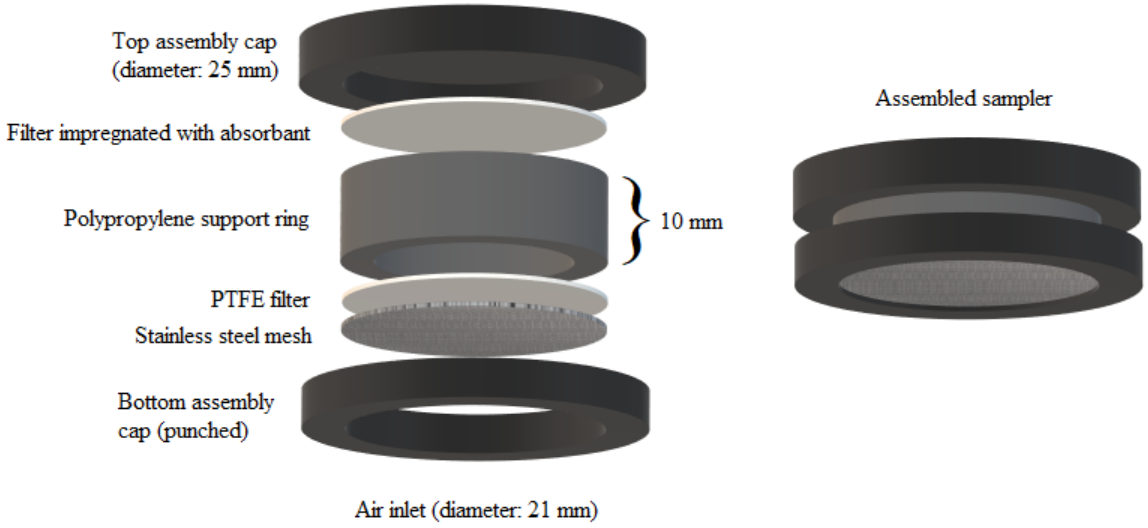

Figure 2.5: Exploded view of a passive diffusive sampler as well as a fully assembled passive diffusive sampler as adapted from Adon *et al.* (2010)

These passive samplers function through physical (the laminar diffusion of pollutant gases through a membrane) and chemical processes (reaction of diffused pollutant trace gases with the absorbing solution on the filter). Diffusion rates of trace gases in the atmosphere into the sampler are governed by diffusion coefficients of these gases and adhere to Fick's principles (Carmichael *et al.*, 2003; Martins *et al.*, 2007). The pollutant gas meets an ash-less medium filter paper disc impregnated with a chemical solution that reacts exclusively with a specific gas and quantitatively traps it on the filter. The limited air volume inside the sampler minimises the gas resistance time and transport distance to the filter paper disc containing the absorbing solution. The chemical reaction between the trace gas and the absorbing solution creates a concentration gradient and a net flux between the atmosphere and the air at the surface of the sorbent (Aiuppa *et al.*, 2004; Carmichael *et al.*, 2003), as indicated in Fig. 2.6.

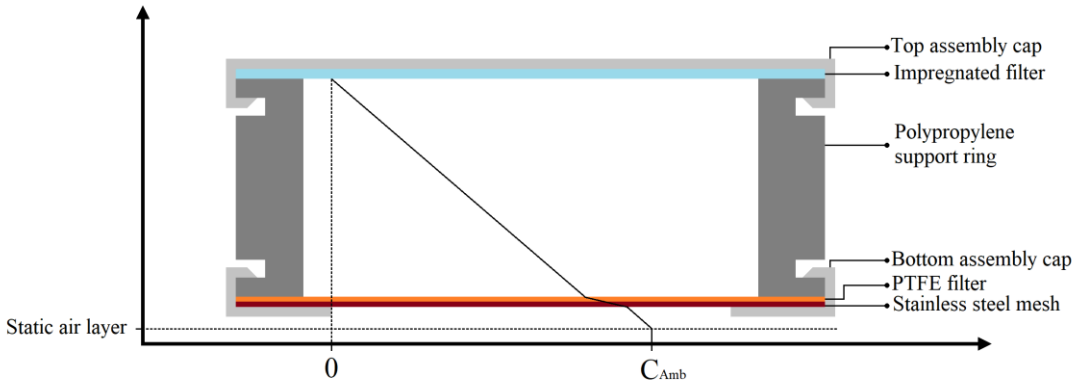

Figure 2.6: Concentration profile of pollutant species in and around the passive diffusive sampler as adapted from Dhammapala (1996)

The rate of diffusion into the passive sampler is governed by Fick's law of diffusion (Carmichael *et al.*, 2003; Ferm, 1991; Martins *et al.*, 2007), which indicates that the net flux Φ ($\mu g \cdot m^{-2} \cdot s^{-1}$) of a pollutant gas is proportional to the concentration C ($\mu g\ m^{-3}$) gradient along the path length L (m) within the sampler (Ferm, 2001);

$$\Phi = -D\left(\frac{dC}{dL}\right) \tag{2.15}$$

with D ($m^2 \cdot s^{-1}$) the diffusion constant and (dC/dL) the instantaneous pollutant concentration gradient in the direction of air flow. Φ can also be defined as the amount of pollutant gas X (µmol) passing through a cross-sectional area A (m^2) along the diffusion path in a given time t;

$$\Phi = \frac{dX/dt}{A} \tag{2.16}$$

which results in the following equation;

$$-D\left(\frac{dC}{dL}\right) = \left(\frac{dX}{dt}\right) / A \tag{2.17}$$

By time integrating equation 2.17 and rearranging, the following equation is obtained;

$$C_{Avg} = \left(\frac{X}{D \cdot t}\right)\left(\frac{L}{A}\right) \tag{2.18}$$

The term (L/A) is calculated as follows;

$$\left(L/A\right) = \left(L_R/A_R\right) + \left(L_F/A_F\right) + \left(L_N/A_N\right) + \left(L_S/A_R\right) \quad (2.19)$$

where L_R, L_F, L_N and L_S are the thickness of the polypropylene support ring, the PTFE filter, the stainless-steel mesh and the static layer underneath the sampler air inlet, respectively, and A_R, A_F and A_N are the cross-sectional areas of the polypropylene support ring, the PTFE filter and the stainless-steel mesh, respectively (Dhammapala, 1996). The inner diameter (21 mm) of the ring is used in calculations, since this is the diameter of the section through which diffusion takes place. According to Ferm (1991), the thickness of the static layer is on average 1.5 mm for outdoor sampling, which implies that the (L/A) ratio for this configuration is therefore 35 m^{-1} (Dhammapala, 1996). The concentration values calculated using equation 2.18 are expressed in mixing ratios (ppb) that translate to volume of pollutant (mm^3) per volume of moist air (m^3) under sampling conditions in order to eliminate pressure dependence (Dhammapala, 1996; Schwartz & Warneck, 1995). Applying the ideal gas law yields the following:

$$C = \left(1000 \cdot X \cdot R \cdot T / M_r \cdot D \cdot t\right)\left(L/A\right) \quad (2.20)$$

where C is the average concentration for the exposure period, R (8.31 $J \cdot K^{-1} \cdot mol^{-1}$) the gas constant, T (K) the average ambient temperature during the sampling period t (s), and M_r ($g \cdot mol^{-1}$) the respective molar mass. The diffusion constants (D) for each gaseous species of interest in this study are 1.30×10^{10} $m^2 \cdot s^{-1}$, 1.52×10^{10} $m^2 \cdot s^{-1}$ and 1.48×10^{10} $m^2 \cdot s^{-1}$ for SO_2, NO_2 and O_3, respectively (Dhammapala, 1996).

The chemical reactions through which SO_2, NO_2 and O_3 are chemically trapped and quantitatively collected with passive samplers are:

$$2SO_2(g) + 4OH^- + O_2 \rightarrow 2H_2O + 2SO_4^{2-} \quad (2.21)$$

$$2NO_2(g) + 3I^- \rightarrow 2NO_2^- + I_3^- \quad (2.22)$$

$$O_3(g) + NO_2^- \rightarrow NO_3^- + O_2 \quad (2.23)$$

Ambient SO_2 reacts with OH^- on the filter to form SO_3^{2-}, which undergoes further oxidation to form SO_4^{2-}. High pH (>13) must be maintained to effectively trap NO_2^-, which is generally ensured by NaOH. pH < 12 can result in the formation of NO_3^- instead of NO_2^-. In addition, the highly reactive NO_2^- can also react with other atmospheric oxidants, which is prevented by

adding I^- that reacts and removes oxidants through the formation of I_2 (Martins, 2009). In order to effectively trap O_3, it is critical that the pH is kept where the reaction constant for Equation 2.23 is at a maximum, i.e. 12, which is accomplished through the addition of K_2CO_3. The hygroscopicity of the sorbent crystals (NO_2^-) is another important factor that must be considered in this reaction. The oxidation potential of O_3 is enhanced with an increase in hygroscopicity, and consequently the collection efficiency is enhanced. Therefore, the hygroscopicity is increased through the addition of glycerol, as well as the use of different nitrite and carbonate salts to form sorbent crystals. Koutrakis *et al.* (1993) speculate that the process of trapping O_3 is a homogenous phase reaction occurring in microscopic droplets of water at the surface of the filter. Although NO_2^- can be oxidised by H_2O_2, the pH in the solution is too high for this to occur. The chemical reaction between HNO_3 and K_2CO_3 also forms NO_3^-, but due to the low ambient concentration of HNO_3 in comparison to O_3, this accounts for less than 5% of accumulated NO_3^-. Although peroxyacetyl nitrate (PAN) is also a strong oxidant in the atmosphere, its low diffusion coefficient and low ambient concentration render its influence mostly negligible (Martins, 2009).

2.4 Weather, climate and teleconnections

Two distinctions are generally made when describing atmospheric phenomena, i.e. *climate* and *weather*. *Weather* refers to pronounced atmospheric fluctuations that occur from hour to hour and from day to day, which includes local temperature, air pressure, humidity, cloud cover, precipitation and wind (Stenseth *et al.*, 2003). *Climate* refers to the prevailing weather that describes the averages, variations and distributions of weather conditions for a particular geographical region. Weather and climate affect the abundance and distribution of atmospheric species. Historically, the focus has been on local weather characteristics; however, recently, large-scale climatic fluctuations have become of interest. The interconnection between atmospheric anomalies at a planetary scale are referred to as teleconnections, which often present as persistent relationships between pressure fields of various geopotential heights at locations that are far apart from one another affecting regional and global weather patterns on global scale. Its effects on temperature, however, remain partially unknown (Sfîcă & Voiculescu, 2014). Examples of large-scale climatic patterns include the total solar irradiance (TSI), the El-Niño southern oscillation (ENSO), the Indian Ocean dipole (IOD), the quasi-

biennial oscillation (QBO) and the Southern annular mode (SAM). TSI is formally defined as the amount of solar radiation that arrives outside the earth's atmosphere, measured on a surface normal to the incident radiation at the mean distance between the earth and the sun and is reported in units of $W.m^{-2}$ (IPCC, 2007). Solar energy is converted into chemical energy through the formation of carbohydrates, which is the basic energy input for the ecosystems of the earth (Connell, 2005). Solar irradiance is therefore regarded as the primary energy input for the Earth (Dewitte *et al.*, 2004). TSI comprises various spectral ranges (ultra-violet UV-A, B and C, X-ray and visible light) that are all absorbed in the atmosphere at different heights, which are all influenced by the same 11-year solar cycle (NASA, 2017). Variations in TSI are expected to result in climatological changes and monitoring thereof is therefore necessary in climate change studies (Dewitte *et al.*, 2004).

Observed warming of equatorial surface waters between the western coast of South America and the International Date Line is referred to as El-Niño (EN), with the cold phase being referred to as La-Niña. The southern oscillation (SO) refers to an atmospheric phenomenon linked to El-Niño and involves air-mass movement between the western and eastern hemispheres (centred in tropical and subtropical latitudes). Although sea surface temperature (SST) fluctuations in this region might be observed without an associated change in SO, EN and SO are so closely associated that atmosphere-ocean interactions throughout the tropical Pacific are described using the term El-Niño southern oscillation (ENSO) (Stenseth *et al.*, 2003).

The spatial distribution, SST, observed in the Indian Ocean is typically characterised by warmer temperatures in the east and a cooler west – in contrast to the Atlantic and Pacific Oceans – that are heavily influenced by monsoons over the northern Indian Ocean and the neighbouring land mass. Furthermore, the thermocline separating the warmer water in the oceanic mixed layer from the colder water underneath is found at deeper depths in the eastern part of the Indian Ocean than in the west. This asymmetry also affects the atmosphere above the sea-surface as evidenced by higher convection being observed over the eastern Indian Ocean than over the western parts. During monsoons, zonal winds over the equatorial Indian Ocean are relatively weak, but stronger westerly winds are observed during the transition periods between monsoons. The monsoons typically occur from April to May and from October to November, coinciding with the boreal spring and fall, respectively. This results in strong currents being driven eastward along the equator transporting warmer water in the upper

layer of the ocean to the east, which lowers the depth of thermocline and causes it to be deeper in the east than in the west. As the eastern part of the Indian Ocean is warmer than the west, it also exhibits a more convective atmosphere than in the west. The Indian Ocean dipole (IOD) refers to this atmosphere-ocean departure from its mean state during certain years (Vinayachandran *et al.*, 2009). Although the origins of IOD events remain unclear, the observed zonal SST gradient anomaly is found to be strongly correlated with ENSO during the boreal fall (Saji & Yamagata, 2003).

The quasi-biennial oscillation (QBO) refers to observed downward propagating easterly and westerly wind systems, which dominates the equatorial stratosphere for slightly more than 28 months. The effects of the QBO are not only limited to tropical regions, as they influence stratospheric airflow from the polar regions. Furthermore, by selectively filtering upward propagating waves of air-mass movement through the equatorial stratosphere, the variability of the mesosphere is also influenced by the QBO and it may also influence the strength of hurricanes in the Atlantic. Circulation patterns and changes in QBO also affect the chemical composition of the atmosphere, as species such as ozone (O_3) and methane, as well as water vapour are transported by the QBO through the atmosphere (Baldwin *et al.*, 2001).

SAM refers to a westerly wind belt that exhibits north to south expansion and contraction over Antarctica, which dominates the middle to high latitudes in the southern hemisphere. The strength and location of cold fronts and storm systems in the mid-latitudes of the southern hemisphere are altered as the position of this belt changes. During positive SAM events, the westerly wind belt contracts towards Antarctica, resulting in weaker westerly winds and higher pressures that inhibit the propagation of cold fronts, whereas the opposite effects are observed during periods of negative SAM events. Strong positive SAM events in recent years have contributed to the observed dry period observed in southern Australia from 1997 to 2010 (BoM, 2012).

2.5 Conclusion

South Africa is the economic hub of southern Africa and is regarded as an important source region of anthropogenic atmospheric pollutants (Laakso *et al.*, 2012; Lourens *et al.*, 2012). The influence of emissions of pollutants in South Africa on local, regional and global atmospheric

chemical composition is signified by an observed NO_2 hotspot over the Mpumalanga Highveld indicated by satellite retrievals (Lourens *et al.*, 2012), being among the top ten largest sulphurous emitters worldwide (Stern, 2006) and plumes from open biomass combustion affecting Australia and South America (Wenig *et al.*, 2003). Numerous studies have indicated the importance of long-term atmospheric measurement to assess atmosphere-biosphere interactions for this region, e.g. gaseous concentration measurements in western and central Africa (Adon *et al.*, 2010), as well as wet deposition reported for DEBITS sites located in the north-eastern interior of South Africa (Conradie *et al.*, 2016; Mphepya *et al.*, 2006; Mphepya *et al.*, 2004). Long-term assessments are crucial when identifying appropriate policy requirements on a local and regional scale, as well as addressing the most topical atmospheric chemistry research questions (IPCC, 2014; Vet *et al.*, 2014).

Research questions that remain unanswered for this region relate to quantifying long-term trends of atmospheric inorganic gaseous species in relation to local, regional and global meteorological patterns, as well as changes in source contribution. Therefore, the influences of various climate drivers (local, regional and global) and source contribution variances on long-term temporal (seasonal and inter-annual) trends of ambient SO_2, NO_2, and O_3 concentrations in the South African atmosphere will be investigated. Long-term datasets of SO_2, NO_2 and O_3 concentrations measured with passive samplers within the framework of the DEBITS programme will be utilised, which include three regional background sites in the north-eastern South African interior and a marine background site. Statistical modelling will be performed with a multiple linear regression model in order to assess the interdependencies between local, regional and global factors (meteorology and source contribution) on long-term SO_2, NO_2 and O_3 concentration trends in order to establish major factors influencing seasonal and inter-annual variability. Furthermore, an assessment of wet deposition will be conducted for the first time for a coastal region in South Africa based on rain samples collected at the marine background site.

CHAPTER 3

EXPERIMENTAL METHODS

3.1 Sampling network

The International Global Atmospheric Chemistry (IGAC) programme initiated the Deposition of Biogeochemically Important Trace Species (DEBITS) project in 1990 in collaboration with the Global Atmosphere Watch (GAW) network of the World Meteorological Organisation (WMO), aiming to conduct long-term assessments of atmospheric biogeochemical species in the tropics, which is a region for which limited data was available (Lacaux *et al.*, 2003). At present, the programme operates within the framework of the third phase of IGAC, within the context of the International Nitrogen Initiative (INI) programme. Historically, the African component of this initiative was referred to as IGAC DEBITS Africa (IDAF). However, in 2015/2016, it was relabelled the International network to study Atmospheric Chemistry and Deposition in Africa (INDAAF) programme. INDAAF comprises 13 monitoring sites strategically positioned in western-, central- and southern Africa representing the most important African ecosystems (http://indaaf.obs-mip.fr). Four southern Africa INDAAF sites were considered in this study, i.e. Amersfoort (AF), Louis Trichardt (LT), Skukuza (SK) and the Cape Point (CPT) Global Atmosphere Watch (GAW) station. AF, LT and SK are semi-arid savannah regional background sites located in the north-eastern interior of South Africa, while CPT GAW is a southern-hemispherical marine background measurement station situated on the south-western coast of South Africa. The geographical locations of these sites are presented in Fig. 3.1.

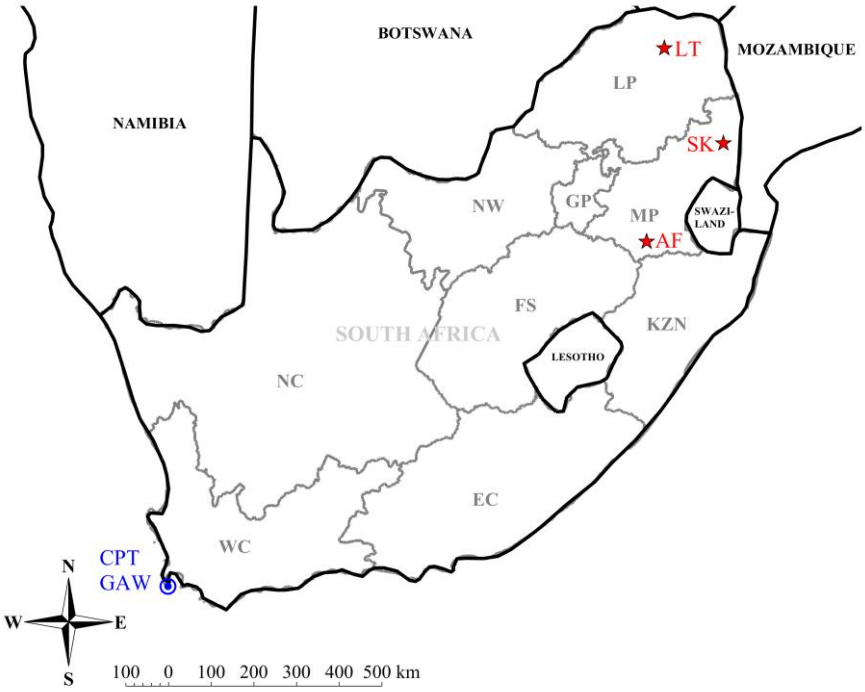

Figure 3.1: Regional South African map indicating the geographical locations of Amersfoort (AF), Louis Trichardt (LT), Skukuza (SK) and Cape Point (CPT GAW)

AF (27°04’13’’S, 29°52’02E) is located at an elevation of 1 628 m amsl in the southern part of Mpumalanga and is impacted by anthropogenic activities from the highly industrialised Mpumalanga Highveld situated approximately 50 km north-west of the region. In addition, the Johannesburg-Pretoria metropole is also located approximately 200 km to the north-west of AF. The measurement site at LT (22°59’10’’S, 30°01’21’’E) is located in the northern parts of the Limpopo Province at an elevation of 1 300 m amsl and is removed from major anthropogenic sources in the Mpumalanga Highveld. LT is considered a rural background site with the surroundings primarily comprising agricultural activities. SK (24°59’35’’S, 31°35’02’’E) is a rural background site located 267 m amsl in northern Mpumalanga within the statutorily conserved Kruger National Park. The nearest anthropogenic pollutant sources to SK are mainly informal settlements (Conradie *et al.*, 2016). CPT GAW (34°21’13’’S, 18°29’23’’E) is located at an elevation of 230 m amsl within the Cape Floral Region Protected Areas (CFRPA), which has been classified as a UNESCO world heritage site since 2004. The site is perched atop a cliff at the most southern tip of the Cape Peninsula that allows a 300° ocean view (Brunke *et al.*, 2004). CPT GAW is located within the Fynbos biome – a fine leaved, sclerophyllic shrub well adapted to a Mediterranean climate (UNESCO, 2015). CPT

GAW is predominantly influenced by air masses passing over the ocean, while it is occasionally impacted by air masses passing over the Cape Town metropole approximately 60 km north of CPT GAW (Brunke *et al.*, 2004).

3.2 Reagents and materials

Chemical reagents utilised in the preparation and analysis of passive samplers include: methanol (MeOH, *Promark Chemicals*); ortho phosphoric acid (o-H_3PO_4, *Promark Chemicals*); potassium carbonate (K_2CO_3, *Saarchem*); sodium iodide (NaI, *Saarchem*); sulphanilamide/4-Aminobenzenesulfonamide ($C_6H_8N_2O_2S$, *Saarchem*); glycerol ($C_3H_8O_3$, *Sigma Aldrich*); N-1-Naphthylethylenediamine dihydrochloride/NEDA ($C_{12}H_{14}N_2.2HCl$, *Sigma Aldrich*); sodium hydroxide (NaOH, *Rochelle Chemicals*); and sodium nitrite ($NaNO_2$, *Associated Chemical Enterprises*). All standards prepared for ion chromatography (IC) analysis were prepared using certified stock solutions manufactured by *SpectraScan* and supplied by *Industrial Analytical*. Buffer solutions and conductivity reference solutions for pH and electroconductivity instruments were manufactured by Hanna Instruments. De-ionised water (18.2 $\mu S.cm^{-1}$) was used for the preparation of all aqueous solutions, as well as for rinsing and washing.

Materials used to assemble passive samplers used in this study include: ash-less hardened medium paper discs with a diameter of 25 mm (*G.I.C. Scientific cc*); Teflon® (PTFE) filter membranes with a diameter of 25 mm and a pore size of 1 micron (*G.I.C. Scientific cc*); top and bottom assembly caps, as well as polypropylene support rings (refer to Fig. 2.5 in section 2.3) manufactured from polypropylene tubes (*Bellco Glass*, *The Scientific Group*) according to specification by the instrument makers of the North-West University; and stainless-steel mesh was supplied and cut (according to specification) by the instrument makers.

Rain samples were collected in single use polyethylene bags, which were transferred to Greiner-type essay-tubes for storage and transport.

3.3 Experimental procedures

3.3.1 General laboratory procedures

The measurement of concentrations of atmospheric trace elements with passive samplers necessitates optimum laboratory cleanliness, as it is estimated that a sample error of up to 50% can result from as little as 20 nmol contamination (Dhammapala, 1996). Sterile conditions were ensured in preparation and analytical laboratories by filtering air flow into the laboratory, maintaining positive pressure, as well as keeping the temperature at 22 °C and the humidity below 40%. All sampler components, with the exception of ash-less paper filters, i.e. the polypropylene snap-on caps and rings, stainless-steel mesh and reusable PTFE filter discs, were cleaned prior to sampler preparation. The cleaning process of these components entailed soaking in 0.2% (v/v) o-H_3PO_4 for four to five hours, which were then rinsed and soaked overnight in a 3% (v/v) Extran® MA O2 solution. After soaking overnight, the components were rinsed thoroughly (three times), sonicated in deionised water and completely dried. The ash-less paper filters were also pre-treated (to remove any debris) by soaking it in methanol followed by sonication in an ultrasonic bath for 30 minutes, which was repeated four times after which they were dried in a vacuum. After drying, the filter discs were sealed in air-tight bags for storage. All glassware, containers and other laboratory equipment used in experimental procedures and analytical techniques were also comprehensively cleaned to prevent sample contamination. All equipment was soaked in a diluted o-H_3PO_4 bath for a minimum of five hours, rinsed and soaked overnight in a soap solution (Extran® MA O2), and then rinsed up to ten times with deionised water and air dried in the laboratory.

3.3.2 Preparation, exposure and analysis of passive samplers

As indicated in section 2.3 (Fig. 2.5) the passive samplers used in this study comprise two snap-on polythene caps, a polypropoplene ring supporting the snap-on caps, a stainless-steel mesh, as well as an impregnated ash-less filter and a PTFE filter. The ash-less paper disc impregnated with a species-specific absorbing solution is placed in the top snap-on cap, while the stainless-steel mesh and the PTFE filter are housed in the bottom snap-on cap (with a hole punched to allow diffusion). Paper filters were impregnated with 50 µL of an absorbing solution that

specifically reacts with the atmospheric gaseous species of interest. All absorbing solutions were prepared in 100 mL volumetric flasks. The absorbing solution for the SO_2 samplers was prepared by diluting 1.00 g NaOH in 100 mL methanol, while the absorbing solution of NO_2 comprised 0.88 g NaOH and 7.90 g NaI dissolved in 5 mL deionised water and 95 mL methanol. The absorbing solution for O_3 consisted of 1.00 g dried $NaNO_2$ (dried in an oven at approximately 70°C), 1.00 g K_2CO_3 and 2 mL glycerol that were dissolved in a 7:3 water-methanol mixture. A duplicate set of samplers was prepared for each of the species measured at the South African DEBITS sites. The passive samplers were sealed off in air-tight containers prior to deployment. A laboratory blank was also prepared each month for each batch of samples, which was sealed in a container and stored in the laboratory.

The prepared passive samplers were either sent with a courier service to the sites or transported by a field technician. In Fig. 3.2, the housing unit in which passive samplers were placed during exposure is presented. The housing unit comprised rails wherein the passive samplers were slid in with the steel mesh opening facing downwards for exposure each month. The housing unit was positioned on a 1.5 m high stand (Fig. 3.2). This aluminium housing unit and stand were also manufactured by the instrument makers of the North-West University. Exposed passive samplers were removed after one month, sealed-off in air tight containers and replaced by new samplers. The exposed passive samplers were transported back to the laboratory, logged and placed in a freezer for storage at 3°C up until analysis.

Figure 3.2: Aluminium stand (left) and the housing unit (right) wherein passive samplers were placed for exposure each month at the South African DEBITS sites (Martins *et al.*, 2007)

The exposed ash-less paper filters were removed from the passive samplers and the collected SO_2 and NO_2 sample leached with 5 mL deionised water, while the O_3 sample was leached with 25 mL deionised water. All laboratory blanks were leached in 5 mL deionised water, which entailed sonication in an ultrasonic bath for 30 minutes. SO_2 and O_3 samples collected during the entire sampling period, as well as NO_2 samples collected after December 2012, were analysed with a suppressed ion chromatograph (IC). Prior to January 2013, NO_2 samples were analysed with ultraviolet/visible (uv/vis) spectroscopy NO_2 and samples were leached with 10 mL water. UV/vis spectroscopy analysis of NO_2 was initially conducted, since the IC method entailed very long running times for NO_2 detection. However, improvements in the development of new columns and the use of eluent gradient methods allowed for the analysis of NO_2 samples with the IC.

A reagent solution (diazotising agent) was prepared for uv/vis spectroscopy (Cary 50 uv/vis spectrophotometer) analysis of NO_2, which included 4 mL o-H_3PO_4, 4 g $C_6H_8N_2O_2S$ and 0.1 g $C_{12}H_{14}N_2.2HCl$ added to a 500 mL volumetric flask filled with deionised water. After the samples were leached, 5 mL diazotising agent was added to each sample prior to uv/vis spectroscopic analysis at 540 nm. A 1 M $NaNO_2$ stock solution that was prepared by dissolving 0.069g $NaNO_2$ in 1 L deionised water was used to prepare standards for uv/vis analysis of NO_2 samples. A second solution was prepared for the standards by dissolving 0.1975 g sodium iodide (NaI) in 50 mL water. The diazotising and NaI solution were added to the standard solutions prior to analysis, from which a five-point collaboration was conducted.

A Dionex ICS-3000 IC system comprising two flow lines was utilised in this study. One flow line was used for the detection of anion species and the other flow line to detect cation species. However, in this study, only the anion flow line used for SO_2, NO_2 and O_3 samples is considered. Prior to January 2013, the anion flow line was equipped with 2 mm AS 18 analytical and 2 mm AG 18 guard columns, a 2 mm CRD 200 carbonate removal device and an ASRS 300 2 mm suppressor. An isocratic eluent programme was employed, which kept the potassium hydroxide (KOH) eluent concentration constant at 18 mM, while the applied current was kept at 33 mA. In January 2013, the analytical and guard columns were replaced by 4 mm AS16 analytical and 4 mm AG16 guard columns. The 2 mm CRD 200 was also replaced by a 4 mm version and the suppressor was replaced by an AERS 500 4 mm suppressor. The eluent concentration and applied suppressor current were adapted to 10 mM and 30 mA, respectively, to accommodate the higher flow rate of 1.2 mL/min. A five-point calibration was performed with standard solutions (0.1, 0.5, 1.0, 2.5 and 5.0 ppm) prepared from 1 000 ppm stock solutions

of SO_4^{2-}, NO_2^- and NO_3^- for SO_2, NO_2 and O_3, respectively. Analysis of the samples commenced only after the relative standard deviation of the calibration curve was below 5%.

In all instances where analytical methods were changed, samplers collected over a period of at least three months were analysed with the previous and new method, which were compared in order to ensure similar results for both methods. Detection limits associated with sample preparation and analysis were calculated by utilising several laboratory blanks. The calculation of detection limits was conducted according to the method specified by the WMO in the bi-annual GAW laboratory inter-comparison study (LIS), which entailed calculating the standard deviation of the laboratory blank samples and multiplying the standard deviation by a factor of 3. The detection limits determined for SO_2, NO_2 and O_3 were 0.16, 0.03 and 0.02 ppm, respectively.

After analyses of the passive samplers, the concentrations of each species are converted to average monthly ambient concentrations with Equation 2.20 (section 2.3). Exposure time and average temperature is considered in the calculation. Since monthly exposure periods did not always commence and end precisely at the beginning and ending of a month, due to logistical reasons, a sampler deployed for a specific month could overlap some days at the end of the previous month or the beginning of the next month. Therefore, exposure periods were also normalised to be only representative of a specific month. Passive sampling data were also evaluated by applying the Q-test to identify and remove outliers.

In addition to passive sampling measurements conducted at the South African DEBITS sites, continuous *in situ* atmospheric O_3 concentration measurements were also conducted at CPT GAW with a Thermo Environmental Instrument (TEI 49C) (Oltmans *et al.*, 2013).

3.3.3 Precipitation

In general, the field protocols of the WMO for precipitation collection (WMO, 2004) were followed. However, due to logistical limitations and the type of rain sampler used, rainwater sampling at CPT GAW did not comply entirely with WMO protocols. An automated wet-only rain sampler designed for use within the IDAF network (Galy-Lacaux *et al.*, 2009) was used for the collection of rain samples at CPT GAW. The sampler has a collection area of 225 cm^2 and is equipped with a sensor that controls a lid that opens when a rain event starts. This type

of wet-only sampler, however, does not close automatically after a rain event and must therefore be manually closed by a site operator. Therefore, since rain water samples could only be collected during scheduled visits to the CPT GAW site, some of the advantages associated with using a wet-only sampler could not be entirely achieved, e.g. minimising contamination. This sampling artefact also contributed to certain collected rain samples being representative of more than one rain event. Furthermore, rain samples were also only collected during the wet season, i.e. May to October at CPT GAW. Rain samples collected in a polyethylene bag in the wet-only sampler were transferred into two 50 mL Greiner-type essay-tubes, which were stored in a freezer at -18°C (Galy-Lacaux *et al.*, 2009). Rain samples were transported to the laboratory in a frozen state for analysis.

Rain samples were unfrozen overnight prior to analysis. Each rain sample was visually inspected to report and remove any visible contamination. Immediate conductivity and pH measurements of 25 mL aliquots of each rain sample were conducted with an HI 255 combined meter (Hanna Instruments) with a low ionic strength electrode. A three-point pH calibration procedure was conducted with pH 4.01, 7.01 and 10.01 buffer solutions, while an 84 $\mu S.cm^{-1}$ electroconductivity reference solution was used for calibration of the conductivity probe.

The remaining rain samples were filtered through a 0.2 µm filter for chemical analysis with the same IC utilised to analyse passive samplers, i.e. a Dionex ICS 3000. For rain water samples, the two-flow line functionality of the IC system was utilised, since anion- and cation species were detected. Analyses of anions were performed with the same analytical setup as previously described for passive samplers. However, a multi-step concentration profile was followed for the eluent (KOH) in order to allow optimum separation of peaks within a reasonable time during anion analysis of rain samples. Cation analyses were conducted with a CS16 analytical column, a CG16 guard column and a CSRS 300 suppressor, at a fixed eluent (methane sulphonic acid, MSA) concentration of 25 mM and a flow of 0.45 mL/min to achieve optimal separation of the cation species. Anion species measured included sodium chloride (Cl^-), sulphate (SO_4^{2-}), nitrate (NO_3^-), fluoride (F^-) and water-soluble organic acids (OA), i.e. formic- (COO^-), acetic- (CH_3COO^-), propionic- ($C_2H_5COO^-$) and oxalic acid ($C_2O_4^{2-}$), while cation species comprised sodium (Na^+), ammonium (NH_4^+), potassium (K^+), calcium (Ca^{2+}) and magnesium (Mg^{2+}). A five-point calibration was also performed for anion and cation analysis, while analysis of the samples commenced only after the relative standard deviation of the calibration curve was below 5% as described above. The detection limits of the IC for the

species analysed were 1 ppb for Na^+, K^+, Mg^{2+} and F^-, 2 ppb for Ca^{2+}, 4 ppb for NH_4^+, 11 ppb for Cl^-, 28 ppb for NO_3^- and 31 ppb for SO_4^{2-} in aqueous solution.

3.3.4 Quality control and -assurance

The passive samplers used during this study were evaluated through participation in several inter-comparison studies (Martins *et al.,* 2007). The most recent was organised by the University of Singapore in 2008 (He & Bala, 2008), in which SO_2 and NO_2 passive samplers were compared to active samplers, as well as to passives samplers used by other international institutions. This study indicated that the SO_2 and NO_2 passive samplers utilised in this study compared very well to active measurements, while having better accuracy compared to similar samplers used by other institutions in most instances. The evaluation of passives samplers is also continuous process, which is currently assessed through comparison to *in situ* measurements at the comprehensively equipped Welgegund measurement station located approximately 100 km west from Johannesburg (Laban *et al.,* 2018). Welgegund was also recently (in 2019) included as a supersite in the INDAAF network.

The IC analytical techniques, as well as the pH and conductivity measurements utilised in this study, were also verified by participating in the bi-annual WMO Laboratory Inter Comparison Study (WMO LIS). A sample set comprising three laboratory-prepared samples is analysed and the results published online. In Fig. 3.3, the results (presented by ring diagrams) of the 58th LIS study in 2018 for the analytical laboratory are presented, which indicate that the IC analytical procedures followed are relatively good. According to the WMO inter-comparison results, the recovery of each ion in standard samples was between 95 and 105%.

WMO LIS 58 Sample 1 WMO LIS 58 Sample 2 WMO LIS 58 Sample 3

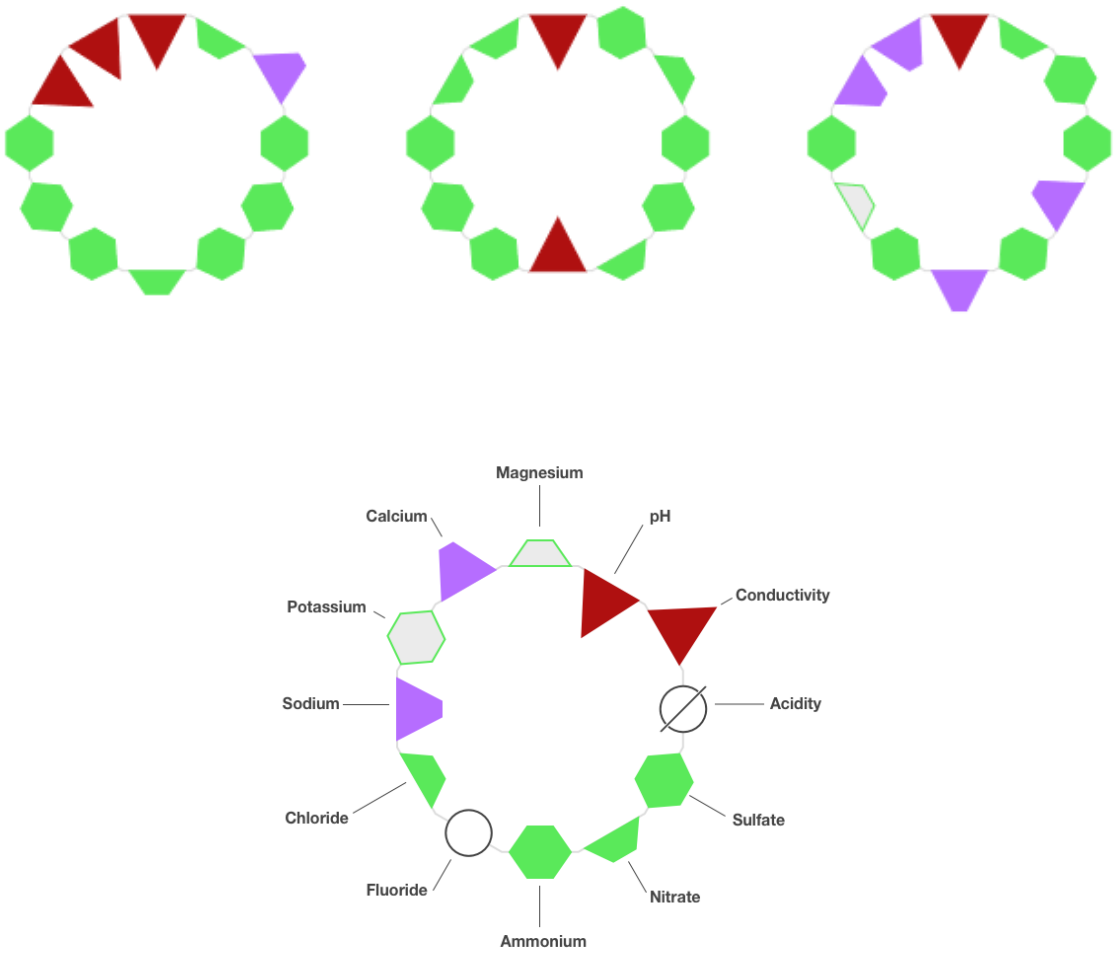

Figure 3.3: Results of the WMO LIS 58 study in July 2018 indicated by ring diagrams with a legend for the ring diagram indicated. Green hexagons indicate good results (measurements are within the interquartile range (IQR), defined as the 25th to 75th percentile or middle half (50%) of the measurements), green trapezoids indicate satisfactory results (measurements are within the range defined by median ± IQR/1.349), purple trapezoids indicate results not within the satisfactory category, but within a range defined by the median ± 2(IQR/1.349), and red triangles indicate that the results are unsatisfactory (measurements are outside the range defined by the median + 2(IQR/1.349)). Measurements below the detection limit are indicated by an open circle, while an open circle with a slash through indicates that no measurement was reported (Qasac-Americas, 2018). IQR/1.349 is the non-parametric estimate of the standard deviation, sometimes called the pseudo-standard deviation (Qasac-Americas, 2018)

The principle of electroneutrality in precipitation requires that the total anion and cation equivalents (AE and CE, respectively) are equal, which is a prerequisite for precipitation collection according to the guidelines of the WMO (WMO, 2004). In order to assess whether a precipitation sample adheres to this criterion, the ion difference percentage (ID%) is calculated using equations 3.1 to 3.3:

$$ID(\%) = 100 \times \left({(CE - AE)} \Big/ {(CE + AE)} \right) \tag{3.1}$$

$$AE = 1000 \times \sum \left({C_{Ai}} \Big/ {(Eq.Wt)_{Ai}} \right) + \left({5.1} \Big/ {10^{6\text{-}Ph}} \right) \tag{3.2}$$

$$CE = 1000 \times \sum \left({C_{Ci}} \Big/ {(Eq.Wt)_{Ci}} \right) + \left(10^{6\text{-}Ph} \right) \tag{3.3}$$

C_{Ai} and $(Eq.Wt)_{Ai}$ in Equation 3.2 refer to the concentration (mg/L) and equivalent weight, respectively, of the i^{th} anion, while the term $(5.1/10^{6\text{-}pH})$ accounts for the calculated bicarbonate concentration at 25°C when sample pH is higher than 5 (Stensland, 2006). In Equation 3.3, C_{Ci} and $(Eq.Wt)_{Ci}$ refer to the concentration (mg/L) and equivalent weight respectively of the i^{th} cation. The ionic equivalent weights, as well as the evaluation criteria values are presented in WMO (2004). Acceptance ranges for the ID%, as indicated in the WMO (2004) report, were applied to all the rain samples collected in this study.

3.4 Multiple linear regression model

The interdependencies between local, regional and global meteorology, as well as variances in source contribution on SO_2, NO_2 and O_3 concentrations measured at CPT GAW, AF, LT and SK were statistically evaluated with a multiple linear regression (MLR) model. This model was similar to the trend-run model developed for trend estimates of O_3 and temperature by Toihir *et al.* (2018) and Bencherif *et al.* (2006), respectively. The relationship between two or more independent variables and a dependant variable by MLR is modelled by fitting a linear equation to the observed data, which can be utilised to calculate values for the dependent variable. In this study, concentrations of SO_2, NO_2 and O_3 were the dependent variable, while meteorological parameters and source contribution variances (e.g. population growth) were the independent variables to yield the following general equation:

$$C(t) = \sum_{k=1}^{p} a(k) \times f(t,k) + R'(t) \quad (3.4)$$

where f(t,k) describes the specific factor k at time t and a(k) is the coefficient calculated by the model for the factor k that minimises the root mean square error (RMSE). The RMSE compares the calculated values with the measured values as follows:

$$\chi^2 = [\sum_t C(t) - \sum_k a(k) \times f(t,k)]^2 \quad (3.5)$$

The residual term, R′(t), accounts for factors that may have an influence on the model that are not considered in the MLR model. The trend was parameterised as linear: Trend (t) = $\alpha_0 + \alpha_1.t$, where t denotes the time range, α_0 is a constant, α_1 is the slope of Trend(t) line that estimates the trend over the time scale. MLR and trend analysis were conducted with appropriate programming software.

In order to assess the significance of each of the independent variables on the calculated C(t), the relative importance weights (RIW) approach was considered, which examines the relative contribution that each independent variable makes to the dependent variable and ranks independent variables in order of importance (Kleynhans *et al.*, 2017; Nathans *et al.*, 2012). The RIW approach was applied with IBM® SPSS® Statistics Version 23, together with program syntaxes and scripts adapted from Kraha *et al.* (2012) and Lorenzo-Seva *et al.* (2010).

3.5 Model input parameter

3.5.1 Local and regional factors

Local and regional meteorological parameters included in the model for CPT GAW, i.e. wind speed (Ws) and -direction (Wd), ambient temperature (T), relative humidity (RH) and rain depth (R) were measured by the South African Weather Service (SAWS) at the CPT GAW site. Meteorological data for AF, LT and SK were obtained from the European Centre for Medium-Range Weather Forecasts (ECMWF) reanalysis-interim archive (ERA), since meteorological parameters were not measured at these sites during the entire long-term measurement periods. In addition, meteorological datasets from nearby SAWS stations had low data coverage percentages (>50%). Local and meteorological data included in the model for AF, LT and SK included the same parameters included for CPT GAW (Ws, Wd, T, RH and R) (www.ecmwf.int/en/forecasts/datasets/archive-datasets/reanalysis-datasets/era-interim). In

addition, similar to Korhonen *et al.* (2014), planetary boundary layer heights were determined with a global weather forecast model operated by the ECMWF for CPT GAW, AF, LT and SK.

Population data (P) from three separate national censuses, i.e. October 2001, October 2011 and May 2016, were obtained from local municipalities and also included in the model at all four South African DEBITS sites as an indicator of increased anthropogenic activities. The population data were interpolated by assuming linear population growth. The influence of source region contribution was also determined at AF, LT and SK by using hourly-arriving back trajectories (discussed in section 3.6). The percentage time that air masses spent over a source region before arriving at each site was calculated, which was included as a factor in the MLR model. The source region that was defined for AF, LT and SK in this study combined source regions defined in previous studies (e.g. Jaars *et al.* (2014) and Booyens *et al.* (2019)), which comprised the Mpumalanga Highveld, Vaal Triangle, the Johannesburg-Pretoria conurbation, the western- and the eastern Bushveld Igneous Complex, as well as a region of anticyclonic recirculation.

Additional data available for CPT GAW that was included in the model comprised *in situ* measurements of CO, CO_2 and ^{222}Rn. ^{222}Rn measurements are mainly conducted at CPT GAW to separate oceanic and continental air masses measured at the site (Botha *et al.*, 2018). CO measurements prior to 2012 were conducted with a reduction gas analyser (RGA3), while subsequent sampling was performed with the Picarro G2302 analyser system (Brunke *et al.*, 2004). A non-dispersive infrared (NDIR) absorption technique was used for CO_2 measurements prior to 2012, after which CO_2 monitoring was conducted with the Picarro G2302 and G2301 systems. ^{222}Rn measurements were conducted with a custom-built instrument designed by the Australian Nuclear Scientific and Technology Organisation (ANSTO) (Brunke *et al.*, 2004).

3.5.2 Global meteorology

Global forcing factors considered as predictor variables in the MLR model include total solar irradiance (TSI), El-Niño southern oscillation (ENSO), Indian Ocean dipole (IOD), quasi-biennial oscillation (QBO) and the Southern annular mode (SAM). Monthly ENSO and QBO

data were obtained from the National Oceanic and Atmospheric Administration (NOAA) database (NOAA, 2015a; NOAA, 2015b), while TSI and IOD datasets were obtained from the Royal Netherlands Meteorological Institute (*"Koninklijk Nederlands Meteorologisch Instituut"*) (KMNI, 2016a; KMNI, 2016b). SAM data were obtained from the National Environmental Research Council's British Antarctic Survey (Marshall, 2018).

3.5.3 Fire frequency

Various parameters, which include burn scars-, fires- and smoke distributions, are measured on a global scale by the National Aeronautics and Space Administration's (NASA) Moderate Resolution Imaging Spectrometer (MODIS) satellite mounted on the polar-orbiting Earth Observation System's (EOS) Terra spacecraft. In this study, MODIS retrievals were used to derive daily fire distribution data from 2000 to 2015, which were retrieved from the NASA Distributed Active Archive Centres (DAAC) (Kaufman *et al.*, 2003). Monthly local fire events (LFE) occurring within 100 km from each site considered in this study were calculated, while regional fire events (RFE) occurring within 1 000 km from AF, LT and SK, as well as 400 km from CPT GAW were also determined.

3.6 Back trajectory analysis

The Hybrid Single-Particle Lagrangian Integrated Trajectory model (HYSPLIT) is generally used to calculate back trajectories by either employing a puff or particle approach (Draxler & Hess, 2004). Trajectories are the integrated advection of a puff or particle, which is calculated from the average of a three-dimensional velocity vector from a starting guess position P(t) at a certain time t, to the position P′(t+Δt) at Δt. These velocity vectors are both space and time interpolated, with the first-guess position and the final position being described by equations 3.6 and 3.7, respectively (Draxler & Hess, 2004);

$$P'(t+\Delta t) = P(t) + V(P,t)\,\Delta t \tag{3.6}$$

$$P(t+\Delta t) = P(t) + 0.5\,[\,V(P,t) + V(P',t+\Delta t)\,]\,\Delta t \tag{3.7}$$

The integration time step (Δt) is computed from the requirement that the advection distance per time step is less than the grid spacing and can therefore change during the simulation (Draxler & Hess, 2004). The maximum transport speed of a puff or particle during the previous hour determines the maximum transport velocity. This model has been used for trajectory analysis in a number of studies (e.g. Petterssen (1940), Draxler (1996), Jaars *et al.* (2014) and Laban *et al.* (2018)).

In this study, version 4.8 of the HYSPLIT model developed by the National Oceanic and Atmospheric Administration (NOAA) Air Resources Laboratory (ARL) (Draxler & Hess, 2004) was used to calculate 96-hour back trajectories arriving hourly at a height of 100 m at each of the South African DEBITS sites considered in this study (AF, LT, SK and CPT GAW). The necessary meteorological data for the HYSPLIT model were obtained from the GDAS archive of the National Centre for Environmental Prediction (NCEP) of the United States National Weather Service. An arrival height of 100 m was chosen, since the orography of HYSPLIT is not well defined for lower arrival heights (Lourens *et al.*, 2011). Back trajectories were overlaid to compile frequency maps by using fit-for-purpose programming software with a colour code indicating the percentage of trajectories passing over 0.2°×0.2° grid cells. As indicated above, back trajectories were also used to quantify air masses passing over the defined source region prior to their arrival at AF, LT and SK, which was included as a factor in the MLR model.

CHAPTER 4

TWENTY-ONE YEARS OF PASSIVE SAMPLING MONITORING OF SO_2, NO_2 AND O_3 AT THE CAPE POINT GAW STATION, SOUTH AFRICA

4.1 Author list, contributions and consent

J.-S. Swartz[1], P. G. Van Zyl[1*], J. P. Beukes[1], C. Labuschagne[2], E.-G. Brunke[1], T. Portafaix[3], C. Galy-Lacaux[4], J. J. Pienaar[1]

[1] Unit for Environmental Sciences and Management, North-West University, Potchefstroom Campus, Potchefstroom, 2520, South Africa

[2] South African Weather Service c/o CSIR, PO Box 320, Stellenbosch, 7599, South Africa

[3] Laboratoire de l'Atmosphére et des Cyclones, UMR CNRS 8105, Universíe de La Ŕeunion, Reunion Island, France

[4] Laboratoire d'Aerologie, UMR 5560, Universit´e Paul-Sabatier (UPS) and CNRS, Toulouse, France

The majority of the work was conducted by the first author, **J.-S. Swartz,** who was responsible for passive sampler preparation, analysis, data processing, interpretation and writing the manuscript. Co-author contributions were as follows: P.G. Van Zyl and J.P. Beukes were the promoters of the study, who assisted in data interpretation and manuscript text editing.

C. Labuschagne and E.-G. Brunke assisted with sample collection and data interpretation.

T. Portafaix contributed to the development of the multiple linear regression model.

C. Galy-Lacaux and J.J. Pienaar made conceptual contributions.

All the co-authors on the article have been informed that the PhD will be submitted in article format and have given their consent.

4.2 Formatting and current status of article

The article was formatted in accordance with the journal specifications to which it was submitted, i.e. *Atmospheric Environment*. The article is presented in the style, format and length prescribed by the journal. The guide for authors that was followed in preparation of the article is available at https://www.elsevier.com/journals/atmospheric-environment/1352-2310/guide-for-authors (Date of access: 29 January 2019). The article was ***submitted*** on 6 December 2018 and ***went into the review process*** on 27 December 2018. As it stands, the article is still under review (https://ees.elsevier.com/atmenv/default.asp).

Twenty-one years of passive sampling monitoring of SO_2, NO_2 and O_3 at the Cape Point GAW station, South Africa

J.-S. Swartz[1], P. G. Van Zyl[1*], J. P. Beukes[1], C. Labuschagne[2], E.-G. Brunke[1], T. Portafaix[3], C. Galy-Lacaux[4], J. J. Pienaar[1]

[1] Unit for Environmental Sciences and Management, North-West University, Potchefstroom Campus, Potchefstroom 2520, South Africa

[2] South African Weather Service c/o CSIR, P.O. Box 320, Stellenbosch 7599, South Africa

[3] Laboratoire de l'Atmosphére et des Cyclones, UMR CNRS 8105, Universiťe de La Ŕeunion, Reunion Island, France

[4] Laboratoire d'Aerologie, UMR 5560, Universit´e Paul-Sabatier (UPS) and CNRS, Toulouse, France

*Corresponding author: P.G. van Zyl (pieter.vanzyl@nwu.ac.za); Postal address: Private Bag X6001, South Africa, Potchefstroom, 2520; Tel: +27 18 299 2395; Fax: +27 18 299 2350

Abstract

Sulphur dioxide (SO_2), nitrogen dioxide (NO_2) and ozone (O_3) are considered typical inorganic gaseous pollutants in the atmosphere. This study assesses long-term seasonal and inter-annual trends of a 21-year SO_2, NO_2 and O_3 passive sampling (monthly means) dataset collected at the Cape Point Global Atmosphere Watch (CPT GAW) station. Comparison of the concentrations of these gaseous species with other IGAC DEBITS Africa measurement sites indicated that levels of these species were generally similar to other African inland ecosystems, but lower compared to an industrial site in southern Africa. The SO_2, NO_2 and O_3 monthly mean concentrations showed seasonal patterns, which can be attributed to various factors influencing levels of these species at CPT GAW. These factors are generally season specific, which include changes in meteorological conditions and source contributions. Higher NO_2 concentrations were also attributed to increased microbial activity in the wet season. The O_3 seasonal pattern corresponded to the NO_2 seasonality, which was attributed to their related chemistry. SO_2 and NO_2 concentrations displayed inter-annual variability, while O_3 did not indicate significant inter-annual fluctuations. The seasonal and inter-annual variability was explored with a multilinear regression model, in which global, regional and local meteorological factors, as well as population growth were included. Modelling results indicated that variances in SO_2 concentrations were predominantly influenced by changes in global forcing factors. Global, regional and local factors played a significant role in NO_2 trends, which

included the influence of population growth and associated increased anthropogenic activities. It was also established that variances in O_3 concentrations were predominantly associated with regional and local factors. Trend analysis indicated that SO_2, NO_2 and O_3 concentrations remained relatively constant over the 21-year sampling period at this background site in the Southern Hemisphere.

Keywords: low-cost sensor, INDAAF, DEBITS, inorganic gaseous species, multiple linear regression, long-term trend

1. Introduction

In recent history, it has become apparent that the atmospheric chemical composition is being altered over a range of scales by means of increased anthropogenic activity (Monks and Leigh, 2009). It is, therefore, necessary to study the spatial and temporal evolution of the chemical composition of the atmosphere in order to evaluate the extent of anthropogenic and natural influences on the atmosphere. Atmospheric chemical species include inorganic trace gases emitted naturally and anthropogenically into the troposphere, which are subjected to various physical and chemical transformations (Seinfeld and Pandis, 2006). Atmospheric trace gases can be transported over long distances before being either deposited directly on to the earth's surface through dry deposition processes or dissolved into airborne moisture and subsequently deposited during precipitation events.

Sulphur dioxide (SO_2), nitrogen dioxide (NO_2) and ozone (O_3) are considered to be typical pollutant atmospheric inorganic gaseous species. Atmospheric SO_2 is usually associated with anthropogenic activities, which generally include the combustion of fossil fuels (Connell, 2005) and pyrometallurgical production processes (Venter et al., 2012; Van Zyl et al., 2014). Nitrogen oxide (NO) is emitted from natural, e.g. lightning and microbial, activity in soils, as well as anthropogenic sources, e.g. fossil fuel combustion, which is rapidly oxidised to NO_2 (Connell, 2005). Tropospheric O_3 is a secondary pollutant formed through the photochemical oxidation of NO_2 in the presence of VOCs and CO (Laban et al., 2018). These species are mainly associated with general air quality, which includes detrimental influences on human health and disturbances of the natural equilibrium of ecosystems. Tropospheric O_3 is also considered to be an important greenhouse gas. In addition to the influence of natural and anthropogenic sources on the atmospheric concentrations of SO_2, NO_2 and O_3, local, regional and global meteorological patterns also influence the atmospheric concentrations of these species.

Comprehensive assessments on air quality (Monks and Leigh, 2009) and atmosphere-biosphere interactions (Fowler et al., 2009; Laban et al., 2018) indicated the importance of long-term atmospheric chemistry measurements. The Deposition of Biogeochemically Important Trace Species (DEBITS) task of the International Global Atmospheric Chemistry (IGAC) programme was initiated in 1990 in collaboration with the Global Atmosphere Watch (GAW) network of the World Meteorological Organisation (WMO) to investigate long-term concentrations and deposition (wet and dry) of atmospheric biogeochemical species (mainly

C, N and S species) for regions in the tropics for which limited long-term datasets exist (Lacaux et al., 2003). The African component of this initiative is known as IGAC DEBITS Africa (IDAF) and consists of ten strategically positioned deposition sites in southern and western Africa that are representative of important African ecosystems (IDAF, 2011). Four of the South African IDAF sites are situated in the north-eastern interior of South Africa, i.e. Louis Trichardt, Amersfoort, Skukuza and the Vaal Triangle, as indicated in Fig. 1. These sites are considered to represent semi-arid and savanna ecosystems. In addition, the coastal Cape Point (CPT) Global Atmosphere Watch (GAW) station, located on the most south-western tip of South Africa (Fig. 1), was also included in the IDAF network in 1995. GAW is a global atmospheric observation network with the main aim to monitor long-term trends in the chemical composition and selected physical parameters of the atmosphere (GAWSIS; Brunke et al., 2004). CPT GAW is a southern-hemispherical background station that is mainly influenced by the maritime sector, but also occasionally by the urban-continental sector. Although the primary objective of CPT GAW is the monitoring of greenhouse gases, various other atmospheric measurements are conducted at the site. This study assesses monthly mean long-term seasonal and inter-annual trends of SO_2, NO_2 and O_3 measured using passive samplers at the CPT GAW atmospheric monitoring station, as well as to determine possible sources of these species based on a 21-year dataset. In addition, the influence of local, regional and global meteorological patterns on the concentrations of these species was also investigated.

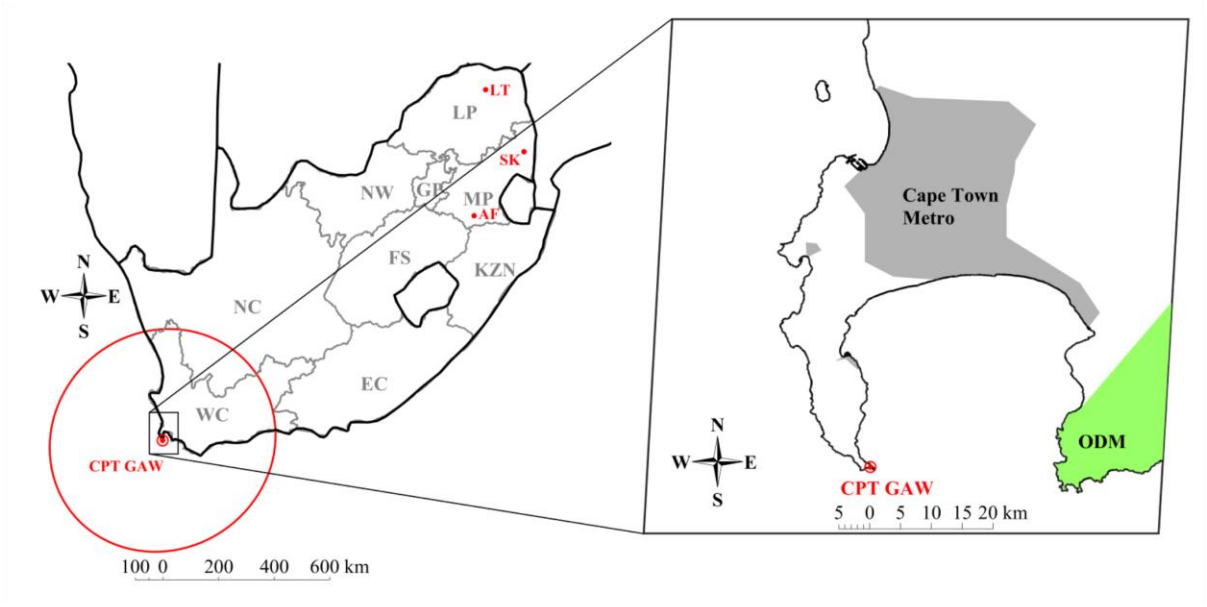

(a)

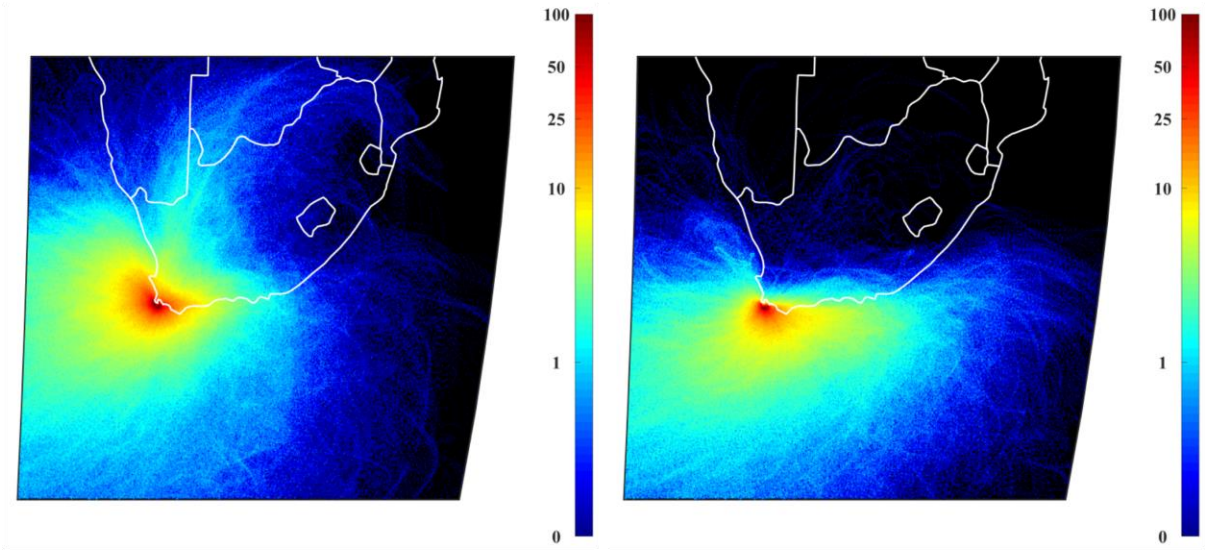

(b) (c)

Figure 1: (a) Regional map of South Africa indicating the location of CPT GAW and other South African IDAF measurement sites, i.e. Amersfoort (AF), Louis Trichardt (LT) and Skukuza (SK), and a zoomed-in map of CPT GAW indicating the Cape Town conurbation (grey area) and the Overberg District Municipality (ODM – green area). The red circle indicates the 400 km radius surrounding CPT GAW. (b) Overlaid hourly-arriving 96-hour back trajectories for air masses arriving at CPT GAW during the wet season (April to September) and (c) the dry season (October to March) for the period 1995 to 2015 with the colour scale indicating the percentage of air masses passing over 0.2° × 0.2° grid cells

2. Measurement site and experimental methods

2.1 Site description

Detailed site descriptions have been presented by Brunke et al. (2010) and Labuschagne et al. (2018). In short, the CPT GAW station (34°21'S, 18°29'E) is perched atop a cliff approximately 230 m above sea-level at the southernmost tip of the peninsula (Fig. 1), resulting in a 300° ocean view (Brunke et al., 2004). The nearby terrain at the CPT GAW station is predominantly rocky and sparsely vegetated. The site is located within the Cape Floral Region Protected Areas (CFRPA), which has been considered a UNESCO world heritage site since 2004. This region forms part of the Fynbos biome and therefore the local vegetation at CPT GAW is dominated by *Fynbos* – a fine-leaved, sclerophyllic shrub that is well adapted to a Mediterranean climate (UNESCO, 2015). Although the site is considered to be a Southern Hemispherical marine background site, predominantly impacted by marine air masses, it is also occasionally impacted by air masses passing over the Cape Town metropole that is located approximately 60 km north of the site (Fig. 1). In addition, the occurrence of biomass burning in the southern parts of Western Cape (mainly the Overberg region) can also have an influence on air masses passing over CPT GAW (Fig. 1).

2.2 Meteorology

The local and regional climate in the Western Cape is characterised by moderate temperatures with a distinct wet season occurring from April to September and a dry season from October to March, i.e. a wet winter and a dry summer season (Slemr et al., 2013), which is the exact opposite of dry winters and wet summers experienced in the interior of South Africa (Jaars et al., 2014). In Fig. 2, the average monthly rainfall for the period January 2004 to December 2013 is presented, which clearly indicates the prominent wet and dry seasons in this region. The dry summers in the Western Cape are also characterised by the occurrence of occasional biomass burning events in the surrounding areas. Rain events during winter are mainly associated with cold fronts moving over the region from the south-west. The CPT GAW station experiences predominantly east-south-easterly to south-easterly winds throughout the year (Botha et al., 2018), as indicated by the wind roses compiled for the wet (April to September) and dry (October to March) seasons from 1995 to 2015 in Fig. 2. In addition, the hourly 96-hour overlay back trajectories compiled for the wet and dry seasons for entire sampling period

(Fig. 1) also indicate that the site is predominantly impacted by air masses passing over the marine background (See Section 2.5). However, the wind roses and back trajectories indicate that CPT GAW is also occasionally impacted by air masses passing over the Cape Town metropole, while the intermittent long-range transport of air masses passing over the industrialised and densely populated northern interior of South Africa is also evident, especially during the wet season. During the dry season, CPT GAW experiences predominantly east-south-easterly to south-easterly winds, which comprise mainly marine air masses influencing CPT GAW. However, during the wet winter season, the frequency of winds originating from the north-north-western to western sector increases, which results in the CPT GAW station being impacted more frequently by air masses passing over the Cape Town conurbation. The overlay back-trajectories also indicate higher frequency of air masses passing over the Cape Town conurbation and South African interior during the winter months.

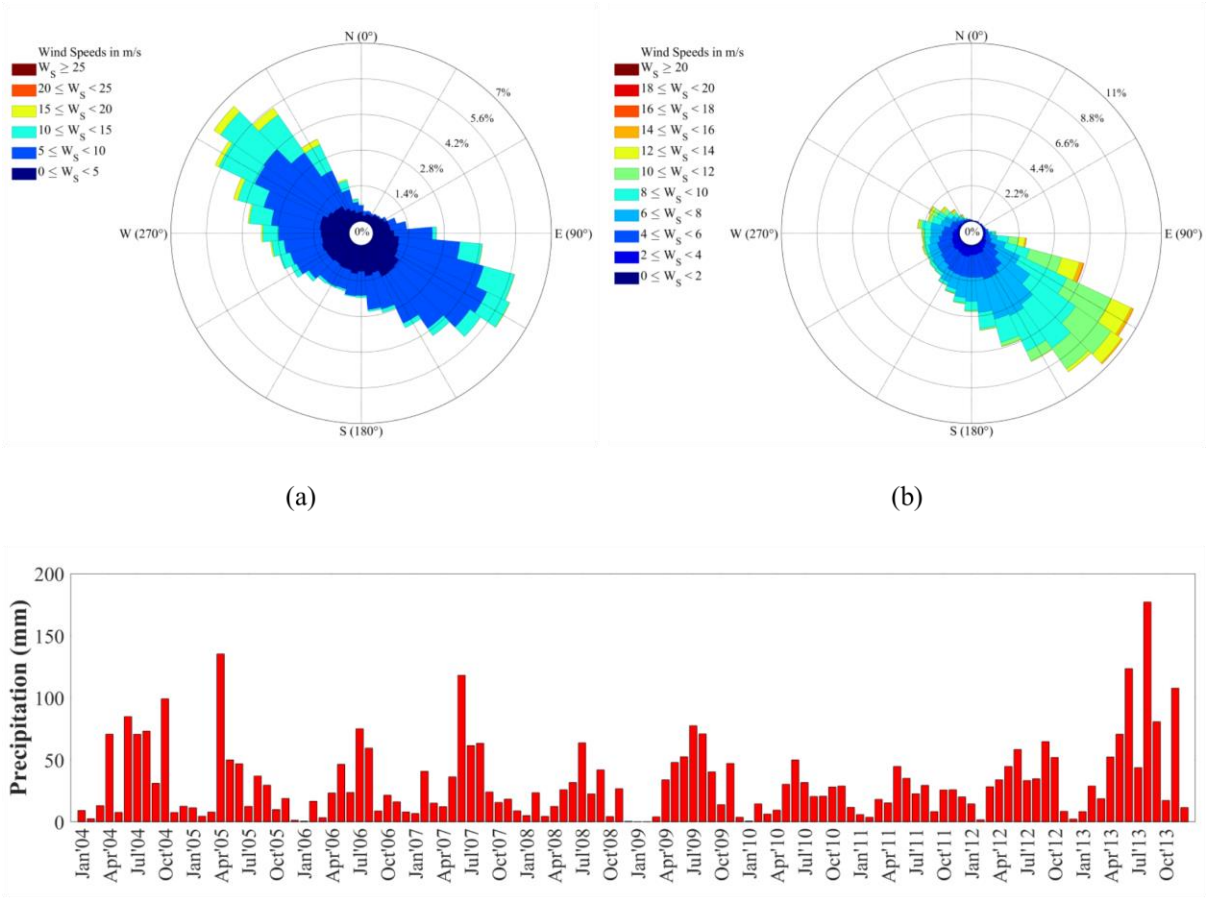

Figure 2: (a) Wind direction frequencies during the wet (April to September) and (b) dry seasons (October to March) from 1995 to 2015, as well as (c) monthly precipitation for the period 2004-2013 at CPT GAW

The global climatic factors considered in this study to possibly influence levels of atmospheric inorganic gaseous species measured at CPT included Total Solar Irradiance (TSI), El-Niño Southern Oscillation (ENSO), the Indian Ocean Dipole (IOD), Quasi-Biennial Oscillation (QBO) and the Southern Annular Mode (SAM). TSI is the main source of energy input into the energy budget of the earth, with even small variations resulting in possible natural forcing with various regional and global responses (IPCC, 2007). ENSO denotes the oscillating sea surface temperatures (SST) observed between the west coast of South America and the International Date Line (Stenseth et al., 2003). Analogous to ENSO, IOD refers to SST differential fluctuations in the tropical western and eastern Indian Ocean, which are strongly connected to various surface wind phenomena in the central area of the Indian Ocean (Saji and Yamagata, 2003; ABM, 2016). QBO depicts the alternating bands of easterly and westerly

winds more than 30 km above the surface of the earth moving downwards through the stratosphere at a rate of approximately 1 km per month (Baldwin et al., 2001). The zonally symmetrical annular atmospheric circulation structure observed around Antarctica is referred to as SAM. It is characterised by westerly winds that alternately strengthen and weaken in conjunction with fluctuating pressure bands between the mid- to high latitudes of the Southern Hemisphere (Ho et al., 2012).

2.3 Sampling and analysis

2.3.1 Sampling procedure

Monthly average atmospheric SO_2, NO_2 and O_3 concentrations were measured with passive samplers for a period of 21 years from January 1995 to December 2015 at CPT GAW. Passive samplers were developed within the framework of the IDAF project at the North-West University and are based on the passive samplers developed by Ferm (1991). The theory, functioning and development of these passive samplers have been described in detail in literature (Ferm, 1991; Dhammapala, 1996; Martins et al., 2007; Adon et al., 2010). Briefly, the functioning of the passive samplers is based on laminar diffusion and chemical reaction. The rates at which gases in ambient air diffuse into the sampler are controlled by the diffusion coefficients of the respective gases. Each passive sampler is loaded with an absorbent capable of reacting specifically with the pollutant of interest. The average concentration of the gaseous species measured during a sampling period is calculated using Fick's first law of diffusion.

Passive samplers were prepared at the North-West University and sealed-off in containers prior to sending the samplers to CPT GAW. The samplers were placed 1.5 m above ground level, in specially manufactured holders to limit natural interferences. Samplers were exposed in duplicate in order to ensure reproducibility and accuracy, as well as to reduce data loss. The diffusive samplers were exposed for one month, after which the exposed samplers were collected, sealed-off in containers, sent back to the laboratory and stored in a fridge prior to analysis.

O_3 levels measured with passive samplers were also compared to active *in situ* O_3 measurements at CPT GAW, which were conducted concurrently during the sampling period with a Thermo Environmental Instruments (TEI 49C) instrument (Oltmans et al., 2013).

2.3.2 Analysis

Collected samples were extracted from paper filters with ultrapure (Milli-Q) water in an ultrasonic bath for 30 minutes. Prior to 2008, SO_2 and O_3 samples were analysed with a Dionex 100 Ion Chromatograph (IC), while NO_2 samples were analysed with a Cary 50 uv/vis spectrometer up until 2012. SO_2 and O_3 samples collected after 2008, and NO_2 samples collected after 2012 were analysed with a Dionex ICS-3000 system. The Dionex ICS-3000 is a significantly improved IC system with the state-of-the-art eluent generator enabling the analysis of NO_2 samples within a reasonable retention time. Standard solutions of ionic species were utilised to perform five-point calibrations.

2.3.3 Quality assurance and quality control

The passive samplers developed by the North-West University and used in this study have been verified through participation in various inter-comparison studies, which is a prerequisite for passive samplers used in the DEBITS programme. Martins et al. (2007) reported various inter-comparison studies performed since the development of the passive samplers in 1994 up until 2003. The most recent evaluation of passive samplers used in this study was an international inter-comparison study that was arranged by the National University of Singapore in 2008. In this evaluation, the precision and accuracy of passive samplers used for the monitoring of SO_2 and NO_2 by various institutions were determined. The final report indicated that the passive samplers used by the North-West University compared very well with active samplers and, in most instances, had better accuracy than similar samplers used by other institutions (He and Bala, 2008). Furthermore, the analytical laboratory participates in the World Meteorological Organisation (WMO) bi-annual Laboratory Inter-Comparison Study (LIS). Conradie et al. (2016) presented the results of the 50th LIS study conducted in 2014, which indicated that the recovery of each ion in standard samples was between 95 and 105%.

For each set of samplers, blank samples were kept sealed in the containers. Detection limits for each of the species were calculated from several laboratory blank samples, which were based on the method specified by the WMO in the bi-annual GAW laboratory inter-comparison study (LIS). The detection limits calculated for each species were: 0.16 ppm for SO_2; 0.03 ppm for NO_2; and 0.02 ppm for O_3. Only data above detection limits are reported. The dataset was also

further refined by applying the Q-test with a 95% confidence threshold in order to reject possible outliers.

2.4 Meteorological data, fire frequencies and back trajectory analysis

Local meteorological data for Cape Point, which include temperature, wind direction and -speed, rain depth and relative humidity were obtained from the South African Weather Services (SAWS). In addition, planetary boundary layer heights were obtained using a global weather forecast model operated by the European Centre for Medium-range Weather Forecasts (ECMWF), as was done by Korhonen et al. (2014). ENSO and QBO data were obtained from the National Oceanic and Atmospheric Administration (NOAA) (NOAA, 2015a; NOAA, 2015b; Conradie et al., 2016). SAM data was obtained from the National Environmental Research Council's British Antarctic Survey (Marshall, 2018). TSI and IOD data was obtained from Koninklijk Nederlands Meteorologisch Instituut (KMNI, 2016a; KMNI, 2016b).

Daily fire distribution data for the period 2000 to 2016 was derived from the National Aeronautics and Space Administration's (NASA) Moderate Resolution Imaging Spectrometer (MODIS) satellite retrievals. MODIS is mounted on the polar-orbiting Earth Observation System's (EOS) Terra spacecraft and globally measures, among others, burn scars, fire and smoke distributions. This dataset was retrieved from the NASA Distributed Active Archive Centres (DAAC) (Kaufman et al., 2003).

The Hybrid Single-Particle Langrangian Integrated Trajectory (HYSPLIT) model version 4.8 developed by the National Oceanic and Atmospheric Administration's (NOAA) Air Resource Laboratory (ARL) was used to determine 96-hour back trajectories for the air masses arriving hourly at Cape Point (Draxler and Hess, 2014). The meteorological data applied in this model was obtained from the Global Data Assimilation System (GDAS) archive of the National Centre for Environmental Prediction (NCEP) of the United States National Weather Service (USNWS). An arrival height of 100 m was chosen in order to reduce error margins associated with lower arrival heights (Venter et al., 2015). Overlay back trajectory frequency maps were compiled with programmable software. A colour code indicates the percentage of trajectories passing over 0.2° x 0.2° grid cells with red being the highest percentage of trajectories passing over a specific cell and dark blue the lowest percentage.

2.5 Multiple linear regression model

A multiple linear regression (MLR) model was utilised in this study in order to statistically evaluate the influence of local, regional and global meteorological patterns on the atmospheric concentrations of inorganic gaseous species at CPT GAW, which is similar to the Trend-Run model utilised at Reunion University for temperature or ozone trend estimates in the southern tropics (Bencherif et al., 2006; Toihir et al., 2018). The MLR approach allows the decomposition of a series of observed data (such as concentrations of SO_2, NO_2 and O_3, noted below C(t)) into different components related to the environmental (e.g. meteorological parameters) or societal factors (population density) (hereinafter referred to as 'forcings' or 'proxies'), and to estimate their importance. This technique requires an in-depth knowledge of these factors influencing the measurement, each represented by a time series comparable to the one analysed.

The following general equation describes the general decomposition performed:

$$C(t) = \sum_{k=1}^{p} a(k) \times f(t,k) + R'(t) \qquad 2$$

where f(t,k) is the forcing k function of time t, and a(k) is the amplitude calculated during the multi-linear regression for k that minimises the root mean square error (RMSE). The RMSE compares the calculated values with the measured values as follows:

$$\chi^2 = [\sum_t C(t) - \sum_k a(k) \times f(t,k)]^2 \qquad 3$$

Therefore, the MLR approach makes it possible to reconstruct the original signal (if all environmental influences have been correctly taken into account) by summing the various calculated contributions. The residual term R(t) then contains the factors that may influence the measured series, but which were not included in the MLR model, as well as the measurement noise. The quality of the model can be estimated using the sum of the residual squares. The trend was parameterised as linear: Trend (t) = $\alpha_0 + \alpha_1.t$, where t denotes the time range, α_0 is a constant, α_1 is the slope of Trend(t) line that estimates the trend over the time scale.

In order to assess the significance of each of the independent variables on the calculated C(t), the relative importance weights (RIW) approach was considered, which examines the relative contribution that each independent variable makes to the dependent variable and ranks

independent variables in order of importance (Nathans et al., 2012; Kleynhans et al., 2017). The RIW approach was applied with IBM® SPSS® Statistics Version 23, together with program syntaxes and scripts adapted from Kraha et al. (2012) and Lorenzo-Seva et al. (2010).

3. Results and discussion

Since CPT GAW is influenced by air masses from both the maritime sector (on average most of the time), as well as from the urban-continental sector, it is subjected to contrasting air-chemical regimes. Therefore, in the case of data obtained with passive samplers, the predicament is that the two datasets, i.e. background and non-background, are not separated, but intermingled to varying proportions as a function of seasonality. During the winter months, the urban-continental proportion could be as high as 60%, while during the summer months it is often as low as 20%. Therefore, the seasonality observed within the mixed dataset is primarily driven by meteorology, which complicates air-chemical interpretations (Botha et al., 2018; Labuschagne et al., 2018). Therefore, it is important to consider this limitation when interpreting composite concentrations of gaseous species determined with passive samplers at CPT GAW. However, in the absence of any continuously active SO_2 and NO_2 measurements at CPT GAW, this 21-year passive sampling dataset is utilised to meaningfully contextualise concentrations of these species, as well as elucidate seasonal patterns and inter-annual variability.

In Fig. A1 the time series of the monthly average SO_2, NO_2 and O_3 concentrations measured with passive samplers during the 21-year sampling period are presented. In subsequent sections this data series will be evaluated in terms of seasonal and inter-annual variability associated with changes in meteorology and source contributions, as well as statistically assessed with a multiple linear regression model as indicated in Section 2.5.

3.1 Contextualisation

In Fig. 3, the atmospheric gaseous concentrations measured at CPT GAW from 1995 to 2015 are compared to the averages of these species also measured with passive samplers at other South African and African IDAF sites. With the exception of Amersfoort, which is in close proximity to industrial sources, all the sites discussed by Conradie et al. (2016), Adon et al.

(2010) and Martins et al. (2007) are considered to be background sites with no local sources of pollutants. The average SO_2 concentration of 2.9 μg/m^3 measured at CPT GAW is similar to the average SO_2 level determined at background sites located in wet and dry savannahs, i.e. Agoufou (2.6 μg/m^3), Djougou (2.1 μg/m^3), Lamto (2.1 μg/m^3) and Louis Trichardt (2.1 μg/m^3). The average SO_2 concentration at CPT GAW is approximately two times lower than the SO_2 level measured at the industrially impacted Amersfoort (Conradie et al., 2016). Much lower SO_2 concentrations are measured in the two sites representative of forest ecosystem, i.e. Bomassa (1.0 μg/m^3) and Zoetele (0.8 μg/m^3), as well as Okaukuejo (1.0 μg/m^3) located in a desert. Reported SO_2 concentrations at two dry savannah sites in western African dry savannah sites (Katibougou and Banizoumbou) are ~50% of that measured at CPT GAW (≤ 1.6 μg/m^3).

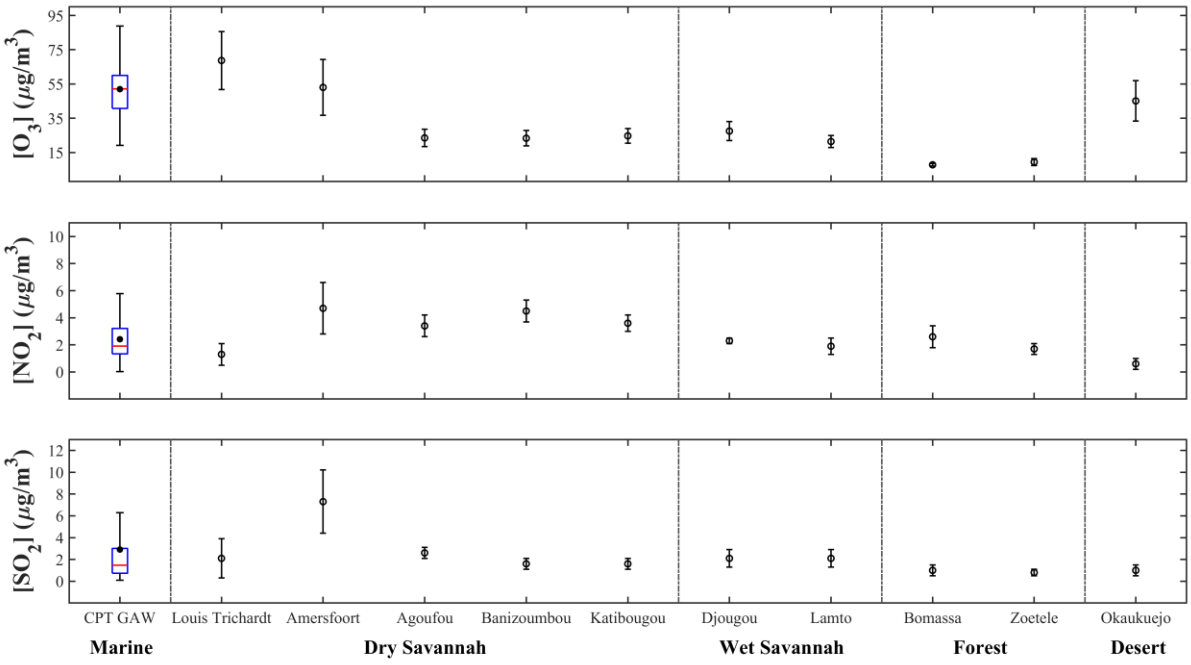

Figure 3: SO_2, NO_2 and O_3 concentrations measured with passive samplers for the entire 21-year sampling period at CPT GAW compared to average SO_2, NO_2 and O_3 concentrations (plotted with standard deviations) determined with passive samplers at other IDAF sites in South, West and Central Africa. †(Martins et al., 2007); ‡(Adon et al., 2010). The red line of each box for CPT GAW represents the median, the top and bottom edges of the box the 25th and 75th percentiles, respectively, the whiskers ±2.7σ (99.3% coverage if the data has a normal distribution) and the black dots the averages

The average NO_2 concentration of 2.4 $\mu g/m^3$ measured at CPT GAW is close to the mean NO_2 levels determined in the wet savannahs at Djougou (2.3 $\mu g/m^3$) and Lamto (1.9 $\mu g/m^3$), as well as in the forest at Bomassa (2.6 $\mu g/m^3$). The average NO_2 concentrations at the anthropogenically impacted Amersfoort (Conradie et al., 2016, Martins et al., 2007) in South Africa, i.e. 4.7 $\mu g/m^3$, are approximately two times higher compared to NO_2 measured at CPT GAW, while the average NO_2 concentration at the South African inland regional background site Louis Trichardt (1.3 $\mu g/m^3$) is approximately two times lower than CPT GAW NO_2 levels. Mean NO_2 levels measured for the dry savannahs in western Africa, i.e. Agoufou (3.4 $\mu g/m^3$), Katibougou (3.6 $\mu g/m^3$) and Banizoumbou (4.5 $\mu g/m^3$) were higher than NO_2 measured at CPT GAW, which were similar to NO_2 concentrations measured at Amersfoort and mainly attributed to the impacts of biomass burning in this region (Adon et al., 2010). Much lower average NO_2 concentrations are observed for the arid Okaukuejo site (0.6 $\mu g/m^3$), which can be attributed to low microbial activity (Ludwig et al., 2001; Hénault et al., 2005; Adon et al., 2010) and no nearby anthropogenic sources.

The average O_3 concentrations measured with passive samplers at CPT GAW (52.0 $\mu g/m^3$) for the 21-year dataset were similar to the average O_3 levels determined from relatively long-term (~10 years) passive sampling datasets at the southern African sites Amersfoort (53.0 $\mu g/m^3$) and Okaukuejo (45.1 $\mu g/m^3$), but lower than the average O_3 concentration at Louis Trichardt (68.7 $\mu g/m^3$) from 1995 to 2005. The passive sampling-derived average O_3 concentration were also similar to the average of active *in situ* O_3 measurements conducted at CPT GAW during the 21-year passive sampling period, i.e. 49.3 $\mu g/m^3$. These average O_3 levels measured at the southern African sites are approximately two times higher than the mean O_3 concentrations measured for dry savannahs at Agoufou (23.5 $\mu g/m^3$), Katibougou (24.7 $\mu g/m^3$) and Banizoumbou (23.3 $\mu g/m^3$), as well as for wet savannahs at Djougou (27.5 $\mu g/m^3$) and Lamto (21.4 $\mu g/m^3$) in western Africa. Much lower average O_3 concentrations were measured for forest ecosystems at Bomassa (7.8 $\mu g/m^3$) and Zoetele (9.4 $\mu g/m^3$) in central Africa. The relatively high O_3 concentrations measured at CPT GAW also reflect the regional O_3 problem in southern Africa (Laban et al., 2018). O_3 concentrations in southern Africa can be attributed to a combination of regional impacts, which include industrial, vehicular, and domestic- and open biomass burning emissions that are often re-circulated through anti-cyclonic air mass processes (Laban et al., 2018). The higher O_3 concentration measured at Louis Trichardt can be ascribed to the additional influence of trans-boundary impacts from biomass burning events in sub-Saharan Africa, especially Mozambique, Zambia, Zimbabwe

and Angola (Tiitta et al., 2014), as well as biomass burning occurring over the central African region (e.g. Democratic Republic of Congo) (Swapt et al., 2003).

3.2 Seasonal patterns

In Fig. 4, the monthly concentrations for each of the gaseous species measured for the entire sampling period are presented. A few instances are observed where the average monthly concentrations were similar to or exceeded the 75th percentiles. These occurrences were attributed to monthly concentrations for specific years being significantly higher, which were not identified as outliers by the Q-test (Fig. A1). SO_2 did not reveal a clear seasonal pattern, although higher SO_2 concentrations were observed during two periods in the year, i.e. January to February, and July to August. More distinct seasonal patterns were observed for NO_2 and O_3. Higher NO_2 levels occurred from April to August with NO_2 concentrations peaking between May and August, while O_3 had higher concentrations between July and October. The seasonal NO_2 and O_3 patterns is also reflected in the time series, while the less distinct trend in monthly SO_2 concentrations is also evident for the 21-year time series (Fig. A1). It is also apparent from the time series that significantly higher SO_2 concentrations measured in 2009 and 2011 (especially in 2009) contributed to box-and-whisker plots of monthly SO_2 concentration having a larger range in July, as well as contributed to monthly average SO_2 levels exceeding the 75th percentiles in January and February (Fig. 4(a)). Significantly higher SO_2 concentrations were also measured in January 2008 and February 2003. Comparison of the passively derived O_3 concentrations with *in-situ* measurements revealed a similar seasonal pattern with relatively good agreement between monthly mean and median values for the 21-year sampling period. In Fig. A2, the time series of the O_3 concentrations determined with passive samplers and *in-situ* measurements are presented, which also indicate good correlations between the two measurement techniques. In addition, a correlation plot between passively derived O_3 concentrations and *in-situ* measurements indicate a very good correlation (0.89) between these two measurement techniques as indicated in Fig. A3. Differences between passive-derived O_3 concentrations and *in-situ* measurements can be attributed to the functioning of the passive O_3 sampler in which O_3 is indirectly measured through the oxidation of NO_2^- to NO_3^- by O_3. Other atmospheric oxidants could contribute to higher O_3 concentrations determined with passive samplers. In addition, fluctuations in relative humidity can also contribute to variability in O_3 levels measured with passive samplers, since the oxidation of

NO_2^- to NO_3^- is enhanced by the presence of water molecules. Lower concentrations measured with passive samplers are usually attributed to decreased diffusion of the pollutant mainly associated with higher wind speeds, while lower relative humidity could also contribute to less effective reaction with NO_2^-. In an effort to explain the observed seasonal patterns for SO_2, NO_2 and O_3, seasonal changes in meteorological conditions, source contributions and ecological process were considered.

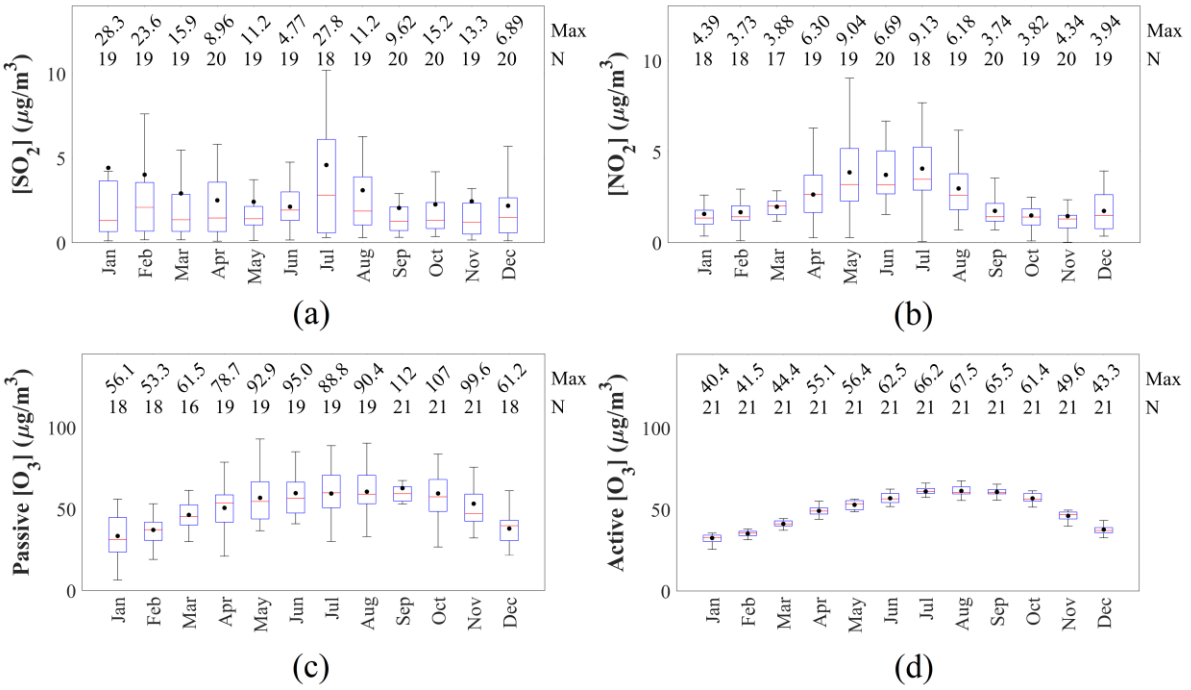

Figure 4: Monthly SO_2 (a), NO_2 (b) and O_3 (c) concentrations measured with passive samplers, as well as monthly averaged *in situ* measured O_3 concentrations (d) for the 21-year sampling period at CPT GAW. The red line of each box represents the median, the top and bottom edges of the box the 25th and 75th percentiles, respectively, the whiskers ±2.7σ (99.3% coverage if the data has a normal distribution) and the black dots the averages. The maximum concentrations and the number of measurements (N) are presented at the top

As indicated in Section 2.2, overlaid back trajectories (Fig. 1) and wind roses (Fig. 2) compiled for the wet and dry seasons revealed that inorganic gas concentrations measured during the dry season generally represent Southern Hemispheric background levels CPT GAW, while the higher frequency of air masses passing over the Cape Town conurbation and South African interior during the wet winter months is evident. Botha et al. (2018) also attributed higher radon

concentrations at CPT GAW (based on 15-year radon measurements) in winter months to an increase in frequency of air masses passing over the continental surface, compared to summer when CPT GAW is more frequently impacted by oceanic air masses. In addition, the monthly carbon monoxide (CO) concentrations at CPT GAW were also indicative of the increased anthropogenic influences from the continent during winter as indicated by higher CO levels measured during winter (Fig. A4). Therefore, the higher SO_2 concentrations observed in July and August, as well as the higher NO_2 levels occurring from April to August, can be partially attributed to an increase in frequency of air masses moving over Cape Town to CPT GAW. Typical sources of SO_2 and NO_2 in the Cape Town conurbation include industrial activities, vehicular emissions, as well as household combustion for cooking and space heating (Ojumu, 2013). In addition, household combustion for space heating will increase during the colder winter months, while more pronounced inversion layers during winter will trap pollutant species near the surface that will lead to higher concentrations of pollutant species in the Cape Town conurbation during winter influencing CPT GAW. Cape Town is also characterised by the occurrence of brown haze events during winter, which is attributed to the build-up of pollutant concentrations within strong inversion layers (Wicking-Baird et al., 1997). The wet season overlay back trajectories also indicate the possible influence of the long-range transport of atmospheric pollutants from the industrialised Highveld in the north-eastern interior of South Africa (Ojumu, 2013; Abiodun et al., 2014). However, it is difficult to quantify the influence of up-country circulation on CPT GAW measurements due to these air masses being obscured by the Cape Town conurbation signal (especially for monthly averages determined with passive samplers), as well as atmospheric residence times of NO_2 and SO_2.

The initial seasonal increase in NO_2 concentrations at CPT GAW also coincides with the onset of the wet season in April. This indicates that NO_2 levels can partially be associated with the emissions of biogenic nitrogen (N) accumulated in the soil (Adon et al., 2010). CPT GAW is situated in a nature reserve where N species from, e.g. guano from the sea birds, can accumulate in the soil during the dry season. After the first rain event occurs, bacterial nitrification is activated, which leads to N consumption that causes the release of large pulses of NO (Ludwig et al., 2001; Hénault et al., 2005; Adon et al., 2010) that is rapidly oxidised to NO_2. In addition, since the passive samplers were deployed relatively close to the surface (1.5 m), passive sampling measurements are exposed to surface effects (soil-nitrogen chemistry), especially under calm winter conditions. Therefore, microbial activity could also contribute to the observed increased NO_2 concentrations at CPT GAW during the wet winter season.

As mentioned, O_3 exhibited a seasonal trend similar to NO_2, with O_3 concentrations also gradually increasing from April. Since atmospheric O_3 is a secondary pollutant formed through the photochemical oxidation of NO_2, O_3 production can be driven by increased NO_2 emissions into the atmosphere. However, O_3 production has a complex and non-linear dependence on precursor emissions, which also include volatile organic compounds (VOCs) and CO (e.g. NRC (1991)). The monthly CO concentrations determined with *in-situ* measurements at CPT GAW during the sampling period also displayed a similar seasonal pattern to O_3 and NO_2 (Fig. A4). O_3 production is generally classified as being either VOC- or NO_x-limited. In a NO_x-limited O_3 production regime, O_3 concentrations will increase with increasing NO_x concentrations, which is typical for background regions with low NO_x emissions (Laban et al., 2018). Therefore, the increase in O_3 concentrations coinciding with increased NO_2 concentrations can be expected at CPT GAW. Adon et al. (2010) indicated a similar observation for dry (semi-arid) savannahs in West Africa, where NO_2 and O_3 levels were also higher during the wet season, while Stewart et al. (2008) also estimated a relatively high O_3 production rate as a result of high NO_X concentrations during the AMMA experiment in the Sahel. O_3 levels remained relatively high at the end of the wet season during August and September, while NO_2 concentrations decreased. This can be attributed to reduced O_3 titration through reaction with NO_2, while August and September are also associated with increased photochemical oxidation due to longer daylight hours in spring. Although daylight hours are even longer during the summer months, O_3 concentrations remain relatively low during summer due to fewer precursor species in the atmosphere, and CPT GAW being impacted more frequently by oceanic air mass.

Biomass burning is considered to be a major source of pollutant species (e.g. NO_2 and O_3) in the interior of South Africa (Vakkari et al., 2013). Therefore, the impacts of local and regional biomass burning on the concentrations of the gaseous species measured were also investigated. In Fig. 5, the monthly average burn frequency for southern Africa from 2000 to 2016, as well as the burn frequency within a 400 km radius from the CPT GAW for the same period obtained from MODIS satellite data is presented. It is evident that the burn frequency is generally higher from June to October in South Africa, peaking in September, which is associated with the dry season in the interior of South Africa. However, limiting the burn frequency within a 400 km radius of the CPT GAW indicates higher burn frequencies coinciding with the dry season in the Western Cape. it is evident from the wind rose compiled for the dry season in Fig. 2 and the 400 km radius surrounding CP GAW indicated in Fig. 1(a) that winds arriving at the CPT

GAW during this period coincide with air masses passing over the Overberg district, which is a large area covered by natural vegetation that is susceptible to biomass burning during the dry season (Brunke et al., 2001). This area also houses two South African national parks, i.e. the Agulhas- and Bontebok National Parks. Furthermore, the continental flow of air masses indicated by overlay back trajectories (Fig. 1(b)) also reflects the possible impact of biomass burning during the dry season on CPT GAW. However, in this study, increased NO_2 and O_3 concentrations, typically associated with biomass burning in South Africa (Lourens et al., 2011; Laban et al., 2018), are not observed at CPT GAW. Higher SO_2 concentrations in January and February did, however, coincide with increased biomass burning. SO_2 emissions are not generally associated with biomass burning and are not well quantified. Although Adon et al. (2010) did consider biomass burning a source of SO_2 at western African savannah background sites, SO_2 concentrations were low, while biomass burning also coincided with increased NO_2 levels. Therefore, higher SO_2 concentrations at CPT GAW measured during January and February are more likely associated with CPT GAW being more frequently impacted by oceanic air masses and oceanic SO_2 sources, e.g. oxidation of dimethyl sulphide (DMS).

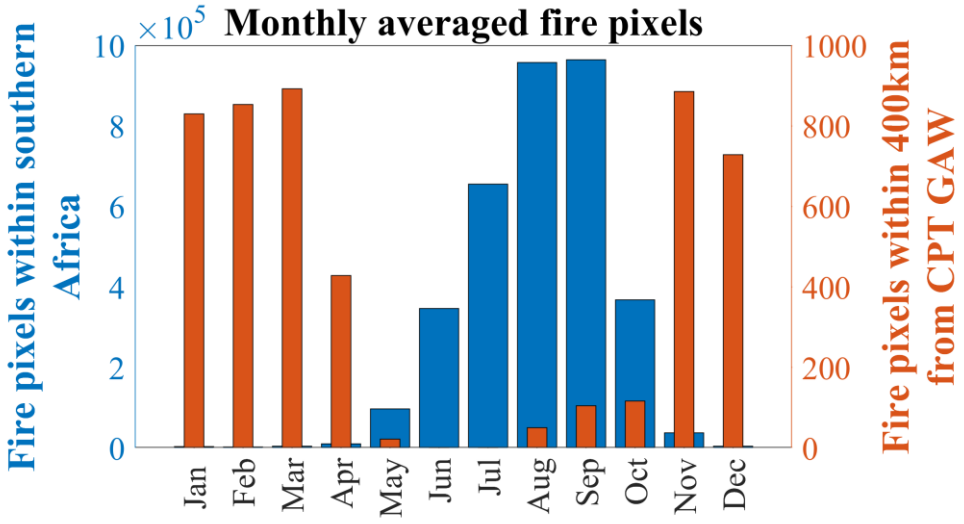

Figure 5: Average monthly fire pixels for the period 2000 to 2016 within the entire southern Africa (10 to 35˚S and 10 to 41˚E), as well as fire pixels within a radius of 400 km around CPT GAW. Data obtained from MODIS collection 5 burned area product (Roy et al., 2008) for the period 2000 to 2016

3.3 Inter-annual variability

In Fig. 6, the annual SO_2, NO_2 and O_3 for the entire sampling period are presented. Small inter-annual variability and a marginal decline are observed for SO_2 from 1995 to 2004, while from 2005 to 2009, a steady increase in average annual SO_2 concentrations is observed, with SO_2 levels reaching an annual average maximum in 2009. The annual average NO_2 concentrations declined from 1996 to 2002, after which the annual average NO_2 levels steadily increased reaching a maximum in 2011, with the exception of 2008 to 2010, during which NO_2 levels were relatively lower. Three-year moving averages of the annual average concentrations of SO_2 and NO_2 indicate a decline in concentrations of both these species from 1996 to 2002, followed by a period of gradual increases in the levels of these species after 2002. The significantly larger range of the 25^{th} and 75^{th} percentiles, as well as average of SO_2 levels measured in 2009 (Fig. 6(a)) can be attributed to substantially higher SO_2 concentrations measured in January, February and July as indicated by the time series in Fig. A1, which can be considered incidental variances in the dataset. The observed inter-annual variations in SO_2 and NO_2 concentrations can be attributed to changes in meteorological conditions and/or fluctuations in source contribution, e.g. economic growth associated with increased energy demand and a larger vehicular fleet. Conradie et al. (2016), for instance, indicated that rain samples collected from 2009 to 2014 at the IDAF sites in the north-eastern interior of South Africa had higher SO_4^{2-} and NO_3^- concentrations compared to rain samples collected in 1986 to 1999 and 1999 to 2002, which were attributed to the increase in economic growth and higher energy demand as indicated by the increase in electricity consumption in South Africa by Inglesi-Lotz and Blignaut, 2011. Furthermore, monthly SO_2 and NO_2 measurements conducted at the IDAF sites in the north-eastern interior of South Africa also indicate increases in SO_2 and NO_2 levels from 2001/2002 (Conradie et al., 2016). The inter-annual variability of SO_2 and NO_2 will be explored further in the subsequent section.

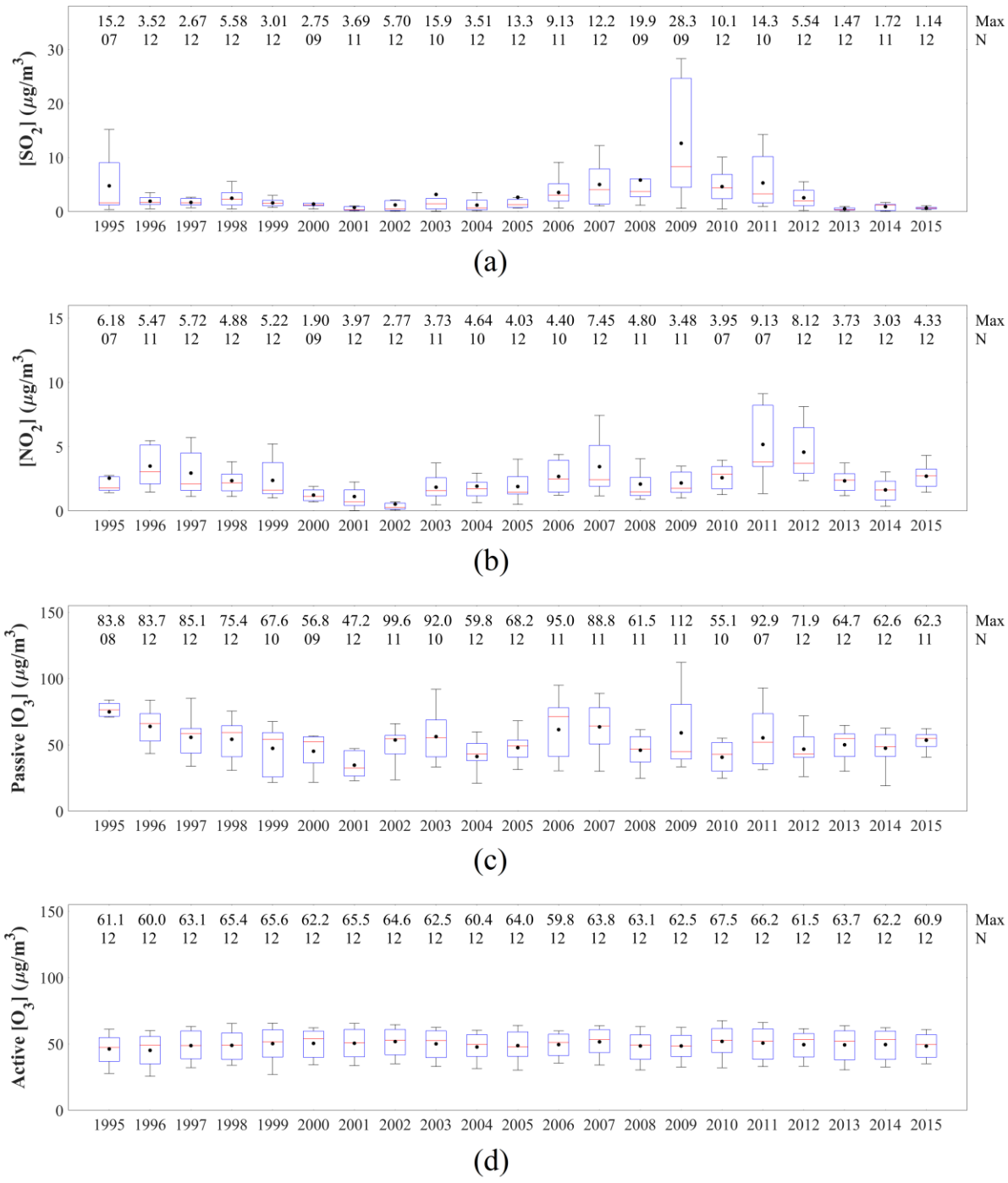

Figure 6: Annual SO_2 (a), NO_2 (b) and O_3 (c) concentrations from 1995 to 2015, as well as the annual O_3 concentrations determined with *in situ* measurements (d) at CPT GAW. The red line of each box represents the median, the top and bottom edges of the box the 25th and 75th percentiles, respectively, the whiskers ±2.7σ (99.3% coverage if the data has a normal distribution) and the black dots the averages. The maximum concentrations and the number of measurements (N) are presented at the top

Although the annual O_3 concentrations determined with passive samplers indicate inter-annual fluctuations, *in-situ* measurements of O_3 levels do not show significant inter-annual variability. As indicated in section 3.2, the functioning of the O_3 passive sampler relies on the measurement of the oxidation potential of the atmosphere (oxidation of NO_2^- to NO_3^-), which is also dependent on the presence of water. Therefore, the occurrence of other atmospheric oxidants can contribute to the higher O_3 concentrations determined with passive samplers, while lower relative humidity can result in the measurement of lower O_3 concentrations. Although Fig. A2 and A3 indicated relatively a good correlation between passive and *in situ* measurements of O_3 during the 21-year sampling period, there are instances and certain years (e.g. 1995 to 1997) for which O_3 concentrations measured with the two sampling techniques differed, which results in the observed inter-annual fluctuations determined with passive samplers. Therefore, from the *in-situ* measurements, it can be deduced that O_3 levels at CPT GAW did not reveal any significant inter-annual variability over the sampling period.

3.4 Modelled variability and linear trend estimates

In an effort to further explore the above-mentioned variability (seasonal and inter-annual) observed for SO_2, NO_2 and O_3, a MLR model was developed in order to statistically evaluate the influence of local, regional and global meteorological patterns on the atmospheric inorganic gaseous species concentrations at CPT GAW. Population data, which was obtained from three separate national censuses, was also included in the model as a proxy for increased anthropogenic activities. Local and regional factors considered in the model included wind speed (Ws), wind direction (Wd), ambient temperature (T), rain depth (R), relative humidity (RH), planetary boundary layer height (PBL), CO and carbon dioxide (CO_2) concentrations, local fire events within 100km from site (LFE), regional fire events between 100km and 400km from site (DFE), and Cape Town metropolitan population (P). Radon data from CPT GAW was used to separate oceanic- (OAM) and continental air mass (CAM) (Botha et al., 2018), which was also included in the model. Global factors considered included TSI, IOD, ENSO, QBO and SAM, as indicated in section 2.2. Although it is recognised that more factors could be considered as input parameters in the model, these global factors were considered to be the most relevant, while the local and regional parameters included were the most complete datasets that could be acquired at CPT GAW. The initial input parameters for the model only included the global force factors for the 21-year sampling period, after which local, regional

and global factors were included in the model for a 15-year period (from 2000). Since data was not available for certain local and regional factors considered in the model for the entire sampling period, and in order to include the optimum number of local and regional factors available for CPT GAW, modelled concentrations could not be calculated for the entire 21-year sampling period when global, regional and local factors were included.

The modelled SO_2, NO_2 and O_3 concentrations are related to the measured SO_2, NO_2 and O_3 levels in Fig. 7, 8 and 9, respectively through the RMSE differences between the modelled and measured concentrations ((a) and (b)), as well as by comparison between the modelled and measured data time series ((c)). In each of these figures, (a) presents the RMSE differences when only global factors are included, while (b) show the influence of the inclusion of local and regional factors in the model on RMSE differences. The RMSE differences are presented as a function of the number of independent variables included in the model with the identities of the most important independent variables also included. The time series of measured concentrations are compared to the modelled values for global factors only, as well as when local and regional factors are included in the model in (c). Also indicated in Fig. 7, 8 and 9 are linear regression trend lines for measured and modelled SO_2, NO_2 and O_3 concentrations. In Table 1, the coefficients associated with each of the independent variables in the optimum MLR equation (i.e. including all independent variables) in conjunction with their respective RIW% are presented for the model including only the global force factors, as well as the MLR equation including the global, regional and local factors for SO_2, NO_2 and O_3.

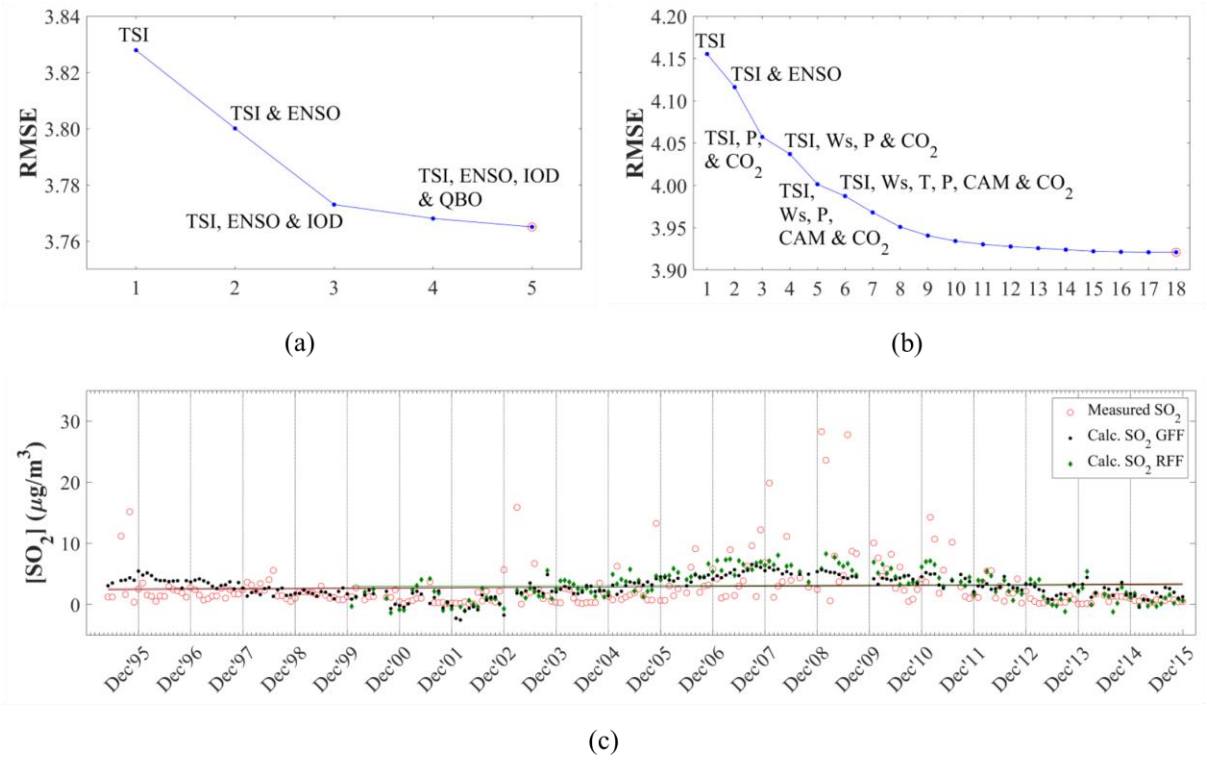

Figure 7: RMSE differences between modelled and measured SO_2 concentrations as a function of the number of independent variables included in the model for (a) global factors only, and (b) for global, regional and local factors, as well as (c) comparison between measured and modelled SO_2 levels for global factor only (black dots), and for global, regional and local factors (green dots)

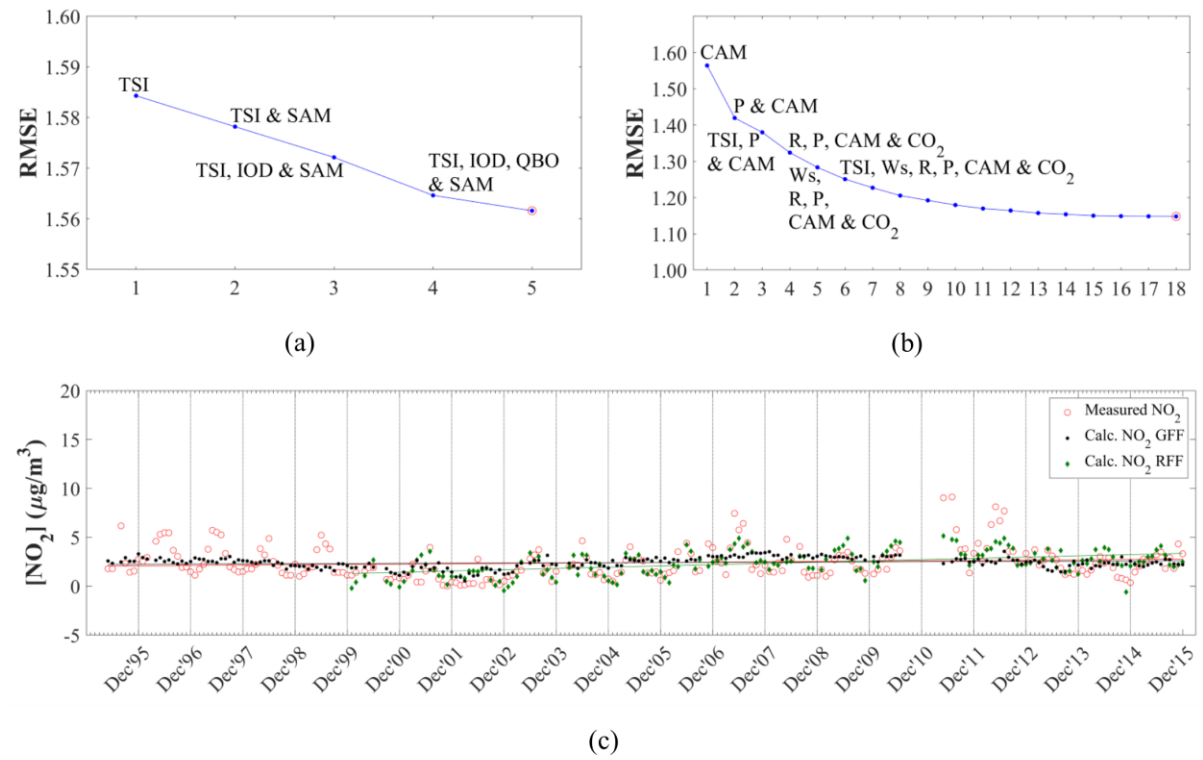

Figure 8: RMSE differences between modelled and measured NO_2 concentrations as a function of the number of independent variables included in the model for (a) global factors only, and (b) for global, regional and local factors, as well as (c) comparison between measured and modelled SO_2 levels for global factor only (black dots), and for global, regional and local factors (green dots)

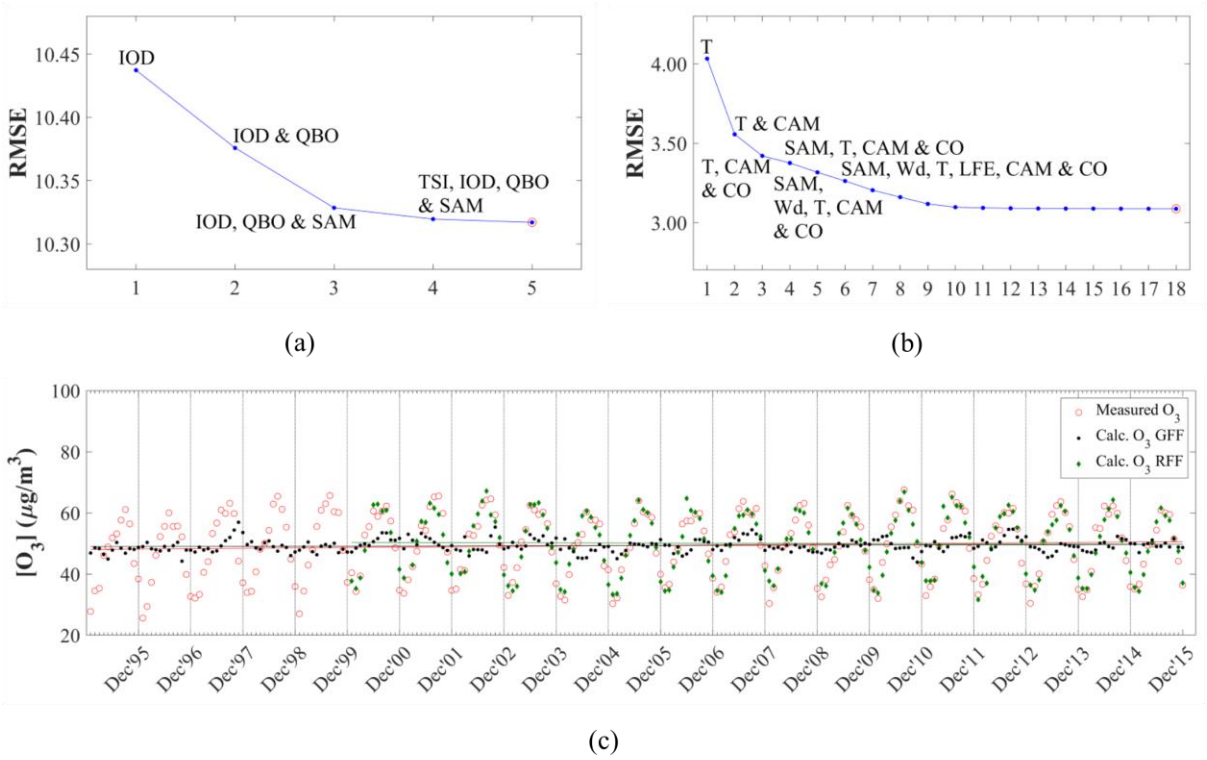

Figure 9: RMSE differences between modelled and measured O_3 concentrations as a function of the number of independent variables included in the model for (a) global factors only, and (b) for global, regional and local factors, as well as (c) comparison between measured and modelled SO_2 levels for global factor only (black dots), and for global, regional and local factors (green dots)

Table 1: Regression coefficients and relative important weight percentage (RIW%) of each independent variable included in the MLR model to calculate SO_2, NO_2 and O_3 concentrations

	SO_2			**NO_2**			**O_3**	
	b	RIW%		*b*	RIW%		*b*	RIW%
i) Global forcing factors								
TSI	-3.791	81.3	TSI	-1.167	74.2	IOD	5.237	43.7
ENSO	-0.856	9.7	IOD	0.708	11.9	SAM	-0.605	28.5
IOD	1.741	6.9	QBO	-0.011	6.2	QBO	-0.076	22.0
SAM	-0.089	1.1	SAM	0.091	6.0	TSI	1.065	2.9
QBO	-0.013	1.0	ENSO	-0.134	1.8	ENSO	-0.312	2.9
ii) Global, regional and local factors								
TSI	-4.666	60.3	CAM	0.033	12.7	T	-3.390	33.5
ENSO	-0.506	5.3	RH	0.023	12.4	CO	0.182	21.2
IOD	1.907	5.2	Ws	-0.671	11.4	CAM	0.179	10.5
T	0.537	4.3	P	1.995×10^{-5}	11.4	RH	-7.237×10^{-3}	10.2
Ws	0.762	4.2	CO_2	-0.716	10.8	LFE	-3.606×10^{-3}	5.1
OAM	-0.021	3.9	TSI	-0.520	7.8	DFE	-1.063×10^{-4}	3.0
P	3.598×10^{-5}	3.8	IOD	1.345	5.8	Wd	-0.018	2.8
CO_2	-1.427	3.8	DFE	-3.370×10^{-4}	5.7	OAM	0.071	2.5
CAM	0.048	1.9	OAM	-6.133×10^{-3}	3.4	RH	0.067	2.4
CO	0.040	1.8	QBO	-0.013	3.0	PBL	1.910×10^{-3}	2.2
Wd	5.723×10^{-3}	1.5	CO	0.017	2.8	IOD	0.476	1.4
SAM	-0.093	0.8	T	0.159	2.6	Ws	-0.072	1.3
RH	9.503×10^{-3}	0.8	ENSO	-0.303	2.3	SAM	-0.467	1.1
PBL	3.382×10^{-4}	0.8	Wd	-7.963×10^{-4}	2.3	P	2.089×10^{-5}	1.1
QBO	-4.310×10^{-3}	0.5	PBL	-7.967×10^{-4}	2.3	CO_2	-0.728	0.9
RH	-0.067	0.4	SAM	0.096	1.5	QBO	-0.012	0.5
DFE	2.533×10^{-4}	0.4	RH	-0.098	1.1	ENSO	-0.990	0.2
LFE	-4.537×10^{-4}	0.3	LFE	5.436×10^{-4}	0.7	TSI	-1.275×10^{-3}	0.1

3.4.1 Sulphur dioxide

It is evident from Fig. 7 that interdependencies between TSI, ENSO and IOD resulted in the largest decrease in RMSE when only global force factors were included for SO_2, while the interdependencies between TSI, Ws, T, P, CAM and CO_2 made the most significant contribution to decreases in RMSE difference between modelled and measured values when regional and local factors were also included The RIW% indicates that TSI made a significant contribution, i.e. 81.3%, to the dependent variable when only global force factors were

considered, while TSI contributed 60.3% of the variance when local and regional parameters were also included. In the optimum solution obtained when all factors were included, the RIW% of ENSO, IOD, T and Ws were 5.3%, 5.2%, 4.3% and 4.2%, respectively. MLR modelling indicates that variances in SO_2 concentrations at Cape Point depend mainly on global forcing factors, i.e. global transport patterns of air masses. This is also supported by Ws being the most relevant regional factor, which is indicative of general air mass flow. Therefore, the MLR model signifies that SO_2 concentrations at CPT GAW are more likely associated with oceanic sources of SO_2 (e.g. oxidation of DMS) as previously mentioned (Section 3.2), which are predominantly dependent on global meteorological patterns. The strong negative correlation with TSI could be attributed to greater oxidation capacity of the atmosphere corresponding to higher temperatures resulting in increased oxidation of oceanic SO_2. However, this correlation cannot be conclusively explained at this stage and must be further investigated. The influence from local and regional factors on SO_2 concentrations is also signified by the influence of T, P and CAM. As indicated in Section 3.2, SO_2 concentrations were slightly higher during June and July in the wet season when CPT GAW is more frequently influenced by air masses passing over the Cape Town conurbation. Therefore, the model also reflects the marginal influence of local and regional factors on seasonal variability in SO_2 levels at CPT GAW. Comparison between modelled and measured SO_2 concentration time series in Fig. 7, indicates, although relatively weak, slight correlations between modelled and measured SO_2 concentrations with an R^2 value of 0.165 when only global factors are included in the model. These correlations are marginally improved when local and regional factors are also included in the model, resulting in an R^2 value of 0.2371. Although relatively weak correlations are observed, the modelled SO_2 concentration time series mimics the general temporal trend of the measured SO_2 time series, with the exception of significantly higher SO_2 concentrations. Differences between modelled and measured values can also be attributed to the limitations of passive sampling measurements at CPT GAW, as previously mentioned.

In Fig. 7(c), it is evident that the slope of the 21-year measurement period trend line has a slight positive value reflecting a marginal increase in SO_2 concentrations over the 21-year period, i.e. 0.05 $\mu g.m^{-3}.y^{-1}$. The 21-year dataset also allowed for the calculation of decadal trends, which were determined to be 1.92 $\mu g.m^{-3}.dec^{-1}$ for the two decades (average SO_2 concentrations from 1995 to 2004 were 1.92 $\mu g.m^{-3}$ and average SO_2 concentrations from 2005 to 2014 were 3.84 $\mu g.m^{-3}$). The annual trends for the two periods identified above as being associated with decreased and increased SO_2 concentrations were calculated to be -0.41 $\mu g.m^{-3}.y^{-1}$ between

1995 and 2002, and 1.20 $\mu g.m^{-3}.y^{-1}$ from 2002 to 2009. Although the 21-year sampling period is characterised by periods with decreased and increased SO_2 levels, it can be deduced that, in general, the observed trend in SO_2 concentrations over the 21-year period remained relatively constant. Linear regression trend lines for the modelled SO_2 concentrations in Fig. 7(c) correlate with the 21-year trend line obtained for the measured SO_2 concentrations. Furthermore, the slope of the trend line for the SO_2 levels modelled with global, regional and local factors is exactly the same as the slope of the trend line for the measured SO_2 concentrations.

3.4.2 Nitrogen dioxide

It is evident from Fig. 8 that the interdependencies between most of the global force factors resulted in the largest decrease in RMSE when only global force factors were included, while RIW% listed in Table 1 indicates that, similar to modelled SO_2 values, TSI also made the most significant contribution, i.e. 74.2% to the variance of the dependent variable (Table 1). IOD made a relatively larger contribution on modelled NO_2 values, i.e. 11.9% compared to its contribution to modelled SO_2. When regional and local factors were included in the MLR model, the interdependencies between CAM, R, P, Ws, TSI and CO_2 made the most significant contribution to decreases in RMSE difference between modelled and measured values. The RIW% of CAM, R, P and Ws in the optimum MLR equation obtained when global, regional and local factors are included indicates that these factors explained 12.7%, 12.4%, 11.4% and 11.4%, respectively, of the variance in NO_2 levels, while TSI contributed to 7.8% of the variance. It is evident from the MLR model that regional and local factors play a more important role in NO_2 trends at Cape Point. In addition, modelled NO_2 concentrations were positively correlated to CAM , indicating higher NO_2 concentrations coinciding with increased frequencies of air masses moving over the continent during the wet season, as indicated by the seasonal NO_2 pattern (Fig. 4b) and discussed in section 3.2. A positive correlation with population growth also signifies the influence of economic growth and increased energy demand. The decrease in NO_2 concentration from 1995 to 2001 is mainly associated with the period during which the new democracy was established in South Africa with companies implementing mitigation technologies in order to comply with international trade requirements (e.g. Westcott et al., 2007). However, it seems that these enhancements in relation to air quality were offset from 2002/2003, which was a period associated with rapid economic and

population growth accompanied with a higher energy demand (Vet, et al., 2014, Inglesi-Lotz and Blignaut, 2011). In addition, although MLR indicated that global meteorology mainly influenced SO_2 variability at CPT GAW, it was also indicated that P was a local and regional factor that influenced SO_2 levels. Therefore, the periods indicate above as being associated with increased and decreased SO_2 levels, can also be attributed to the changes in the energy demand. Similarly to SO_2, the influence of TSI on NO_2 could be ascribed to increased oxidation capacity of the atmosphere. However, as previously mentioned, the influence of TSI on SO_2 and NO_2 variability cannot be decisively explained at this stage.

It is evident from Fig. 8(c) that, similar to SO_2, relatively weak correlations are observed between measured and modelled NO_2 concentrations when only global factors are included into the MLR model, with an R^2 value of 0.112, which is lower than the R^2 value for SO_2. However, the correlation between measured and modelled NO_2 levels significantly improves when local and regional factors are included, yielding an R^2 value of 0.549, which can be considered a moderate correlation (Kleynhans et al., 2017). This emphasises the importance of local and regional factors on NO_2 concentrations at Cape Point. From Fig. 8(c), it seems that the model, in particular, does not give good estimations for very high NO_2 levels. However, in general, the modelled NO_2 concentrations correlate relatively well to the observed variability of the measured NO_2 concentrations when global, regional and local factors are included.

The slopes of the trend lines for the measured and modelled NO_2 concentrations for the 21-year period correlate very well with the annual trend calculated for the measured NO_2 levels, i.e. 0.035 $\mu g.m^{-3}.y^{-1}$, indicating a slight inter-annual increase. In addition, the slope of the trend line for the NO_2 levels modelled with global, regional and local factors is exactly the same as the slope of the trend line for measured NO_2 concentrations (Fig. 8(c)). The calculated decadal trend for the measured dataset was 0.68 $\mu g.m^{-3}.dec^{-1}$ for the two decades (average NO_2 concentrations from 1995 to 2004 were 2.03 $\mu g.m^{-3}$ and average NO_2 concentrations from 2005 to 2014 were 2.71 $\mu g.m^{-3}$). The annual trends for the two periods identified as being associated with decreased and increased NO_2 concentrations were calculated to be - 0.34 $\mu g.m^{-3}.y^{-1}$ from 1995 to 2001 and 0.29 $\mu g.m^{-3}.y^{-1}$ from 2002 to 2011. In general, it can also be deduced that the trend in NO_2 concentrations over the 21-year measurement period was relatively constant, although characterised by periods of annual decrease and increase in NO_2 concentrations.

3.4.3 Ozone

Since *in-situ* measured O_3 concentrations were available for CPT GAW, modelled O_3 levels were correlated to these measurements, which curtailed the limitations associated with passive sampling of ambient O_3. In Fig. 9, the modelled and measured O_3 concentrations are related, which indicate weak correlations (R^2 value of 0.039) between measured and modelled O_3 levels when only global force factors are considered (Fig. 9(c)). However, the correlations are significantly improved (R^2 value of 0.910) when regional and local factors are included in the MLR model. This indicates that regional and local factors play a significant role in O_3 variability at Cape Point. The very good correlation between modelled and *in-situ* measured O_3 concentrations is also indicative of the limitation associated with passive samplers, especially for a site such as CPT GAW that is influenced by two distinct types of air masses. Comparison of modelled O_3 levels to passively derived O_3 concentrations yielded R^2 values of 0.082 when only global factors were considered, and 0.338 when global, regional and local factors are included in the model. Therefore, although comparison of the O_3 concentrations determined with passive samplers with modelled O_3 levels also reflect the important influence of local and regional factors on O_3 variability, weaker correlation between measured and modelled values are determined.From the RMSE, plotted as a function of the number of interdependent variables, it is evident that the interdependencies between T, CO, CAM and SAM yield the largest decrease in RMSE when global, regional and local factors are included. The RIW% of T, CO and CAM were 33.5%, 21.2% and 10.5, respectively, which made the most significant contributions in explaining the variances (Table 1). IOD had the largest RIW% (43.7%) when only global factors were included, while it also had the highest, although very low (1.4%), RIW% of the global factors when all factors were included in the model. The interdependency between T, CO and CAM resulting in the largest decrease in differences between modelled and measured O_3 concentrations, as well as their respective highest RIW% values, signifies the important role of local and regional factors on O_3 variability at CPT GAW, as mentioned above. Modelled O_3 concentrations are negatively correlated to T, while it is positively correlated to CO and CAM. Therefore, higher O_3 concentrations correspond to lower temperatures, as well as increased frequencies of air masses moving over the continent and higher CO concentrations during the winter months, as indicated and discussed in section 3.2.

The linear regression trend line of the measured O_3 concentrations in Fig. 9 indicates a relatively small positive slope for the 21-year period, i.e. 0.06 $\mu g.m^{-3}.y^{-1}$. The decadal trend

was calculated to be 0.79 $\mu g.m^{-3}dec^{-1}$ (average O_3 concentration from 1995 to 2004 was 49.0 $\mu g.m^{-3}$ and average O_3 concentration from 2005 to 2014 was 49.8 $\mu g.m^{-3}$). As observed in Fig. 6, trend analysis also indicates that O_3 concentrations remained relative constant during the 21-year sampling period. Furthermore, here, the slope of trend line for modelled O_3 values when global, regional and local factors are included, is the same as the slope of trend line of the measured O_3 concentrations.

4. Summary and conclusions

A 21-year passive sampled dataset for atmospheric SO_2, NO_2 and O_3 at CPT GAW was explored for their inter-annual and seasonal features. Comparison of SO_2, NO_2 and O_3 measured at CPT GAW with measurements at other IDAF measurement sites utilising passive samplers indicated that concentrations at CPT GAW were lower than an industrially impacted site, while being generally similar to other African inland ecosystems (with the exception of levels of these gaseous species over forests). SO_2, NO_2 and O_3 showed seasonal patterns, which were attributed to different factors influencing their levels at CPT GAW. It was indicated that SO_2 and NO_2 levels are predominantly influenced by the more frequent occurrences of air masses passing over the Cape Town Metropole in the wet winter season and stronger inversions. Increased microbial activity during the wet season can partially explain increased NO_2 concentrations. The O_3 seasonal pattern corresponded to the NO_2 seasonality, which can be expected in a NO_x-limited regional background site. Although increased SO_2 in January and February coincided with increased biomass burning, the influence of regional biomass burning in the Western Cape was not reflected by NO_2 and O_3 concentrations.

SO_2 and NO_2 did indicate inter-annual variability, having periods associated with decreased and increased concentrations. O_3, however, did not show any significant inter-annual variability. Seasonal and inter-annual SO_2, NO_2 and O_3 variability was further explored with MLR modelling, in which the interdependencies between global, regional and local meteorological factors, as well as population growth, were investigated. Modelling results indicated that variances in SO_2 concentrations were predominantly influenced by global force factors, while global, regional and local factors were indicated as playing a significant role in NO_2 fluctuations. It was also indicated that variances in O_3 concentrations were predominantly associated with regional and local factors. The 21-year trend analysis indicated that SO_2, NO_2 and O_3 concentrations remained relatively constant.

In this study, the value of a long-term atmospheric measurement dataset is clearly illustrated. This dataset was useful to indicate that SO_2, NO_2 and O_3 concentrations at CPT GAW are influenced by various contributing factors, which resulted in seasonal and inter-annual variability of these inorganic gaseous species. However, future *in-situ* NO_x an SO_2 analysers at CPT GAW would be most helpful to resolve some of the proposed inferences/deductions, e.g. episodes of anomalous SO_2 levels could be linked to emissions from the Saldanha iron smelter. A statistical model could be applied to this long-term dataset, which also signified the most important factors contributing to long-term trends. However, availability of measurements of other factors that could be included in such a model should yield more accurate correlations between modelled and measured values.

Acknowledgements

The authors would like to acknowledge the International Global Atmospheric Chemistry programme for endorsing the DEBITS programme, as well as Sasol and Eskom for financial support of the South African IDAF project. Assistance with sample deployment and collection by Ms Thumeka Mkololo is also acknowledged. The authors also acknowledge support from the Atmospheric Research in Southern Africa and Indian Ocean (ARSAIO) programme established by the National Center for Scientific Research (CNRS) in France and the National Research Foundation (NRF) in South Africa.

References

Abiodun, B. J., Ojumu, A. M., Jenner, S. & Ojumu, T. V. 2014. The transport of atmospheric NO_X and HNO_3 over Cape Town. *Atmospheric Chemistry & Physics,* 14**,** 559-575, doi: 10.5194/acp-14-559-2014.

ABM. 2016. *Indian Ocean influences on Australian climate* [Online]. Available: http://www.bom.gov.au/climate/iod/ [Accessed 26 November 2018].

Adon, M., Galy-Lacaux, C., Yoboué, V., Delon, C., Lacaux, J. P., Castera, P., Gardrat, E., Pienaar, J. J., Al Ourabi, H., Laouali, D., Diop, B., Sigha-Nkamdjou, L., Akpo, A., Tathy, J. P., Lavenu, F. & Mougin, E. 2010. Long-term measurements of sulfur dioxide, nitrogen dioxide, ammonia, nitric acid and ozone in Africa using passive samplers. *Atmospheric Chemistry and Physics,* 10**,** 7467-7487, doi: 10.5194/acp-10-7467-2010.

Baldwin, M. P., Gray, L. J., Dunkerton, T. J., Hammilton, K., Haynes, P. H., Randel, W. J., Holton, J. R., Alexander, M. J., Hirota, I., Horinouchi, T., Jones, D. B. A., Kinnersley, J. S., Marquardt, C., Sato, K. & Takahashi, M. 2001. The quasi-biennial oscillation. *Reviews of Geophysics,* 39**,** 179-229, doi: 10.1029/1999RG000073.

Bencherif, H., Diab, R. D., Portafaix, T., Morel, B., Keckhut, P. & Moorgawa, A. 2006. Temperature climatology and trend estimates in the UTLS region as observed over a southern subtropical site, Durban, South Africa. *Atmospheric Chemistry and Physics,* 6**,** 5121-5128, doi: 10.5194/acp-6-5121-2006.

Botha, R., Labuschagne, C., Williams, A. G., Bosman, G., Brunke, E. G., Rossouw, A. & Lindsay, R. 2018. Characterising fifteen years of continuous atmospheric radon activity observations at Cape Point (South Africa). *Atmospheric Environment,* 176**,** 30-39, doi: 10.1016/j.atmosenv.2017.12.010.

Brunke, E. G., Labuschagne, C., Ebinghaus, R., Kock, H. H. & Slemr, F. 2010. Gaseous elemental mercury depletion events observed at Cape Point during 2007-2008. *Atmospheric Chemistry and Physics,* 10**,** 1121-1131, doi: 10.5194/acp-10-1121-2010.

Brunke, E. G., Labuschagne, C., Parker, B., Scheel, H. E. & Whittlestone, S. 2004. Baseline air mass selection at Cape Point, South Africa: application of ^{222}Rn and other filter criteria to CO_2. *Atmospheric Environment,* 38**,** 5693-5702, doi: 10.1016/j.atmosenv.2004.04.024.

Brunke, E.-G, Labuschagne, C & Scheel, H.E. 2001. Trace gas variations at Cape Point, South Africa, during May 1997 following a regional biomass burning episode, *Atmospheric Environment*, 35 (4), 777-786, https://doi.org/10.1016/S1352-2310(00)00260-0

Connell, D. W. 2005. *Basic concepts of environmental chemistry,* CRC Press.

Conradie, E. H., Van Zyl, P. G., Pienaar, J. J., Beukes, J. P., Galy-Lacaux, C., Venter, A. D. & Mkhatshwa, G. V. 2016. The chemical composition and fluxes of atmospheric wet deposition at four sites in South Africa. *Atmospheric Environment,* 146**,** 113-131, doi: 10.1016/j.atmosenv.2016.07.033.

Dhammapala, R. S. 1996. *Use of diffusive samplers for the sampling of atmospheric pollutants.* MSc, Potchefstroom University for CHE.

Draxler, R. R. & Hess, G. D. 2014. Description of the HYSPLIT_4 modelling system. 7 ed. Silver Spring, Maryland: Air Resources Laboratory.

Ferm, M. 1991. A sensitive diffusional sampler. *IVL Report L91*. Göteborg, Sweden: Swedish Environmental Research Institute.

Fowler, D., Pilegaard, K., Sutton, M. A., Ambus, P., Raivonen, M., Duyzer, J., Simpson, D., Fagerli, H., Fuzzi, S., Schjoerring, J. K., Granier, C., Neftel, A., Isaksen, I. S. A., Laj, P., Maione, M., Monks, P. S., Burkhardt, J., Daemmgen, U., Neirynck, J., Personne, E., Wichink-Kruit, R., Butterbach-Bahl, K., Flechard, C., Tuovinen, J. P., Coyle, M., Gerosa, G., Loubet, B., Altimir, N., Gruenhage, L., Ammann, C., Cieslik, S., Paoletti, E., Mikkelsen, T. N., Ro-Poulsen, H., Cellier, P., Cape, J. N., Horváth, L., Loreto, F., Niinemets, Ü., Palmer, P. I., Rinne, J., Misztal, P., Nemitz, E., Nilsson, D., Pryor, S., Gallagher, M. W., Vesala, T., Skiba, U., Brüggemann, N., Zechmeister-Boltenstern, S., Williams, J., O'dowd, C., Facchini, M. C., De Leeuw, G., Flossman, A., Chaumerliac, N. & Erisman, J. W. 2009. Atmospheric composition

change: Ecosystems-Atmosphere interactions. *Atmospheric Environment,* 43**,** 5193-5267, doi: 10.1016/j.atmosenv.2009.07.068.

GAWSIS. *Global Atmosphere Watch Station Information System* [Online]. Available: https://gawsis.meteoswiss.ch/GAWSIS//index.html#/ [Accessed 23 November 2018].

He, J. & Bala, R. 2008. Draft report on passive sampler inter-comparison under Malé Declaration. *Malé Declaration on Control and Prevention of Air Pollution and its Likely Transboundary Effect for South Asia.* Singapore: National University of Singapore.

Hénault, C., Bizouard, F., Laville, P., Gabrielle, B., Nicoullaud, B., Germon, J. C. & Cellier, P. 2005. Predicting in situ soil N2O emission using NOE algorithm and soil database. *Global Change Biology,* 11**,** 115-127, doi: 10.1111/j.1365-2486.2004.00879.x.

Ho, M., Kiem, A. S. & Verdon-Kidd, D. C. 2012. The Southern Annular Mode: a comparison of indices. *Hydrology and Earth System Sciences,* 16**,** 15, doi: 10.5194/hess-16-967-2012.

IDAF. 2011. *Network* [Online]. Available: http://idaf.sedoo.fr/spip.php?rubrique45 [Accessed 29 June 2017].

Inglesi-Lotz, R. & Blignaut, J.N., 2011. South Africa's electricity consumption: a sectoral decomposition analysis. Applied Energy 88 (12), 4779e4784

IPCC 2007. Climate change 2007: The Physical Science Basis. *In:* Solomon, S., Qin, D., Manning, M., Chen, Z., Marquis, M., Averyt, K. B., Tignor, M. & Miller, H. L. (eds.) *Contribution of Working Group I to the Fourth Assessment Report of the Intergovernmental Panel on Climate Change.* Cambridge, United Kingdom and New York, NY, USA.

Jaars, K., Beukes, J. P., Van Zyl, P. G., Venter, A. D., Josipovic, M., Pienaar, J. J., Vakkari, V., Aaltonen, H., Laakso, H., Kulmala, M., Tiitta, P., Guenther, A., Hellén, H., Laakso, L. & Hakola, H. 2014. Ambient aromatic hydrocarbon measurements at Welgegund, South Africa. *Atmospheric Chemistry and Physics Discussions,* 14**,** 7075-7089, doi: 10.5194/acp-14-7075-2014.

Kaufman, Y. J., Ichoku, C., Giglio, L., Korontzi, S., Chu, D. A., Hao, W. M., Li, R. R. & Justice, C. O. 2003. Fire and smoke observed from the Earth Observing System MODIS instrument: products, validation, and operational use. *International Journal of Remote Sensing,* 24**,** 1765-1781, doi: 10.1080/01431160210144741.

Kleynhans, E., Beukes, J. P., Van Zyl, P. G., Bunt, J., Nkosi, N. & Venter, M. 2017. The Effect of Carbonaceous Reductant Selection on Chromite Pre-reduction. *Metallurgical & Materials Transactions B,* 48**,** 827-840, doi: 10.1007/s11663-016-0878-4.

KMNI. 2016a. *monthly DMI HadISST1* [Online]. Available: http://climexp.knmi.nl/getindices.cgi?WMO=UKMOData/hadisst1_dmi&STATION=DMI_HadISST1&TYPE=i&id=someone@somewhere [Accessed 22 December 2016].

KMNI. 2016b. *monthly measured total solar irradiance* [Online]. Available: http://climexp.knmi.nl/getindices.cgi?WMO=PMODData/tsi&STATION=measured_total_solar_irradiance&TYPE=i&id=someone@somewhere [Accessed 22 December 2016].

Korhonen, K., Giannakaki, E., Mielonen, T., Pfüller, A., Laakso, L., Vakkari, V., Baars, H., Engelmann, R., Beukes, J. P., Van Zyl, P. G., Ramandh, A., Ntsangwane, L., Josipovic, M., Tiitta, P., Fourie, G., Ngwana, I., Chiloane, K. & Komppula, M. 2014. Atmospheric boundary layer top height in South Africa: measurements with lidar and radiosonde compared to three atmospheric models. *Atmospheric Chemistry and Physics,* 14**,** 4263-4278, doi: 10.5194/acp-14-4263-2014.

Kraha, A., Turner, H., Nimon, K., Reichwein Zientek, L. & Henson, R. K. 2012. Tools to support interpreting multiple regression in the face of multicollinearity. *Frontiers in Psychology,* 3**,** 1-16, doi: 10.3389/fpsyg.2012.00044.

Laban, T. L., Van Zyl, P. G., Beukes, J. P., Vakkari, V., Jaars, K., Borduas-Dedekind, N., Josipovic, M., Thompson, A. M., Kulmala, M. & Laakso, L. 2018. Seasonal influences on surface ozone variability in continental South Africa and implications for air quality. *Atmospheric Chemistry and Physics* 15491-15514, doi: 10.5194/acp-18-15491-2018.

Labuschagne, C., Kuyper, B., Brunke, E.-G., Mokolo, T., Van Der Spuy, D., Martin, L., Mbambalala, E., Parker, B., Khan, M. a. H., Davies-Coleman, M. T., Shallcross, D. E. & Joubert, W. 2018. A review of four decades of atmospheric trace gas measurements at Cape Point, South Africa. *Transactions of the Royal Society of South Africa,* 73**,** 113-132, doi: 10.1080/0035919X.2018.1477854.

Lacaux, J. P., Tathy, J. P. & Sigha, L. 2003. Acid wet deposition in the tropics: Two case studies using DEBITS measurements. *IGACtivities Newsletter of the International Global Atmospheric Chemistry Project.*

Lorenzo-Seva, U., Ferrando, P. J. & Chico, E. 2010. Two SPSS programs for interpreting multiple regression results. *Behavior Research Methods,* 42**,** 29-35, doi: 10.3758/BRM.42.1.29.

Lourens, A. S., Beukes, J. P., Van Zyl, P. G., Fourie, G. D., Burger, J. W., Pienaar, J. J., Read, C. E. & Jordaan, J. H. 2011. Spatial and temporal assessment of gaseous pollutants in the Highveld of South Africa. *South African Journal of Science,* 107**,** 1-8, doi: 10.4102/sajs.v107i1/2.269.

Ludwig, J., Meixner, F. X., Vogel, B. & Förstner, J. 2001. Soil-air exchange of nitric oxide: an overview of processes, environmental factors, and modeling studies. *Biogeochemistry,* 52**,** 225-257, doi: 10.1023/A:1006424330555.

Marshall, G. 2018. *An observation-based Southern Hemisphere Annular Mode Index* [Online]. United Kingdom. Available: http://www.nerc-bas.ac.uk/icd/gjma/sam.html [Accessed 28 August 2018].

Martins, J. J., Dhammapala, R. S., Lachmann, G., Galy-Lacaux, C. & Pienaar, J. J. 2007. Long-term measurements of sulphur dioxide, nitrogen dioxide, ammonia, nitric acid and ozone in southern Africa using passive samplers. *South African Journal of Science,* 103**,** 336-342, doi:

Monks, P. & Leigh, R. 2009. Tropospheric chemistry and air pollution. *In:* Hewitt, C. N. & Jackson, A. V. (eds.) *Atmospheric science for environmental scientists.* United Kingdom: Wiley-Blackwell.

Nathans, L. L., Oswald, F. L. & Nimon, K. 2012. Interpreting multiple linear regression: A guidebook of variable importance. *Practical Assessment, Research & Evaluation,* 17**,** 1-19, doi:

NOAA. 2015a. *Climate Indices: Monthly Atmospheric and Ocean Time Series* [Online]. Available: https://www.esrl.noaa.gov/psd/data/climateindices/list/ [Accessed 22 December 2016].

NOAA. 2015b. *Monthly Atmospheric and SST Indices* [Online]. Available: http://www.cpc.ncep.noaa.gov/data/indices/ [Accessed 22 December 2016].

NRC 1991. *Rethinking the Ozone Problem in Urban and Regional Air Pollution,* Washington, DC, The National Academies Press.

Ojumu, A. M. 2013. *Transport of nitrogen oxides and nitric acid pollutants over South Africa and air pollution in Cape Town.* MSc, University of South Africa.

Oltmans, S. J., Lefohn, A. S., Shadwick, D., Harris, J. M., Scheel, H. E., Galbally, I., Tarasick, D. W., Johnson, B. J., Brunke, E. G., Claude, H., Zeng, G., Nichol, S., Schmidlin, F., Davies, J., Cuevas, E., Redondas, A., Naoe, H., Nakano, T. & Kawasato, T. 2013. Recent tropospheric ozone changes: A pattern dominated by slow or no growth. *Atmospheric Environment,* 67**,** 331-351, doi: 10.1016/j.atmosenv.2012.10.057.

Roy, D. P., Boschetti, L., Justice, C. O. & Ju, J. 2008. The collection 5 MODIS burned area product: global evaluation by comparison with the MODIS active fire product. *Remote Sensing of Environment,* 112**,** 3690-3707, doi: 10.1016/j.rse.2008.05.013.

Saji, N. H. & Yamagata, T. 2003. Possible impacts of Indian Ocean Dipole mode events on global climate. *Climate Research,* 25**,** 151-169, doi: 10.3354/cr025151.

Seinfeld, J. H. & Pandis, S. N. 2006. *Atmospheric Chemistry and Physics: From Air Pollution to Climate Change*, Wiley.

Slemr, F., Brunke, E. G., Whittlestone, S., Zahorowski, W., Ebinghaus, R., Kock, H. H. & Labuschagne, C. 2013. 222Rn-calibrated mercury fluxes from terrestrial surface of southern Africa. *Atmospheric Chemistry & Physics,* 13**,** 6421-6428, doi: 10.5194/acp-13-6421-2013.

Stenseth, N. C., Ottersen, G., Hurrell, J. W., Mysterud, A., Lima, M., Chan, K., Yoccoz, N. G. & Ådlandsvik, B. 2003. Review article. Studying climate effects on ecology through the use of climate indices: the North Atlantic Oscillation, El Niño Southern Oscillation and beyond. *Proceedings of the Royal Society of London B,* 270**,** 2087 2096, doi: 10.1098/rspd.2003.2415.

Stewart, D. J., Taylor, C. M., Reeves, C. E. & Mcquaid, J. B. 2008. Biogenic nitrogen oxide emissions from soils: impact on NO_X and ozone over west Africa during AMMA (African Monsoon Multidisciplinary Analysis): observational study. *Atmospheric Chemistry and Physics,* 8**,** 2285-2297, doi: 10.5194/acp-8-2285-2008.

Swap, R. J., Annegarn, H. J., Suttles, J. T., King, M. D. Platnick, S., Privette, J. L. & Scholes, R. J. 2003. Africa burning: A thematic analysis of the Southern African Regional Science Initiative (SAFARI 2000), Journal of Geophysical Researcg, 108 (D13), 8465, doi:10.1029/2003JD003747

Tiitta, P., Vakkari, V., Croteau, P., Beukes, J. P., Zyl, P. G. V., Josipovic, M., Venter, A. D., Jaars, K., Pienaar, J. J., Ng, N. L., Canagaratna, M. R., Jayne, J. T., Kerminen, V. M., Kokkola, H., Kulmala, M., Laaksonen, A., Worsnop, D. R. & Laakso, L. 2014. Chemical composition, main sources and temporal variability of PM_1 aerosols in southern African grassland. *Atmospheric Chemistry and Physics,* 14**,** 1909-1927, doi: 10.5194/acp-14-1909-2014.

Toihir, A. M., Portafaix, T., Sivakumar, V., Bencherif, H., Pazmiño, A. & Bègue, N. 2018. Variability and trend in ozone over the southern tropics and subtropics. *Annales Geophysicae,* 36**,** 381-404, doi: 10.5194/angeo-36-381-2018.

UNESCO. 2015. *Cape Floral Region Protected Areas* [Online]. Available: http://whc.unesco.org/en/list/1007/ [Accessed 20 June 2017].

Vakkari, V., Beukes, J. P., Laakso, H., Mabaso, D., Pienaar, J. J., Kulmala, M. & Laakso, L. 2013. Long-term observations of aerosol size distributions in semi-clean and polluted savannah in South Africa. *Atmospheric Chemistry and Physics,* 13**,** 1751-1770, doi: 10.5194/acp-13-1751-2013.

Van Zyl, P. G., Beukes, J. P., Du Toit, G., Mabaso, D., Hendriks, J., Vakkari, V., Tiitta, P., Pienaar, J. J., Kulmala, M. & Laakso, L. 2014. Assessment of atmospheric trace metals in the western Bushveld Igneous Complex, South Africa. *South African Journal of Science,* 110**,** 1-11, doi: 10.1590/sajs.2014/20130280.

Venter, A. D., Jaars, K., Booyens, W., Beukes, J. P., Van Zyl, P. G., Josipovic, M., Hendriks, J., Vakkari, V., Hellen, H., Hakola, H., Aaltonen, H., Ruiz-Jimenez, J., Riekkola, M. L. & Laakso, L. 2015. Plume characterization of a typical South African braai: research article. *South African Journal of Chemistry,* 68**,** 181-194, doi: 10.17159/0379-4350/2015/v68a25.

Venter, A. D., Vakkari, V., Beukes, J. P., Van Zyl, P. G., Laakso, H., Mabaso, D., Tiitta, P., Josipovic, M., Kuimala, M., Pienaar, J. J. & Laakso, L. 2012. An air quality assessment in the industrialized western Bushveld Igneous Complex, South Africa. *South African Journal Science,* 108**,** 10, doi: 10.4102/sajs.V108i9/10.1059.

Vet, R., Artx, R.S., Carou, S., Shaw, M., Ro, C., Aas, W., Baker, A., Bowersox, V.C., Dentener, F., Galy-Lacaux, C., Hou, A., Pienaar, J.J., Gillet, R., Forti, M.C., Gromov, S., Hara, H., Khodzher, T., Mahowald, N.M., Nickovic, S., Rao, P.S.P. & Reid, N.W. 2014. A global assessment of precipitation chemistry and deposition of sulfur, nitrogen, sea salt, base cations, organic acids, acidity and pH, and phosphorus. *Atmospheric Environment,* 93:3-100.

Westcott, G., Tacke, M., Schoeman, N. & Morgan, N., 2007. Impala Platinum Smelter, Rustenburg: An integrated smelter off-gas treatment solution. *The Journal of the Southern African Institute of Mining and Metallurgy,* 107:281-287.

Wicking-Baird, M. C., De Villiers, M. G. & Dutkiewicz, R. 1997. The Cape Town brown haze study.

Appendix

Figure A1: Time series of monthly average SO_2, NO_2 and O_3 concentrations measured with passive samplers

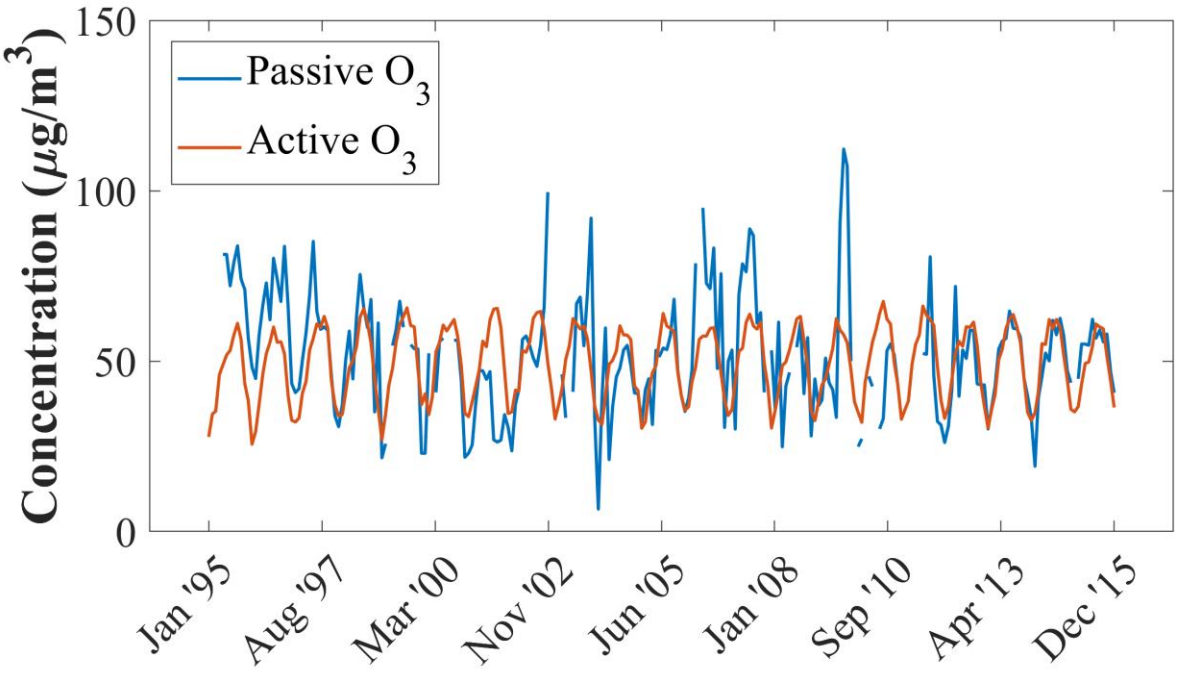

Figure A2: Time series of O_3 concentrations measured with passive samplers and *in situ* measurements at CPT GAW

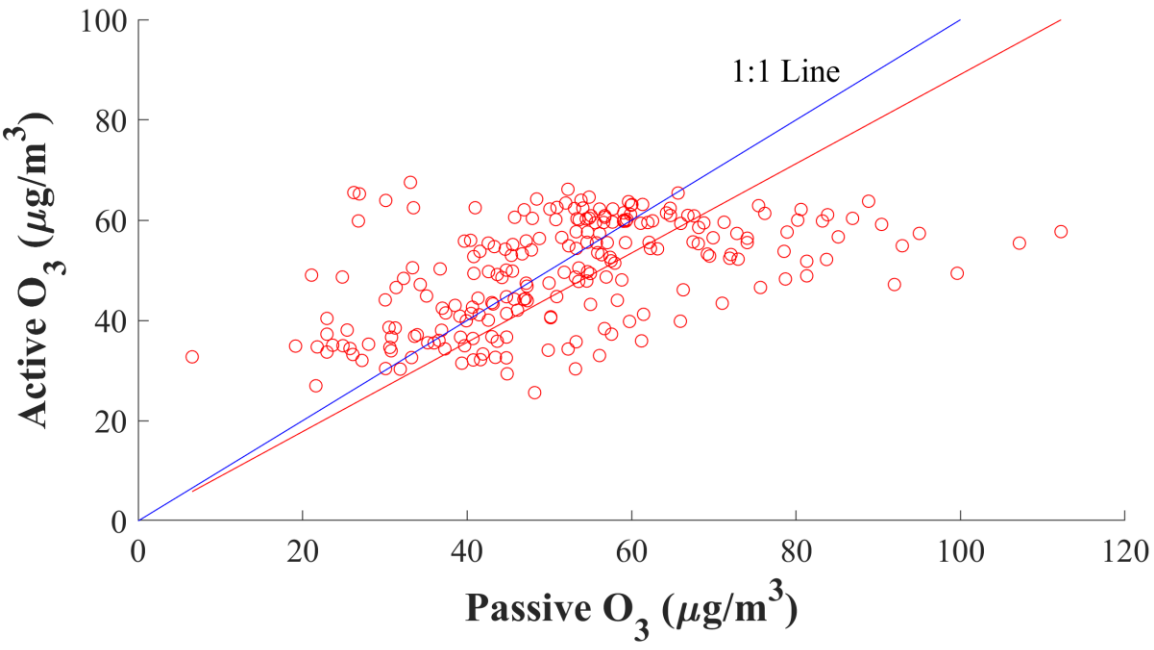

Figure A3: Correlation between O_3 concentrations measured with passive samplers and *in situ* measurements at CPT GAW

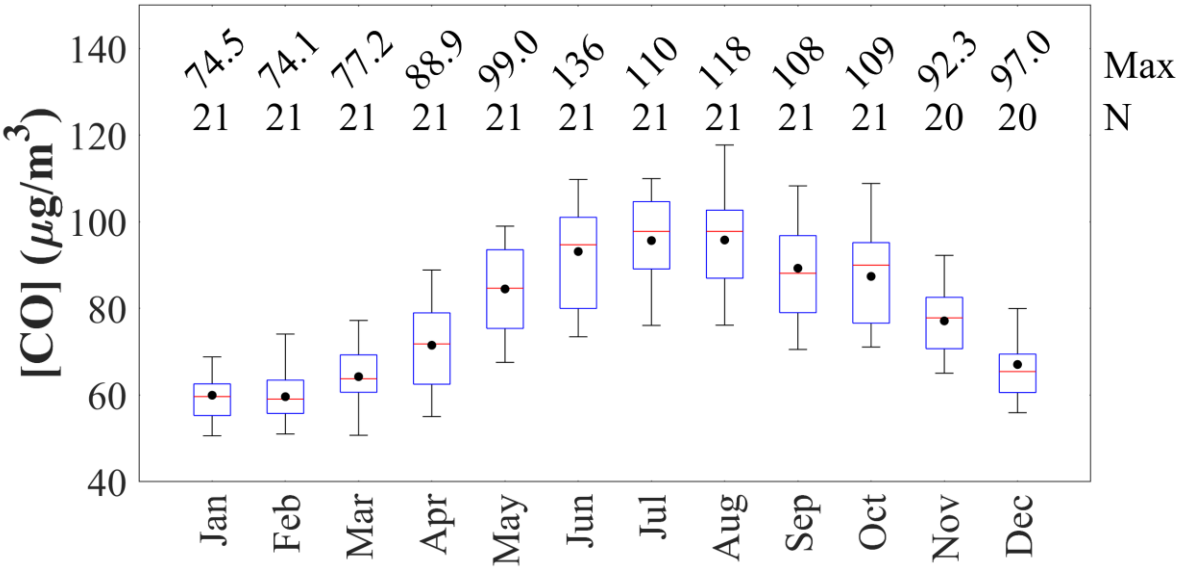

Figure A4: Monthly averaged *in situ* measured CO concentrations for the 21-year sampling period at CPT GAW. The red line of each box represents the median, the top and bottom edges of the box the 25th and 75th percentiles, respectively, the whiskers ±2.7σ (99.3% coverage if the data has a normal distribution) and the black dots the averages. The maximum concentrations and the number of measurements (N) are presented at the top

CHAPTER 5

STATISTICAL MODELLING OF LONG-TERM ATMOSPHERIC SO_2, NO_2 AND O_3 TRENDS WITHIN THE INTERIOR OF SOUTH AFRICA

5.1 Author list, contributions and consent

J.-S. Swartz[1], P.G. Van Zyl[1], J.P. Beukes[1], C. Galy-Lacaux[2], J.J. Pienaar[1]

[1] Unit for Environmental Sciences and Management, North-West University, Potchefstroom Campus, Potchefstroom, 2520, South Africa

[2] Laboratoire d'Aerologie, UMR 5560, Universit´e Paul-Sabatier (UPS) and CNRS, Toulouse, France

Most of the work was done by the first author, **J.-S. Swartz,** who was responsible for passive sampler preparation, analysis, data processing, interpretation and writing the manuscript. Co-author contributions are as follows: P.G. Van Zyl and J.P. Beukes were the promoters of the study, who assisted in data interpretation and writing the manuscript. C. Galy-Lacaux and J.J. Pienaar made conceptual contributions.

All co-authors have been informed that the PhD will be submitted in article format and have given their consent.

5.2 Formatting and current status of article

The article was formatted in accordance with the journal specifications to which it will be submitted, i.e. *Atmospheric Environment*. The article is presented in the style, format and length prescribed by the journal. The guide for authors that was followed in preparation of the article is available at https://www.elsevier.com/journals/atmospheric-environment/1352-

2310/guide-for-authors (Date of access: 29 January 2019). At the time when this PhD was submitted for examination, this article had not yet been submitted for review, but the intention is to submit it soon thereafter.

Statistical modelling of long-term atmospheric SO_2, NO_2 and O_3 trends within the interior of South Africa

J.-S. Swartz[a], P.G. Van Zyl[a]*, J.P. Beukes[a], C. Galy-Lacaux[c], J.J. Pienaar[a]

[a] Unit for Environmental Sciences and Management, North-West University, Potchefstroom Campus, Potchefstroom, 2520, South Africa

[b] Laboratoire de l'Atmosphére et des Cyclones, UMR CNRS 8105, Universit́e de La Ŕeunion, Reunion Island, France

[c] Laboratoire d'Aerologie, UMR 5560, Universit´e Paul-Sabatier (UPS) and CNRS, Toulouse, France

*Corresponding author: P.G. van Zyl (pieter.vanzyl@nwu.ac.za); Postal address: Private Bag X6001, South Africa, Potchefstroom, 2520; Tel: +27 18 299 2395; Fax: +27 18 299 2350

Abstract

South Africa is considered an important source region of atmospheric pollutants, which is compounded by high population- and industrial growth. However, this region is understudied, especially with regard to evaluating long-term trends of atmospheric pollutants. The aim of this study was to perform statistical modelling of SO_2, NO_2 and O_3 long-term trends based on 21-, 19- and 16-year passive sampling datasets available for three South African INDAAF (International network to study Atmospheric Chemistry and Deposition in Africa) sites, which are regionally representative of the industrialised north-eastern interior. The interdependencies between local, regional and global parameters on variances in SO_2, NO_2 and O_3 levels were investigated in the model. Long-term temporal trends indicated seasonal and inter-annual variability at all three sites, which could be ascribed to changes in meteorological conditions and/or variances in source contribution. Local, regional and global parameters contributed to SO_2 variability, with total solar irradiation (TSI) being the most significant factor at the regional background site, Louis Trichardt (LT). Temperature (T) was the most important factor at Skukuza (SK), located in the Kruger National Park, while population growth (P) made the most substantial contribution at the industrially impacted Amersfoort (AF) site. Air masses passing over the source region also contributed to SO_2 levels at SK and LT. Local and regional factors made more substantial contributions to modelled NO_2 levels, with P being the most significant factor explaining NO_2 variability at all three sites, while relative humidity (RH) was the most important local and regional meteorological factor. The important contribution of P on modelled SO_2 and NO_2 concentrations was indicative of the impact of increased anthropogenic activities and energy demand in the north-eastern interior of South Africa. Higher SO_2

concentrations, associated with lower temperatures, as well as the negative correlation of NO_2 levels to RH, reflected the influence of pollution build-up and increased household combustion during winter. ENSO made a significant contribution to modelled O_3 levels at all three sites, while the influence of local and regional meteorological factors was also evident. Trend lines for SO_2 and NO_2 at AF indicated an increase in SO_2 and NO_2 concentrations over the 19-year sampling period, while an upward trend in NO_2 levels at SK signified the influence of growing rural communities. Marginal trends were observed for SO_2 at SK, as well as SO_2 and NO_2 at LT, while O_3 remained relatively constant at all three sites. SO_2 and NO_2 concentrations were higher at AF, while the regional O_3 problem was evident at all three sites.

Keywords: Low-cost sensors; passive sampling; atmospheric inorganic gases; DEBITS; multiple-linear regression

1. Introduction

Although Africa is regarded as one of the most sensitive continents with regard to air pollution and climate change, it is the least studied (Laakso et al., 2012). South Africa is considered an important source region of atmospheric pollutants within the African continent, which is attributed to its highly industrialised economy with the most significant industrial activities including mining-, metallurgical- and petrochemical activities, as well as large-scale coal-fired electricity generation (Rorich and Galpin, 1998; Tiitta et al., 2014). Atmospheric pollution associated with South Africa is compounded by high population growth that, in turn, drives further economic and industrial growth leading to an ever-increasing energy demand (Tiitta et al., 2014). The extent of air pollution in South Africa is illustrated by the well-known NO_2 pollution hotspot revealed by satellite data over the Mpumalanga Highveld, where 11 coal-fired power stations are located (Lourens et al., 2011), which was also recently indicated by the newly launched European Space Agency Sentinel 5P satellite (Meth, 2018).

The importance of long-term atmospheric chemical measurements has been indicated by numerous studies on atmosphere-biosphere interactions (Fowler et al., 2009) and air quality (Monks et al., 2009). These long-term assessments are crucial in identifying relevant policy requirements on local and global scales, as well as the most topical atmospheric chemistry research questions (Vet et al., 2014; IPCC, 2014). In 1990, the International Global Atmospheric Chemistry (IGAC) programme, in collaboration with the Global Atmosphere Watch (GAW) network of the World Meteorological Organisation (WMO) initiated the Deposition of Biogeochemically Important Trace Species (DEBITS) project with the aim to conduct long-term assessments of atmospheric biogeochemical species in the tropics – a region for which limited data existed (Lacaux et al., 2003). The programme is currently operated within the framework of the third phase of IGAC and within the context of the International Nitrogen Initiative (INI) programme. The African component of this initiative was historically referred to as IGAC DEBITS Africa (IDAF), which was relabelled in 2015/2016 under the International Network to study Atmospheric Chemistry and Deposition in Africa (INDAAF) programme. The INDAAF long-term network currently consists of 13 monitoring sites, strategically positioned in southern-, western- and central Africa, which are representative of the most important African ecosystems (http://indaaf.obs-mip.fr). Typical measurements at the INDAAF sites include wet-only rain collection, aerosol composition and inorganic gaseous concentrations, determined with passive samplers.

Long-term measurements have been conducted at three dry-savannah southern African INDAAF sites, which include Amersfoort (AF), Louis Trichardt (LT) and Skukuza (SK) located within the north-eastern interior of South Africa. Measurement of inorganic gaseous pollutant species i.e. sulphur dioxide (SO_2), nitrogen dioxide (NO_2) and ozone (O_3), have been conducted since 1995 at LT, 1997 at AF and 2000 at SK utilising passive samplers. These gaseous species are generally associated with the above-mentioned major sources of atmospheric pollutants in South Africa (Connell, 2005). Moreover, a large number of these sources are located within the north-eastern interior of South Africa, and include the Mpumalanga Highveld, the Johannesburg-Pretoria conurbation and the Vaal Triangle. Laban et al. (2018), for instance, recently indicated high O_3 levels in this north-eastern interior of South Africa, while it was also indicated that O_3 formation in this region can be considered NO_x-limited due to high NO_2 concentrations. Therefore, the South African INDAAF sites were strategically positioned to be representative of the South African interior, with AF an industrially influenced site, LT a rural background site and SK a background site located in the Kruger National Park, as indicated in Fig. 1.

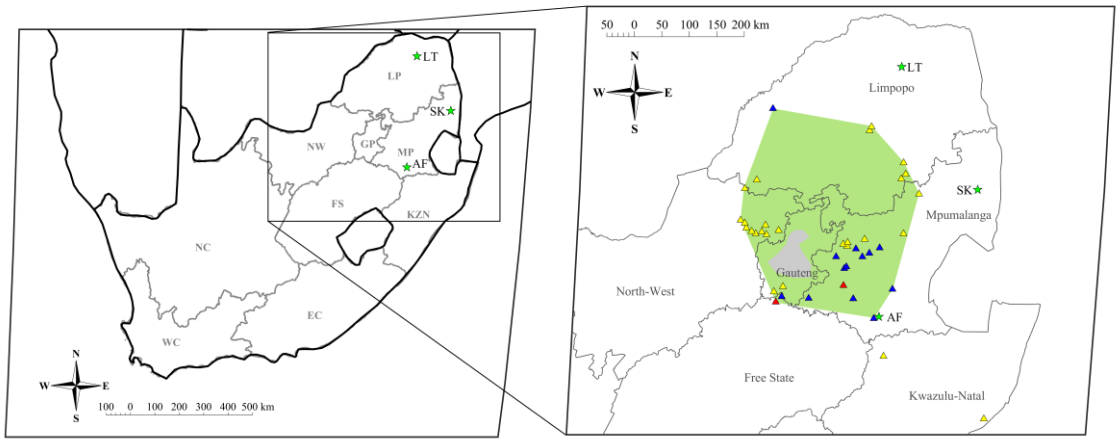

Figure 1: Regional map of South Africa indicating the measurement sites at Amersfoort (AF), Louis Trichardt (LT) and Skukuza (SK) with green stars. A zoomed-in map indicates the defined source region, the Johannesburg-Pretoria Megacity (grey polygon) and large point sources, i.e. power stations (blue triangles), petrochemical plants (red triangles) and pyrometallurgical smelters (yellow triangles)

A number of studies have been reported on measurements conducted within the INDAAF network (Martins et al., 2007; Adon et al., 2010; Josipovic et al., 2011; Adon et al., 2013),

presenting inorganic gaseous concentrations at southern-, as well as western- and central African sites, respectively. Conradie et al. (2016) recently reported on precipitation chemistry at the South African INDAAF sites, while Maritz et al. (2019) conducted an assessment of particulate organic- and elemental carbon at these sites. However, in-depth analysis of long-term trends of atmospheric pollutants at the INDAAF sites has not been conducted due to the non-availability of long-term data. Therefore, the aim of this study was to perform statistical modelling of SO_2, NO_2 and O_3 long-term trends based on 21-, 19- and 16-year datasets available for LT, AF and SK, respectively. The influences of sources together with local, regional and global meteorological patterns on the atmospheric concentrations of SO_2, NO_2 and O_3 were considered in the model.

2 Measurement site and experimental methods

2.1 Site description

Detailed site descriptions have been presented in literature, e.g. Mphepya et al. (2004), Mphepya et al. (2006) and Conradie et al. (2016). AF (1 628 m amsl) and LT (1 300 m amsl) are located within the South African Highveld, while SK is situated in the South African Lowveld. As indicated in Fig.1, AF is in close proximity to the major industrial activities in the Mpumalanga Highveld (~50 to 100 km north-west) and ~200 km east of the Johannesburg-Pretoria conurbation. LT is located in a rural region mainly associated with agricultural activity, while SK (267 m amsl) is situated in the Kruger National Park, i.e. natural bushveld in a protected area.

A summary of the regional meteorology of the South African interior, especially relating to the north-eastern part, was presented by Laakso et al. (2012) and Conradie et al. (2016). Meteorology in the South African interior exhibits strong seasonal variability. This region is characterised by anticyclonic air mass circulation, which is especially predominant during winter, resulting in pronounced inversion layers trapping pollutants near the surface (Tyson et al., 1996; Garstang et al., 1996). In addition, the north-eastern interior (as most parts of the South African interior) is also characterised by distinct wet and dry seasons, with the wet season occurring typically from mid-spring up to autumn (mid-October to mid-May) (Hewitson and Crane, 2006; Conradie et al., 2016).

In Fig. 2, the air mass history for LT, AF and SK for the entire sampling periods at each site is presented by means of overlaid back trajectories. 96-hour back trajectories arriving hourly at

each site at a height of 100 m were calculated with the Hybrid Single-Particle Langrangian Integrated Trajectory (HYSPLIT) model (version 4.8), developed by the National Oceanic and Atmospheric Administration (NOAA) Air Resources Laboratory (ARL) (Draxler and Hess, 2014).

Meteorological data was obtained from the GDAS archive of the National Centre for Environmental Prediction (NCEP) of the United States National Weather Service. Back trajectories were overlaid with fit-for-purpose programming software on a map area divided into grid cells of 0.2° x 0.2°. A colour scale presents the frequency of back trajectories passing over each grid cell, with dark blue indicating the lowest and dark red the highest percentage. The predominant anticyclonic air mass circulation over the interior of South Africa is reflected by the overlay back trajectories at each site, while it also indicates that AF is frequently impacted by air masses passing over the major sources in the north-eastern interior. In addition, it is also evident that the rural background sites (LT and SK) are also impacted by the regional circulation of air masses passing over the major sources.

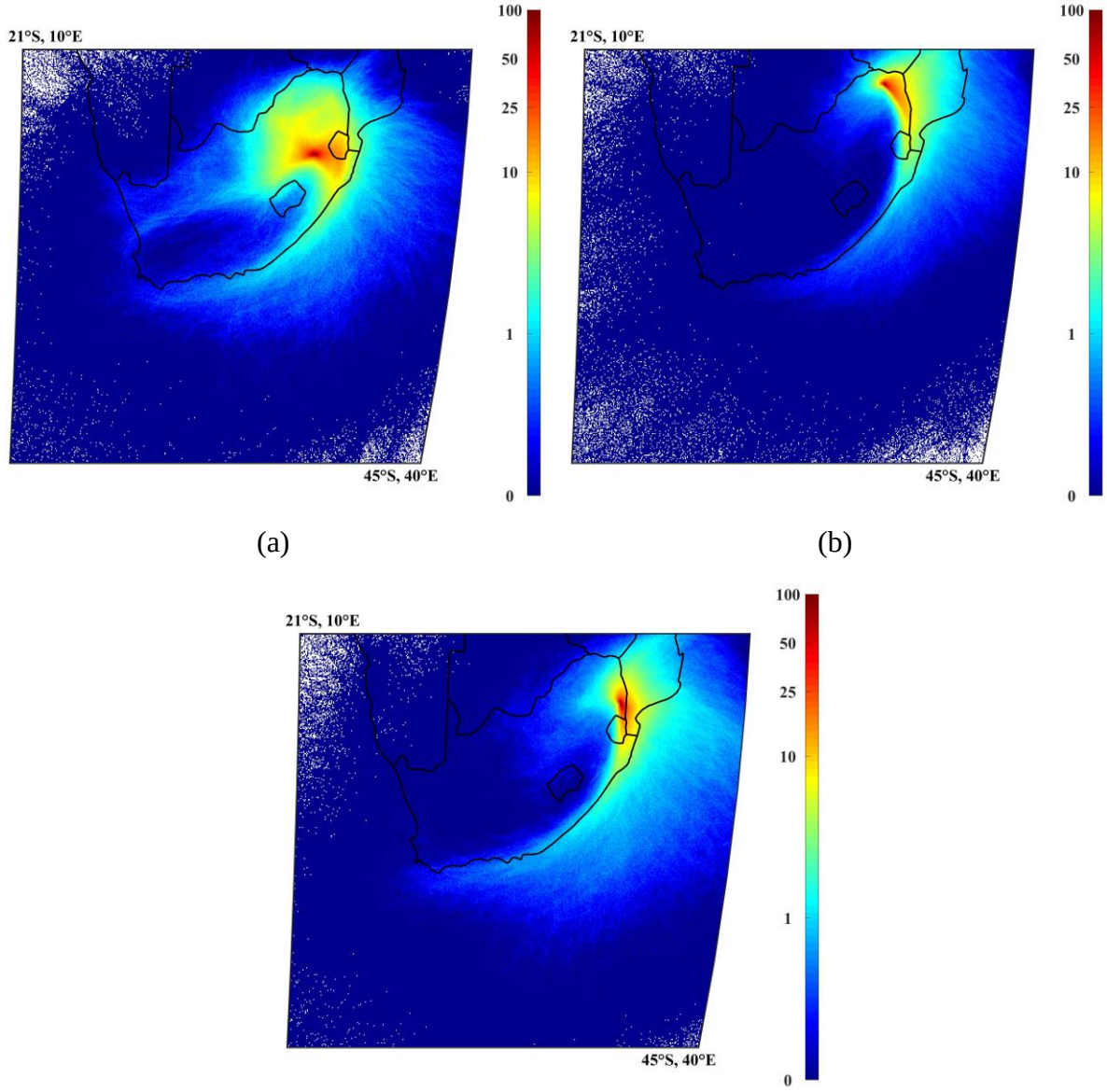

Figure 2: Overlaid hourly arriving 96-hour back-trajectories for air masses arriving at (a) AF from 1997 to 2015, (b) LT from 1995 to 2015 and (c) SK from 2000-2015

2.2 Sampling, analysis and data quality

Passively derived SO_2, NO_2 and O_3 concentrations were available from 1995 to 2015, 1997 to 2015 and 2000 to 2015 for LT, AF and SK, respectively. Gaseous SO_2, NO_2 and O_3 concentrations were measured utilising passive samplers manufactured at the North-West University, which are based on the Ferm (1991) passive sampler. Detailed descriptions on the theory and functioning of these passive samplers, which are based on laminar diffusion and chemical reaction of the atmospheric pollutant of interest, have been presented in literature

(Ferm, 1991; Dhammapala, 1996; Martins et al., 2007; Adon et al., 2010). In addition, the passive samplers utilised in this study have been substantiated through a number of inter-comparison studies (Martins et al., 2007; He and Bala, 2008).

Samplers were exposed in duplicate sets for each gaseous species at each measurement site (1.5 m above ground level) for a period of approximately one month and returned to the laboratory for analysis. Blank samples were kept sealed in the containers for each set of exposed samplers. Prior to 2008, SO_2 and O_3 passive samples were analysed with a Dionex 100 Ion Chromatograph (IC), while NO_2 samples were analysed with a Cary 50 uv/vis spectrometer up until 2012. SO_2 and O_3 samples collected after 2008, and NO_2 samples collected after 2012, were analysed with a Dionex ICS-3000 system. Data quality of the analytical facilities is ensured through participation in the World Meteorological Organisation (WMO) bi-annual Laboratory Inter-Comparison Study (LIS). The results of the 50th LIS study in 2014 indicated that the recovery of each ion in standard samples was between 95 and 105% (Conradie et al., 2016). Analysed data was also subjected to the Q-test, with a 95% confidence threshold to identify, evaluate and reject outliers in the datasets.

2.3 Multiple linear regression model

Similar to the approach employed by Swartz et al. (2019) for the Cape Point GAW station, a multiple linear regression (MLR) model was utilised to statistically evaluate the influence of sources and meteorology on the concentrations of SO_2, NO_2 and O_3 at AF, LT and SK. This model was also utilised by Toihir et al. (2018) and Bencherif et al. (2006) for trend estimates of O_3 and temperature, respectively,. MLR analysis models the relationship between two or more independent variables and a dependant variable by fitting a linear equation to the observed data, which can be utilised to calculate values for the dependent variable. In this study, concentrations of inorganic gaseous species (SO_2, NO_2 and O_3) were considered the dependent variable (C(t)), while local, regional and global factors were considered independent variables to yield the following general equation:

$$C(t) = \sum_{k=1}^{p} a(k) \times f(t,k) + R'(t) \quad 1$$

where f(t,k) describes the specific factor k at time t; a(k) is the coefficient calculated by the model for the factor k that minimises the root mean square error (RMSE); and R′(t) is the residual term that accounts for factors that may have an influence on the model, which are not

considered in the MLR model. The RMSE compares the calculated values with the measured values as follows;

$$\chi^2 = [\sum_t C(t) - \sum_k a(k) \times f(t,k)]^2 \quad 2$$

The trend was parameterised as linear: Trend (t) = $\alpha_0 + \alpha_1.t$, where t denotes the time range, α_0 is a constant, α_1 is the slope of Trend(t) line that estimates the trend over the time scale.

The significance of each of the independent variables on the calculated C(t) was evaluated by the relative importance weights (RIW) approach, which examines the relative contribution that each independent variable makes to the dependent variable and ranks independent variables in order of significance (Nathans et al., 2012; Kleynhans et al., 2017). The RIW approach was applied with IBM® SPSS® Statistics Version 23, together with program syntaxes and scripts adapted from Kraha et al. (2012) and Lorenzo-Seva et al. (2010).

2.4 Input data

Global meteorological factors considered in the model included Total Solar Irradiation (TSI), the El-Niño Southern Oscillation (ENSO), the Indian Ocean Dipole (IOD), the Quasi-Biennial Oscillation (QBO) and the Southern Annular Mode (SAM). Data for the ENSO and QBO cycles was obtained from the National Oceanic and Atmospheric Administration (NOAA) (NOAA, 2015a; NOAA, 2015b), while TSI and IOD data was obtained from the Royal Netherlands Meteorological Institute (*"Koninklijk Nederlands Meteorologisch Instituut"*) (KMNI, 2016a; KMNI, 2016b). SAM data was obtained from the National Environmental Research Council's British Antarctic Survey (Marshall, 2018). The initial input parameters for the model only included the global force factors in order to assess the importance of individual global predictors on measured gaseous concentrations.

Local and regional meteorological parameters included in the model were rain depth (RF), relative humidity (RH) and ambient temperature (T), as well as monthly averaged wind direction (Wd) and -speed (Ws). Since meteorological parameters were not measured at the three sites during the entire sampling period, meteorological data was obtained from the European Centre for Medium-Range Weather Forecasts (ECMWF) reanalysis-interim archive (ERA). Although meteorological measurements were conducted by the South African Weather Service within relative proximity of the locations of the three sites, the data coverage for all the meteorological parameters for the entire sampling period was relatively low (<50%).

Planetary boundary layer (PBL) heights were obtained from the global weather forecast model operated by the ECMWF (Korhonen et al., 2014). Population data (P) from three separate national censuses was obtained from local municipalities and was also included in the model.

Daily fire distribution data from 2000 to 2015 was derived from the National Aeronautics and Space Administration's (NASA) Moderate Resolution Imaging Spectrometer (MODIS) satellite retrievals. MODIS is mounted on the polar-orbiting Earth Observation System's (EOS) Terra spacecraft and globally measures, among others, burn scars, fire and smoke distributions. This dataset was retrieved from the NASA Distributed Active Archive Centres (DAAC) (Kaufman et al., 2003). Fire events were separated into local fire events (LFE), occurring within a 100 km radius from a respective site, and regional fire events (DFE), taking place between 100 km and 1 000 km from each site.

Hourly arriving back trajectories (as discussed above) were also used to calculate the percentage time that air masses spent over a predefined source region (Fig. 1) before arriving at each of the sites for each month, which was also a parameter (SR) included in the statistical model. The source region is a combination of source regions defined in previous studies, e.g. Jaars et al. (2014) and Booyens et al. (2019), which comprised the Mpumalanga Highveld, Vaal Triangle, the Johannesburg-Pretoria conurbation, the western- and the eastern Bushveld Igneous Complex, as well as a region of anticyclonic recirculation (Fig. 1).

Since data was not available for certain local and regional factors considered in the model for the entire sampling periods at AF, LT and SK, and, in an effort to include the optimum number of local and regional factors available for each site, modelled concentrations could not be calculated for the entire sampling periods when global, regional and local factors were included in the MLR model.

3 Results

Fig. A1, A2 and A3 present the time series of monthly average SO_2, NO_2 and O_3 concentrations measured at AF (1997 - 2015), LT (1995 - 2015) and SK (2000 - 2015). Seasonal and inter-annual variability associated with changes in the prevailing meteorology and source contributions will be evaluated and statistically assessed using multiple linear regression model in subsequent sections.

3.1 Seasonal and inter-annual variability

In Fig. 3, 4 and 5, the monthly SO_2, NO_2 and O_3 concentrations, respectively at AF, LT and SK, determined for the entire sampling periods, are presented. Monthly variability in concentrations of these species at these three sites is expected. The north-eastern interior of South Africa, where these sites are located, is generally characterised by increased concentrations in pollutant species during the dry winter months (June to September) due to the prevailing meteorological conditions (Conradie et al., 2016). More pronounced inversion layers trap pollutants near the surface, which, in conjunction with increased anticyclonic recirculation and decreased wet deposition, leads to the build-up pollutant levels (Conradie et al., 2016; Laban et al., 2018). In addition, increased household combustion for space heating during winter also contributes to higher levels of atmospheric pollutants, while open biomass burning (wild fires) is also a significant source of atmospheric species in late winter and spring (August to November). Species typically associated with biomass burning (open or household) include particulate matter (PM), CO and NO_2, while household combustion can also contribute to SO_2 emissions depending on the type of fuel consumed. CO and NO_2 are also important precursors of tropospheric O_3, which also lead to increased surface O_3 concentrations, especially with increased photochemical activity in spring (Laban et al., 2018). From Fig. 3, it is evident that SO_2 concentrations peaked in winter months at LT and SK, while SO_2 levels did not reveal significant monthly variability at AF throughout the year. NO_2 and O_3 concentrations at all three sites are higher during August to November, coinciding with open biomass burning. NO_2 and O_3 levels at AF do not reflect the influence of pollutant build-up in winter, although the whiskers in July do indicate more instances of higher NO_2 concentrations. SK did indicate higher NO_2 and O_3 concentrations during June and July, while LT also had relatively higher O_3 concentrations during July.

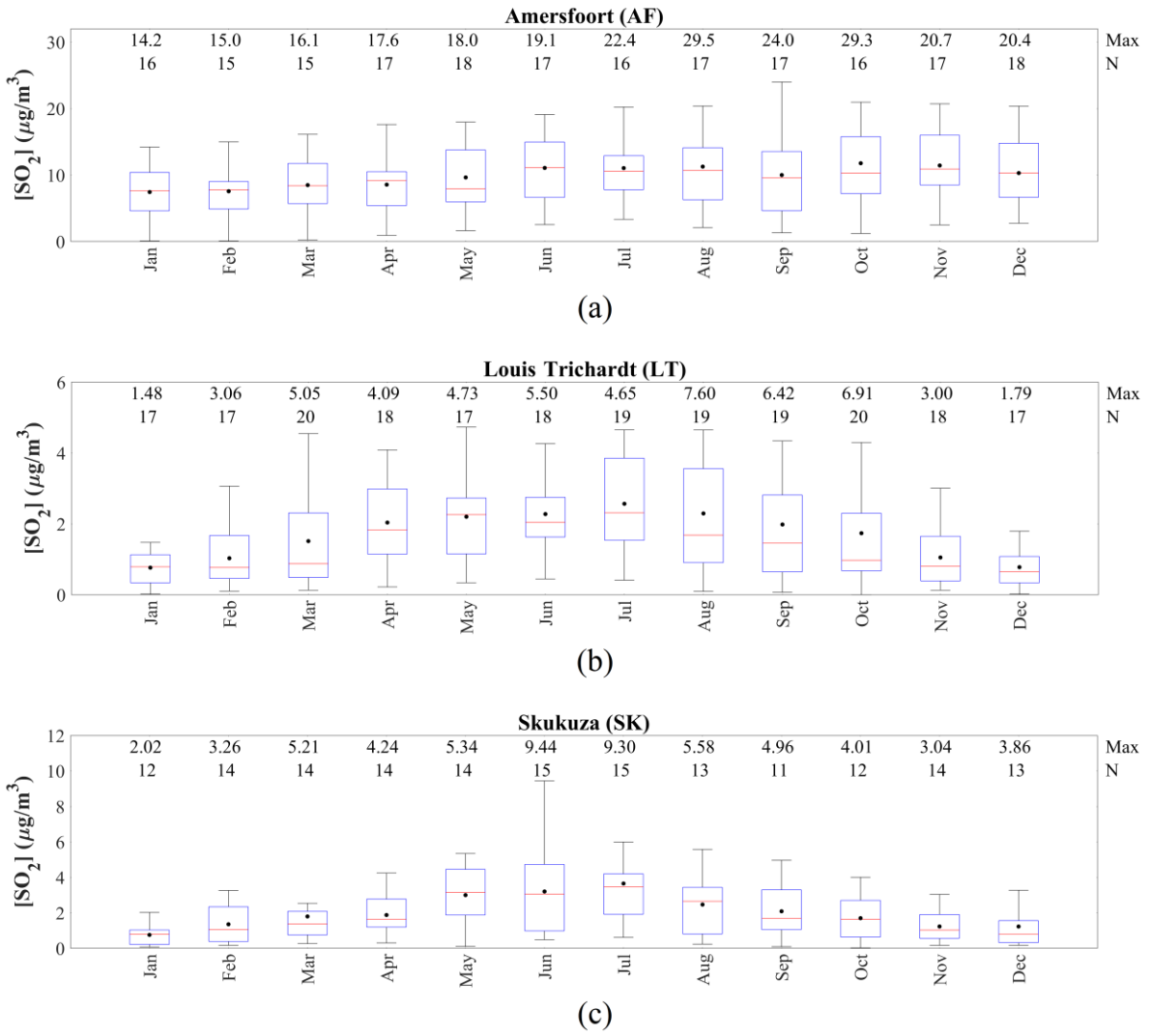

Figure 3: Monthly SO_2 concentrations measured at (a) AF from 1997 to 2015, (b) LT from 1995 to 2015 and (c) SK from 2000 to 2015. The red line of each box represents the median, the top and bottom edges of the box the 25th and 75th percentiles, respectively, the whiskers ±2.7σ (99.3% coverage if the data has a normal distribution) and the black dots the averages. The maximum concentrations and the number of measurements (N) are presented at the top

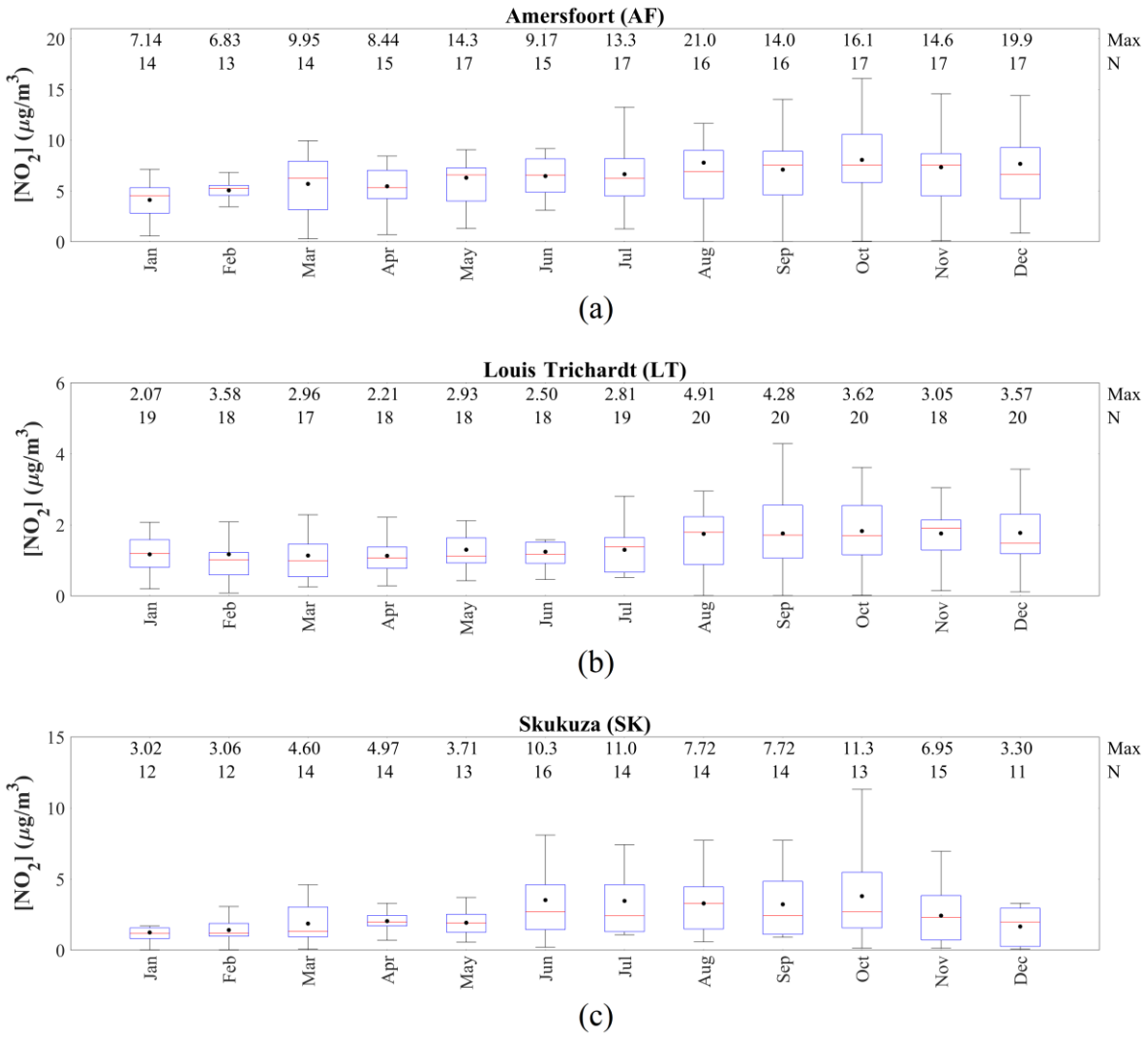

Figure 4: Monthly NO_2 concentrations measured at (a) AF from 1997 to 2015, (b) LT from 1995 to 2015 and at (c) SK from 2000 to 2015. The red line of each box represents the median, the top and bottom edges of the box the 25th and 75th percentiles, respectively, the whiskers ±2.7σ (99.3% coverage if the data has a normal distribution) and the black dots the averages. The maximum concentrations and the number of measurements (N) are presented at the top

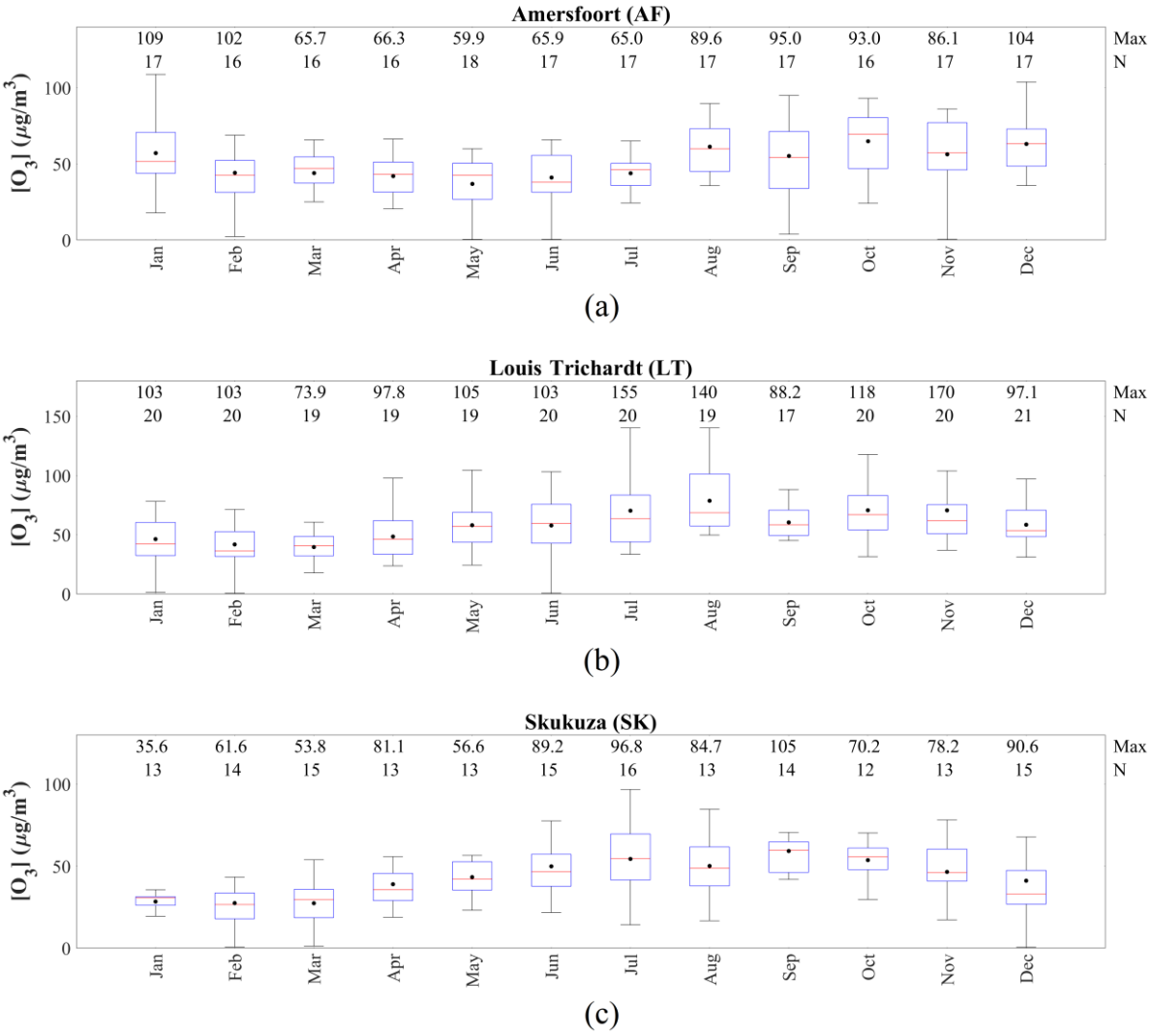

Figure 5: Monthly O_3 concentrations measured at (a) AF from 1997 to 2015, (b) LT from 1995 to 2015 and (c) SK from 2000 to 2015. The red line of each box represents the median, the top and bottom edges of the box the 25th and 75th percentiles, respectively, the whiskers ±2.7σ (99.3% coverage if the data has a normal distribution) and the black dots the averages. The maximum concentrations and the number of measurements (N) are presented at the top

The inter-annual variability of SO_2, NO_2 and O_3 levels is presented in Fig. 6, 7 and 8, respectively for AF, LT and SK. Noticeable from the SO_2 and NO_2 inter-annual fluctuations at all three sites is that the annual average SO_2 and NO_2 concentrations decreased up until 2003/2004 and 2002, respectively, which is followed by a period during which levels of SO_2 and NO_2 increased up until 2009 and 2007, respectively. After 2009, annual average SO_2 concentrations remained relatively constant, while NO_2 showed relatively large inter-annual variability, with annual NO_2 concentrations reaching a maximum in 2011 and 2012. These

observed periods of decreased and increased SO_2 and NO_2 levels are also indicated by the three-year moving averages of the annual mean SO_2 and NO_2 concentrations at all three sites. Since these trends are observed at all three sites, located several kilometres apart in the north-eastern interior, these inter-annual trends seem real and not merely a localised artefact. Furthermore, monthly SO_2 and NO_2 measurements conducted at the Cape Point Global Atmosphere Watch station on the west coast of South Africa also indicate similar periods of increase and decrease in SO_2 and NO_2 levels (Swartz et al., 2019). Although annual O_3 concentrations indicate inter-annual variances, annual average O_3 concentrations remained relatively constant at all three sites, with the exception of a decreasing trend observed from 1995 to 2001 at LT corresponding to the period during which SO_2 and NO_2 decreased. Similar to seasonal variances, inter-annual fluctuations can also be ascribed to changes in meteorological conditions and/or variances in source contribution. Conradie et al. (2016), for example, indicated that rain samples collected from 2009 to 2014 at these three sites had higher SO_4^{2-} and NO_3^- concentrations compared to rain samples collected in 1986 to 1999 and 1999 to 2002, which is attributed to increased energy demand and a larger vehicular fleet associated with economic- and population growth.

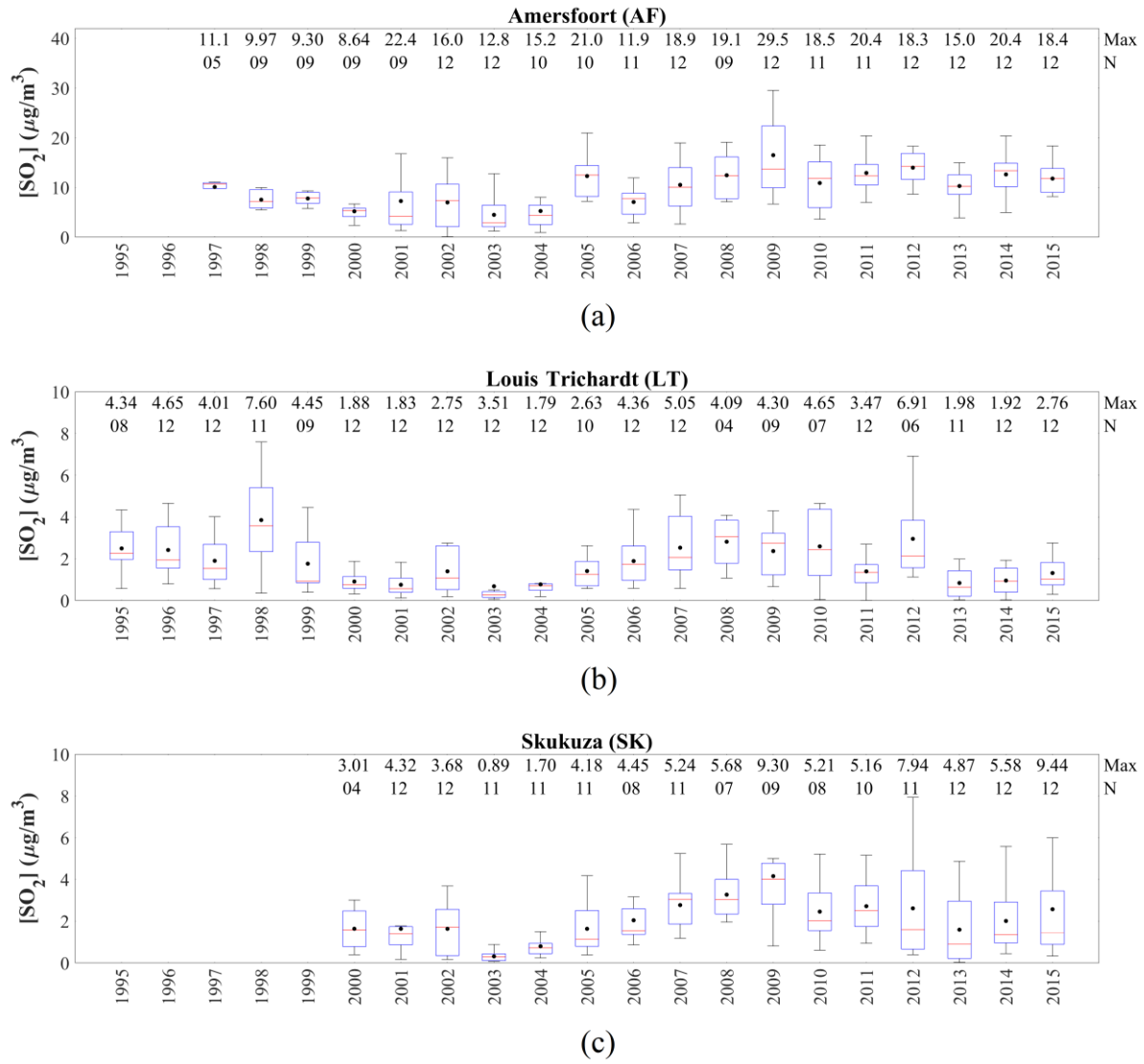

Figure 6: Annual SO_2 concentrations at (a) AF, (b) LT and (c) SK. The red line of each box represents the median, the top and bottom edges of the box the 25th and 75th percentiles, respectively, the whiskers ±2.7σ (99.3% coverage if the data has a normal distribution) and the black dots the averages. The maximum concentrations and the number of measurements (N) are presented at the top

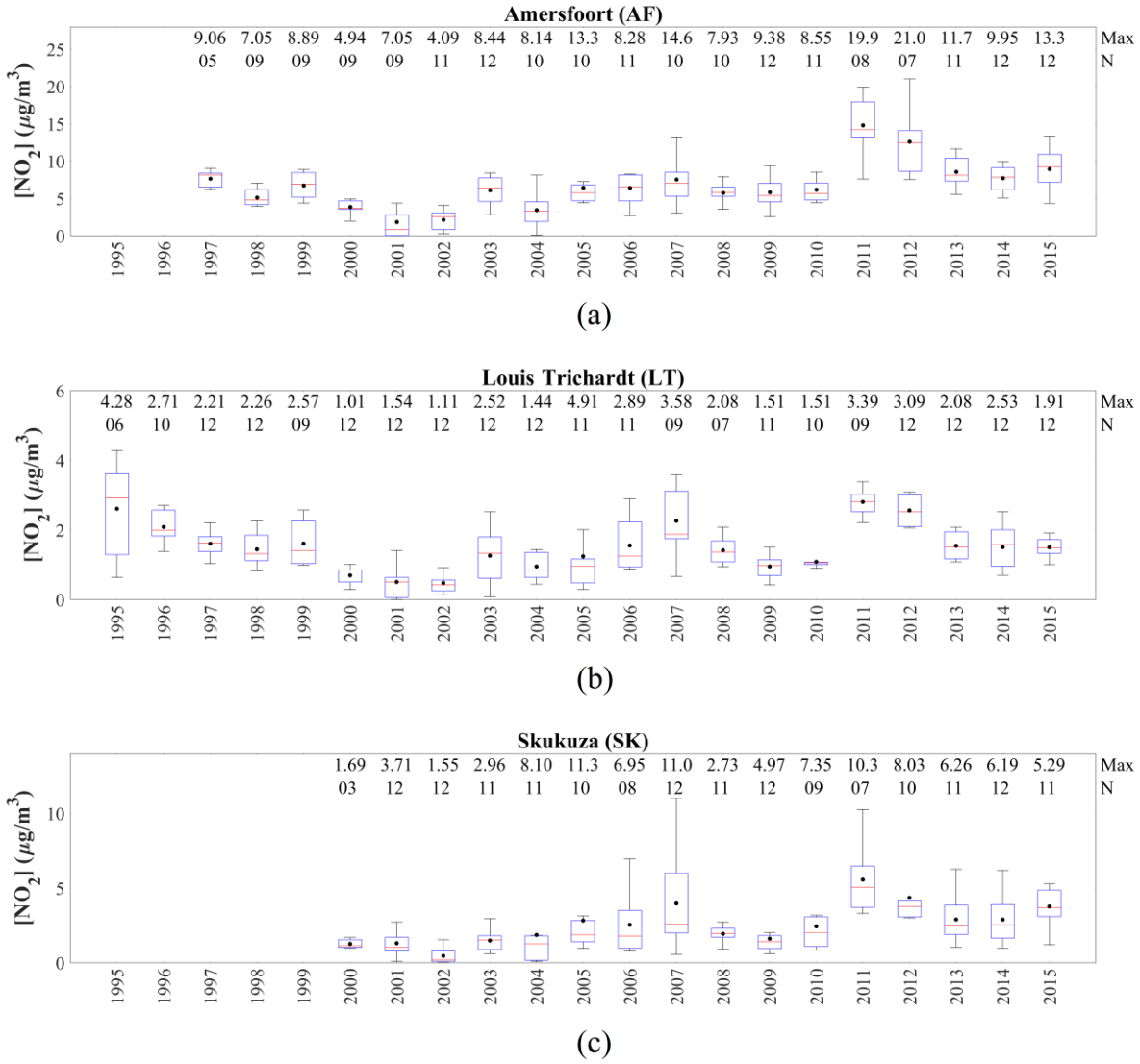

Figure 7: Annual NO_2 concentrations at (a) AF, (b) LT and (c) SK. The red line of each box represents the median, the top and bottom edges of the box the 25th and 75th percentiles, respectively, the whiskers ±2.7σ (99.3% coverage if the data has a normal distribution) and the black dots the averages. The maximum concentrations and the number of measurements (N) are presented at the top

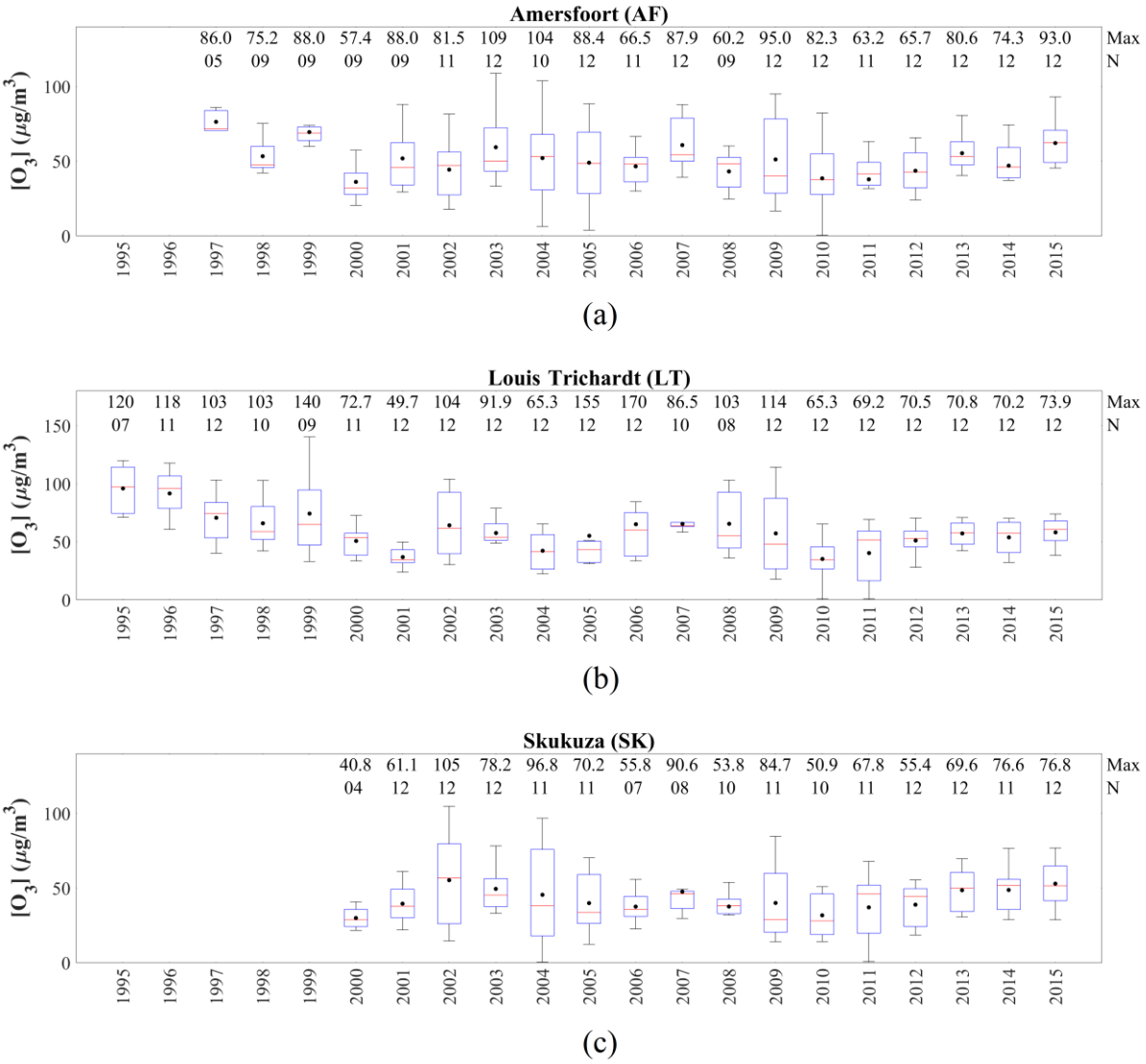

Figure 8: Annual O_3 concentrations at (a) AF, (b) LT and (c) SK. The red line of each box represents the median, the top and bottom edges of the box the 25th and 75th percentiles, respectively, the whiskers ±2.7σ (99.3% coverage if the data has a normal distribution) and the black dots the averages. The maximum concentrations and the number of measurements (N) are presented at the top

3.2 Statistical modelling of variability

3.2.1 Sulphur dioxide (SO_2)

The SO_2 concentrations calculated with the MLR model are compared to measured SO_2 levels in Fig. 9 for AF (Fig. 9a), LT (Fig. 9b) and SK (Fig. 9c). In each sub-figure, the RMSE differences between measured and modelled SO_2 concentrations are presented as a function of the number of independent variables included in the model (i and ii), while the differences between modelled and measured SO_2 levels for each sample are also indicated (iii). As

indicated above, in the initial run of the model, only global factors were included (i and iii), after which all factors (local, regional and global) were incorporated in the model (ii and iii). In Table 1, the coefficients and RIW% of each of the independent variables are included in the optimum MLR equation containing all global factors, as well as in the optimum MLR equation when all local, regional and global factors are included. It is evident from Fig. 9 (iii) that the correlations between measured and modelled SO_2 levels are significantly improved when all factors are considered in the MLR model compared to only including global factors at all three sites. The R^2 values are improved from 0.122 to 0.330, 0.078 to 0.257, and 0.100 to 0.389 at AF, LT and SK, respectively. Although relatively weak correlations are observed between modelled and measured SO_2 levels, the general trend of the measured SO_2 concentrations is mimicked by the modelled values, even when only global factors are included in the MLR model. In addition, the R^2 values at AF and SK when all factors are considered (0.330 and 0.389) can be considered moderate correlations (Kleynhans et al., 2017). It also seems that very high and low SO_2 levels are underestimated by the model. Swartz et al. (2019) attributed differences between monthly concentrations of species measured with passive samplers at CPT GAW and modelled levels to the limitations associated with the use of passive samplers.

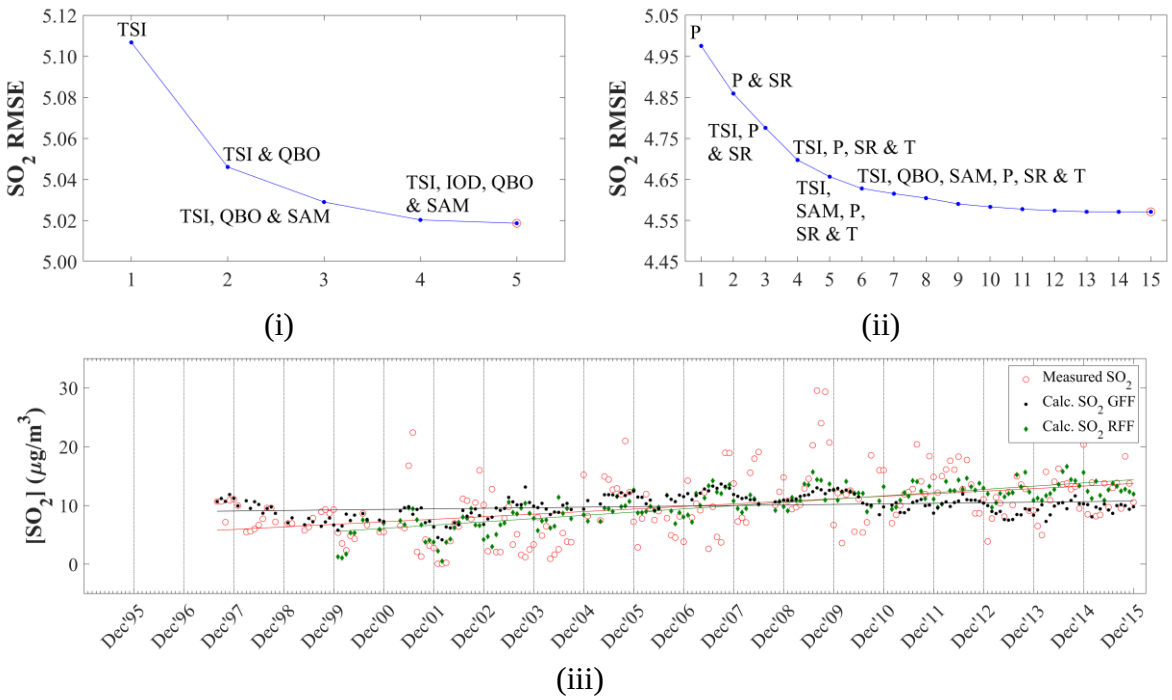

Figure 9a: (i and ii) RMSE differences between modelled and measured SO_2 concentrations as a function of the number of independent variables included in the model, as well as comparison between modelled and measured SO_2 levels (iii) for global force factors only (GFF), and for global, regional and local factors (RFF) determined for AF

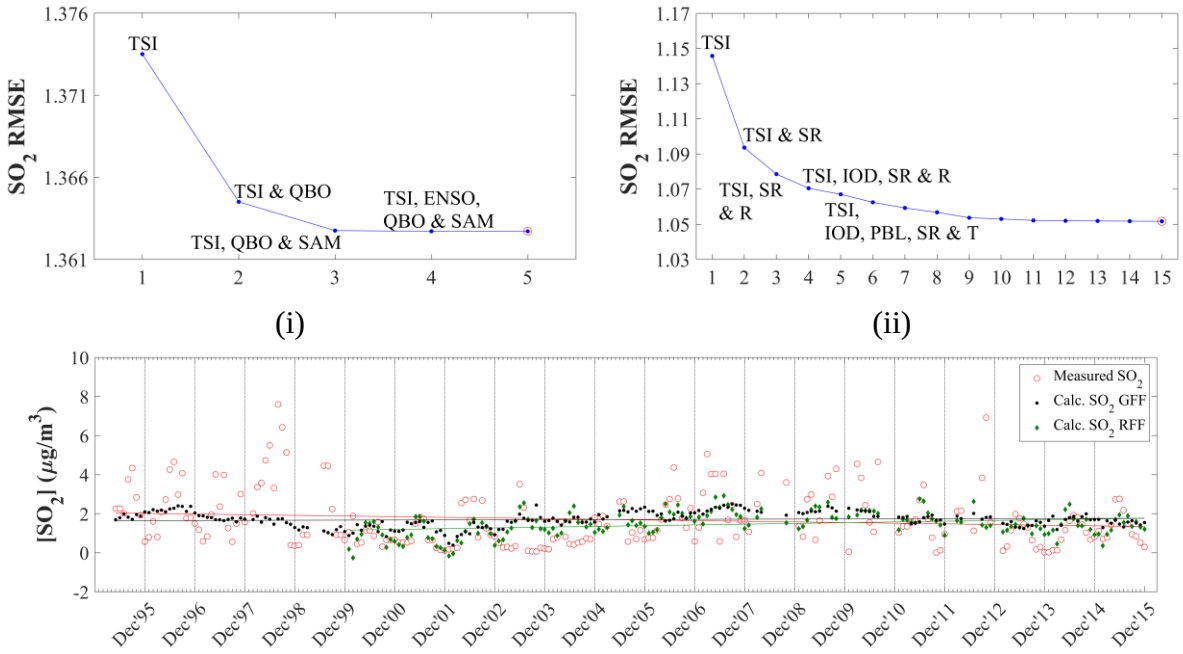

Figure 9b: (i and ii) RMSE differences between modelled and measured SO_2 concentrations as a function of the number of independent variables included in the model, as well as comparison between modelled and measured SO_2 levels (iii) for global force factors only (GFF), and for global, regional and local factors (RFF) determined for LT

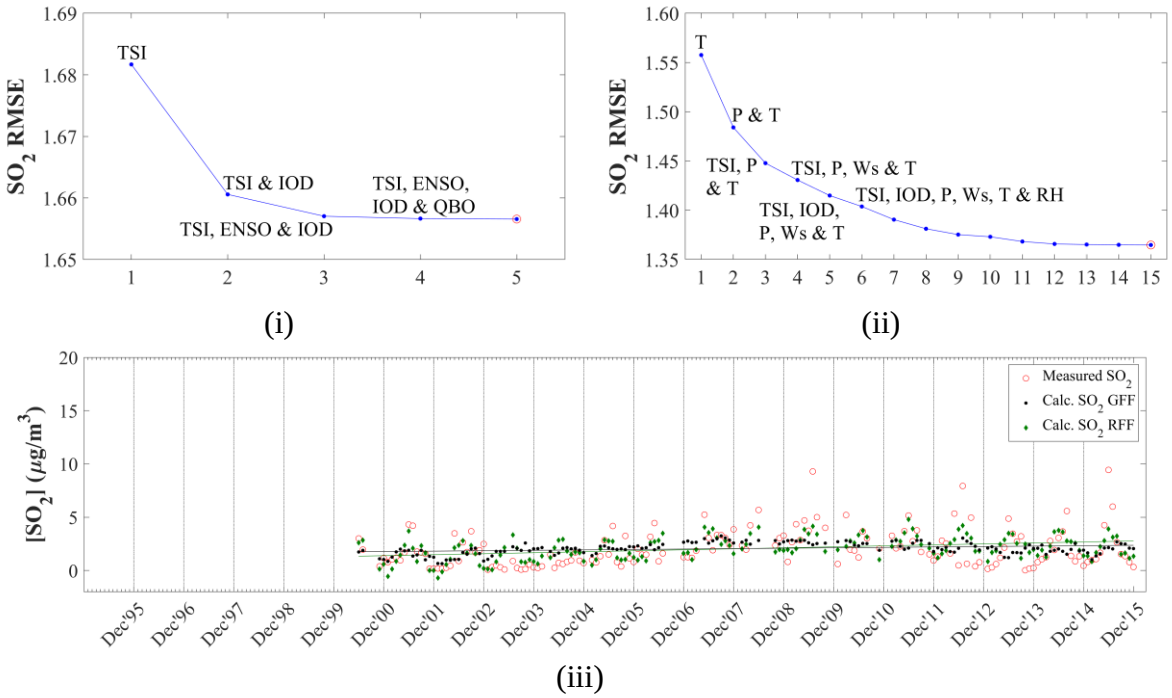

Figure 9c: (i and ii) RMSE differences between modelled and measured SO_2 concentrations as a function of the number of independent variables included in the model, as well as comparison between modelled and measured SO_2 levels (iii) for global force factors only (GFF), and for global, regional and local factors (RFF) determined for SK

Table 1: Regression coefficients (b) and relative important weight percentage (RIW%) of each independent variable included in the MLR model to calculate SO_2 concentrations at AF, LT and SK

	AF			**LT**			**SK**	
	b	***RIW%***		***b***	***RIW%***		***b***	***RIW%***
i) Global forcing factors								
TSI	-3.563	66.2	TSI	-0.875	80.2	TSI	-0.988	61.6
QBO	-0.057	21.2	QBO	-0.011	15.2	IOD	1.183	33.8
IOD	0.818	5.5	SAM	-0.042	3.9	ENSO	-0.158	3.7
SAM	-0.209	5.0	IOD	-0.011	0.5	QBO	-2.500×10^{-3}	0.7
ENSO	0.170	2.0	ENSO	-0.012	0.2	SAM	-0.010	0.3
ii) Global, regional and local factors								
P	1.927×10^{-3}	54.5	TSI	-0.827	34.7	T	-0.281	15.9
TSI	-2.373	14.6	SR	0.069	11.3	TSI	-0.820	12.0
SR	0.189	6.2	T	-0.109	9.9	SR	0.076	9.9
T	-0.588	4.5	IOD	0.588	8.0	P	5.610×10^{-6}	9.1
QBO	-0.034	4.4	R	6.448×10^{-4}	6.7	Ws	-1.357	9.1
RH	0.043	3.9	RH	-0.014	6.2	PBL	3.134×10^{-3}	8.4
PBL	6.396×10^{-3}	2.8	Ws	-0.404	5.1	R	9.233×10^{-4}	7.4
SAM	-0.406	2.6	PBL	1.520×10^{-3}	4.9	RH	-0.024	7.0
R	-1.104×10^{-3}	1.8	Wd	2.746×10^{-3}	3.1	IOD	1.011	6.7
Ws	0.076	1.5	P	-1.035×10^{-6}	2.7	Wd	-4.034×10^{-4}	5.6
IOD	-0.674	0.9	SAM	-0.049	2.4	LFE	5.827×10^{-5}	4.5
LFE	1.114×10^{-4}	0.9	DFE	-2.892×10^{-7}	2.0	DFE	-3.355×10^{-6}	2.2
Wd	-3.502×10^{-3}	0.6	QBO	-6.471×10^{-3}	1.6	ENSO	-0.260	1.7
DFE	-1.319×10^{-5}	0.5	LFE	-8.706×10^{-5}	0.8	SAM	-0.078	0.5
ENSO	-0.310	0.3	ENSO	-0.034	0.6	QBO	-2.726×10^{-3}	0.2

The interdependencies between TSI and QBO at AF and LT, as well as TSI and IOD at SK yielded the largest decreases in RMSE when only global parameters were considered. The RIW% calculated for these parameters in the optimum MLR equation containing all global factors also indicates that these factors are the most significant. When all factors (local, regional and global) were considered in the model, the combinations between P, TSI, SR and T at AF, TSI, SR, IOD and R at LT, and T, TSI, P and Ws contributed to the most significant decrease in RMSE for each of the sites. According to the RIW% calculated for each parameter in the optimum MLR equation containing all factors P (54.5%) and TSI (14.6%) at AF, TSI (34.7%), SR (11.3%), T (9.9%) and IOD (8.0%) at LT, and T (15.9%), TSI (12.0%), SR (9.9%), P (9.1%) and Ws (9.1%) at SK were the most important factors contributing to variances. From the MLR

model, it is evident that global meteorological factors contribute to SO_2 variability at each of these sites located in the north-eastern interior of South Africa. The model also indicates that the influence of global factors is more significant at the rural background site LT, where TSI made the largest contribution to the modelled value, while IOD also made a relatively important contribution. Although TSI was the second most significant factor at AF and SK, local and regional parameters were more important to variances in modelled SO_2 levels at these sites.

Population growth had the most substantial contribution to the dependent variable at the industrially influenced AF, which is indicative of the impacts of increased anthropogenic activities and energy demand in this region. Therefore, it is most-likely that the observed inter-annual variability observed at AF, i.e. periods of decreased and increased SO_2 levels, can mainly be attributed to changes in source contribution. The decrease in SO_2 concentrations up until 2003/2004 is associated with a period post-1994 (when the new democracy was established) during which many companies obtained environmental accreditation (ISO 14000 series, ISO survey (2015)) and implemented mitigation technologies in order to comply with international trade requirements, e.g. certain large metallurgical smelters applied desulphurisation technologies (e.g. Westcott et al., 2007). The period was characterised by an increased awareness of air pollution and its impacts in South Africa. However, it seems that these improvements made with regard to air pollution were offset from 2003/2004 due to rapid economic growth associated with increased industrial activities, e.g. increased production by pyrometallurgical industries (ICDA, 2012), as well as the increase in population growth accompanied by higher energy demand (Vet et al., 2014). Electricity consumption is a good indicator of increased anthropogenic activities, with Inglesi-Lotz and Blignaut (2011) indicating that electricity consumption in South Africa increased by 131 024 GWh from 1993 to 2006. In 2007/2008, the global financial crisis occurred, which forced numerous South African commodity-based producers (e.g. platinum group metal, base metal, ferrochromium, ferromanganese, ferrovanadium and steel smelters) to completely discontinue production. Ferrochromium production in South Africa, for instance, decreased by approximately 35% from 2007 to 2009 (ICDA, 2013), while energy consumption in the manufacturing sector dropped by approximately 34% from 2007 to 2008 (Statistics South Africa, 2012). Furthermore, these variances in source contribution associated with anthropogenic activities are also observed at LT and SK distant from the major sources due to these sites also being impacted by the regional circulation of air masses passing over major sources, as indicated in Fig. 2. In addition, the RIW% associated with P (9.1%) in the optimum MLR equation

containing all factors at SK is also indicative of not only the influence of population growth within the source region (Fig. 1), but also the increased populations of rural communities on the border of the Kruger National Park. Maritz et al. (2019) attributed higher organic- and elemental carbon concentrations measured at SK to increased biomass burning by these rural communities.

Temperature had the largest contribution to the variances of the modelled SO_2 at SK, while it was also an important parameter at LT. In addition, the source region (SR) factor made significant contributions to the dependent variable at SK and LT, while it also made a relative contribution at AF. These two factors are indicative of the influence of changes in local and regional meteorological conditions on SO_2 concentrations, as well as the important influence of air mass movement over the source region. The contribution of SR at all the sites indicated that months and/or years coinciding with these sites being more frequently impacted by air masses passing over the defined source region (Fig. 1) corresponded to increased SO_2 concentrations, while it also substantiates the afore-mentioned deduction that increased anthropogenic activities in the source region also influenced LT and SK. As indicated in section 3.1, SK and LT revealed the expected higher SO_2 levels during winter, while AF had a less distinct seasonal pattern. Therefore, the strong negative correlation between temperature and modelled SO_2 concentrations at SK and LT, i.e. higher SO_2 levels associated with lower temperature, reflects the influence of local and regional meteorology on monthly SO_2 variability, i.e. build-up of pollutant concentrations during winter. At SK, the influence of local meteorology is also indicated by the relative strong negative correlation to Ws, i.e. more stable conditions in winter coinciding with higher SO_2 concentrations. Furthermore, the influence of the rural communities in proximity of SK on SO_2 levels is also signified by T being the most significant factor contributing to modelled SO_2 values at this site. The less distinct seasonal pattern at AF can be attributed to the proximity of AF to the industrial SO_2 sources, with the major point sources consistently emitting the same levels of SO_2 throughout the year. Therefore, the average monthly SO_2 concentrations measured with passive samplers at AF do not reflect the influence of local and regional meteorology on atmospheric SO_2 concentrations.

The slopes of the trend lines of SO_2 values calculated when only global factors were included in the model did not correspond with the trend lines of the measured SO_2 concentrations at all the sites, with the exception of LT that showed slightly better correlations, signifying the stronger influence of global factors at this site (Pane iii in Fig. 9a, b and c). However, the slopes of the linear regression trend lines for the measured SO_2 concentrations and the modelled SO_2

levels when all the factors are included in the model are exactly the same at AF, LT and SK when the same period is considered for both the modelled and measured values. A positive slope for the 19-year trend line for measured SO_2 concentrations is observed at AF (Fig. 9a(iii)), indicating an increase in SO_2 levels over the 19-year sampling period, i.e. 0.43 $\mu g.m^{-3}.y^{-1}$. An increase in SO_2 concentration, i.e. 0.09 $\mu g.m^{-3}.y^{-1}$ is also determined for the 16-year measurement period at SK (Fig. 9b(iii)), which is significantly smaller than the upwards trend at AF. In contrast to AF and SK, LT indicates a slight net negative slope with SO_2 decreasing on average by 0.03 $\mu g.m^{-3}.y^{-1}$ during the 21-year sampling period (Fig. 9c(iii)). The 19- and 21-year datasets at AF and LT also allowed for the calculation of decadal trends, which were determined to be 5.24 $\mu g.m^{-3}.dec^{-1}$ (average SO_2 concentrations from 1997 to 2006 were 7.20 $\mu g.m^{-3}$ and average SO_2 concentrations from 2007 to 2015 were 12.44 $\mu g.m^{-3}$) and 0.18 $\mu g.m^{-3}.dec^{-1}$ (average SO_2 concentrations from 1995 to 2004 were 1.64 $\mu g.m^{-3}$ and average SO_2 concentrations from 2005 to 2014 were 1.82 $\mu g.m^{-3}$), respectively, for the two decades. Trend lines are also presented for the periods characterised by increased (1995, 1997 to 2003) and decreased (2004 to 2008/2009) SO_2 concentrations at LT and AF. The average annual trend between 1997 and 2003 at AF was -0.53 $\mu g.m^{-3}.y^{-1}$, while the annual trend from 2004 to 2009 was 1.87 $\mu g.m^{-3}.y^{-1}$. At LT, the average annual SO_2 concentrations decreased by -0.26 $\mu g.m^{-3}.y^{-1}$ from 1995 to 2002, and increased by 0.37 $\mu g.m^{-3}.y^{-1}$ from 2003 to 2007.

3.2.2 Nitrogen dioxide (NO_2)

In Fig. 10, the measured NO_2 concentrations are related to the modelled NO_2 levels, while Table 2 presents the coefficients and RIW% of each of the independent variables included in the optimum MLR equation modelling NO_2 concentrations. Similar to SO_2, the relationships between measured and modelled NO_2 are also significantly improved when local, regional and global factors are included in the model at all three sites (Pane iii in Fig. 10a, b and c). However, inclusion of only global factors in the model yielded modelled NO_2 concentrations that mimicked the general measured NO_2 trend. The R^2 values, when only global factors are included, i.e. 0.171, 0.170 and 0.099 at AF, LT and SK, respectively, are enhanced to 0.498, 0468 and 0.362 at AF, LT and SK, respectively, when all factors are considered in the MLR model. The R^2 values, when all factors are included, especially AF and LT, can be considered relatively good correlations (Sheskin, 2003). In general, modelled NO_2 concentrations

corresponded well with the observed variances in measured NO_2 levels when all factors are included in the model at all three sites, with the exception of very high NO_2 concentrations.

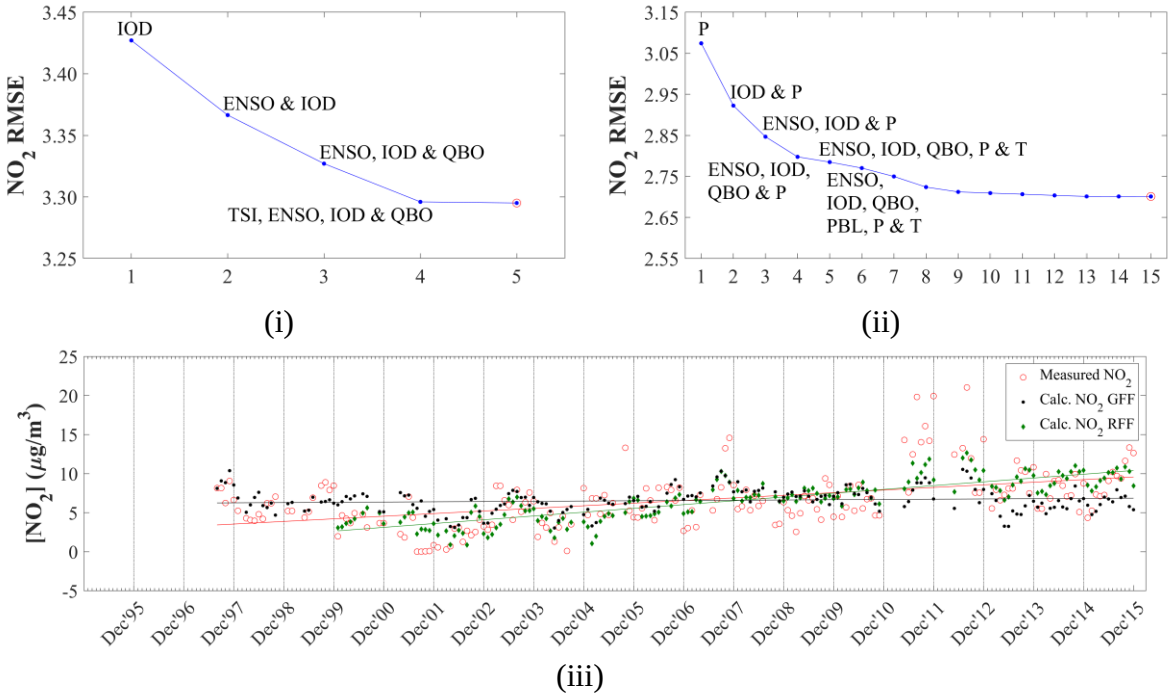

Figure 10a: (i and ii) RMSE differences between modelled and measured NO_2 concentrations as a function of the number of independent variables included in the model, as well as comparison between modelled and measured NO_2 levels (iii) for global force factors only (GFF), and for global, regional and local factors (RFF) determined for AF

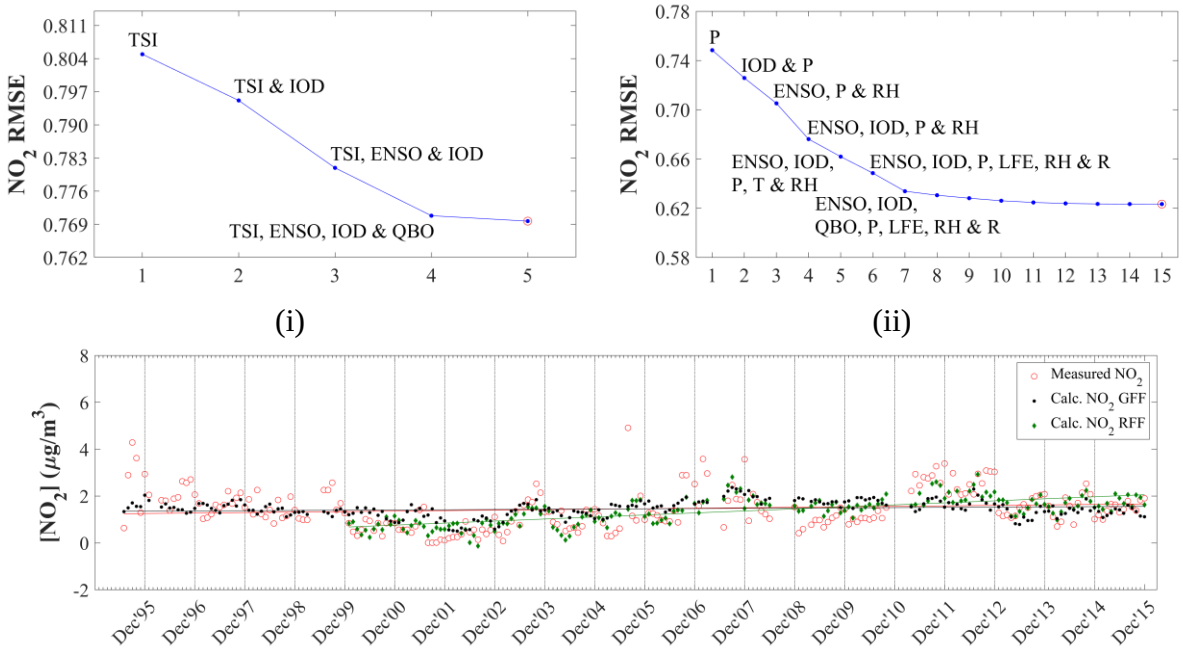

Figure 10b: (i and ii) RMSE differences between modelled and measured NO_2 concentrations as a function of the number of independent variables included in the model, as well as comparison between modelled and measured NO_2 levels (iii) for global force factors only (GFF), and for global, regional and local factors (RFF) determined for LT

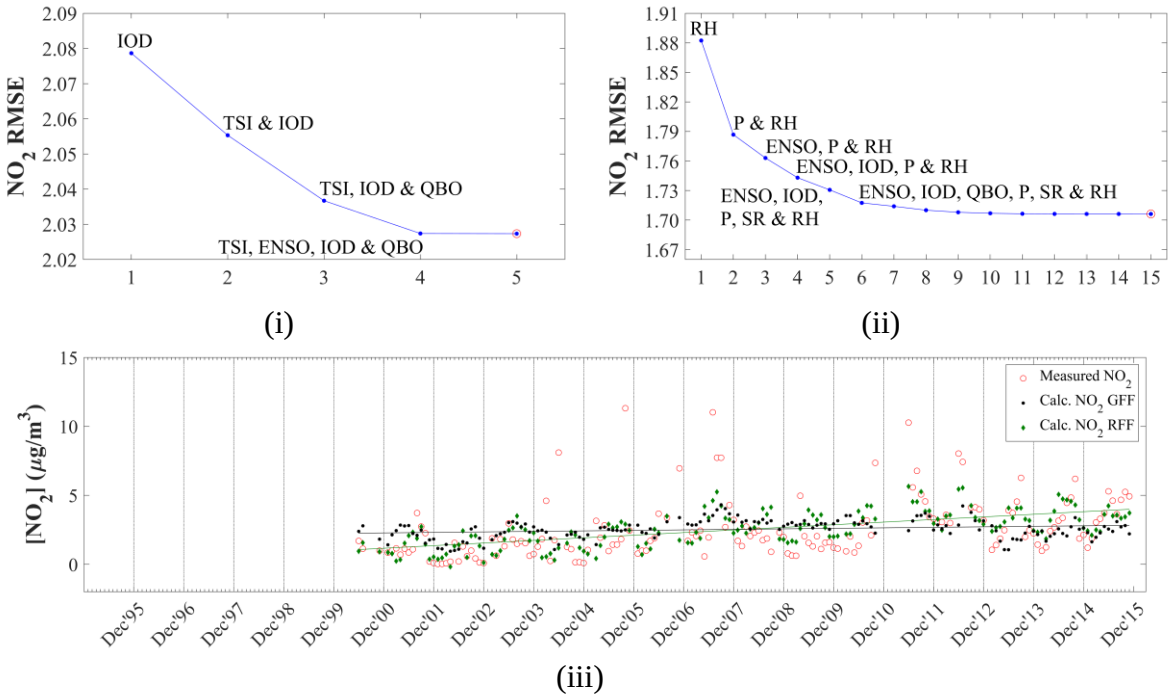

Figure 10c: (i and ii) RMSE differences between modelled and measured NO_2 concentrations as a function of the number of independent variables included in the model, as well as comparison between modelled and measured NO_2 levels (iii) for global force factors only (GFF), and for global, regional and local factors (RFF) determined for SK

Table 2: Regression coefficients (b) and relative important weight percentage (RIW%) of each independent variable included in the MLR model to calculate NO_2 concentrations at AF, LT and SK

	AF			**LT**			**SK**	
	b	***RIW%***		***b***	***RIW%***		***b***	***RIW%***
i) Global forcing factors								
IOD	4.718	65.3	TSI	-0.625	52.4	IOD	1.954	49.4
TSI	-1.156	15.1	IOD	0.723	25.5	TSI	-0.698	27.6
QBO	-0.037	10.5	QBO	-9.326×10^{-3}	11.8	QBO	-0.018	15.4
ENSO	-0.798	8.6	ENSO	-0.186	8.9	ENSO	-0.301	7.1
SAM	0.047	0.5	SAM	0.025	1.4	SAM	-8.422×10^{-3}	0.5
ii) Global, regional and local factors								
P	1.444×10^{-3}	53.7	P	1.512×10^{-5}	29.9	P	1.366×10^{-5}	29.8
IOD	3.861	17.8	RH	-0.056	16.6	RH	-0.090	20.6
RH	-0.036	6.0	IOD	0.916	15.2	IOD	1.032	7.1
QBO	-0.028	3.5	TSI	-0.186	8.4	DFE	1.473×10^{-7}	6.9
PBL	5.119×10^{-3}	3.2	ENSO	-0.327	6.8	R	3.833×10^{-3}	6.1
TSI	0.040	2.8	QBO	-9.368×10^{-3}	6.5	LFE	3.800×10^{-6}	4.1
ENSO	-0.965	2.7	R	2.482×10^{-3}	3.8	SR	0.073	4.0
Ws	0.075	2.7	DFE	-6.055×10^{-7}	2.9	T	-0.072	3.8
T	-0.415	2.5	PBL	-1.225×10^{-3}	2.5	TSI	-0.160	3.7
R	0.014	1.5	T	0.069	1.9	QBO	-0.015	3.6
LFE	-1.229×10^{-4}	1.0	LFE	-2.134×10^{-4}	1.8	ENSO	-0.441	3.1
DFE	-5.044×10^{-6}	0.9	Ws	0.107	1.5	Ws	0.313	3.0
SR	0.028	0.6	SAM	0.021	0.8	Wd	4.912×10^{-4}	1.9
Wd	-1.419×10^{-3}	0.6	SR	0.010	0.8	PBL	1.567×10^{-4}	1.8
SAM	-0.141	0.5	Wd	-1.587×10^{-4}	0.6	SAM	-0.025	0.5

The annual trend calculated from the slope of the 19-year measured NO_2 dataset at AF indicates an annual increase of 0.33 $\mu g.m^{-3}.y^{-1}$, while the 16-year measured NO_2 concentrations indicate an upwards trend of 0.19 $\mu g.m^{-3}.y^{-1}$ at SK. The trend line of measured NO_2 concentrations at LT also indicated a marginal increase, i.e. 0.02 $\mu g.m^{-3}.y^{-1}$ in NO_2 levels over the 21-year sampling period. Decadal trends were determined to be 3.43 $\mu g.m^{-3}.dec^{-1}$ (average NO_2 concentrations from 1997 to 2006 were 4.86 $\mu g.m^{-3}$ and average NO_2 concentrations from 2007 to 2015 were 8.29 $\mu g.m^{-3}$) and 0.45 $\mu g.m^{-3}.dec^{-1}$ (average NO_2 concentrations from 1995 to 2004 were 1.23 $\mu g.m^{-3}$ and average NO_2 concentrations from 2005 to 2014 were 1.68 $\mu g.m^{-3}$), respectively, for the two decades. Trend lines were also calculated for the periods coinciding with increases and decreases in measured NO_2 concentrations at AF and LT. The average

annual trend between 1997 and 2003 at AF was -0.26 $\mu g.m^{-3}.y^{-1}$, while the annual trend from 2004 to 2009 was 0.37 $\mu g.m^{-3}.y^{-1}$. At LT, the average annual NO_2 concentrations decreased by -0.29 $\mu g.m^{-3}.y^{-1}$ from 1995 to 2002, and increased by 0.28 $\mu g.m^{-3}.y^{-1}$ from 2003 to 2007. Similar to SO_2, the slopes of the linear regression trend lines for the measured NO_2 concentrations and the modelled NO_2 levels when all the factors are included in the model are exactly the same at AF, LT and SK (Pane iii in Fig. 10a, b and c). However, with the exception of LT, the slopes of the trend lines of NO_2 levels calculated including only global factors in the model did not correspond with the trend lines of the measured NO_2 concentrations, indicating the significance of local and regional factors on measured NO_2 concentrations (Pane iii in Fig. 10a, b and c).

The RMSE differences between the modelled and measured NO_2 concentrations (Pane i Fig. 10a, b and c) indicated that the linear combination between most of the global force factors, i.e. IOD, TSI, QBO and ENSO, resulted in the largest decrease in RMSE when only global force factors were included. The RIW% listed in Table 2 for the optimum MLR equation, including only global factors, indicates that IOD (65.3% and 49.4%, respectively) was the most significant parameter at AF and SK, while TSI (52.4%) was the most important factor at LT. The inclusion of local, regional and global factors in the MLR model indicated that the interdependencies between P, IOD, QBO, ENSO and T at AF, P, RH, IOD, ENSO and T at LT, and P, RH, IOD and ENSO at SK, yielded the largest decrease in RMSE difference. The RIW% determined for each independent variable in the optimum MLR equation containing all parameters indicated the most important factors explaining variances in the dependent variable (i.e. NO_2 levels) were P (53.7%) and IOD (17.8%) at AF, P (29.9%), RH (16.6%) and IOD (15.5%) at LT, and P (29.8%) and RH (20.6%) at SK. It is evident from these interdependencies of the dependent variable and RIW% of parameters included in the MLR model that local and regional factors were more significant to NO_2 variability at AF, LT and SK, while global meteorological factors also contributed to variances in NO_2 levels.

Population growth made the most significant contribution to modelled NO_2 concentrations at all three sites, and not only at AF, as observed for SO_2. Therefore, the influence of increased population growth and associated anthropogenic activities is reflected in ambient NO_2 concentrations modelled for the entire north-eastern interior region. Therefore, the periods coinciding with decreased (up until 2002) and increased (2003 to 2007) NO_2 inter-annual variability can be attributed to similar variances in source contribution, as discussed above for SO_2, with regional circulation of air masses passing over major sources also influencing LT and SK (Fig. 2). However, the significant contribution of population growth to the modelled

NO_2 levels at two rural background sites (LT and SK) also points to increased household combustion associated with enlarged populations within rural communities being a major source of NO_2 in this part of South Africa. The influence of increased seasonal household combustion is also indicated by higher NO_2 concentrations determined in June and July at SK (Fig. 4), which also signifies the impacts of the growing rural communities in proximity of SK.

RH made the second most important contribution in explaining variances in modelled NO_2 concentrations at LT and SK, while it was the third most important factor at AF as indicated by RIW%. Therefore, RH can be considered the factor representing the influence of changes in local and regional meteorology at these sites. Although T was indicated as a factor included in the linear combination of parameters yielding the largest decrease in RMSE at AF and SK, its relative importance in explaining modelled variances is not indicated by its RIW% in Table 2. The strong negative correlation with RH is indicative of increased NO_2 corresponding with months (or years) when dry meteorological conditions prevail, i.e. winter and early spring months in the north-eastern interior of South Africa. As indicated in Fig. 4, higher NO_2 concentrations did correspond with dry months (August to November) associated with increased biomass burning. However, the model does not reflect significant contributions of the two parameters included in the model to represent biomass burning, i.e. LFE and DFE to NO_2 variability with relatively higher RIW% observed for DFE (6.9%) and LFE (4.1%) only at SK. Furthermore, higher annual average NO_2 concentrations observed in 2011 and 2012 (Fig. 7) at all the sites are also not explained by the MLR model.

3.2.3 Ozone (O_3)

Modelled and measured O_3 concentrations at AF, LT and SK are presented in Fig.11, while Table 3 presents the coefficients and the RIW% of independent variables considered in the optimum MLR equation. When only global factors are considered in the model, the linear combinations between ENSO, TSI, IOD and SAM at AF, ENSO, TSI and SAM at LT, and ENSO and IOD at SK resulted in the largest RMSE differences between measured and modelled O_3 levels. However, according to RIW% values calculated, the most significant global factor contributing to O_3 variability was ENSO at all three sites (84.1%, 41.8% and 96.7% at AF, LT and SK, respectively). The interdependencies between parameters when local, regional and global factors were included in the models, as well as the RIW% contributions of all factors included in the optimum MLR equation also indicated the significance of ENSO in

explaining variances in atmospheric O_3 concentrations at all three sites. Interdependencies between ENSO, IOD, PBL, LFE and R at AF, ENSO, PBL, T, RH and R at LT, and ENSO, PBL, T, RH and R at SK yielded the largest decrease in RMSE differences between measured and modelled O_3 levels, while RIW% indicated that the largest contributions made by factors explaining O_3 variability were ENSO (22.6%), R (14.6%) and Ws (10.1%) at AF, RH (23.1%), ENSO (16.8%) and T (10.5%) at LT, and T (24.6%), ENSO (19.5%), RH (11.3%) and DFE (10.1%) at SK when local, regional and global factors were included in the model.

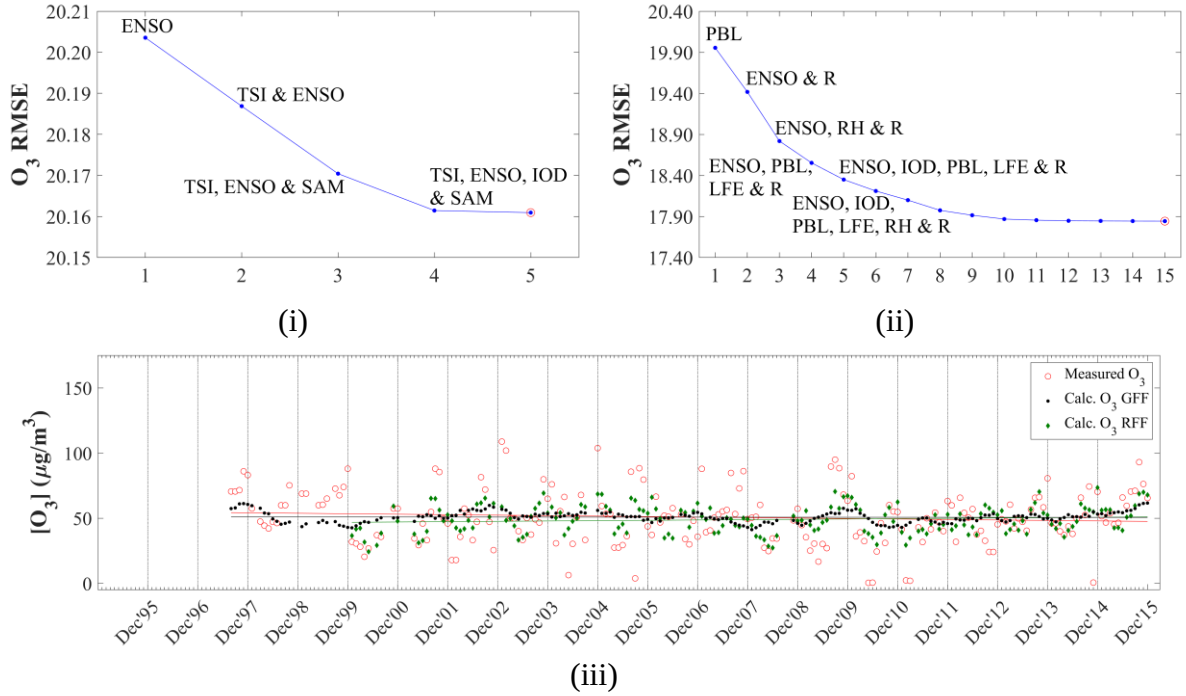

Figure 11a: (i and ii) RMSE differences between modelled and measured O_3 concentrations as a function of the number of independent variables included in the model, as well as comparison between modelled and measured O_3 levels (iii) for global force factors only (GFF), and for global, regional and local factors (RFF) determined for AF

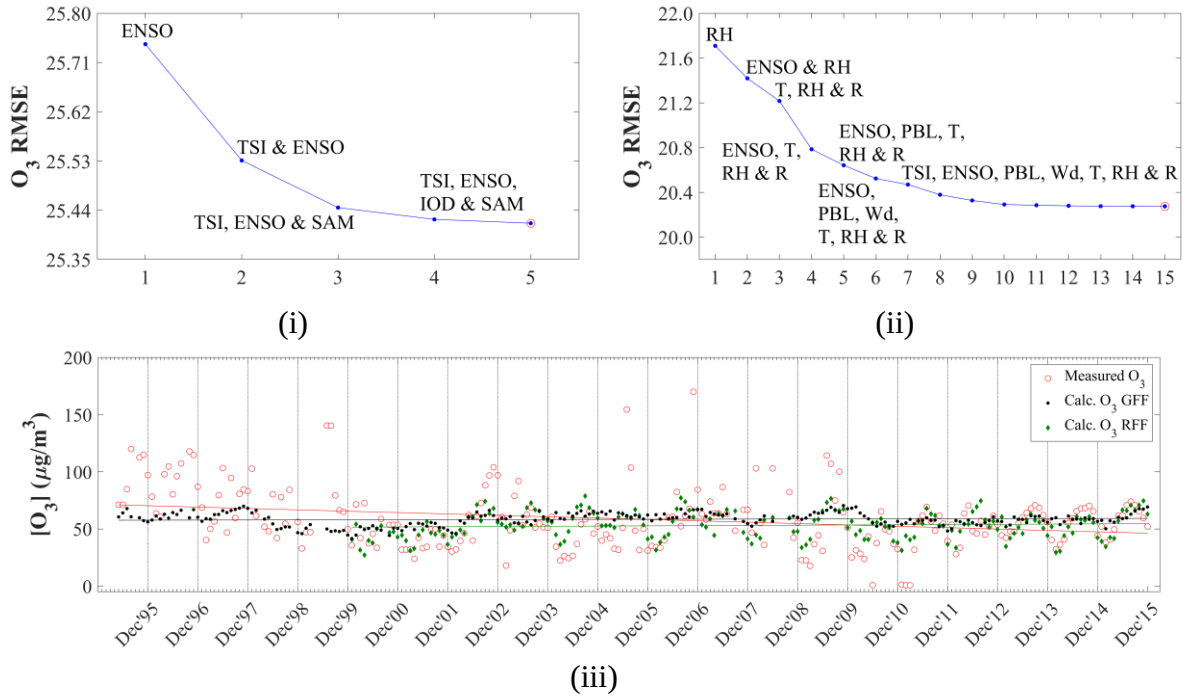

Figure 11b: (i and ii) RMSE differences between modelled and measured O_3 concentrations as a function of the number of independent variables included in the model, as well as comparison between modelled and measured O_3 levels (iii) for global force factors only (GFF), and for global, regional and local factors (RFF) determined for LT

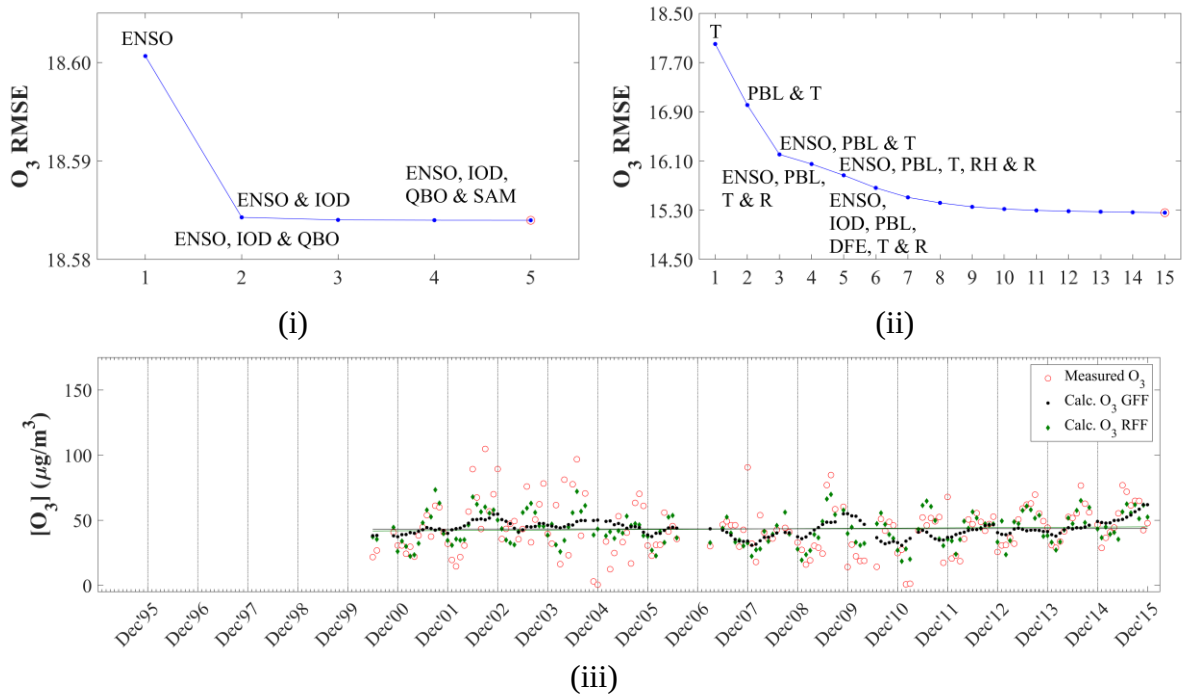

Figure 11c: (i and ii) RMSE differences between modelled and measured O_3 concentrations as a function of the number of independent variables included in the model, as well as comparison between modelled and measured O_3 levels (iii) for global force factors only (GFF), and for global, regional and local factors (RFF) determined for SK

Table 3: Regression coefficients (b) and relative important weight percentage (RIW%) of each independent variable included in the MLR model to calculate O_3 concentrations at AF, LT and SK

	AF			**LT**			**SK**	
	b	***RIW%***		***b***	***RIW%***		***b***	***RIW%***
i) Global forcing factors								
ENSO	4.923	84.1	ENSO	4.732	41.8	ENSO	8.353	96.7
SAM	-0.539	7.9	TSI	-8.397	36.3	IOD	-3.151	1.5
IOD	-2.337	5.2	SAM	-1.313	18.0	TSI	-0.034	1.5
TSI	1.844	2.5	IOD	-4.231	2.6	SAM	-0.020	0.2
QBO	0.010	0.2	QBO	0.044	1.2	QBO	-6.823×10^{-3}	0.1
ii) Global, regional and local factors								
ENSO	7.478	22.6	RH	-0.966	23.1	T	-5.378	24.6
R	0.122	14.6	ENSO	5.135	16.8	ENSO	7.458	19.5
Ws	5.988	10.1	T	-3.542	10.5	RH	-0.276	11.3
SR	0.474	9.4	DFE	1.070×10^{-5}	9.7	DFE	3.886×10^{-5}	10.1
PBL	2.287×10^{-3}	7.7	PBL	0.043	7.2	PBL	0.070	8.6
T	0.306	7.5	R	0.166	6.5	SR	1.376	8.2
LFE	9.076×10^{-4}	6.8	Wd	-0.087	4.7	R	0.100	4.3
Wd	-0.029	5.1	SR	0.340	4.5	LFE	-5.803×10^{-4}	3.7
RH	-0.257	4.7	IOD	4.900	4.4	Wd	-0.036	3.3
DFE	1.185×10^{-5}	4.2	Ws	-0.601	4.2	Ws	-2.536	2.8
IOD	-12.736	3.7	TSI	-4.195	3.2	IOD	-11.527	1.4
P	6.657×10^{-4}	1.2	LFE	-5.076×10^{-3}	2.3	P	3.013×10^{-5}	1.0
SAM	-0.339	1.2	P	-1.834×10^{-4}	1.5	TSI	1.670	1.0
TSI	-2.989	0.6	SAM	0.101	0.9	QBO	0.038	0.1
QBO	0.018	0.4	QBO	0.031	0.1	SAM	-0.279	0.1

The significant contribution of ENSO on variances of the dependent variable (modelled O_3 concentrations) is evident at all three sites, with RIW% indicating ENSO to be the major factor at AF, and the second most important factor at LT and SK when local, regional and meteorological factors are included in the model. Therefore, inter-annual variability in O_3 concentrations can most likely be attributed to ENSO cycles. El Niño periods are associated with drier and warmer conditions in the South African interior, which are conducive to O_3 formation, while cloudy and increased rainfall conditions related to La Niña hinder O_3 production (Balashov et al., 2014). Balashov et al. (2014) indicated that surface O_3 concentrations on the South African Highveld are sensitive to ENSO, with the El Niño period amplifying O_3 formation. The influence of local and regional meteorological conditions is also

indicated by the substantial contributions of R and Ws at AF, as well as T and RH at LT and SK on modelled O_3 levels. At LT, RH made the most substantial contribution to the dependent variable, while T made the most significant contribution to modelled O_3 levels. The negative correlation to T and RH at LT and SK is indicative of higher O_3 concentrations corresponding with drier colder months, as indicated in Fig. 5. Laban et al. (2018) indicated the significance of RH to surface O_3 concentrations in the north-eastern part of South Africa through the statistical analysis of *in situ* O_3 measurements conducted in this region, with RH also negatively correlated to surface O_3 levels. The positive correlation to R and Ws at AF reflects higher O_3 concentrations measured during late spring and summer at AF, i.e. October to January, which is a period associated with increased rainfall and less stable meteorological conditions (Fig. 5). The influence of regional open biomass burning during late winter and spring (August to November) on surface O_3 concentrations in this part of South Africa is indicated by the relatively significant contribution of DFE on modelled O_3 concentrations at LT and SK. A recent paper reporting tropospheric O_3 levels measured at four sites in the north-eastern interior of South Africa indicated that O_3 is a regional problem, with O_3 concentration measured at these four sites being similar to levels thereof measured at AF, LT and SK (Laban et al., 2018). A time series of O_3 levels measured from 2010 to 2015 at one of the sites presented by Laban et al. (2018) also indicated higher O_3 concentration corresponding to drier years associated with the ENSO cycle.

As indicated in Fig. 8, inter-annual O_3 concentrations at LT decreased from 1995 to 2001, which corresponded to the period when SO_2 and NO_2 concentrations decreased, as discussed in section 3.1. This period of inter-annual decrease in O_3 levels is not reflected in the statistical model. Since LT is a rural background site with low NO_x emissions, it can be considered to be located in a NO_x-limited O_3 production regime where O_3 concentrations correspond with NO_x concentrations, i.e. increase/decrease with increasing/decreasing NO_x. Therefore, the decrease in O_3 concentrations from 1995 to 2001 can be attributed to decreasing NO_2 concentrations during this period, and the factors influencing NO_2 concentrations at LT, i.e. mainly population growth, as discussed above (section 3.2.2).

The comparisons between modelled and measured O_3 concentrations (Pane iii in Fig. 11a, b and c) also indicated, as observed for SO_2 and NO_2, that the correlations are significantly improved when local, regional and global factors are included in the model. The R^2 values, when only global factors are included, i.e. 0.042, 0.048 and 0.094 at AF, LT and SK, respectively, are improved to 0.259, 0.241 and 0.389 at AF, LT and SK, respectively. These

correlations can be considered relatively weak, with the exception of a moderate correlation at SK (Sheskin, 2003). These generally weaker correlations can be attributed to the complexity associated with tropospheric O_3 chemistry. Tropospheric O_3 is a secondary atmospheric pollutant with several factors contributing to its variability. In addition, Laban et al. (2018) indicated the significance of the precursor species CO to surface O_3 concentrations in the north-eastern interior of South Africa, which were not measured at any of the sites and included in the model. Swartz et al. (2019) also compared passively derived O_3 concentrations with active O_3 measurements and illustrated limitations associated with the use of passive samplers to determine O_3 concentrations. However, the general trend of measured O_3 concentrations is mimicked by the modelled O_3 values when local, regional and global factors are included in the model, while the overall trend is weakly followed when only global factors are included. Higher and lower O_3 concentrations are underestimated by the MLR model.

The trend lines for the O_3 concentrations measured during the entire sampling periods indicate slight negative slopes at AF and LT (Fig. 11a(iii) and 11b(iii), respectively), and a small positive slope at SK (Fig. 11c(iii)). Annual average decreases in O_3 levels of 0.37 $\mu g.m^{-3}.y^{-1}$ and 1.20 $\mu g.m^{-3}.y^{-1}$ were calculated at AF and LT, respectively, while an average annual increase of 0.21 $\mu g.m^{-3}.y^{-1}$ was calculated at SK. However, in general, it seems that O_3 concentrations remained relatively constant at all three sites for the entire 19-, 21- and 16-year sampling periods at AF, LT and SK, respectively. Decadal trends of -3.46 (average O_3 concentrations from 1997 to 2006 were 52.56 $\mu g.m^{-3}$ and average O_3 concentrations from 2007 to 2015 were 49.10 $\mu g.m^{-3}$) and -9.15 $\mu g.m^{-3}.dec^{-1}$ (average O_3 concentrations from 1995 to 2004 were 63.16 $\mu g.m^{-3}$ and average O_3 concentrations from 2005 to 2014 were 53.01 $\mu g.m^{-3}$) were calculated for AF and LT, respectively, for two decades. Similar to SO_2 and NO_2, the slopes of the linear regression trend lines for the measured and modelled O_3 concentrations when local, regional and global factors are included are exactly the same at AF, LT and SK (Pane iii in Fig. 11a, b and c), which indicates that measured and modelled O_3 trends compares well in spite of low R^2 values. In addition, relatively good correlations are observed between the slopes of the trend lines of measured O_3 concentrations and modelled O_3 values calculated when only global factors are included at all the sites, signifying the influence of global factors, especially ENSO, as indicated above, on O_3 variability (Pane iii in Fig. 11a, b and c).

3.3 Contextualisation

In order to contextualise the long-term SO_2, NO_2 and O_3 concentrations measured with passive samplers at AF, LT and SK located in the north-eastern interior of South Africa, the statistical spread of the concentrations of these species determined during the entire sampling period at each site are compared to average concentrations of these species determined with passive samplers during other studies in South Africa and Africa, as well as regional sites in other parts of the world. SO_2, NO_2 and O_3 concentrations determined in this study are related to levels reported elsewhere in Fig. 12, 13 and 14, respectively.

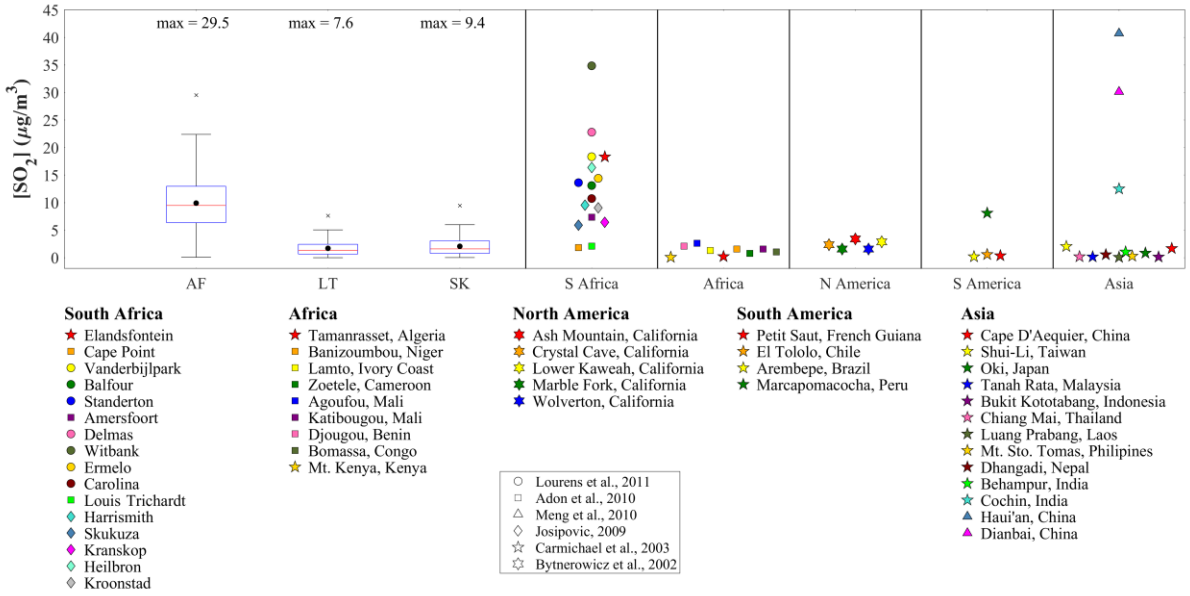

Figure 12: Statistical spread of SO_2 concentrations determined during the entire measuring period at each site compared to mean levels determined with passive samplers elsewhere. The red line of each box represents the median, the top and bottom edges of the box the 25th and 75th percentiles, respectively, the whiskers ± 2.7σ (99.3% coverage if the data has a normal distribution) and the black dots the average concentrations

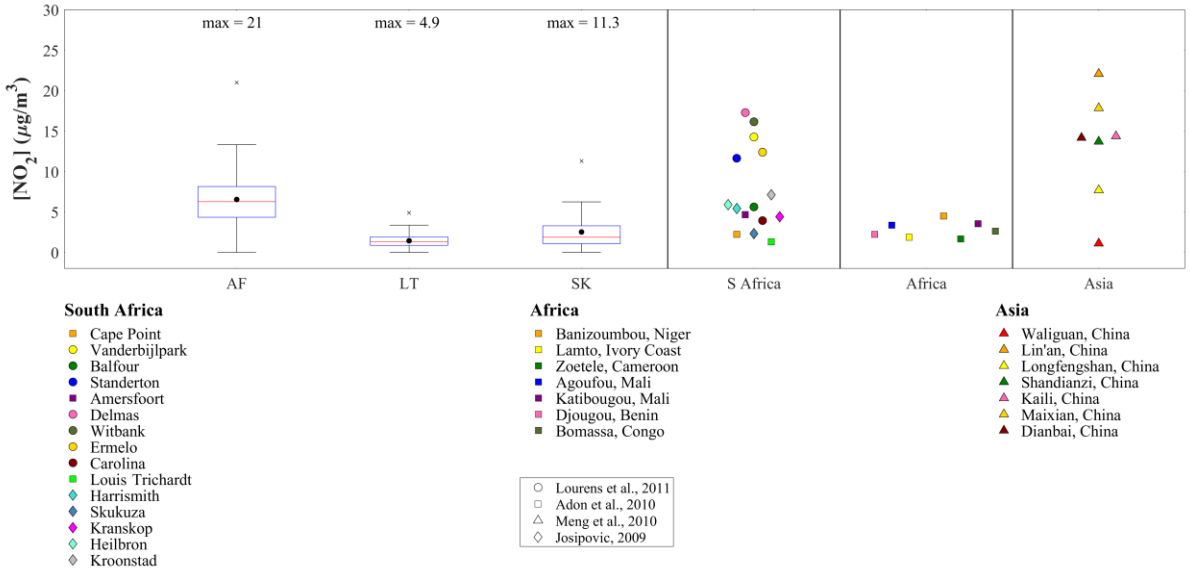

Figure 13: Statistical spread of NO_2 concentrations determined during the entire measuring period at each site compared to mean levels determined with passive samplers elsewhere. The red line of each box represents the median, the top and bottom edges of the box the 25th and 75th percentiles, respectively, the whiskers ± 2.7σ (99.3% coverage if the data has a normal distribution) and the black dots the average concentrations

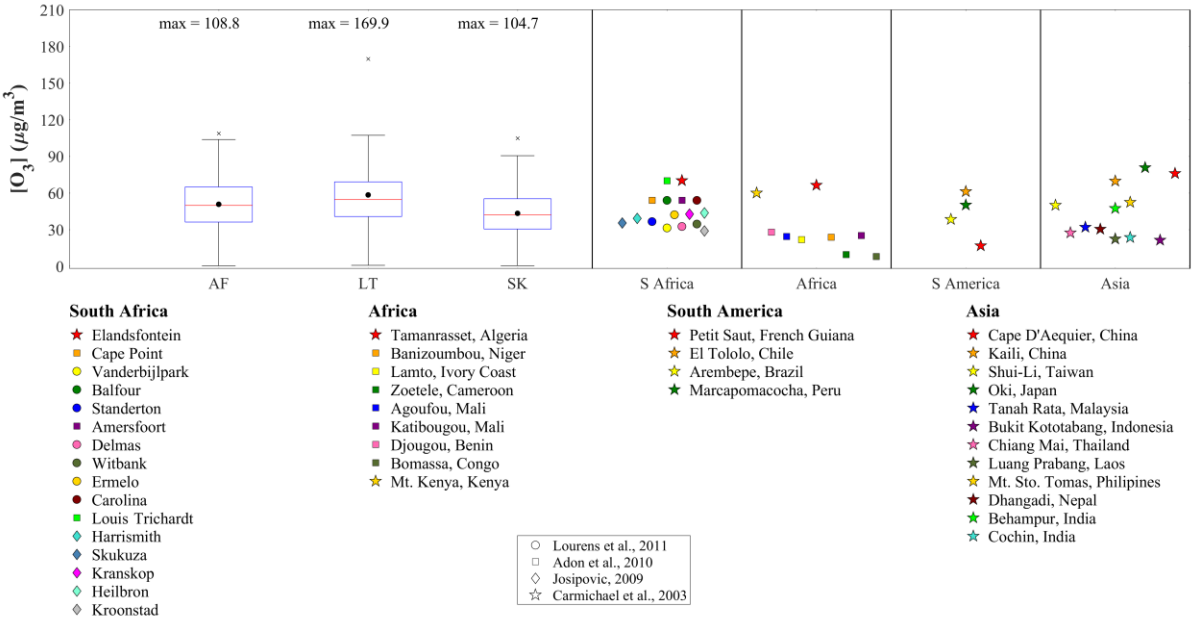

Figure 14: Statistical spread of O_3 concentrations determined during the entire measuring period at each site compared to mean levels determined with passive samplers elsewhere. The red line of each box represents the median, the top and bottom edges of the box the 25th and 75th percentiles, respectively, the whiskers ± 2.7σ (99.3% coverage if the data has a normal distribution) and the black dots the average concentrations

As expected, the average and median SO_2 concentrations determined at the industrially impacted AF (9.91 μg.m^{-3} and 9.48 μg.m^{-3}, respectively) site were higher compared to average and median SO_2 levels determined at the rural background sites LT (1.70 μg.m^{-3} and 1.35 μg.m^{-3}, respectively) and SK (2.07 μg.m^{-3} and 1.60 μg.m^{-3}, respectively) for the entire sampling period at each site. Geospatial maps of SO_2 column amount in the planetary boundary layer and NO_2 tropospheric column density averaged over the period 2005 to 2015 over southern Africa (Fig. A4 and A5 respectively) indicate higher average SO_2 and NO_2 concentrations being observed over the region where AF is located. Much lower average SO_2 and NO_2 concentrations are observed over the northernmost parts of the country, where LT is located, as well as the western region where SK is situated. Therefore, the influence of coal-fired power stations on SO_2 (and NO_2) levels measured at AF is evident. The average SO_2 levels at AF were similar to average SO_2 concentrations determined at other sites located in the Mpumalanga Highveld, for which the measurement period was from August 2007 to July 2008 (Lourens et al., 2011). However, the average SO_2 level at AF was significantly lower than the mean SO_2 levels at Elandsfontein, Delmas and Witbank. Elandsfontein and Delmas are situated

within closer proximity to major industrial activities in the Mpumalanga Highveld, while Witbank is a relatively large urban area with numerous large industrial point sources (Lourens et al., 2011). In addition, the average SO_2 concentrations at Vanderbijlpark – an urban area located within the highly industrialised Vaal Triangle region – were also higher compared to levels thereof at AF. Average SO_2 concentrations determined at regional sites in South America and India, i.e. Marcapomacocha and Cochin, respectively, were also similar to mean SO_2 levels determined at AF (Carmichael et al., 2003). The measurement period of the Carmichael et al. (2003) study was 12 months, starting in September 1999 (Carmichael et al., 2003). SO_2 concentrations reported for two rural sites in China, i.e. Dianbai and Haui'an were similar to SO_2 levels determined at Witbank (Meng et al., 2010). Meng et al. (2010) presented results obtained during a two-year study that commenced in January 2007. The mean SO_2 concentrations determined at LT and SK were similar to average SO_2 concentrations determined at regional background sites in west- and central African sites (Carmichael et al., 2003; Adon et al., 2010), as well as mean SO_2 levels determined at most of the regional sites in North America – measured between May and November 1999, South America and Asia (Bytnerowicz et al., 2002; Carmichael et al., 2003). Adon et al. (2010) presented ambient SO_2, NO_2 and O_3 concentrations measured from 1998 to 2007 at Katibougou in Mali, Banizoumbou in Niger, Lamto in Ivory Coast and Zoetele in Cameroon. The measurement periods for Agoufou in Mali and Djougou in Benin was from 2005 to 2007, while for Bomassa in Congo measurements were reported between 1998 and 2006 (Adon et al., 2010).

Similar to SO_2, the mean and median NO_2 levels determined for the respective sampling periods at each site were higher at AF (6.56 $\mu g.m^{-3}$ and 6.29 $\mu g.m^{-3}$, respectively) compared to mean and median levels thereof at LT (1.45 $\mu g.m^{-3}$ and 1.32 $\mu g.m^{-3}$, respectively) and SK (2.54 $\mu g.m^{-3}$ and 1.89 $\mu g.m^{-3}$, respectively). Relatively higher NO_2 concentrations were determined at SK compared to LT, which can be attributed to the influence of growing rural communities on the border of the Kruger National Park (Maritz et al., 2019). The mean NO_2 concentrations at AF were lower compared to most of the average NO_2 levels determined at other sites located in the Mpumalanga Highveld within closer proximity to industrial sources, while being similar to mean NO_2 concentrations measured at Balfour and Carolina. In addition, average NO_2 levels at AF were also lower than average NO_2 concentrations determined in the Vaal Triangle (Lourens et al., 2011). Average NO_2 concentrations determined at rural and regional sites in China were higher than mean NO_2 levels at AF, with the exception of Longfengshan that had similar NO_2 concentrations to AF (Meng et al., 2010), which reflects the scale of atmospheric

pollution in China. The average NO_2 concentrations at LT and SK were also similar to mean NO_2 levels determined at regional sites in west- and central African sites (Carmichael et al., 2003; Adon et al., 2010), as well as a remote site (Waliguan) in China (Meng et al., 2010).

The statistical distribution of O_3 concentrations determined at AF, LT and SK indicates similar surface O_3 levels at all three sites with marginally higher O_3 concentrations determined at LT (58.44 $\mu g.m^{-3}$ and 54.67 $\mu g.m^{-3}$, respectively) compared to AF (50.77 $\mu g.m^{-3}$ and 49.84 $\mu g.m^{-3}$, respectively) and SK (43.36 $\mu g.m^{-3}$ and 42.20 $\mu g.m^{-3}$, respectively). Higher O_3 levels are expected at the rural background LT site due to decreased O_3 titration compared to polluted regions, while LT is also impacted by aged air masses passing over the Mpumalanga Highveld source region as previously indicated. However, the regional O_3 problem in the South Africa interior is reflected by high O_3 concentrations also measured at the industrially influenced AT site, as well as similar O_3 levels determined at other sites in the Mpumalanga Highveld (Lourens et al., 2011). Laban et al. (2018) attributed high regional O_3 concentrations in the north-eastern interior of South Africa to the influence of household combustion and widespread open biomass burning impacting this region. In addition, the influence of rural communities is also reflected by the slightly lower average O_3 levels at SK. O_3 concentrations measured at west- and central Africa sites were lower than South African O_3 levels (Adon et al., 2010), with the exception of Mt Kenya and a site in northern Africa that had similar O_3 concentrations (Carmichael et al., 2003). Similar O_3 concentrations were determined at the South American regional sites, except for Petit Saut that had lower O_3 concentrations (Carmichael et al., 2003). Average O_3 levels determined at some of the regional Asian sites were in the same range as O_3 concentrations over the interior of South Africa, while certain sites in Asia had lower mean O_3 levels (Carmichael et al., 2003).

4. Summary and conclusions

In this study, long-term trends of atmospheric SO_2, NO_2 and O_3 concentrations measured with passive samplers at three sites located in the north-eastern interior of South Africa are presented. This paper illustrates the value of low-cost atmospheric sampling techniques in order to obtain long-term data, especially for regions restricted by logistical accessibility and limited capacity. A 19-year (1997 to 2015), 21-year (1995 to 2015) and 16-year (2000 to 2015) dataset for AF, LT and SK could be evaluated. Long-term temporal trends indicated seasonal and inter-annual variability at all three sites, which could be ascribed to changes in meteorological

conditions and/or variances in source contribution. Inter-annual variability indicated periods up until 2003/2004 and 2002 during which SO_2 and NO_2 concentrations, respectively, decreased, followed by periods during which SO_2 and NO_2 levels increased up until 2009 and 2007, respectively. These long-term trends were assessed with an MLR model in order to establish the influence of sources, as well as local, regional and global meteorology on atmospheric SO_2, NO_2 and O_3 concentrations.

Interdependencies between local, regional and global parameters included in the statistical model indicated the influence of global meteorology on SO_2 variability at all three sites, especially at the rural background site LT. However, population growth was the most substantial factor in the statistical model at the industrially impacted AF site, while the significance of local and regional meteorology was also evident with T being the most significant factor at SK. The important contribution of population growth on modelled SO_2 levels at AF was indicative of the impact of increased anthropogenic activities and energy demand in the north-eastern interior of South Africa. Higher SO_2 concentrations associated with lower temperatures reflected the influence of pollution build-up during winter, while the influence of air masses passing over the source region is also evident at SK and LT. Although global parameters contributed to variances in NO_2 concentrations, local and regional factors made more substantial contributions to modelled NO_2 levels. The most significant factor explaining NO_2 variability at all three sites was population growth, while RH was the most important local and regional meteorological factor. Therefore, similar to SO_2, the influence of population growth and associated increases in anthropogenic activities in the north-eastern interior is also reflected in NO_2 levels, while the impacts of increased household combustion associated with growing rural communities are also evident, especially at SK. The negative correlation to RH indicates higher NO_2 levels associated with drier months, i.e. winter, which contribute to seasonal variances. ENSO was shown to make a significant contribution to modelled O_3 levels at all three sites, while the important influence of local and regional meteorological factors was also evident, especially through significant negative correlations with T and RH at SK and LT. Inter-annual O_3 variability in this part of South Africa can therefore most likely be attributed to ENSO cycles, while seasonal patterns are attributed changes in local and regional meteorology.

The decreases in SO_2 and NO_2 concentrations from 1995 were attributed to the implementation of mitigation policies by industries post the establishment of the new democracy in South Africa. However, these improvements were offset from 2002 due to rapid economic growth

associated with increased industrial activities, as well as the increase in population growth accompanied by higher energy demand. The 19-year trend lines for SO_2 and NO_2 at AF indicated an increase in SO_2 and NO_2 concentrations over the 19-year sampling period. In addition, an upwards trend in NO_2 levels was also evident at SK, signifying the influence of the growing rural communities on the border of the Kruger National Park. Marginal trends were observed for SO_2 at SK, as well as SO_2 and NO_2 at LT. Trend analysis of O_3 at all three sites indicated that O_3 concentrations remained relatively constant at all three sites for the entire 19-, 21- and 16-year sampling periods at AF, LT and SK, respectively.

As expected, SO_2 and NO_2 concentrations were higher at AF compared to levels thereof at the rural background sites LT and SK. SO_2 levels at AF were similar to levels of these species determined with passive samplers at other sites within the Mpumalanga Highveld with the exception of sites closer to the major industrial sources. NO_2 levels at AF were generally lower than NO_2 concentrations determined at sites within the source region, as well as than regional sites in China. SO_2 and NO_2 concentrations determined at LT and SK were similar to levels thereof determined with passive samplers at regional and rural sites in Africa and other parts of the world. The regional problem of O_3 in the interior of South Africa was also evident, with similar O_3 levels determined at all three sites.

Acknowledgements

The authors would like to thank the International Global Atmospheric Chemistry programme for endorsing the DEBITS programme, as well as Sasol and Eskom for financial support of the South African INDAAF project. Assistance with sample deployment and collection by Ms Carin van der Merwe is also acknowledged, as well as the site operators, who include: Memory Deacon at AF; Chris James at LT; and Navashni Govender, Walter Kubheka, Eva Gardiner and Joel Tleane at SK. The authors also thank the Atmospheric Research in Southern Africa and Indian Ocean (ARSAIO) programme established by the National Center for Scientific Research (CNRS) in France and the National Research Foundation (NRF) in South Africa.

References

Adon, M., Galy-Lacaux, C., Delon, C., Yoboue, V., Solmon, F. & Kaptue Tchuente, A. T. 2013. Dry deposition of nitrogen compounds (NO_2, HNO_3, NH_3), sulfur dioxide and ozone in west and central African ecosystems using the inferential method. *Atmospheric Chemistry and Physics,* 13**,** 11351-11374, doi: 10.5194/acp-13-11351-2013.

Adon, M., Galy-Lacaux, C., Yoboué, V., Delon, C., Lacaux, J. P., Castera, P., Gardrat, E., Pienaar, J. J., Al Ourabi, H., Laouali, D., Diop, B., Sigha-Nkamdjou, L., Akpo, A., Tathy, J. P., Lavenu, F. & Mougin, E. 2010. Long term measurements of sulfur dioxide, nitrogen dioxide, ammonia, nitric acid and ozone in Africa using passive samplers. *Atmospheric Chemistry and Physics,* 10**,** 7467-7487, doi: 10.5194/acp-10-7467-2010.

Balashov, N. V., Thompson, A. M., Piketh, S. J. & Langerman, K. E. 2014. Surface ozone variability and trends over the South African Highveld from 1990 to 2007. *Journal of Geophysical Research: Atmospheres,* 119**,** 20, doi: 10.1002/2013JD020555.

Bencherif, H., Diab, R. D., Portafaix, T., Morel, B., Keckhut, P. & Moorgawa, A. 2006. Temperature climatology and trend estimates in the UTLS region as observed over a southern subtropical site, Durban, South Africa. *Atmospheric Chemistry and Physics,* 6**,** 5121-5128, doi: 10.5194/acp-6-5121-2006.

Booyens, W., Beukes, J. P., Van Zyl, P. G., Ruiz-Jimenez, J., Kopperi, M., Riekkola, M.-L., Josipovic, M., Vakkari, V. & Laakso, L. 2019. Assessment of polar organic aerosols at a regional background site in southern Africa. *Submitted to Journal of Atmospheric Chemistry*.

Bytnerowicz, A., Tausz, M., Alonso, R., Jones, D., Johnson, R. & Grulke, N. 2002. Summer-time distribution of air pollutants in Sequoia National Park, California. *Environmental Pollution,* 118**,** 187-203, doi: 10.1016/S0269-7491(01)00312-8.

Carmichael, G. R., Ferm, M., Thongboonchoo, N., Woo, J.-H., Chan, L. Y., Murano, K., Viet, P. H., Mossberg, C., Bala, R., Boonjawat, J., Upatum, P., Mohan, M., Adhikary, S. P., Shrestha, A. B., Pienaar, J. J., Brunke, E. B., Chen, T., Jie, T., Guoan, D., Peng, L. C., Dhiharto, S., Harjanto, H., Jose, A. M., Kimani, W., Kirouane, A., Lacaux, J.-P., Richard, S., Barturen, O., Cerda, J. C., Athayde, A., Tavares, T., Cotrina, J. S. & Bilici, E. 2003. Measurements of sulfur dioxide, ozone and ammonia concentrations in Asia, Africa, and South America using passive samplers. *Atmospheric Environment,* 37**,** 1293-1308, doi: 10.1016/S1352-2310(02)01009-9.

Connell, D. W. 2005. *Basic concepts of environmental chemistry,* CRC Press.

Conradie, E. H., Van Zyl, P. G., Pienaar, J. J., Beukes, J. P., Galy-Lacaux, C., Venter, A. D. & Mkhatshwa, G. V. 2016. The chemical composition and fluxes of atmospheric wet deposition at four sites in South Africa. *Atmospheric Environment,* 146**,** 113-131, doi: 10.1016/j.atmosenv.2016.07.033.

Dhammapala, R. S. 1996. *Use of diffusive samplers for the sampling of atmospheric pollutants.* M.Sc, Potchefstroom University for CHE.

Draxler, R. R. & Hess, G. D. 2014. Description of the HYSPLIT_4 modelling system. 7 ed. Silver Spring, Maryland: Air Resources Laboratory.

Ferm, M. 1991. A Sensitive Diffusional Sampler. *IVL Report L91*. Göteborg, Sweden: Swedish Environmental Research Institute.

Fowler, D., Pilegaard, K., Sutton, M. A., Ambus, P., Raivonen, M., Duyzer, J., Simpson, D., Fagerli, H., Fuzzi, S., Schjoerring, J. K., Granier, C., Neftel, A., Isaksen, I. S. A., Laj, P., Maione, M., Monks, P. S., Burkhardt, J., Daemmgen, U., Neirynck, J., Personne, E., Wichink-Kruit, R., Butterbach-Bahl, K., Flechard, C., Tuovinen, J. P., Coyle, M., Gerosa, G., Loubet, B., Altimir, N., Gruenhage, L., Ammann, C., Cieslik, S., Paoletti, E., Mikkelsen, T. N., Ro-Poulsen, H., Cellier, P., Cape, J. N., Horváth, L., Loreto, F., Niinemets, Ü., Palmer, P. I., Rinne, J., Misztal, P., Nemitz, E., Nilsson, D., Pryor, S., Gallagher, M. W., Vesala, T., Skiba, U., Brüggemann, N., Zechmeister-Boltenstern, S., Williams, J., O'dowd, C., Facchini, M. C., De Leeuw, G., Flossman, A., Chaumerliac, N. & Erisman, J. W. 2009. Atmospheric composition change: Ecosystems–Atmosphere interactions. *Atmospheric Environment,* 43**,** 5193-5267, doi: 10.1016/j.atmosenv.2009.07.068.

Garstang, M., Tyson, P. D., Swap, R., Edwards, M., Kållberg, P. & Lindesay, J. A. 1996. Horizontal and vertical transport of air over southern Africa. *Journal of Geophysical Research Atmospheres,* 101**,** 16, doi: 10.1029/95JD00844.

He, J. & Bala, R. 2008. Draft Report on passive sampler inter-comparison under Malé declaration. *Malé Declaration on Control and Prevention of Air Pollution and its Likely Transboundary Effect for South Asia.* Singapore: National University of Singapore.

Hewitson, B. C. & Crane, R. G. 2006. Consensus between GCM climate change projections with empirical downscaling: precipitation downscaling over South Africa. *International Journal of Climatology,* 26**,** 1315-1337, doi: 10.1002/joc.1314.

ICDA (International Chromium Development Association) 2012. High carbon charge grade ferrochromium Statistics. *Statistical Bulletin 2012.* Paris, France: International Chromium Development Association.

ICDA 2013. Statistical Bulletin 2013 (based on 2012 data). International Chromium Development Association.

ISO Survey 2015. Available: http://www/iso/org/iso/iso-survey [Accessed 23 January 2017].

Inglesi-Lotz, R. & Blignaut, J. 2011. Estimating the price elasticity for demand for electricity by sector in South Africa. *South African Journal of Economic and Management Sciences, Vol 14, Iss 4, Pp 449-465 (2011)***,** 449, doi: 10.4102/sajems.v14i4.134.

Jaars, K., Beukes, J. P., Van Zyl, P. G., Venter, A. D., Josipovic, M., Pienaar, J. J., Vakkari, V., Aaltonen, H., Laakso, H., Kulmala, M., Tiitta, P., Guenther, A., Hellén, H., Laakso, L. & Hakola, H. 2014. Ambient aromatic hydrocarbon measurements at Welgegund, South Africa. *Atmospheric Chemistry and Physics Discussions,* 14**,** 7075-7089, doi: 10.5194/acp-14-7075-2014.

Josipovic, M. 2009. *Acidic deposition emanating from the South African Highveld: A critical levels and critical loads assessment.* PhD, University of Johannesburg.

Josipovic, M., Annegarn, H. J., Kneen, M. A., Pienaar, J. J. & Piketh, S. J. 2011. Atmospheric dry and wet deposition of sulphur and nitrogen species and assessment of critical loads of acidic

deposition exceedance in South Africa. *South African Journal Science,* 107**,** 10, doi: 10.4102/sajs.v107i3/4.478.

Kaufman, Y. J., Ichoku, C., Giglio, L., Korontzi, S., Chu, D. A., Hao, W. M., Li, R. R. & Justice, C. O. 2003. Fire and smoke observed from the Earth Observing System MODIS instrument - products, validation, and operational use. *International Journal of Remote Sensing,* 24**,** 1765-1781, doi: 10.1080/01431160210144741.

Kleynhans, E., Beukes, J. P., Van Zyl, P. G., Bunt, J., Nkosi, N. & Venter, M. 2017. The Effect of Carbonaceous Reductant Selection on Chromite Pre-reduction. *Metallurgical & Materials Transactions B,* 48**,** 827-840, doi: 10.1007/s11663-016-0878-4.

KMNI. 2016a. *monthly DMI HadISST1* [Online]. Available: http://climexp.knmi.nl/getindices.cgi?WMO=UKMOData/hadisst1_dmi&STATION=DMI_HadISST1&TYPE=i&id=someone@somewhere [Accessed 22 December 2016].

KMNI. 2016b. *monthly measured total solar irradiance* [Online]. Available: http://climexp.knmi.nl/getindices.cgi?WMO=PMODData/tsi&STATION=measured_total_solar_irradiance&TYPE=i&id=someone@somewhere [Accessed 22 December 2016].

Korhonen, K., Giannakaki, E., Mielonen, T., Pfüller, A., Laakso, L., Vakkari, V., Baars, H., Engelmann, R., Beukes, J. P., Van Zyl, P. G., Ramandh, A., Ntsangwane, L., Josipovic, M., Tiitta, P., Fourie, G., Ngwana, I., Chiloane, K. & Komppula, M. 2014. Atmospheric boundary layer top height in South Africa: measurements with lidar and radiosonde compared to three atmospheric models. *Atmospheric Chemistry and Physics,* 14**,** 4263-4278, doi: 10.5194/acp-14-4263-2014.

Kraha, A., Turner, H., Nimon, K., Reichwein Zientek, L. & Henson, R. K. 2012. Tools to support interpreting multiple regression in the face of multicollinearity. *Frontiers In Psychology,* 3**,** 1-16, doi: 10.3389/fpsyg.2012.00044.

Laakso, L., Vakkari, V., Virkkula, A., Laakso, H., Backman, J., Kulmala, M., Beukes, J. P., Van Zyl, P. G., Tütta, P., Josipovic, M., Pienaar, J. J., Chiloane, K., Gilardoni, S., Vignati, E., Wiedensohler, A., Tuch, T., Birmili, W., Piketh, S., Collett, K. & Fourie, G. D. 2012. South African EUCAARI measurements: seasonal variation of trace gases and aerosol optical properties. *Atmospheric Chemistry & Physics,* 12**,** 1847-1864, doi: 10.5194/acp-12-1847-2012.

Laban, T. L., Van Zyl, P. G., Beukes, J. P., Vakkari, V., Jaars, K., Borduas-Dedekind, N., Josipovic, M., Thompson, A. M., Kulmala, M. & Laakso, L. 2018. Seasonal influences on surface ozone variability in continental South Africa and implications for air quality. *Atmospheric Chemistry and Physics* 15491-15514, doi: 10.5194/acp-18-15491-2018.

Lacaux, J. P., Tathy, J. P. & Sigha, L. 2003. Acid wet deposition in the tropics: Two case studies using DEBITS measurements. *IGACtivities Newsletter of the International Global Atmospheric Chemistry Project.*

Lorenzo-Seva, U., Ferrando, P. J. & Chico, E. 2010. Two SPSS programs for interpreting multiple regression results. *Behavior Research Methods,* 42**,** 29-35, doi: 10.3758/BRM.42.1.29.

Lourens, A. S., Beukes, J. P., Van Zyl, P. G., Fourie, G. D., Burger, J. W., Pienaar, J. J., Read, C. E. & Jordaan, J. H. 2011. Spatial and temporal assessment of gaseous pollutants in the

Highveld of South Africa. *South African Journal of Science,* 107**,** 1-8, doi: 10.4102/sajs.v107i1/2.269.

Maritz, P., Beukes, J. P., Van Zyl, P. G., Liousse, C., Gardrat, E., Ramandh, A. & Mkhatshwa, G. V. 2019. Spatial, temporal and source assessments of organic and elemental carbon at DEBITS sites in South Africa. *Submitted to Environmental Monitoring and Assessment.*

Marshall, G. 2018. *An observation-based Southern Hemisphere Annular Mode Index* [Online]. United Kingdom. Available: http://www.nerc-bas.ac.uk/icd/gjma/sam.html [Accessed 28 August 2018].

Martins, J. J., Dhammapala, R. S., Lachmann, G., Galy-Lacaux, C. & Pienaar, J. J. 2007. Long-term measurements of sulphur dioxide, nitrogen dioxide, ammonia, nitric acid and ozone in southern Africa using passive samplers. *South African Journal of Science,* 103**,** 336-342.

Meng, Z.-Y., Xu, X.-B., Wang, T., Zhang, X.-Y., Yu, X.-L., Wang, S.-F., Lin, W.-L., Chen, Y.-Z., Jiang, Y.-A. & An, X.-Q. 2010. Ambient sulfur dioxide, nitrogen dioxide, and ammonia at ten background and rural sites in China during 2007–2008. *Atmospheric Environment,* 44**,** 2625-2631, doi: 10.1016/j.atmosenv.2010.04.008.

Meth, O. 2018. *New satellite data reveals the world's largest air pollution hotspot is Mpumalanga – South Africa* [Online]. Available: https://www.greenpeace.org/africa/en/issues/inspirethemovement/4202/new-satellite-data-reveals-the-worlds-largest-air-pollution-hotspot-is-mpumalanga-south-africa/ [Accessed 17 January 2019].

Monks, P. S., Granier, C., Fuzzi, S., Stohl, A., Williams, M. L., Akimoto, H., Amann, M., Baklanov, A., Baltensperger, U., Bey, I., Blake, N., Blake, R. S., Carslaw, K., Cooper, O. R., Dentener, F., Fowler, D., Fragkou, E., Frost, G. J., Generoso, S., Ginoux, P., Grewe, V., Guenther, A., Hansson, H. C., Henne, S., Hjorth, J., Hofzumahaus, A., Huntrieser, H., Isaksen, I. S. A., Jenkin, M. E., Kaiser, J., Kanakidou, M., Klimont, Z., Kulmala, M., Laj, P., Lawrence, M. G., Lee, J. D., Liousse, C., Maione, M., Mcfiggans, G., Metzger, A., Mieville, A., Moussiopoulos, N., Orlando, J. J., O'dowd, C. D., Palmer, P. I., Parrish, D. D., Petzold, A., Platt, U., Pöschl, U., Prévôt, A. S. H., Reeves, C. E., Reimann, S., Rudich, Y., Sellegri, K., Steinbrecher, R., Simpson, D., Ten Brink, H., Theloke, J., Van Der Werf, G. R., Vautard, R., Vestreng, V., Vlachokostas, C. & Von Glasow, R. 2009. Atmospheric composition change – global and regional air quality. *Atmospheric Environment,* 43**,** 5268-5350, doi: 10.1016/j.atmosenv.2009.08.021.

Mphepya, J. N., Galy-Lacaux, C., Lacaux, J. P., Held, G. & Pienaar, J. J. 2006. Precipitation Chemistry and Wet Deposition in Kruger National Park, South Africa. *Journal of Atmospheric Chemistry,* 53**,** 169-183, doi: 10.1007/s10874-005-9005-7.

Mphepya, J. N., Pienaar, J. J., Galy-Lacaux, C., Held, G. & Turner, C. R. 2004. Precipitation Chemistry in Semi-Arid Areas of Southern Africa: A Case Study of a Rural and an Industrial Site. *Journal of Atmospheric Chemistry,* 47**,** 24, doi: 10.1023/B:JOCH.0000012240.09119.c4.

Nathans, L. L., Oswald, F. L. & Nimon, K. 2012. Interpreting Multiple Linear Regression: A Guidebook of Variable Importance. *Practical Assessment, Research & Evaluation,* 17**,** 1-19.

NOAA. 2015a. *Climate Indices: Monthly Atmospheric and Ocean Time Series* [Online]. Available: https://www.esrl.noaa.gov/psd/data/climateindices/list/ [Accessed 22 December 2016].

NOAA. 2015b. *Monthly Atmospheric and SST Indices* [Online]. Available: http://www.cpc.ncep.noaa.gov/data/indices/ [Accessed 22 December 2016].

Rorich, R. P. & Galpin, J. S. 1998. Air quality in the Mpumalanga Highveld region, South Africa. *South African Journal of Science,* 94**,** 109.

Sheskin, D. J. 2003. *Handbook of Parametric and Nonparametric Statistical Procedures,* Boca Raton, Chapman and Hall/CRC Press.

Swartz, J.-S., Van Zyl Pieter, G., Beukes Johan, P., Labuschagne, C., Brunke, E.-G., Portafaix, T., Galy-Lacaux, C. & Pienaar Jacobus, J. 2019. Twenty-one years of passive sampling monitoring of SO_2, NO_2 and O_3 at the Cape Point GAW station, South Africa. *Submitted to Atmospheric Environment*.

Tiitta, P., Vakkari, V., Croteau, P., Beukes, J. P., Zyl, P. G. V., Josipovic, M., Venter, A. D., Jaars, K., Pienaar, J. J., Ng, N. L., Canagaratna, M. R., Jayne, J. T., Kerminen, V. M., Kokkola, H., Kulmala, M., Laaksonen, A., Worsnop, D. R. & Laakso, L. 2014. Chemical composition, main sources and temporal variability of PM_1 aerosols in southern African grassland. *Atmospheric Chemistry and Physics,* 14**,** 1909-1927, doi: 10.5194/acp-14-1909-2014.

Toihir, A. M., Portafaix, T., Sivakumar, V., Bencherif, H., Pazmiño, A. & Bègue, N. 2018. Variability and trend in ozone over the southern tropics and subtropics. *Annales Geophysicae,* 36**,** 381-404, doi: 10.5194/angeo-36-381-2018.

Tyson, P. D., Garstang, M. & Swap, R. 1996. Large-Scale Recirculation of Air over Southern Africa. *Journal of Applied Meteorology,* 35**,** 18, doi: 10.1175/1520-0450(1996)035<2218:LSROAO>2.0.CO;2.

Vet, R., Artz, R. S., Carou, S., Shaw, M., Ro, C.-U., Aas, W., Baker, A., Bowersox, V. C., Dentener, F., Galy-Lacaux, C., Hou, A., Pienaar, J. J., Gillett, R., Forti, M. C., Gromov, S., Hara, H., Khodzher, T., Mahowald, N. M., Nickovic, S., Rao, P. S. P. & Reid, N. W. 2014. A global assessment of precipitation chemistry and deposition of sulfur, nitrogen, sea salt, base cations, organic acids, acidity and pH, and phosphorus. *Atmospheric Environment,* 93**,** 3-100, doi: 10.1016/j.atmosenv.2013.10.060.

Westcott, G., Tacke, M., Schoeman, N. & Morgan, N. 2007. Impala Platinum Smelter, Rustenburg: An integrated smelter off-gas treatment solution. *The Journal of the Southern African Institute of Mining and Metallurgy,* 107**,** 7.

Appendix

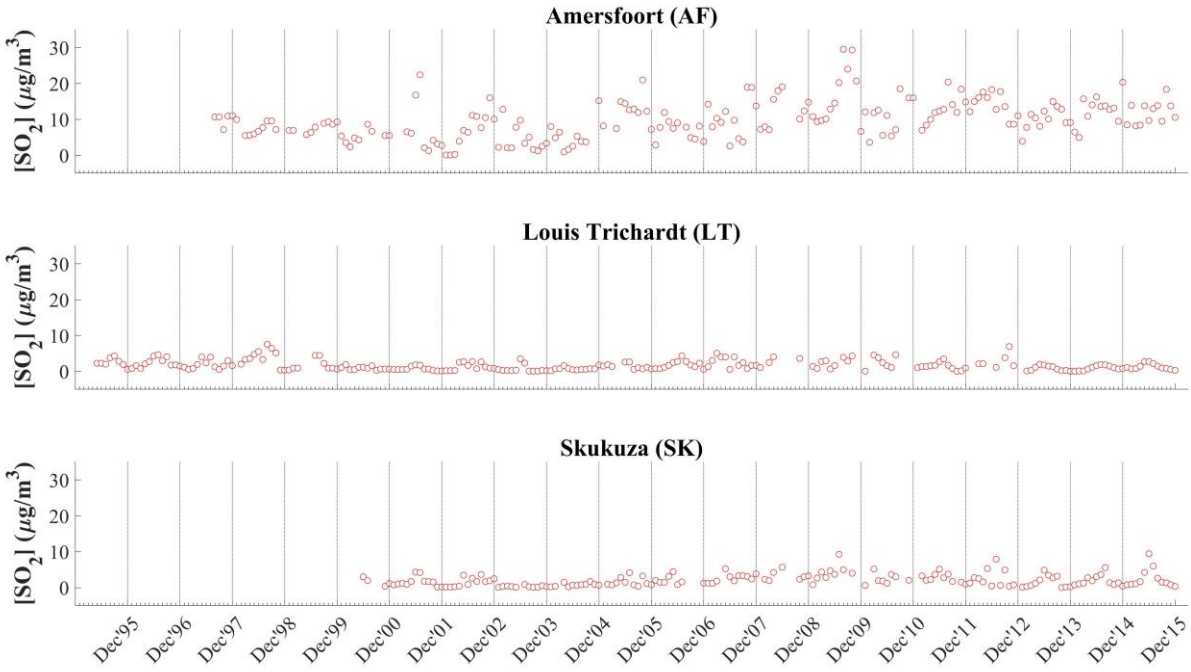

Figure A1: Time series of monthly average SO_2 concentrations measured at Amersfoort (AF), Louis Trichardt (LT) and Skukuza (SK) using passive samplers over the relevant measurement periods

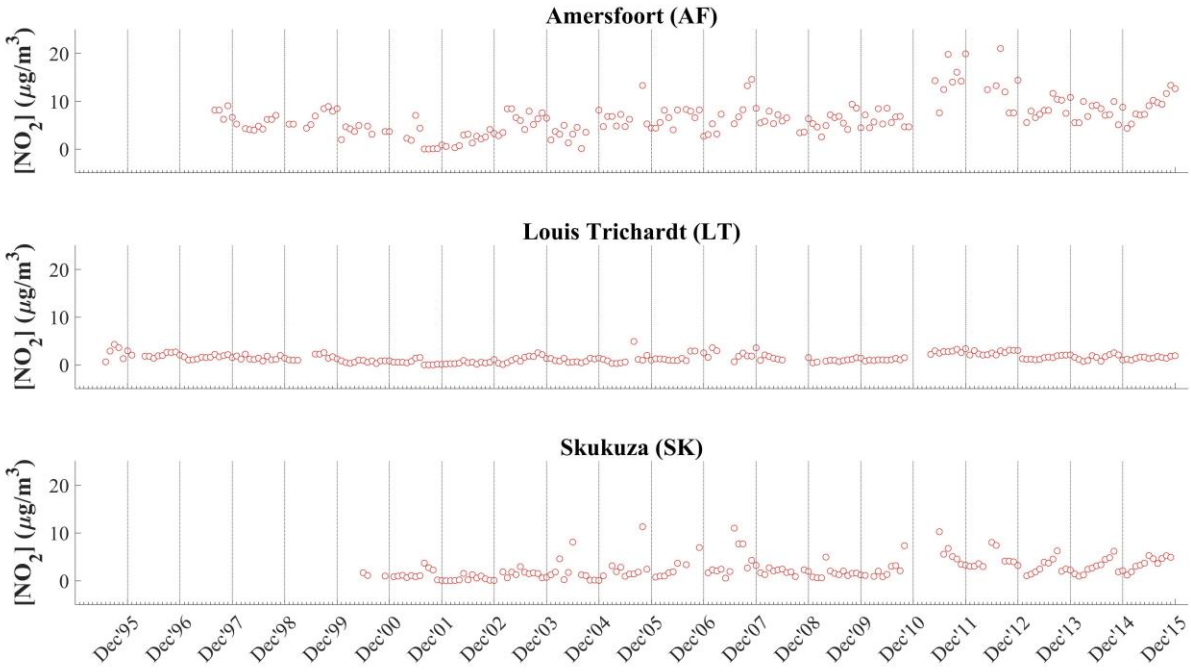

Figure A2: Time series of monthly average NO_2 concentrations measured at Amersfoort (AF), Louis Trichardt (LT) and Skukuza (SK) using passive samplers over the relevant measurement periods

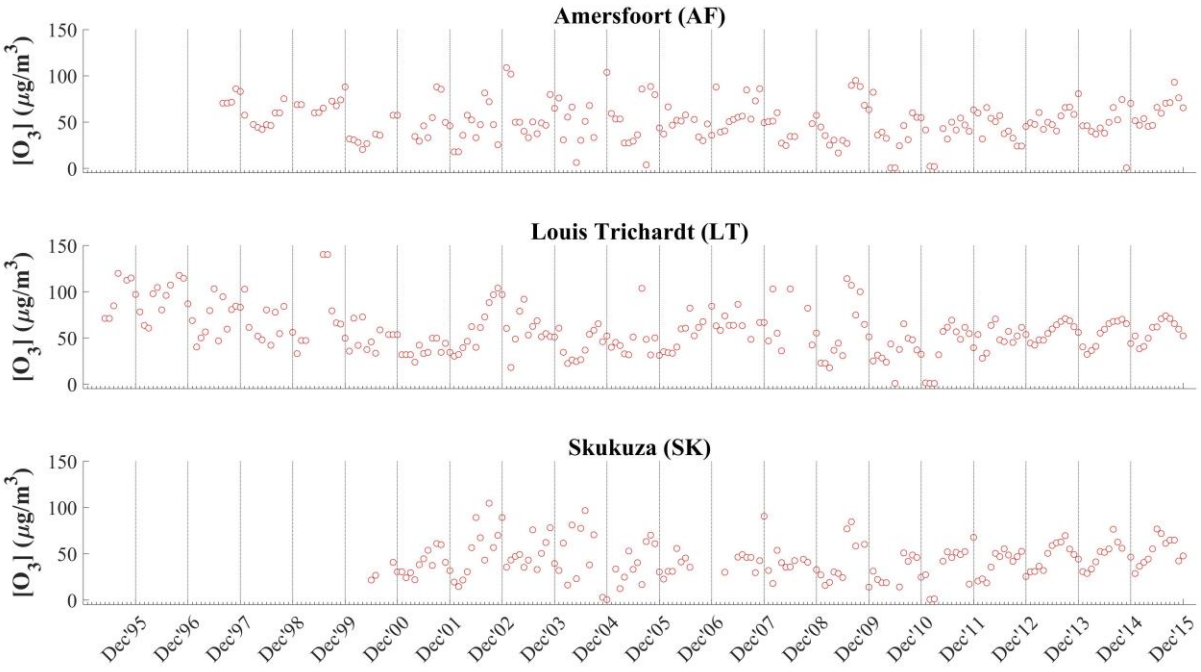

Figure A3: Time series of monthly average O_3 concentrations measured at Amersfoort (AF), Louis Trichardt (LT) and Skukuza (SK) using passive samplers over the relevant measurement periods

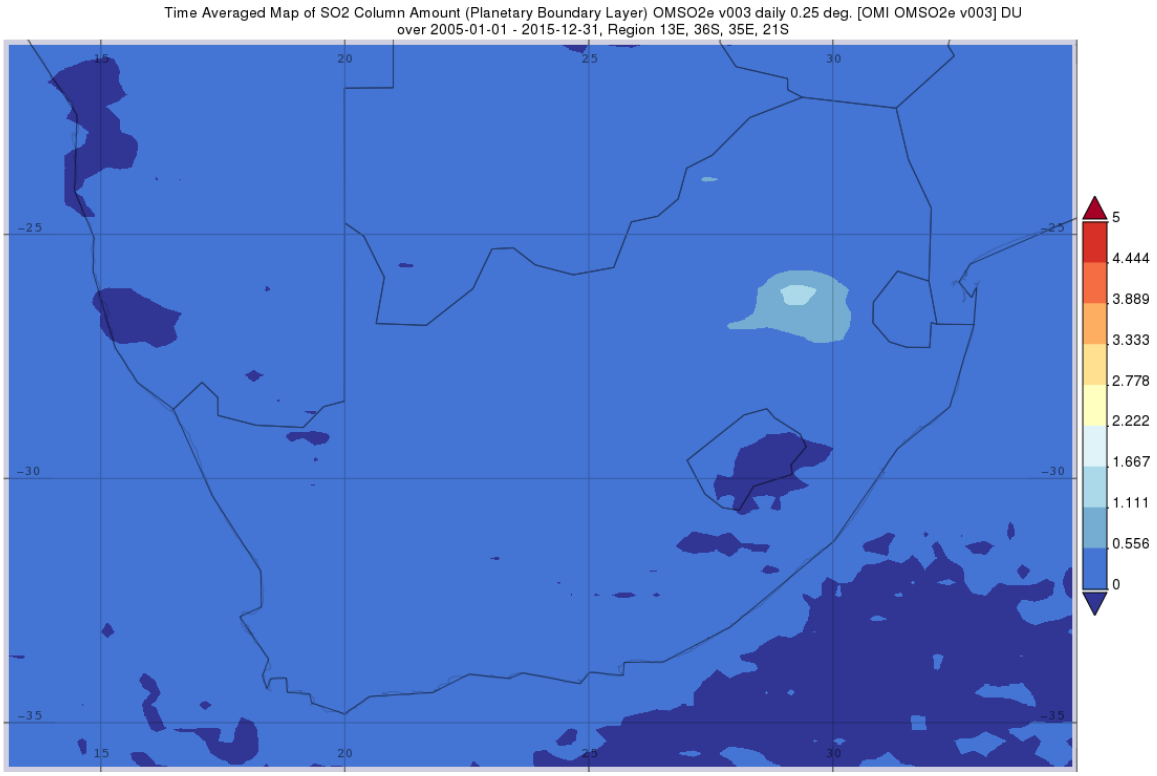

Figure A4: Geospatial map of southern Africa depicting the SO_2 column amount averaged over the period 2005 to 2015 obtained using the data from the NASA Giovanni satellite (https://giovanni.gsfc.nasa.gov/giovanni/)

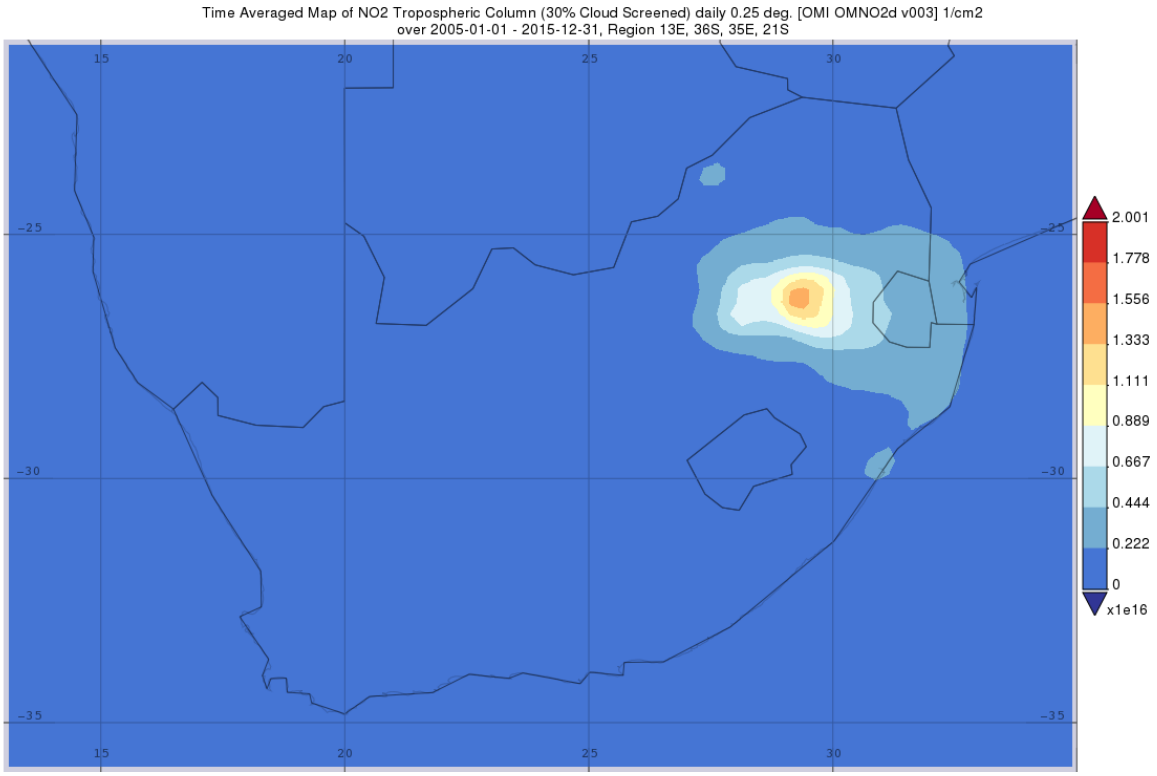

Figure A5: Geospatial map of southern Africa depicting the NO_2 tropospheric column density averaged over the period 2005 to 2015 obtained using the data from the NASA Giovanni satellite (https://giovanni.gsfc.nasa.gov/giovanni/)

CHAPTER 6

CHEMICAL COMPOSITION OF ATMOSPHERIC WET DEPOSITION AT THE CAPE POINT GAW SITE, SOUTH AFRICA

6.1 Author list, contributions and consent

J.-S. Swartz[1], P.G. Van Zyl[1], J.P. Beukes[1], C. Galy-Lacaux[2], C. Labuschagne[3], E.-G. Brunke[1], T. Mkololo[3] and J.J. Pienaar[1]

[1] Unit for Environmental Sciences and Management, North-West University, Potchefstroom Campus, Potchefstroom, 2520, South Africa

[2] Laboratoire d'Aérologie, 14, Av. Edouard Belin, 31400, Toulouse, France

[3] South African Weather Service, c/o CSIR, PO Box 320, Stellenbosch, 7599, South Africa

The bulk of the work was conducted by the first author, **J.-S. Swartz,** who was responsible for analysis, data processing, interpretation, and writing the research paper. Co-author contributions include: P.G. Van Zyl and J.P. Beukes were the promoters, who assisted in data interpretation and manuscript text editing. C. Labuschagne, E.-G. Brunke and T. Mkololo assisted with data collection. C. Galy-Lacaux and J.J. Pienaar made conceptual contributions.

All the co-authors on the article have been informed that the PhD will be submitted in article format and have given their consent.

6.2 Formatting and current status of article

The article was formatted in accordance with the journal specifications to which it will be submitted, i.e. *Atmospheric Environment*. The article is presented in the style, format and length required by the journal. The guide for authors that was followed in preparation of the

article is available at https://www.elsevier.com/journals/atmospheric-environment/1352-2310/guide-for-authors (Date of access: 29 January 2019). At the time when this PhD was submitted for examination, this article had not yet been submitted for review, but the intention is to submit it soon thereafter.

Chemical composition of atmospheric wet deposition at the Cape Point GAW site, South Africa

J.-S. Swartz[1], P.G. Van Zyl[1], J.P. Beukes[1], C. Galy-Laczaux[2], C. Labuschagne[3], E.-G. Brunke[1], T. Mkololo[3] and J.J. Pienaar[1]

[1] Unit for Environmental Sciences and Management, North-West University, Potchefstroom Campus, Potchefstroom, 2520, South Africa

[2] Laboratoire d'Aérologie, 14, Av. Edouard Belin, 31400, Toulouse, France

[3] South African Weather Service, c/o CSIR, P.O. Box 320, Stellenbosch 7599, South Africa

Correspondence to: P.G. van Zyl (Pieter.VanZyl@nwu.ac.za)

Abstract

The measurement of precipitation chemistry enables the assessment of the temporal and spatial evolution of the chemical composition of the atmosphere associated with atmospheric physical and chemical mechanisms. The aims of this study were to report the chemical composition of rainwater collected at a marine environment, i.e. the Cape Point Global Atmosphere Watch (CPT GAW) station from 2004 to 2012, as well as the associated wet deposition fluxes of ionic species. The volume weighted mean (VWM) concentrations of Na^+ and Cl^- were significantly higher compared to the VWM concentrations of other ionic species, as well as compared to the VWM concentrations thereof at the sites in the South African interior. The average pH of rainwater was slightly lower than the pH of unpolluted rainwater, mainly due to NO_3^- associated with the occasional influence of the Cape Town metropole. In contrast to the sites situated in the north-eastern South African interior, where anthropogenic SO_4^{2-} was the major constituent in rainwater, SO_4^{2-} at CPT GAW was entirely associated with marine air with no anthropogenic contribution. Sulphur and nitrogen deposition at CPT GAW were two orders of magnitude lower than sulphur and nitrogen deposition in the South African interior. It was also indicated that 94% of the chemical content at CPT GAW can be attributed to the marine source.

1. Introduction

Atmospheric pollutants are emitted into the atmosphere from various natural sources (e.g. marine, biogenic and crustal sources) and anthropogenic sources (e.g. fossil fuel combustion, traffic emissions and household combustion) (Mphepya et al., 2004). One of the mechanisms by which pollutants are removed from the atmosphere is through wet deposition (Josipovic et al., 2011). Many atmospheric pollutants are water soluble and are dissolved in cloud water and rain droplets (Waldman et al., 1992). The chemical analysis of rainwater enables the assessment of the temporal and spatial evolution of the chemical composition of the atmosphere, which reflects the numerous atmospheric physical and chemical mechanisms (Mphepya et al., 2006). Rainwater chemistry also reveals changes in atmospheric composition attributed to variances in natural and anthropogenic source contribution and/or meteorology (Vet et al., 2014). In addition, wet deposition can also be considered a source of nutrients (e.g. nitrogen, N and sulphur, S) to ecosystems or transport toxic species to the environment depending on its chemical composition (Duce et al., 2009).

Conradie et al. (2016) recently presented the chemical composition and fluxes of atmospheric wet deposition at four sites located in the interior of South Africa, which are considered to be regionally representative of semi-arid and savannah ecosystems. These sites form part of the South African component of the Deposition of Biogeochemically Important Trace Species (DEBITS) project, which was initiated in 1990 by the Global Atmosphere Watch (GAW) network of the World Meteorological Organisation (WMO) and currently endorsed by the International Global Atmospheric Chemistry (IGAC) programme. The main objectives of DEBITS entail long-term assessments of atmospheric biogeochemical species (mainly carbon (C), N and S species) in the tropics, as well as wet and dry deposition of these species (Lacaux et al., 2003). Also included in the South African DEBITS network is the globally significant Cape Point (CPT) Global Atmosphere Watch (GAW) station, which is a coastal site representative of southern-hemispherical marine air masses (Fig. 1). CPT GAW is, however, occasionally influenced by air masses passing over the urban-continental region (Fig.1). The aims of this study were to (i) assess the chemical composition of rainwater collected at CPT GAW from 2004 to 2012, (ii) determine S and N wet deposition fluxes, (iii) establish the major sources of ionic species, and (iv) relate ionic composition and wet deposition fluxes at CPT GAW to the South African interior in order to compliment that precipitation chemistry presented for the other South African DEBITS sites by Conradie et al. (2016).

2. Methods

2.1 Site Description

Detailed descriptions of the CPT GAW station are presented in a number of studies (Brunke et al., 2010; Labuschagne et al., 2018). As indicated in Fig. 1, the CPT GAW site (34°21'S, 18°29'E) is located at the southernmost tip of the peninsula on a cliff approximately 230 m above sea-level and approximately 60 km south of the Cape Town metropole (Brunke et al., 2004). The site is situated within a nature reserve within the Cape Floral Region Protected Areas (CFRPA), which has been afforded UNESCO world heritage status since 2004 (UNESCO, 2015). As mentioned, the site is a southern-hemispherical marine background site predominantly impacted by marine air masses, while it is also occasionally impacted by continental air masses passing over the Cape Town metropole as indicated by the overlay back trajectories presented in Fig. 1b.

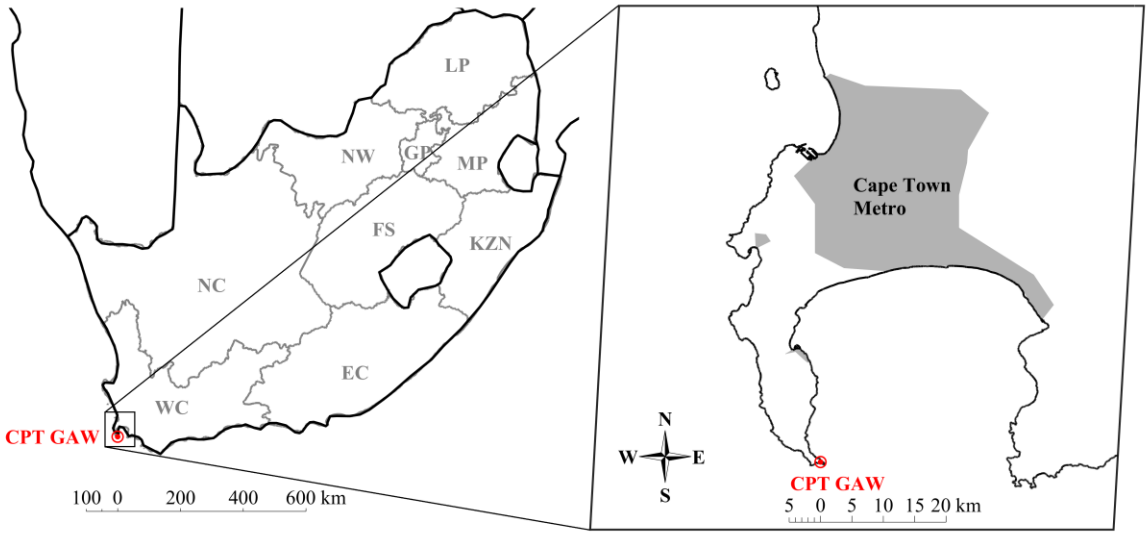

(a)

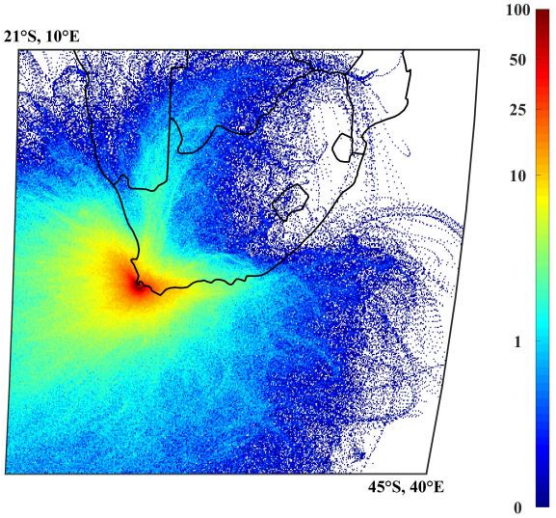

(b)

Figure 1: Regional map of South Africa indicating the location of the measurement station at Cape Point (34°21'S, 18°29'E) along with a zoomed-in map of the region around the site depicting the Cape Town metropole (a) and normalised overlaid hourly-arriving 72-hour back-trajectories (b) arriving at Cape Point during the measurement period 2004 to 2012 with the colour bar indicating overpass intensity over 0.2° by 0.2° grid cells

2.2 Back trajectory analysis

Air mass origins and their movement in the 72 hours prior to their arrival at the measurement station at CPT GAW is presented in Fig. 1b as normalised hourly arriving overlay back trajectories arriving at a height of 100m. These trajectories were calculated using the Hybrid

Single-Particle Langrangian Integrated Trajectory (HYSPLIT) model (version 4.8) that was developed by the National Oceanic and Atmospheric Administration (NOAA) Air Resources Laboratory (ARL) (Draxler and Hess, 2014). The necessary meteorological data was obtained from the GDAS archive of the National Centre for Environmental Prediction (NCEP) of the United States National Weather Service. Using fit for purpose mathematical programming software the back trajectories were overlaid on a map of southern Africa and the map area divided into 0.2° x 0.2° grid cells. The frequency with which trajectories pass over each grid cell is represented by a colour scale where dark blue indicates the lowest proportion, and dark red the highest.

2.3 Sampling procedures

Rainwater samples were collected on an event basis with an automated wet-only sampler similar to those used at the western and central African DEBITS sites (Galy-Lacaux et al., 2008) from January 2004 and December 2012. Although the field protocols of the WMO for precipitation chemistry measurements (WMO, 2004) were followed in general, rainwater sampling at CPT GAW did not entirely comply with WMO protocols. A limitation of the wet-only sampler used at the CPT GAW station was that the lid did not close automatically after a rain event. Furthermore, rain water samples were only collected during scheduled visits to the CPT GAW site due to logistical restraints. Therefore, some of the advantages associated with using a wet-only sampler, which include minimising contamination of rain samples and delays related to manual operations, were not realised. In addition, some rain samples also comprised composite samples of more than one rain event. However, in the absence of any other precipitation chemistry measurements for a marine environment in South Africa, as well as within the logistical limitations, rainwater samples collected at CPT GAW can be considered representative of rainwater chemistry for a southern-hemispherical marine background site.

An automatic precipitation sampler was designed for use within the IDAF network (Galy-Lacaux et al., 2008) and used for the collection of precipitation samples at CPT GAW. The sampler was equipped with a precipitation sensor that would control the cover of the sampler, opening when rain was detected, and hermetically sealing a single-use polyethylene bag in which the rain water was collected. The precipitation collection area was 225 cm^2. After a rain event, or as soon as practically possible, the collected rainwater was distributed between two

50 ml Greiner-type essay-tubes and placed in cold storage – either refrigerated (4°C) or frozen (-18°C) (Galy-Lacaux et al., 2008).

2.4 Analysis

The same analytical procedures were followed as presented by Conradie et al. (2016) for the four South African DEBITS sites in the interior of South Africa. In short, samples were unfrozen overnight and analysed immediately. Initial analysis entailed pH and conductivity measurements with an HI 255 combined meter (Hanna Instruments) utilising a low ionic strength electrode. A Dionex ICS 3000 ion chromatograph (IC) was used to determine cation and anion species, i.e. sodium (Na^+), ammonium (NH_4^+), potassium (K^+), calcium (Ca^{2+}), magnesium (Mg^{2+}), nitrate (NO_3^-), chloride (Cl^-), sulphate (SO_4^{2-}), as well as water-soluble organic acids (OA), including formic- (COO^-), acetic- (CH_3COO^-), propionic- ($C_2H_5COO^-$) and oxalic acid ($C_2O_4^{2-}$) in rainwater samples. Details of the IC analytical setup, as well as detection limits of these species are presented by Conradie et al. (2016).

2.5 Quality assurance / quality control

Data quality was ensured in accordance with the WMO Data Quality Objectives (DQO) stated in the WMO precipitation chemistry manual (WMO, 2004). All rainwater samples were visually inspected in order to identify visible contaminants, e.g. dust, insects and plant matter, which were removed by filtering the sample through a 0.2 μm filter (supplied by Sigma Aldrich) prior to chemical analysis. Any visible contamination was also recorded. All analytical methods utilised in rainwater analysis (IC, pH and conductivity measurements) were also verified bi-annually through participation in the inter-laboratory comparison study (LIS) of the WMO. The most recent results, i.e. the 58th LIS study of 2018, are presented in Fig. 2 as an example of the general performance of the analytical laboratory, t which indicate that the recovery of each ion in standard samples was between 95 and 105%. The ionic balance of each rain sample was also considered by calculating the ion difference (ID) with the following equation (WMO, 2004):

$$ID(\%) = 100 \times \left({(CE - AE)} \Big/ {(CE + AE)} \right) \quad 1$$

where AE is the total of the anions in μeqL^{-1} and CE is the total of the cations in μeqL^{-1}. Acceptance ranges for the ID, as indicated in the WMO (2004) report, were applied to all the rain samples collected in this study. Only samples that passed WMO ID% criteria are reported in this paper.

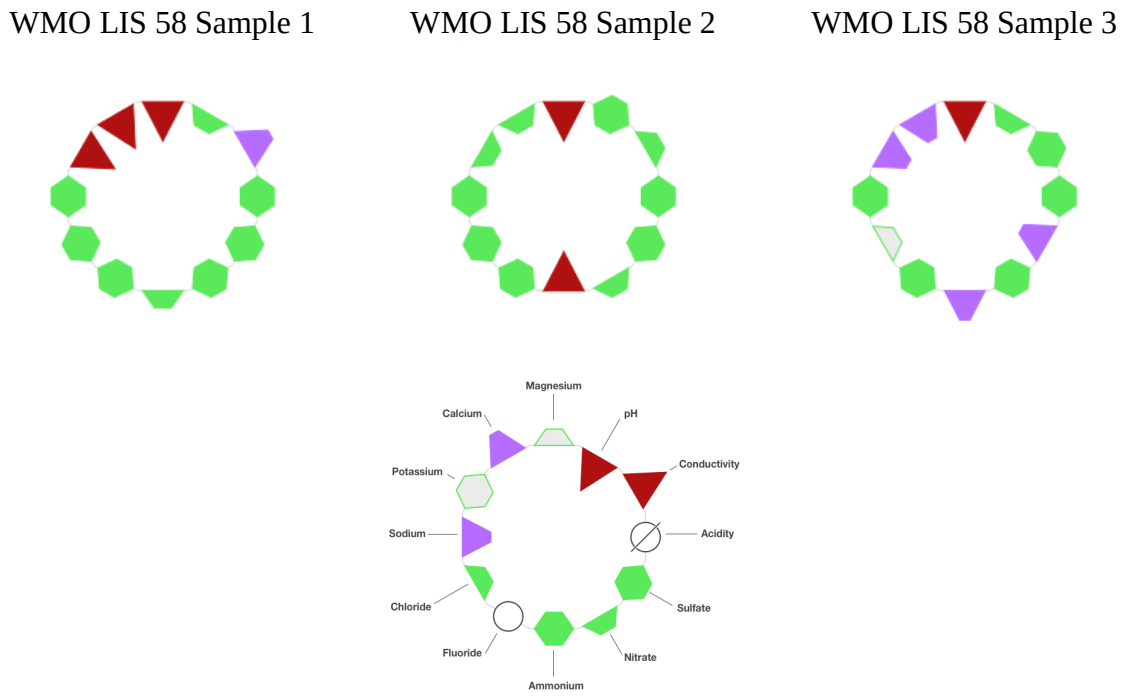

Figure 2: Results of the WMO LIS 58 study in July 2018 indicated by ring diagrams with a legend for the ring diagram indicated. Green hexagons indicate good results (measurements are within the interquartile range (IQR), defined as the 25th to 75th percentile or middle half (50%) of the measurements), green trapezoids indicate satisfactory results (measurements are within the range defined by median ± IQR/1.349), purple trapezoids indicate results not within the satisfactory category, but within a range defined by the median ± 2(IQR/1.349), and red triangles indicate that the results are unsatisfactory (measurements are outside the range defined by the median + 2(IQR/1.349)). Measurements below the detection limit are indicated by an open circle, while an open circle with a slash through indicates that no measurement was reported (Qasac-Americas, 2018). IQR/1.349 is the non-parametric estimate of the standard deviation, sometimes called the pseudo-standard deviation (Qasac-Americas, 2018)

In Table 1, the total numbers of rainwater samples collected for chemical analysis are presented. All these samples passed the WMO ID% criteria, were of sufficient volume (> 0.2 mm) and were not associated with any analytical errors. As mentioned previously, due to limitations associated with the wet-only samplers utilised at CPT GAW, as well as logistical

restraints related to sample collection, rainwater samples did not completely adhere to WMO protocols (e.g. some rainwater samples could contain an accumulation of several rain events). In addition, samples were only collected during the wet season at CPT GAW, i.e. May to October. Therefore, the percentage rainfall collected for the entire sampling period at CPT GAW, i.e. 43% is not within the WMO percentage total precipitation (%TP) acceptance range, i.e. %TP ≥ 70%. The %TP is the percentage of total rainfall depth measured associated with valid precipitation chemistry data. However, in the absence of any other rain chemistry measurements in this region, and within the logistical restraints associated with rainwater collection at CPT GAW, these rainwater samples could be considered representative of this marine ecosystem. Furthermore, the percentage of rainfall collected during the wet season represents 60% of total precipitation occurring during the wet season, which were the only samples considered in calculations during this study (i.e. 122 samples). In addition, the percentage of the samples that passed the WMO ID% criteria and were not discarded due to analytical errors were 100%, which is in the WMO %TP acceptance range and can be considered very good.

Table 1: Summary of wet deposition samples collected at CAT GAW from 2004 to 2012

	2004	***2005***	***2006***	***2007***	***2008***	***2009***	***2010***	***2011***	***2012***	***Total***
Number of samples collected (wet season)	10	15	13	16	14	16	12	8	18	122
Collected rainfall (wet season)	223.9	107.0	126.0	191.6	106.6	239.6	91.6	40.8	213.8	1340.9
Total rainfall (mm)	483.5	366.2	304.1	422.3	264.0	393.0	254.0	256.2	378.0	3121.3
Average rainfall (mm)										346.8
% TP	46.3	29.2	41.4	45.4	40.4	61.0	36.1	15.9	56.6	43.0

2.6 Calculations

Similar calculations than those conducted by Conradie et al. (2016) for the South African DEBITS sites in the interior were performed for rainwater samples collected at CPT GAW. The annual volume weighted mean (VWM) concentration of each ionic species was determined as follows (Conradie et al., 2016):

$$VWM(\mu eq.L^{-1}) = \sum_{i=1}^{N} C_i P_i \Big/ \sum_{i=1}^{N} P_i \qquad 2$$

where C_i and P_i representing the concentration ($\mu eq.L^{-1}$) of a given ion and the rain depth (mm) of each precipitation event, respectively, while N is the total number of rain samples (Table 1). Multiplying the calculated annual VWM with the total annual rain depth and the equivalent weight of the specific ion yields the annual wet deposition (WD) fluxes ($kg.ha^{-1}.yr^{-1}$) of each species (Galy-Lacaux et al., 2008). As indicated in the WMO guidance manual, the total annual rainfall amount includes rain depth of all events reported in the year and not only events utilised in the calculation of VWM ionic concentrations (WMO, 2004), which implies, among others, rain depth associated with rain samples collected during the wet season at CPT GAW. The average wet deposition fluxes for the entire sampling period were calculated using the average annual rainfall from 2004 to 2012 (Table 1). The H^+ concentrations were calculated from the measured pH values.

A general method utilised to estimate the contribution of sea salt to the ionic composition is to calculate the excess concentrations of K^+, Mg^{2+}, Ca^{2+}, Cl^- and SO_4^{2-} with respect to sea salt using Na^+ as a reference, i.e. assuming Na^+ was completely of marine origin. Reference ratios of these species in relation to Na^+ in seawater, as presented by Keene et al. (1986), were used. The sea salt fractions (ssf) of any of these species, X, with respect to Na^+ are:

$$[X]_{ssf} = [Na^+]_{rain} \times \left([X] \Big/ [Na^+] \right)_{seawater} \qquad 3$$

where $[X]_{ssf}$ is the sea salt contribution of X, $[Na^+]_{rain}$ is the Na^+ concentration in rain, and $[X / Na^+]_{seawater}$ is the seawater concentration ratio (Keene et al., 1986). The non-sea salt fraction (nssf) of X is then calculated by:

$$[X]_{nssf} = [X]_{rain} - ssf_X \qquad 4$$

where $[\ X\ ]_{rain}$ is the concentration of species X in rainwater. The seawater enrichment factors (EF) of species X with regard to the reference ratio were also calculated as follows (Quiterio et al., 2004; Chao and Wong, 2002):

$$EF_X = \left(X / [\ Na^+\ ] \right)_{rain} \Big/ \left(X / [\ Na^+\ ] \right)_{seawater} \quad 5$$

Water-soluble OA in wet deposition was considered as reference species for biomass burning (Helas and Pienaar, 1996; Conradie et al., 2016). Neutralisation of sulphuric and nitric acids by base cations can be evaluated by calculating the neutralisation factors (NF) with the following equation (Laouali et al., 2012; Possanzini et al., 1988):

$$NF_X = X / (SO_4^{2-} + NO_3^-) \quad 6$$

where X is the base cation of interest, i.e. Mg^{2+}, Ca^{2+} and NH_4^+.

3. Results and discussion

3.1 Ionic composition

In Table 2, the VWM concentrations and wet deposition fluxes of each ionic species, together with the averaged pH and electrical conductivity (EC) values determined at CPT GAW from 2004 to 2012, are listed. The water-soluble organic acids (OA) are presented as the sum of VWM concentrations of COO^-, CH_3COO^-, $C_2H_5COO^-$ and $C_2O_4^{2-}$. The rainwater chemistry and wet deposition fluxes reported by Conradie et al. (2016) for the four South African DEBITS sites in the interior from 2009 to 2014 are also presented.

Table 2: VWM concentrations ($\mu Eq.L^{-1}$) and wet deposition fluxes ($kg.ha^{-1}.yr^{-1}$) of ionic species, as well as pH and EC at CPT GAW from 2004 to 2012. Also indicated are VWM, wet deposition flux, pH and EC at the four South African DEBITS sites from 2009 to 2014 (Conradie et al., 2016)

	CPT GAW		***AF***		***LT***		***SK***		***VT***	
	VWM	***Flux***	***VWM***	***Flux***	***VWM***	***Flux***	***VWM***	***Flux***	***VWM***	***Flux***
pH	5.49	---	4.32	---	4.89	---	4.66	---	4.51	---
EC	80.98	---	42.6	---	13.1	---	22.9	---	33.6	---
H^+	7.16	0.02	61.18	0.45	15.24	0.11	22.24	0.13	44.64	0.43
Na^+	298.64	1.04	17.79	2.98	7.75	1.30	13.17	1.77	3.50	0.77
NH_4^+	13.41	0.05	28.50	3.75	10.85	1.42	12.80	1.35	29.06	5.01
K^+	11.28	0.04	7.35	2.10	5.12	1.46	2.08	0.48	1.41	0.53
Mg^{2+}	59.36	0.21	5.54	0.49	1.93	0.17	3.27	0.23	4.55	0.53
Ca^{2+}	18.57	0.06	16.39	2.40	6.25	0.91	4.69	0.55	16.18	3.10
NO_3^-	10.01	0.03	33.40	15.11	7.49	3.38	13.20	4.77	22.97	13.62
Cl^-	354.18	1.23	17.96	4.65	10.83	2.80	15.73	3.25	4.52	1.53
SO_4^{2-}	33.59	0.12	67.21	23.56	12.37	4.33	18.66	5.23	55.00	25.27
TOA	3.47	0.01	14.64	5.57	12.14	4.54	9.69	2.93	12.51	6.10
DOA	3.14	0.01	13.24	---	11.10	---	8.69	---	11.49	---

TOA refers to total organic acids and DOA refers to total dissolved organic acids

It is evident from Table 2 that Na^+ and Cl^- were the most abundant ionic species at CPT GAW, with significantly higher VWM concentrations compared to other ionic species. In addition, Na^+ and Cl^- concentrations were also substantially higher than levels thereof at the four sites in the interior of South Africa, as well as concentrations reported for other DEBITS sites in Africa (Galy-Lacaux et al., 2008). These higher recorded values for Na^+ and Cl^- can be expected for a site predominantly influenced by marine air masses. This is also observed for other marine measurement sites such as Cape Grimm, Tasmania (Ayers and Ivey, 1988) and remote islands and coastal East Asian sites (Vet et al., 2014). The significantly higher Na^+ and Cl^- concentrations also contributed to noticeably higher EC of rainwater samples collected at CPT GAW compared to the other South African DEBITS sites.

The second and third most abundant species were Mg^+ and SO_4^{2-}, respectively, which are also most likely mainly associated with marine air, as indicated in subsequent paragraphs. SO_4^{2-} was the most abundant species at the four sites in the South African interior, which was attributed, by Conradie et al. (2016), to sulphur emissions from anthropogenic activities in this region. Although CPT GAW is on occasion influenced by air masses passing over the Cape Town metropole (Fig.1), a significantly lower impact of anthropogenic emissions on rainwater chemistry is expected, which is also signified by the lower VWM concentration of NO_3^-

compared to the two industrially impacted AF and VT sites. Substantially lower values are also reported for OA at CPT GAW compared to the other South African DEBITS sites, which reflects a less significant influence of biomass burning on rain chemistry at CPT GAW. Swartz et al. (2019) also indicated that seasonal open biomass burning in the Overberg region did not contribute substantially to the NO_2 and O_3 concentrations at CPT GAW.

3.2 Acidity

The average pH of rainwater at CPT GAW was 5.49, which is slightly lower than the pH of unpolluted rainwater, i.e. 5.60 (Eby, 2004). Average rainwater pH at GPT GAW was higher than the average pH at all the sites located in the South African interior, including the rural background sites LT and SK. Evidently, the resultant H^+ concentration was also lower at CPT GAW, especially being significantly lower than H^+ levels at AF and LT in proximity of anthropogenic emissions. In Fig. 3, the pH frequency distribution of rain events occurring during the wet season at CPT GAW is presented. It is evident that most of rain events had pH values ranging between 5.2 and 5.8. It was found that 85% of rain events had pH > 5.2, while 35% had pH > 5.6. The average pH value of rainwater at CPT GAW reflects the less significant impacts of anthropogenic activities and biomass burning on rainwater chemistry at CPT GAW. However, the occasional influence of anthropogenic activities is indicated by the largest number of rain events having pH values between 5.2 and 5.4, while 9.8% had pH < 5.0.

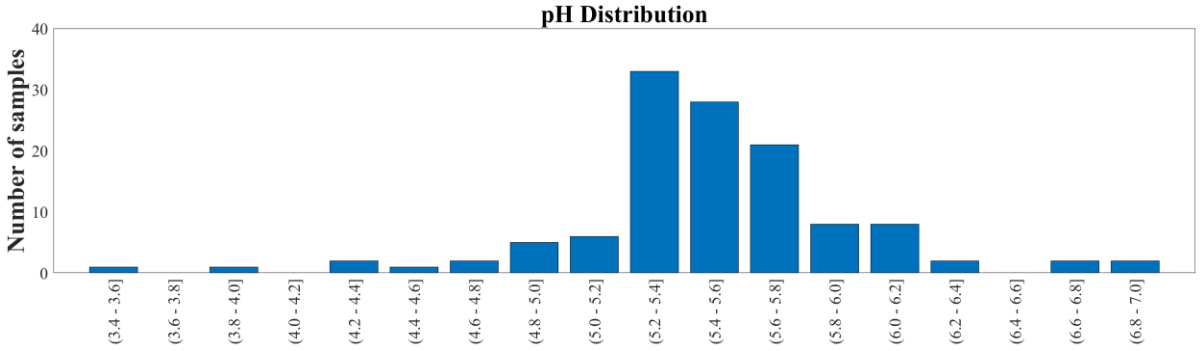

Figure 3: pH distribution of precipitation samples collected during the annual wet season (May-October) at CPT GAW during the period 2004 to 2012

The acidity potential (pA), presented in Table 3, is the sum of the potential acidic compounds, which include sulphuric acid (anthropogenic SO_4^{2-}), nitric acid (NO_3^-) and OA (Mphepya et

al., 2004; Laouali et al., 2012). Empirical estimations indicated that SO_4^{2-} in rainwater at CPT GAW was entirely from marine origin, i.e. completely in the sea-salt fraction (Equation 4). Therefore, terrigenous and anthropogenic sources did not contribute to any SO_4^{2-} measured in rainwater. The measured acidity (H^+, measured) at CPT GAW is lower than the estimated acidity (total H^+, estimated from the pA), which can be ascribed to neutralisation by basic cation species such as Ca^{2+}, NH_4^+ and Mg^{2+}. Neutralisation factors were calculated (Equation 6) to evaluate the neutralisation of nitric acid by these bases, which indicated that Mg^{2+} is the major ionic species in rainwater that neutralises nitric acid (Table 4). The calculated potential contribution of the mineral acids (nitric acid) at CPT GAW is 76.1%, which forms the greatest part of free acidity. Therefore, the marginal acidity of rain water at CPT GAW, as well as rain events with pH < 5, can be attributed to the influence of anthropogenic activities associated with the Cape Town metropole.

Table 3: Contributions of mineral and organic acids to the total acidity

	***μeq.L*$^{-1}$**	***%***
‡Sulphuric acid	0	0
Nitric acid	10.01	76.1
OA	3.14	23.9
Estimated total H^+ (pA)	13.15	100
Measured H^+	7.16	54.4

‡Anthropogenic sulphates

Table 4: Acid neutralisation factors (NF_X) of CPT GAW wet seasonal wet deposition for 2004 to 2012

	***NF*$_X$**
Ca^{2+}	1.85
Mg^{2+}	5.93
NH_4^+	1.34

3.3 Wet deposition fluxes

The wet deposition fluxes of the ionic species resembled the relative concentrations of these species in rainwater, i.e. species with higher VWM concentrations had higher wet deposition fluxes. The wet deposition flux of sulphur was 0.013 $kgS.ha^{-1}.yr^{-1}$, while the total wet

deposition flux of nitrogen (total nitrogen in NO_3^- and NH_4^+) was 0.007 kgN.ha^{-1}.yr^{-1}. The wet deposition fluxes of sulphur and nitrogen at CPT GAW were two orders of magnitude lower than the fluxes determined at the four sites in the interior of South Africa (Conradie et al., 2016). Furthermore, sulphur and nitrogen wet deposition fluxes were respectively eight and three times higher at the two industrially impacted sites (AF and VT) compared to the two rural sites (LT and SK).

3.4 Sources

Explorative statistical analysis, i.e. Pearson correlation calculations, was conducted in order to establish relationships between the different ionic species, which could be indicative of similar sources of species. It is evident from Table 5 that good correlations are observed between all species considered to be associated with marine air masses, i.e. Na^+, Cl^-, Mg^{2+}, K^+, Ca^{2+} and SO_4^{2-}. However, correlations between some of these species could also be attributed to terrigenous sources (e.g. Ca^{2+} and Mg^{2+}), which will be explored in subsequent paragraphs. In contrast to Conradie et al. (2016), no correlation is observed between SO_4^{2-} and NO_3^-, which signifies different sources, i.e. marine and anthropogenic, respectively, of these species at CPT GAW. It is also of interest to note that moderate correlations are observed between TOA and species associated with marine air masses (e.g. Na^+ and Cl^-), which are indicative of some of these species also being of marine origin. In addition, weak correlations are observed between H^+ and acidic ions, which correspond to the low acidity of rainwater.

Table 5: Pearson correlation for ionic species measured in CPT GAW wet deposition samples collected during the wet season for the period 2004 to 2012

	H^+	Na^+	NH_4^+	K^+	Mg^{2+}	Ca^{2+}	NO_3^-	Cl^-	SO_4^{2-}	F^-	TCarb	TOA
H^+	1.00											
Na^+	-0.05	1.00										
NH_4^+	-0.02	0.51	1.00									
K^+	-0.10	0.77	0.34	1.00								
Mg^{2+}	-0.02	0.91	0.56	0.47	1.00							
Ca^{2+}	-0.10	0.94	0.56	0.72	0.88	1.00						
NO_3^-	0.02	0.12	0.09	0.00	0.14	0.13	1.00					
Cl^-	0.05	0.99	0.51	0.75	0.91	0.93	0.14	1.00				
SO_4^{2-}	0.03	0.86	0.51	0.73	0.77	0.84	-0.20	0.85	1.00			
F^-	-0.05	0.56	0.31	0.59	0.37	0.55	-0.10	0.55	0.63	1.00		
TCarb	-0.52	0.25	0.41	0.15	0.30	0.43	-0.08	0.25	0.27	0.11	1.00	
TOA	-0.06	0.51	0.38	0.60	0.32	0.49	0.19	0.51	0.43	0.48	0.12	1.00

The ssf and nssf were calculated for the VWM concentrations of Cl^-, Mg^{2+}, K^+, Ca^{2+} and SO_4^{2-} with Equations 3 and 4, as discussed in section 2.5 in order to estimate the marine and non-marine contributions, while it was assumed that Na^+ was entirely from a marine source. The nssf of Cl^-, Mg^{2+}, K^+, Ca^{2+} and SO_4^{2-} was considered to be terrigenous. The sum of the VWM concentrations of the ssf and nssf of the species comprised the marine and terrigenous contributions, respectively. As indicated in the previous section, SO_4^{2-} was completely of marine origin and an anthropogenic fraction was not calculated. It can be assumed that NO_3^- at CPT GAW is predominantly associated with anthropogenic activities in the Cape Town metropole, e.g. vehicular emissions and household combustion. Swartz et al. (2019) attributed increased NO_2 concentrations at CP GAW to air masses passing over the Cape Town conurbation. NH_4^+ in precipitation is usually attributed to agricultural activities. However, guano from the sea birds could potentially be a more significant source at CPT GAW. OA concentrations can be considered a proxy for the biomass burning contribution. In Fig. 4, a summary of the estimations of the source group contributions to the chemical composition of rainwater at CPT GAW is presented. It is evident from Fig. 4 that the chemical content of rainwater collected at CPT GAW was dominated by the marine contribution, i.e. 94%, while the other sources contributed ≤ 2% each. This source group distribution for CPT GAW is completely unique in comparison to the source group distribution reported for the four other South African DEBITS sites located in the north-eastern interior where SO_4^{2-} and NO_3^- dominated rainwater composition (Mphepya, 2004, 2006, Conradie et al., 2016). The main sources of ionic species in rain water in the north-eastern interior of South African were the combustion of fossil fuels.

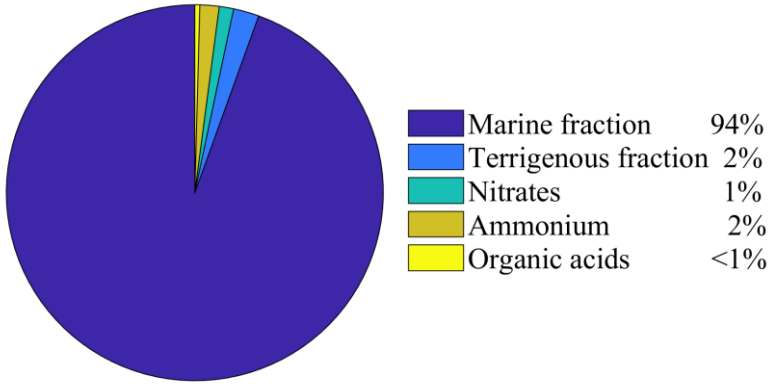

Figure 4: Estimated source contributions to the chemical composition of rainwater at CPT GAW

The ratios of Cl^-, Mg^{2+}, K^+, Ca^{2+} and SO_4^{2-} with regard to Na^+ are presented together with the EFs (Equation 5) in relation to the reference seawater ratios (Keene et al., 1986) in Table 6. It is evident that the Cl^-/Na^+, Mg^{-+}/Na^+ and SO_4^{2-}/Na^+ ratios were similar to seawater ratios, with EFs very close to one. Calculation of nssf with Equation 4 indicated that Mg^{2+} and SO_4^{2-} were completely in the ssf, while Cl^- was almost entirely (98%) in the ssf. Comparison of rain- and seawater ratios of K^+/Na^+ and Ca^{2+}/Na^+ ratios, as well as EFs indicated that these were not only of marine origin. K^+ and Ca^{2+} were also estimated to be from terrigenous sources, which mainly comprised the terrigenous contribution to the chemical content of rainwater. Therefore, correlations between these species (Table 5) could also be attributed to terrigenous/crustal sources.

Table 6: Comparison of rainwater ratios at CPT GAW with seawater ratios (Keene et al., 1986) and corresponding enrichment factors (EF)

	Rain	***Seawater***	***EF***
Mg^{2+} / Na^+	020	0.23	0.88
Cl^- / Na^+	1.19	1.16	1.02
Ca^{2+} / Na^+	0.06	0.04	1.41
K^+ / Na^+	0.04	0.02	1.72
SO_4^{2-} / Na^+	0.11	0.12	0.93

4. Conclusions

A total of 122 rainwater samples were collected during only the wet season (May to October) at CPT GAW from 2004 to 2012. Although the WMO criteria for precipitation collection were generally followed, logistical and instrumental limitations did not allow for sample collection to adhere completely to the WMO guidelines. Therefore, only 43% of the total rain depth from 2004 to 2012 was collected. However, 100% of the samples passed the WMO ID% criteria and none of the samples were discarded due to analytical errors, while samples represented 60% of the wet season rainfall.

Na^+ and Cl^- were the most abundant ionic species at CPT GAW, with VWM concentrations significantly higher compared to other ionic species, as well as higher than VWM concentrations of Na^+ and Cl^- measured at other South African DEBITS sites in the interior. The average pH of rainwater at this marine site was slightly lower than the pH of unpolluted rainwater, while it is indicated that mainly NO_3^- contributed to the marginal acidity due to the occasional influence of air masses passing over the Cape Town metropole. It was also indicated that SO_4^{2-} in rainwater at CPT GAW was entirely associated with marine air mass with no anthropogenic contribution, which is in contrast to the DEBITS sites situated in the South African interior, where anthropogenic SO_4^{2-} was the major constituent in rainwater. Sulphur and nitrogen depositions at CPT GAW were two orders of magnitude lower than sulphur and nitrogen deposition at the South African DEBITS located in the north-eastern interior impacted by anthropogenic activities. Estimations of source contribution indicated that 94% of the chemical content at CPT GAW can be attributed to the marine source, which signifies that CPT GAW is representative of southern-hemispherical marine air masses.

Valuable conclusions could be drawn from rain samples collected for a region and ecosystem in Southern Africa, for which no precipitation chemistry has been reported. The significance of the influence of anthropogenic activities on precipitation chemistry in the South African interior is also highlighted by the rainwater chemistry for a clean marine background site. It is recommended that future precipitation chemistry studies should include more sites representative of different regions and ecosystems in Southern Africa, while precipitation collection should continue at the current South African DEBITS sites in order to reflect changes in source contributions and meteorology.

Acknowledgements

The authors wish to thank the International Global Atmospheric Chemistry programme for endorsing the DEBITS programme. The authors also thank the Atmospheric Research in Southern Africa and Indian Ocean (ARSAIO) programme established by the National Centre for Scientific Research (CNRS) in France, and the National Research Foundation (NRF) in South Africa for their support.

References

Ayers, G. P. & Ivey, J. P. 1988. Precipitation composition at Cape Grim, 1977-1985. *Tellus. Series B: Chemical and Physical Meteorology,* 40B**,** 297-307, doi: 10.3402/tellusb.v40i4.15919.

Brunke, E. G., Labuschagne, C., Ebinghaus, R., Kock, H. H. & Slemr, F. 2010. Gaseous elemental mercury depletion events observed at Cape Point during 2007–2008. *Atmospheric Chemistry and Physics,* 10**,** 1121-1131, doi: 10.5194/acp-10-1121-2010.

Brunke, E. G., Labuschagne, C., Parker, B., Scheel, H. E. & Whittlestone, S. 2004. Baseline air mass selection at Cape Point, South Africa: application of ^{222}Rn and other filter criteria to CO_2. *Atmospheric Environment,* 38**,** 5693-5702, doi: 10.1016/j.atmosenv.2004.04.024.

Chao, C. Y. & Wong, K. K. 2002. Residential indoor PM_{10} and $PM_{2.5}$ in Hong Kong and the elemental composition. *Atmospheric Environment,* 36**,** 13, doi: 10.1016/S1352-2310(01)00411-3.

Conradie, E. H., Van Zyl, P. G., Pienaar, J. J., Beukes, J. P., Galy-Lacaux, C., Venter, A. D. & Mkhatshwa, G. V. 2016. The chemical composition and fluxes of atmospheric wet deposition at four sites in South Africa. *Atmospheric Environment,* 146**,** 113-131, doi: 10.1016/j.atmosenv.2016.07.033.

Draxler, R. R. & Hess, G. D. 2014. Description of the HYSPLIT_4 modelling system. 7 ed. Silver Spring, Maryland: Air Resources Laboratory.

Duce, R. A., Galloway, J. N. & Liss, P. S. 2009. The impacts of atmospheric deposition to the ocean on marine ecosystems and climate'. *WMO Bulletin 58.*

Galy-Lacaux, C., Laouali, D., Descroix, L., Gobron, N. & Liousse, C. 2008. Long term precipitation chemistry and wet deposition in a remote dry savanna site in Africa (Niger). *Atmospheric Chemistry & Physics Discussions,* 8**,** 5761-5812, doi: 10.5194/acpd-8-5761-2008.

Helas, G. & Pienaar, J. J. 1996. Chapter 3: "Biomass Burning Emissions. *In:* Held, G., Gore, B. J., Surridge, A. D., Tosen, G. R., Turner, C. R. & Walmsley, R. D. (eds.) *Air Pollution and its Impacts on the South African Highveld.* Cleveland: Environmental Scientific Association.

Josipovic, M., Annegarn, H. J., Kneen, M. A., Pienaar, J. J. & Piketh, S. J. 2011. Atmospheric dry and wet deposition of sulphur and nitrogen species and assessment of critical loads of acidic deposition exceedance in South Africa. *South African Journal Science,* 107**,** 10, doi: 10.4102/sajs.v107i3/4.478.

Keene, W. C., Pszenny, A. A., Galloway, J. N. & Hawley, M. E. 1986. Sea-salt corrections and interpretation of constituent ratios in marine precipitation. *Journal of Geophysical Research,* 91**,** 12, doi: 10.1029/JD091iD06p06647.

Labuschagne, C., Kuyper, B., Brunke, E.-G., Mokolo, T., Van Der Spuy, D., Martin, L., Mbambalala, E., Parker, B., Khan, M. a. H., Davies-Coleman, M. T., Shallcross, D. E. & Joubert, W. 2018. A review of four decades of atmospheric trace gas measurements at Cape Point, South Africa. *Transactions of the Royal Society of South Africa,* 73**,** 113-132, doi: 10.1080/0035919X.2018.1477854.

Lacaux, J. P., Tathy, J. P. & Sigha, L. 2003. Acid wet deposition in the tropics: Two case studies using DEBITS measurements. *IGACtivities Newsletter of the International Global Atmospheric Chemistry Project.*

Laouali, D., Galy-Lacaux, C., Diop, B., Delon, C., Orange, D., Lacaux, J. P., Akpo, A., Lavenu, F., Gardrat, E. & Castera, P. 2012. Long term monitoring of the chemical composition of precipitation and wet deposition fluxes over three Sahelian savannas. *Atmospheric Environment,* 50**,** 314-327, doi: 10.1016/j.atmosenv.2011.12.004.

Mphepya, J. N., Galy-Lacaux, C., Lacaux, J. P., Held, G. & Pienaar, J. J. 2006. Precipitation Chemistry and Wet Deposition in Kruger National Park, South Africa. *Journal of Atmospheric Chemistry,* 53**,** 169-183, doi: 10.1007/s10874-005-9005-7.

Mphepya, J. N., Pienaar, J. J., Galy-Lacaux, C., Held, G. & Turner, C. R. 2004. Precipitation Chemistry in Semi-Arid Areas of Southern Africa: A Case Study of a Rural and an Industrial Site. *Journal of Atmospheric Chemistry,* 47**,** 24, doi: 10.1023/B:JOCH.0000012240.09119.c4.

Possanzini, M., Buttini, P. & Di Palo, V. 1988. Characterization of a rural area in terms of dry and wet deposition. *Science of the Total Environment,* 74**,** 10.

Qasac-Americas. 2018. *Lab Intercomparison Study Data* [Online]. Available: http://www.qasac-americas.org/ringdiagram [Accessed 18 January 2019].

Quiterio, S. L., Da Silva, C. R. S., Arbilla, G. & Escaleira, V. 2004. Metals in airborne particulate matter in the industrial district of Santa Cruz, Rio de Janeiro, in an annual period. *Atmospheric Environment,* 32**,** 11, doi: 10.1016/j.atmosenv.2003.09.017.

Swartz, J.-S., Van Zyl Pieter, G., Beukes Johan, P., Labuschagne, C., Brunke, E.-G., Portafaix, T., Galy-Lacaux, C. & Pienaar Jacobus, J. 2019. Twenty-one years of passive sampling monitoring of SO_2, NO_2 and O_3 at the Cape Point GAW station, South Africa. *Submitted to Atmospheric Environment*.

UNESCO. 2015. *Cape Floral Region Protected Areas* [Online]. Available: http://whc.unesco.org/en/list/1007/ [Accessed 20 June 2017].

Vet, R., Artz, R. S., Carou, S., Shaw, M., Ro, C.-U., Aas, W., Baker, A., Bowersox, V. C., Dentener, F., Galy-Lacaux, C., Hou, A., Pienaar, J. J., Gillett, R., Forti, M. C., Gromov, S.,

Hara, H., Khodzher, T., Mahowald, N. M., Nickovic, S., Rao, P. S. P. & Reid, N. W. 2014. A global assessment of precipitation chemistry and deposition of sulfur, nitrogen, sea salt, base cations, organic acids, acidity and pH, and phosphorus. *Atmospheric Environment,* 93**,** 3-100, doi: 10.1016/j.atmosenv.2013.10.060.

Waldman, K. E., Munger, W. J. & Jacob, D. J. 1992. Measurement methods for atmospheric acidity and acid deposition. *In:* Radojević, M. & Harrison, R. M. (eds.) *Atmospheric acidity: Sources, consequences and abatement.* New York: Elsevier.

WMO 2004. WMO/GAW report no. 160, Manual for the GAW precipitation chemistry programme,WMO TD No. 1251.

CHAPTER 7

PROJECT EVALUATION AND FUTURE PERSPECTIVES

7.1 Project evaluation

As indicated in Chapter 1, the general aim of this study was to conduct long-term assessments of measurements conducted within the DEBITS programme at sites in South Africa. These assessments included evaluations of long-term inorganic gaseous measurements with passive samplers at three sites in the South African interior, i.e. Amersfoort (AF), Louis Trichardt (LT) and Skukuza (SK), as well as the marine Cape Point Global Atmosphere Watch (CPT GAW) site. A statistical model was developed for inorganic gaseous measurements at CPT GAW, which was applied to the other sites in the South African interior. In addition, rainwater chemistry and wet deposition fluxes based on relatively long-term rain collection are also reported for CPT GAW. The study is critically evaluated in view of the successes and shortcomings in accordance with each of the specific objectives listed in Chapter 1, while a few future perspectives drawn from the results are also discussed.

Objective I: Assessment of monthly mean long-term seasonal and inter-annual trends of SO_2, NO_2 and O_3 measured with passive samplers at the CPT GAW atmospheric monitoring station, as well as determining possible sources of these species

A 21-year passive sampling dataset, containing monthly mean concentrations of SO_2, NO_2 and O_3 collected at the CPT GAW, was successfully investigated in this study. A limitation of the dataset, however, was that passive samplers comprised composite concentrations of inorganic gaseous species, which represented two different air-chemical regimes at CPT GAW, i.e. a maritime- and an urban-continental sector varying as a function of seasonality (Botha *et al.*, 2018; Laban *et al.*, 2018). Notwithstanding this limitation, as well as in the absence of any other data for this region, this passive sampling dataset for SO_2, NO_2 and O_3 could be utilised to interpret seasonal patterns and inter-annual variability. In addition, continuous *in-situ*

measurements were available for O_3, which could be utilised to compare passive and *in-situ* measurements. Comparison revealed a similar seasonal pattern for the passively derived O_3 concentrations and the *in-situ* measurements, with relatively good agreement between monthly mean and median values for the 21-year dataset.

The distinct seasonal patterns observed for SO_2, NO_2 and O_3 concentrations measured at CPT GAW could be attributed to various influencing factors. It was shown that SO_2 and NO_2 concentrations were influenced by increased air mass movement over the Cape Town Metropole, and stronger inversions during the winter months. In addition, increased NO_2 concentrations could also be attributed, in part, to increased microbial activity during the wet season (Adon *et al.*, 2010). NO_2 and O_3 seasonal peaks also coincided, which is expected for a NO_X-limited regional background site. Although increased SO_2 in January and February coincided with increased biomass burning, the influence of regional biomass burning in the Western Cape was not reflected by NO_2 and O_3 concentrations. Higher SO_2 concentrations at CPT GAW measured during January and February are more likely associated with CPT GAW being more frequently impacted by oceanic air masses and oceanic SO_2 sources, e.g. oxidation of dimethyl sulphide (DMS). Inter-annual variability was observed for SO_2 and NO_2 concentrations, which was further explored with a statistical model. Passively derived O_3 concentrations and *in situ* O_3 measurements indicated no significant inter-annual variability.

Objective II: Developing and employing a statistical model to establish the influence of local and regional meteorology together with source contribution, as well as global climate drivers at CPT GAW on long-term trends

In order to elucidate the inter-annual variability, as well as to substantiate factors identified as contributing to seasonal variability, a multiple linear regression model was successfully developed and employed in this study. The influence of variances in source contributions (with population growth included as a proxy for changes in anthropogenic activities), as well as the local, regional and global meteorological factors could be explored in the model. Results obtained from this model indicated that fluctuations in SO_2 concentrations were mainly influenced by global forcing factors, whereas NO_2 concentration variations were a function of global, regional and local factors. O_3 concentration variances were predominantly associated with regional and local factors. Trend analysis of the 21-year dataset could be performed, which

indicated a relatively constant trend in SO_2, NO_2 and O_3 concentrations over the measurement period. However, two periods coinciding with decrease and increase in annual SO_2 and NO_2 concentrations were identified. Although a model was successfully developed in this study to evaluate long-term trends, the model was limited in view of the parameters included, especially factors pertaining to source contribution variability.

Objective III: Conducting statistical modelling of SO_2, NO_2 and O_3 long-term trends in the north-eastern interior of South Africa by utilising long-term passive sampling datasets available for AF, LT and SK in order to determine the influence of changes in source contributions, as well as local, regional and global meteorological parameters on long-term temporal trends

Passive samplers were successfully deployed at AF, LT and SK, for which 19-, 21- and 16-year, respectively, long-term SO_2, NO_2 and O_3 concentrations were determined. These datasets illustrate the value of cost-effective techniques for atmospheric measurements, especially in regions where accessibility and capacity might be limited (Adon *et al.*, 2010; Lacaux *et al.*, 2003). Seasonal and inter-annual variability was observed in SO_2, NO_2 and O_3 concentrations at all three sites, which was ascribed to the influence of changes in source contributions and meteorological conditions. Inter-annual variability indicated periods during which SO_2 and NO_2 concentrations decreased, followed by periods during which SO_2 and NO_2 levels increased. These long-term trends were successfully statistically modelled with the multiple linear regression model developed for CPT GAW, in which interdependencies between source contributions together with local, regional and global meteorological parameters could be evaluated.

Although the influence of global meteorology on SO_2 concentrations was evident, local and regional factors contributed significantly to SO_2 variability. Global meteorology made the largest contribution in explaining SO_2 variances at the rural background LT site, while local and regional factors, i.e. source contribution and meteorology, were the most important parameters at AF and SK. Local and regional factors made the most substantial contributions to modelled NO_2 levels at all three sites. It could be indicated that population growth played a significant role in SO_2 and NO_2 long-term trends. The period associated with a decrease in SO_2 and NO_2 concentrations could be attributed to the implementation of mitigation policies

deployed by industries in South Africa during the 1990s, coinciding with establishing a new democracy in order to comply with international trade requirements. However, these improvements were offset in the early part of the next decade due to rapid economic growth associated with increased industrial activities, as well as the increase in population growth accompanied by higher energy demand (Inglesi-Lotz & Blignaut, 2011; Vet *et al.*, 2014). Trend analysis indicated increases in SO_2 and NO_2 concentrations at AF during the long-term measurement periods, while the influence of increased household combustion associated with population growth was also signified with increasing NO_2 levels at SK. It was also indicated that seasonal SO_2 and NO_2 variability was mainly attributed to the influence of pollution build-up during winter, while the influence of air masses passing over the source region was also evident at the rural background sites (SK and LT). Modelled O_3 concentrations at all three South African DEBITS sites in the interior were shown to be most significantly influenced by ENSO. However, the influence of local and regional meteorology on O_3 variability was also evident, especially on seasonal trends. Inter-annual O_3 variability in this part of South Africa can therefore most likely be attributed to ENSO cycles (Balashov *et al.*, 2014). O_3 concentrations remained relatively constant over the long-term periods.

Objective IV: Contextualising SO_2, NO_2 and O_3 concentrations measured at South African DEBITS sites with other regions

SO_2, NO_2 and O_3 concentrations measured at AF, LT, SK and CPT GAW could be contextualised with levels of these species measured with passive samplers at other IDAF sites, as well as at other parts of the world. SO_2, NO_2 and O_3 concentrations at CPT GAW were lower than the industrially impacted AF site, while being similar in magnitude to other inland South African and African ecosystems (Adon *et al.*, 2010). There were, however, exceptions for sites located in African forest ecosystems. Higher SO_2 and NO_2 concentrations were also determined at AF in relation to levels thereof at the rural background sites (LT and SK). SO_2 levels at AF were similar to levels of these species determined at other sites located within the Mpumalanga Highveld (Lourens *et al.*, 2011). However, sites in closer proximity to the major industrial sources in the Mpumalanga Highveld had higher concentrations, while certain rural background sites in China also had higher SO_2 concentrations compared to SO_2 levels at AF (Carmichael *et al.*, 2003). NO_2 levels at AF were generally lower than NO_2 concentrations determined at sites within the Mpumalanga Highveld source region, as well as than most

regional sites in China. SO_2 and NO_2 concentrations determined at LT and SK were similar to levels thereof determined with passive samplers at regional and rural sites in Africa and other parts of the world. The regional problem of O_3 in the interior of South Africa was also indicated in this study, with relatively high O_3 levels determined at all three sites (Laban *et al.*, 2018).

Objective V: Assessment of the chemical composition of rainwater and wet deposition fluxes at CPT GAW

122 rainwater samples were successfully collected at the CPT GAW station over the period 2004 to 2012. Although the WMO precipitation collection criteria were generally followed, logistical restraints and limitations associated with wet-only samplers resulted in precipitation collection not completely complying with the guidelines of the WMO. In addition, rainwater could only be collected during the wet season at CPT GAW. However, considering these limitations associated with precipitation sampling at CPT GAW, 43% of the total rain depth during the entire sampling period could be collected, from which valuable deductions could be made for a region and ecosystem in Southern Africa for which no precipitation chemistry has been reported. These samples were also adequate to successfully contextualise rain chemistry at CPT GAW in relation to the South African interior. Furthermore, the collected rain samples represented 60% of the total rain depth during the wet season, while 100% of the samples passed the WMO ID% criteria and none of the samples were discarded due to analytical errors.

It could be indicated that Na^+ and Cl^- dominated the rainwater at CPT GAW, while concentrations of these species were also substantially higher compared to levels thereof in rain samples collected in the South African interior (Conradie *et al.*, 2016). The rainwater pH at CPT GAW was slightly more acidic than that of unpolluted water, which was mainly attributed to NO_3^- associated with the occasional influence of air masses passing over the Cape Town metropole. Furthermore, it could also be shown that no SO_4^{2-} in the rainwater at CPT GAW was associated with anthropogenic sources, which is in contrast to rainwater collected in the interior of South Africa where anthropogenic SO_4^{2-} dominated (Conradie *et al.*, 2016). Sulphur and nitrogen depositions were significantly lower at CPT GAW, while it was also indicated that the marine source contributed to 94% of the ionic content of rainwater at CPT GAW.

In summary, this study signified the value of conducting long-term measurements of atmospheric species. It contributed to a better understanding of seasonal and inter-annual trends

observed in SO_2, NO_2 and O_3 concentrations at CPT GAW, AF, LT and SK, which were shown to be a combination of local, regional and global factors. Furthermore, this study, together with the study by Conradie *et al.* (2016), indicated the value of long-term precipitation chemistry in order to assess the temporal and spatial evolution of the chemical composition of the atmosphere.

7.2 Future perspectives

In view of the some of the limitations identified in the previous section, as well as the value of long-term measurements and the use of low-cost samplers indicated in this study, the following recommendation for future work are made:

- Although passive samplers provided a cost-effective method to establish long-term trends of atmospheric inorganic gaseous species, it is recommended that future studies should incorporate *in-situ* measurements of these species, especially at sites such as CPT GAW that is influenced by air masses passing over different sectors, i.e. marine and urban-continental. *In-situ* measurements at CPT GAW would allow for separation of the influence of different air-chemical regimes on concentrations of inorganic gaseous species. The comprehensively equipped and continuously operated Welgegund measurement site, located in the interior of South Africa, could also support measurements conducted at remote sites in the South African interior for which *in-situ* measurements are logistically limited.

- It is also recommended that the spatial resolution for measurements of atmospheric species in Southern Africa is increased by utilising low-cost samplers, such as the passive samplers utilised in this study, especially for regions in South Africa that are not currently considered by government to be priority areas with regard to air pollution. Low-cost samplers will assist in identifying pollution hotspots in other parts of South Africa, which will allow investment in costly continuous atmospheric measurement infrastructure in essential areas.

- Long-term trend measurement at sites included in this study should also be continued in order to obtain and improve the evaluation of decadal trends of atmospheric species in southern Africa.

- Although criteria of inorganic gaseous pollutants (SO_2, NO_2 and O_3) were investigated in this study, it is also recommended that other gaseous species not currently measured at these sites, such as NH_4^+, HNO_3, VOCs and CO (not measured at the South African interior sites), are also measured in future.

- Measurements of other factors that can be included in the statistical model utilised in this study should significantly improve correlations between modelled and measured values, while *in situ* measurements of SO_2, NO_2 and O_3 will also improve the relation between modelled and measured values as indicated for O_3 at CPT GAW. Although local and meteorological data were successfully utilised in this model, it is also recommended that field measurements of meteorological parameters are improved.

- Future precipitation chemistry studies must include more sites representative of different regions and ecosystems in Southern Africa, while precipitation collection should continue at the current South African DEBITS sites in order to reflect changes in source contributions and meteorology.

- Rain collection percentages could also be improved at CPT GAW, by utilising a more fit-for-purpose wet-only sampler.

BIBLIOGRAPHY

Abiodun, B.J., Ojumu, A.M., Jenner, S. & Ojumu, T.V. 2014. The transport of atmospheric NO_X and HNO_3 over Cape Town. *Atmospheric Chemistry and Physics*, 14(2):559-575.

Adon, M., Galy-Lacaux, C., Yoboué, V., Delon, C., Lacaux, J.P., Castera, P., Gardrat, E., Pienaar, J.J., Al Ourabi, H., Laouali, D., Diop, B., Sigha-Nkamdjou, L., Akpo, A., Tathy, J.P., Lavenu, F. & Mougin, E. 2010. Long-term measurements of sulfur dioxide, nitrogen dioxide, ammonia, nitric acid and ozone in Africa using passive samplers. *Atmospheric Chemistry and Physics*, 10(15):7467-7487.

Aiuppa, A., Bellomo, S., D'Alessandro, W., Federico, C., Ferm, M. & Valenza, M. 2004. Volcanic plume monitoring at Mount Etna by diffusive (passive) sampling. *Journal of Geophysical Research*, 109:11.

Andreae, M.O. & Rosenfeld, D. 2008. Aerosol-cloud-precipitation interactions. Part 1. The nature and sources of cloud-active aerosols. *Earth-Science Reviews*, 89(1-2):13-41.

Atkinson, R. 2000. Atmospheric chemistry of VOCs and NOx. *Atmospheric Environment*, 34:2063-2101.

Ayers, G.P., Cainey, J.M., Gillett, R.W., Saltzman, E.S. & Hooper, M. 1997. Sulfur dioxide and dimethyl sulfide in marine air at Cape Grim, Tasmania. *Tellus*, 49B(3):292-294.

Baker, P.G.L., Brunke, E.G., Slemr, F. & Crouch, A.M. 2002. Atmospheric mercury measurements at Cape Point, South Africa. *Atmospheric Environment*, 36(14):2459-2465.

Balashov, N.V., Thompson, A.M., Piketh, S.J. & Langerman, K.E. 2014. Surface ozone variability and trends over the South African Highveld from 1990 to 2007. *Journal of Geophysical Research: Atmospheres*, 119(7):20.

Baldwin, M.P., Gray, L.J., Dunkerton, T.J., Hammilton, K., Haynes, P.H., Randel, W.J., Holton, J.R., Alexander, M.J., Hirota, I., Horinouchi, T., Jones, D.B.A., Kinnersley, J.S.,

Marquardt, C., Sato, K. & Takahashi, M. 2001. The quasi-biennial oscillation. *Reviews of Geophysics*, 39:179-229.

Bencherif, H., Diab, R.D., Portafaix, T., Morel, B., Keckhut, P. & Moorgawa, A. 2006. Temperature climatology and trend estimates in the UTLS region as observed over a southern subtropical site, Durban, South Africa. *Atmospheric Chemistry and Physics*, 6(12):5121-5128.

BoM. 2012. Record-breaking La Niña events. Melbourne, Australia.

Booyens, W., Beukes, J.P., Van Zyl, P.G., Ruiz-Jimenez, J., Kopperi, M., Riekkola, M.-L., Josipovic, M., Vakkari, V. & Laakso, L. 2019. Assessment of polar organic aerosols at a regional background site in southern Africa. *Submitted to Journal of Atmospheric Chemistry*.

Botha, R., Labuschagne, C., Williams, A.G., Bosman, G., Brunke, E.G., Rossouw, A. & Lindsay, R. 2018. Characterising fifteen years of continuous atmospheric radon activity observations at Cape Point (South Africa). *Atmospheric Environment*, 176:30-39.

Brasseur, G., Orlando, J.J. & Tyndall, G.S. 1999. Atmospheric chemistry and global change: New York : Oxford University Press, 1999.

Brunke, E.G., Labuschagne, C., Ebinghaus, R., Kock, H.H. & Slemr, F. 2010. Gaseous elemental mercury depletion events observed at Cape Point during 2007-2008. *Atmospheric Chemistry and Physics*, 10(3):1121-1131.

Brunke, E.G., Labuschagne, C., Parker, B., Scheel, H.E. & Whittlestone, S. 2004. Baseline air mass selection at Cape Point, South Africa: application of ^{222}Rn and other filter criteria to CO_2. *Atmospheric Environment*, 38(33):5693-5702.

Carmichael, G.R., Ferm, M., Thongboonchoo, N., Woo, J.-H., Chan, L.Y., Murano, K., Viet, P.H., Mossberg, C., Bala, R., Boonjawat, J., Upatum, P., Mohan, M., Adhikary, S.P., Shrestha, A.B., Pienaar, J.J., Brunke, E.B., Chen, T., Jie, T., Guoan, D., Peng, L.C., Dhiharto, S., Harjanto, H., Jose, A.M., Kimani, W., Kirouane, A., Lacaux, J.-P., Richard, S., Barturen, O., Cerda, J.C., Athayde, A., Tavares, T., Cotrina, J.S. & Bilici, E. 2003. Measurements of sulfur dioxide, ozone and ammonia concentrations in Asia, Africa, and South America using passive samplers. *Atmospheric Environment*, 37:1293-1308.

Chameides, W.L., Kasibhatla, P.S., Yienger, J. & H. Levy, I. 1994. Growth of continental-scale metro-agro-plexes, regional ozone pollution, and world food production. *Science*, (5155):74.

Connell, D.W. 2005. Basic concepts of environmental chemistry. 2: CRC Press.

Conradie, E.H. 2018. Spatial and temporal deposition of selected biogeochemical important trace species in South Africa. North-West University, Potchefstroom.

Conradie, E.H., Van Zyl, P.G., Pienaar, J.J., Beukes, J.P., Galy-Lacaux, C., Venter, A.D. & Mkhatshwa, G.V. 2016. The chemical composition and fluxes of atmospheric wet deposition at four sites in South Africa. *Atmospheric Environment*, 146:113-131.

Cox, R.M. 2003. The use of passive sampling to monitor forest exposure to O_3, NO_2 and SO_2: a review and some case studies. *Environmental Pollution*, 126:301-311.

Dewitte, S., Crommelynck, D., Mekaoui, S. & Joukoff, A. 2004. Measurement and uncertainty of the long-term total solar irradiance trend. *Solar Physics*, 224(1/2):209-216.

Dhammapala, R.S. 1996. Use of diffusive samplers for the sampling of atmospheric pollutants. South Africa: Potchefstroom University for CHE.

Draxler, R.R. 1996. Trajectory optimization for balloon flight planning. *NOAA/Air Resources Laboratory, Silver Spring, Maryland*.

Draxler, R.R. & Hess, G.D. 2004. Description of the HYSPLIT_4 modelling system. Silver Spring, Maryland.

Eby, G.N. 2004. Principles of environmental geochemistry: Australia ; Pacific Grove, CA : Thomson-Brooks/Cole, c2004.

Felzer, B.S., Cronin, T., Melillo, J.M., Reilly, J.M. & Wang, X. 2007. Impacts of ozone on trees and crops. *Comptes Rendus – Geoscience*, 339(11-12):784-798.

Ferm, M. 1991. A sensitive diffusional sampler. Göteborg, Sweden.

Ferm, M. 2001. The theories behind diffusive sampling. (*In ed^eds*. International Conference on Measuring Air Pollutants by Diffusive Sampling organised by Montpellier, France. p. 31-40).

Fields, S. 2004. Global nitrogen: Cycling out of control. *Environmental Health Perspectives*, (10):A556-A563.

Galbally, I., G. Schultz, M., Buchmann, B., Gilge, S., Guenther, F., Koide, H., Oltmans, S., Patrick, L., Scheel, H.E., Smit, H., Steinbacher, M., Steinbrecht, W., Tarasova, O., Viallon, J., Volz-Thomas, A., Weber, M., Wielgosz, R. & Zellweger, C. 2013. Guidelines for Continuous Measurement of Ozone in the Troposphere.

Galloway, J.N., Schlesinger, W.H., Levy, H., Michaels, A. & Schnoor, J.L. 1995. Nitrogen fixation: Anthropogenic enhancement-environmental response. *Global Biogeochemical Cycles*, 9(2):235-252.

Galy-Lacaux, C., Laouali, D., Descroix, L., Gobron, N. & Liousse, C. 2009. Long-term precipitation chemistry and wet deposition in a remote dry savanna site in Africa (Niger). *Atmospheric Chemistry and Physics*, 9(5):16.

Hao, W.M. & Liu, M.H. 1994. Spatial and temporal distribution of tropical biomass burning. *Global Biogeochemical Cycles*, 8(4):495-503.

Harrison, R.M. 1999. Understanding our environment : an introduction to environmental chemistry and pollution. Cambridge, U.K.: Royal Society of Chemistry.

He, J. & Bala, R. 2008. Draft report on passive sampler inter-comparison under Malé Declaration. Singapore.

IDAF. 2011. Network. http://idaf.sedoo.fr/spip.php?rubrique45 Date of access: 29 June 2017.

Inglesi-Lotz, R. & Blignaut, J. 2011. Estimating the price elasticity for demand for electricity by sector in South Africa. *South African Journal of Economic and Management Sciences*, 14(4):449-465

IPCC. 2007. Climate change 2007: The physical science basis. Cambridge, United Kingdom and New York, NY, USA,.

IPCC. 2013. *(In* Stocker, T.F., Qin, D., Plattner, G.-K., Tignor, M., Allen, S.K., Boschung, J., Nauels, A., Xia, Y., Bex, V. & Midgley, P.M., *eds*. Climate change 2013: The Physical Science Basis. Contribution of working group I to the Fifth Assessment Report of the

Intergovernmental Panel on Climate Change. Cambridge, United Kingdom and New York, NY, USA: Cambridge University Press.

IPCC. 2014. Climate Change 2014: Synthesis Report. Contribution of Working Groups I, II and III to the Fifth Assessment Report of the Intergovernmental Panel on Climate Change. Geneva, Switzerland: IPCC.

Jaars, K., Beukes, J.P., van Zyl, P.G., Venter, A.D., Josipovic, M., Pienaar, J.J., Vakkari, V., Aaltonen, H., Laakso, H., Kulmala, M., Tiitta, P., Guenther, A., Hellén, H., Laakso, L. & Hakola, H. 2014. Ambient aromatic hydrocarbon measurements at Welgegund, South Africa. *Atmospheric Chemistry and Physics Discussions*, 14(13):7075-7089.

Jerrett, M., Burnett, R.T., Pope, C.A., III, Ito, K., Thurston, G., Krewski, D., Li, Y.S., Calle, E. & Thun, M. 2009. Long-term ozone exposure and mortality. *New England Journal of Medicine*, 360(11):1085-1095.

Josipovic, M., Annegarn, H.J., Kneen, M.A., Pienaar, J.J. & Piketh, S.J. 2011. Atmospheric dry and wet deposition of sulphur and nitrogen species and assessment of critical loads of acidic deposition exceedance in South Africa. *South African Journal Science*, 107(3/4):10.

Josipovic, M., Annegarn, H.J., Kneen, M.A., Piketh, S. & Pienaar, J.J. 2007. A regional-scale passive monitoring study of SO_2, NO_2 and ozone in South Africa.

Kajino, M. & Aikawa, M. 2015. A model validation study of the washout/rainout contribution of sulfate and nitrate in wet deposition compared with precipitation chemistry data in Japan. *Atmospheric Environment*, 117:124-134.

Kampa, M. & Castanas, E. 2008. Human health effects of air pollution. *Environmental Pollution*, 151:362-367.

Kaufman, Y.J., Ichoku, C., Giglio, L., Korontzi, S., Chu, D.A., Hao, W.M., Li, R.R. & Justice, C.O. 2003. Fire and smoke observed from the Earth Observing System MODIS instrument:n Products, validation, and operational use. *International Journal of Remote Sensing*, 24(8):1765-1781.

Keene, W.C., Pszenny, A.A., Galloway, J.N. & Hawley, M.E. 1986. Sea-salt corrections and interpretation of constituent ratios in marine precipitation. *Journal of Geophysical Research*, 91(D6):12.

Kleynhans, E., Beukes, J.P., Van Zyl, P.G., Bunt, J., Nkosi, N. & Venter, M. 2017. The effect of carbonaceous reductant selection on chromite pre-reduction. *Metallurgical & Materials Transactions B*, 48(2):827-840.

KMNI. 2016a. monthly DMI HadISST1. http://climexp.knmi.nl/getindices.cgi?WMO=UKMOData/hadisst1_dmi&STATION=DMI_HadISST1&TYPE=i&id=someone@somewhere Date of access: 22 December 2016.

KMNI. 2016b. monthly measured total solar irradiance. http://climexp.knmi.nl/getindices.cgi?WMO=PMODData/tsi&STATION=measured_total_solar_irradiance&TYPE=i&id=someone@somewhere Date of access: 22 December 2016.

Korhonen, K., Giannakaki, E., Mielonen, T., Pfüller, A., Laakso, L., Vakkari, V., Baars, H., Engelmann, R., Beukes, J.P., Van Zyl, P.G., Ramandh, A., Ntsangwane, L., Josipovic, M., Tiitta, P., Fourie, G., Ngwana, I., Chiloane, K. & Komppula, M. 2014. Atmospheric boundary layer top height in South Africa: measurements with lidar and radiosonde compared to three atmospheric models. *Atmospheric Chemistry and Physics*, 14(8):4263-4278.

Koutrakis, P., Wolfson, J.M. & Bunyaviroch, A. 1993. Measurement of ambient ozone using a nitrite-coated filter. *Analytical Chemistry*, 65:209-214.

Kraha, A., Turner, H., Nimon, K., Reichwein Zientek, L. & Henson, R.K. 2012. Tools to support interpreting multiple regression in the face of multicollinearity. *Frontiers In Psychology*, 3(44):1-16.

Krupa, S., McGrath, M.T., Andersen, C.P., Booker, F.L., Burkey, K.O., Chappelka, A.H., Chevone, B.I., Pell, E.J. & Zilinskas, B.A. 2001. Ambient ozone and plant health. *Plant Disease*, 85(1):4-12.

Kulmala, M., Josipov, M., Vakkari, V., Worsnop, D., Pienaar Jacobus, J., Beukes Johan, P., Jaars, K., Laakso, L., Venteric Andrew, D., Tiitta, P., Van Zyl Pieter, G. & Tiitta, P. 2013. Source region plume characterisation of the interior of South Africa as observed at Welgegund. *Clean Air Journal = Tydskrif vir Skoon Lug*, (1):7.

Laakso, L., Vakkari, V., Virkkula, A., Laakso, H., Backman, J., Kulmala, M., Beukes, J.P., van Zyl, P.G., Tütta, P., Josipovic, M., Pienaar, J.J., Chiloane, K., Gilardoni, S., Vignati, E., Wiedensohler, A., Tuch, T., Birmili, W., Piketh, S., Collett, K. & Fourie, G.D. 2012. South African EUCAARI measurements: seasonal variation of trace gases and aerosol optical properties. *Atmospheric Chemistry & Physics*, 12(4):1847-1864.

Laban, T.L., van Zyl, P.G., Beukes, J.P., Vakkari, V., Jaars, K., Borduas-Dedekind, N., Josipovic, M., Thompson, A.M., Kulmala, M. & Laakso, L. 2018. Seasonal influences on surface ozone variability in continental South Africa and implications for air quality. *Atmospheric Chemistry and Physics*, 15491-15514.

Lacaux, J.P., Tathy, J.P. & Sigha, L. 2003. Acid wet deposition in the tropics: Two case studies using DEBITS measurements.

Laj, P., Klausen, J., Bilde, M., Plaß-Duelmer, C., Pappalardo, G., Clerbaux, C., Baltensperger, U., Hjorth, J., Simpson, D., Reimann, S., Coheur, P.F., Richter, A., De Mazière, M., Rudich, Y., McFiggans, G., Torseth, K., Wiedensohler, A., Morin, S., Schulz, M., Allan, J.D., Attié, J.L., Barnes, I., Birmili, W., Cammas, J.P., Dommen, J., Dorn, H.P., Fowler, D., Fuzzi, S., Glasius, M., Granier, C., Hermann, M., Isaksen, I.S.A., Kinne, S., Koren, I., Madonna, F., Maione, M., Massling, A., Moehler, O., Mona, L., Monks, P.S., Müller, D., Müller, T., Orphal, J., Peuch, V.H., Stratmann, F., Tanré, D., Tyndall, G., Abo Riziq, A., Van Roozendael, M., Villani, P., Wehner, B., Wex, H. & Zardini, A.A. 2009. Measuring atmospheric composition change. *Atmospheric Environment*, 43:5351-5414.

Likens, G.E., Driscoll, C.T. & Buso, D.C. 1996. Long-term effects of acid rain: Response and recovery of a forest ecosystem. *Science*, (5259):244.

Lorenzo-Seva, U., Ferrando, P.J. & Chico, E. 2010. Two SPSS programs for interpreting multiple regression results. *Behavior Research Methods*, 42(1):29-35.

Lourens, A.S., Beukes, J.P., Van Zyl, P.G., Fourie, G.D., Burger, J.W., Pienaar, J.J., Read, C.E. & Jordaan, J.H. 2011. Spatial and temporal assessment of gaseous pollutants in the Highveld of South Africa. *South African Journal of Science*, 107(1/2):1-8.

Lourens, A.S.M., Beukes, J.P., Van Zyl, P.G., Pienaar, J.J., Butler, T.M., Beirle, S., Wagner, T.K., Heue, K.P., Fourie, G.D. & Lawrence, M.G. 2012. Re-evaluating the NO_2 hotspot over the South African Highveld. *South African Journal of Science*, 108(11-12).

Marshall, G. 2018. An observation-based Southern Hemisphere Annular Mode Index. http://www.nerc-bas.ac.uk/icd/gjma/sam.html Date of access: 28 August 2018.

Martins, J.J. 2009. Concentrations and deposition of atmospheric species at regional sites in southern Africa. North-West University, Potchefstroom Campus. (Thesis).

Martins, J.J., Dhammapala, R.S., Lachmann, G., Galy-Lacaux, C. & Pienaar, J.J. 2007. Long-term measurements of sulphur dioxide, nitrogen dioxide, ammonia, nitric acid and ozone in southern Africa using passive samplers. *South African Journal of Science*, 103(7-8):336-342.

McGranahan, G. & Murray, F. 2003. Air pollution and health in rapidly developing countries: London, Sterling, VA: Earthscan, 2003.

Monks, P. & Leigh, R. 2009. *(In* Hewitt, C.N. & Jackson, A.V., *eds*. Atmospheric science for environmental scientists. United Kingdom: Wiley-Blackwll).

Monroe, J.S., Wicander, R. & Hazlett, R.W. 2007. Physical geology : exploring the Earth. 6th ed. Belmont, CA: Thomson Brooks/Cole.

Mphepya, J.N., Galy-Lacaux, C., Lacaux, J.P., Held, G. & Pienaar, J.J. 2006. Precipitation chemistry and wet deposition in Kruger National Park, South Africa. *Journal of Atmospheric Chemistry*, 53(2):169-183.

Mphepya, J.N., Pienaar, J.J., Galy-Lacaux, C., Held, G. & Turner, C.R. 2004. Precipitation chemistry in semi-arid areas of Southern Africa: A case study of a rural and an industrial site. *Journal of Atmospheric Chemistry*, 47:24.

NASA. 2017. Solar irradiance. https://www.nasa.gov/mission_pages/sdo/science/solar-irradiance.html Date of access: 14 January 2019.

Nathans, L.L., Oswald, F.L. & Nimon, K. 2012. Interpreting Multiple Linear Regression: A Guidebook of Variable Importance. *Practical Assessment, Research & Evaluation*, 17(9):1-19.

Nixon, S.W., Ammerman, J.W., Atkinson, L.P., Berounsky, V.M., Billen, G., Boicourt, W.C., Boynton, W.R., Church, T.M., Ditoro, D.M., Elmgren, R., Garber, J.H., Giblin, A.E., Jahnke, R.A., Owens, N.J.P., Pilson, M.E.Q. & Seitzinger, S.P. 1996. The fate of nitrogen and phosphorus at the land-sea margin of the North Atlantic Ocean. *Biogeochemistry*(1):141.

NOAA. 2015a. Climate indices: Monthly atmospheric and ocean time series. https://www.esrl.noaa.gov/psd/data/climateindices/list/ Date of access: 22 December 2016.

NOAA. 2015b. Monthly atmospheric and SST indices. http://www.cpc.ncep.noaa.gov/data/indices/ Date of access: 22 December 2016.

NRC. 1991. Rethinking the ozone problem in urban and regional air pollution. Washington, DC: The National Academies Press.

Ojumu, A.M. 2013. Transport of nitrogen oxides and nitric acid pollutants over South Africa and air pollution in Cape Town. University of South Africa.

Oltmans, S.J., Lefohn, A.S., Shadwick, D., Harris, J.M., Scheel, H.E., Galbally, I., Tarasick, D.W., Johnson, B.J., Brunke, E.G., Claude, H., Zeng, G., Nichol, S., Schmidlin, F., Davies, J., Cuevas, E., Redondas, A., Naoe, H., Nakano, T. & Kawasato, T. 2013. Recent tropospheric ozone changes: A pattern dominated by slow or no growth. *Atmospheric Environment*, 67:331-351.

Petäjä, T., Vakkari, V., Pohja, T., Kerminen, V.-M. & Laakso, L. 2013. Transportable aerosol characterization trailer with trace gas chemistry: design, instruments and verification. *Aerosol and Air Quality Research*, 13:14.

Petterssen, S. 1940. Weather analysis and forecasting: A textbook on synoptic meteorology. New York and London: McGraw-Hill Book Company, Inc.Popescu, F. & Ionel, I. 2010. *(In* Kumar, A., *ed.* Air Quality. Sciyo. p. 382)

Qasac-Americas. 2018. Lab intercomparison study data. http://www.qasac-americas.org/ringdiagram Date of access: 18 January 2019.

Rorich, R.P. & Galpin, J.S. 1998. Air quality in the Mpumalanga Highveld region, South Africa. *South African Journal of Science*, 94(3):109.

Saji, N.H. & Yamagata, T. 2003. Structure of SST and surface wind variability during Indian Ocean dipole mode events : COADS Observations. *Journal of Climate*, (16):2735.

Saltzman, E.S., Yvon, S.A. & Matrai, P.A. 1993. Low-level atmospheric sulfur dioxide measurement using HPLC/fluorescence detection. *Journal of Atmospheric Chemistry*, (17/1):73-90.

Schimel, D., Enting, I.G., Heimann, M., Wigley, T.M.L., Raynaud, D., Alves, D. & Siegenthaler, U. 1995. *(In* Houghton, J.T., Meira Filho, L.G., Bruce, J., Lee, H., Callander, B.A., Haites, E., Harris, N. & Maskell, K., *eds*. Climate change 1994: Radiative Forcing of Climate Change and An Evaluation of the IPCC IS92 Emission Scenarios. New York: Cambridge University Press.

Schmid, P. & Niyogi, D. 2012. A method for estimating planetary boundary layer heights and its application over the ARM Southern Great Plains Site. *Journal of Atmospheric & Oceanic Technology*, 29(3):316-322.

Scholes, M.C., Olbrich, K.A. & Van Rensburg, E. 1996. The environmental impact of atmospheric pollution in the industrial Highveld and adjacent regions: Crops, indigenous vegetation and commercial forests.

Schwartz, S.E. & Warneck, P. 1995. Units for use in atmospheric chemistry. *Pure and Applied Chemistry*, 67(8/9):1377-1406.

Seinfeld, J.H. & Pandis, S.N. 2006. Atmospheric chemistry and physics: From air pollution to climate change: Wiley.

Sfîcă, L. & Voiculescu, M. 2014. Possible effects of atmospheric teleconnections and solar variability on tropospheric and stratospheric temperatures in the Northern Hemisphere. *Journal of Atmospheric and Solar-Terrestrial Physics*, 109:7-14.

Sivertsen, B., Matale, C. & Pereira, L.M.R. 1995. Sulphur emissions and trans-frontier air pollution in southern Africa. Maseru, Lesotho.

Stenseth, N.C., Ottersen, G., Hurrell, J.W., Mysterud, A., Lima, M., Chan, K., Yoccoz, N.G. & Ådlandsvik, B. 2003. Review article. Studying climate effects on ecology through the use

of climate indices: the North Atlantic Oscillation, El Niño Southern Oscillation and beyond. *Proc. R. Soc. Lond. B*, 270(1529):2087-2096.

Stensland, G.J. 2006. *(In* Pfafflin, J.R. & Ziegler, E.N., *eds*. Encyclopedia of Environmental Science and Engineering. 5th ed. Boca Raton, Florida: CPR Press, Taylor & Francis Group p. 1-13).

Stern, D.I. 2006. Reversal of the trend in global anthropogenic sulfur emissions. *Global Environmental Change*, 16(2):207-220.

Takemura, T. 2005. Simulation of climate response to aerosol direct and indirect effects with aerosol transport-radiation model. *Journal of Geophysical Research*, 110(D2).

Tiitta, P., Vakkari, V., Croteau, P., Beukes, J.P., Zyl, P.G.v., Josipovic, M., Venter, A.D., Jaars, K., Pienaar, J.J., Ng, N.L., Canagaratna, M.R., Jayne, J.T., Kerminen, V.M., Kokkola, H., Kulmala, M., Laaksonen, A., Worsnop, D.R. & Laakso, L. 2014. Chemical composition, main sources and temporal variability of PM_1 aerosols in southern African grassland. *Atmospheric Chemistry and Physics*, 14(4):1909-1927.

Toihir, A.M., Portafaix, T., Sivakumar, V., Bencherif, H., Pazmiño, A. & Bègue, N. 2018. Variability and trend in ozone over the southern tropics and subtropics. *Annales Geophysicae*, 36(2):381-404.

Thompson, A.M., Tao W., Pickering K.E., Scala, J.R & Simpson, J. 1997. Tropical Deep Convection and Ozone Formation. *Bulletin of the American Meteorological Society*, 78(6):1043-1054.

UNESCO. 2015. Cape Floral Region Protected Areas. http://whc.unesco.org/en/list/1007/ Date of access: 20 June 2017.

USEPA. 2014. Sulphur dioxide: Health. http://www.epa.gov/oaqps001/sulfurdioxide/health.html Date of access: 10 October 2014.

USNPS. 2013. Sulphur dioxide effects on health. http://www.nature.nps.gov/air/AQBasics/understand_so2.cfm Date of access: 10 October 2014.

Vakkari, V., Beukes, J.P., Laakso, H., Mabaso, D., Pienaar, J.J., Kulmala, M. & Laakso, L. 2013. Long-term observations of aerosol size distributions in semi-clean and polluted savannah in South Africa. *Atmospheric Chemistry and Physics*, 13(4):1751-1770.

Venter, A.D., Vakkari, V., Beukes, J.P., Van Zyl, P.G., Laakso, H., Mabaso, D., Tiitta, P., Josipovic, M., Kuimala, M., Pienaar, J.J. & Laakso, L. 2012. An air quality assessment in the industrialized western Bushveld Igneous Complex, South Africa. *South African Journal Science*, 108(9/10):10.

Vet, R., Artz, R.S., Carou, S., Shaw, M., Ro, C.-U., Aas, W., Baker, A., Bowersox, V.C., Dentener, F., Galy-Lacaux, C., Hou, A., Pienaar, J.J., Gillett, R., Forti, M.C., Gromov, S., Hara, H., Khodzher, T., Mahowald, N.M., Nickovic, S., Rao, P.S.P. & Reid, N.W. 2014. A global assessment of precipitation chemistry and deposition of sulfur, nitrogen, sea salt, base cations, organic acids, acidity and pH, and phosphorus. *Atmospheric Environment*, 93:3-100.

Vinayachandran, P.N., Francis, P.A. & Rao, S.A. 2009. Indian Ocean Dipole: Processes and impacts. *Current Trends in Science*:569-589.

Vitousek, P.M. & Howarth, R.W. 1991. Nitrogen limitation on land and in the sea: How can it occur? *Biogeochemistry*(2):87.

Waldman, K.E., Munger, W.J. & Jacob, D.J. 1992. *(In* Radojević, M. & Harrison, R.M., *eds*. Atmospheric acidity: Sources, consequences and abatement. New York: Elsevier.

Wenig, M., Beirle, S., Wagner, T., Jähne, B., Platt, U., Spichtinger, N., Stohl, A. & Held, G. 2003. Intercontinental transport of nitrogen oxide pollution plumes. *Atmospheric Chemistry and Physics*, 3(2):387-393.

Wilson, S.R., Solomon, K.R. & Tang, X. 2007. Changes in tropospheric composition and air quality due to stratospheric ozone depletion and climate change. *Photochemical & Photobiological Sciences*, 6(3):301-310.

WMO. 2004. WMO/GAW report no. 160, Manual for the GAW precipitation chemistry programme,WMO TD No. 1251.

Zbieranowski, A.L. & Aherne, J. 2012. Ambient concentrations of atmospheric ammonia, nitrogen dioxide and nitric acid across a rural-urban-agricultural transect in southern Ontario, Canada. *Atmospheric Environment*, 62:481-491.